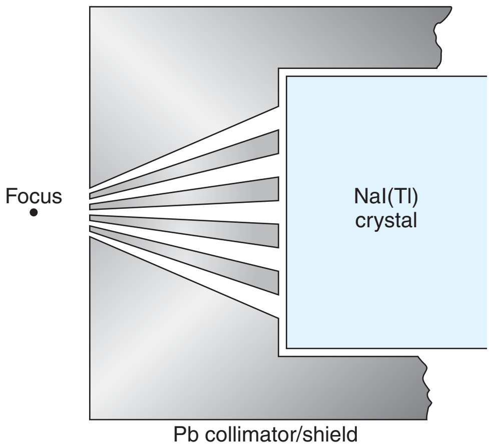

Figure 11-63 Schematic drawing of a scintillation crystal with a Pb collimator to define a focus, a gamma camera. As the detector is moved around the patient, the intensity of the gamma radiation yields information about the location and concentration of the source radioisotope in the body, which can be used by a computer to produce an image of the distribution. Actual gamma cameras incorporate collimators with hundreds or even thousands of tiny channels for the gamma rays to reach the crystal.

Just as with ordinary x-ray radiographs, the images formed by the gamma camera are two-dimensional projections of a three-dimensional distribution. Thus, radiographs provide no depth information, a very serious disadvantage. G. Hounsfield and A. Cormack solved this problem in 1972 with the invention of the computer-assisted tomography (CT or CAT) scanner.[26] A fan-shaped x-ray beam collimated to a thickness of a few millimeters is rotated about the patient and the transmitted fan beam is recorded by an arc of detectors opposite the source, as illustrated in Figure 11-64. The measurements are then reconstructed into an image of a two-dimensional image (*not* a projection) of a transverse slice of the body—a tomograph. By simultaneously making a series of two-dimensional projections with a gamma camera and combining the results with the CT scan, the distribution of the trace radioisotopes in two-dimensional transverse sections can be constructed. The combination system is called *single-photon emission computer tomography*, or SPECT.

It had been recognized early on that the collimators that were essential to the operation of CT scanners and gamma cameras placed a serious restriction on their sensitivity. It was also recognized that the collimators could be eliminated and the sensitivity

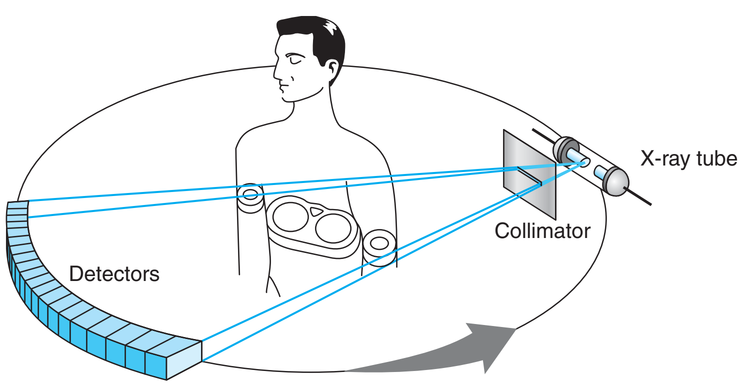

Figure 11-64 Sections of the patient's body transverse to the long axis are imaged by the CT scanner. The fan-shaped x-ray beam, a few millimeters thick, and the bank of detectors, typically proportional or wire counters, rotate about the long axis to produce each complete image. The patient is moved slowly along the axis while the scanner produces successive images, their sum constituting a full three-dimensional composite.

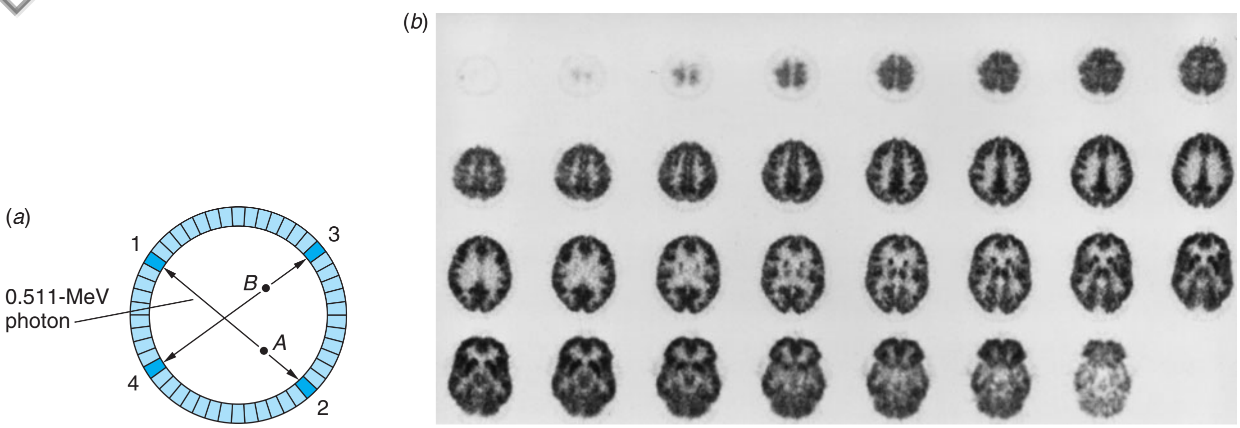

Figure 11-65 (*a*) Nuclei emit positrons at *A* and *B*. The oppositely directed 0.511-MeV photons from each annihilation are detected by a pair of BGO crystal detectors in the annular ring around the subject (not shown). Electronic coincidence circuits establish the line along which each pair of photons traveled. (*b*) The pattern of coincidence measurements is used by a computer to construct an image of the distribution of the radioisotope in the plane of the detector ring. This sequence of PET scans shows the utilization of glucose in the brain, traced by 7 mCi of a positron emitter. The sequence begins in the upper left. [*Courtesy of D. W. Townsend, Division of Nuclear Medicine, University Hospital of Geneva, Geneva, Switzerland.*]

significantly enhanced if the trace radioisotope employed was a positron emitter. The reason is that the positron is stopped within a few millimeters in the tissue and its subsequent annihilation results in two 0.511-MeV photons emitted in opposite directions. Detection of the photons by counters 180° apart whose outputs are analyzed by a time-of-flight coincidence spectrometer yields a precise location for the decay. (See Figure 11-65.) However, this idea did not find its way into a useful diagnostic scanner until the mid-1980s because of the absence of detectors with good efficiency for the 0.511-MeV photons and small enough to localize the incident photons to within a millimeter or so. This problem was solved with the invention by C. Thompson and his co-workers of the bismuth germanate (BGO) crystal. Currently, nearly all commercial positron emission tomography (PET) scanners rely on detector rings made of BGO crystals, as illustrated in Figure 11-65*a*. A PET scan of brain activity made with BGO detectors is shown in Figure 11-65*b*. The availability of PET scans is limited to locations in the proximity of cyclotron facilities because most biologically useful positron emitters, those that readily participate in reactions in the body, are ^{11}C, ^{13}N, ^{15}O, and ^{18}F. They have short half-lives of 20 min, 10 min, 2 min, and 110 min, respectively, and supplies must be regularly replenished by nuclear reactions.

Technetium ($Z = 43$) does not occur in nature. Predicted by Moseley in 1914 and first produced by Segrè in 1937, ^{99}Tc is by far the most widely used radioisotope in nuclear medicine research and diagnosis. Its decay produces a 140-keV gamma ray easily detected by scintillation and germanium detectors.

Radioactive Dating

Radioactivity occurs in nature as a result of (1) decays within the three decay chains originating with long-lived α emitters discussed in Section 11-4, (2) the existence of isolated long-lived primordial radioisotopes such as ^{40}K ($t_{1/2} = 1.25 \times 10^9$ y), and (3) the production of isolated radioisotopes due to reactions between cosmic ray protons and neutrons and nuclei in the atmosphere. Each of these provides a means by which the age of materials, such as rocks and archeological artifacts, can be measured. As one might guess, the very long-lived isotopes, such as ^{40}K and ^{232}Th ($t_{1/2} = 1.24 \times 10^{10}$ y), are used in determining the ages of "old" rocks, while shorter-lived isotopes are employed in determining the ages of "younger" rocks, other inorganic materials, and archeological samples containing carbon, such as charcoal.

Table 11-8 Selected naturally occurring isolated radioactive nuclides

Nuclide	$t_{1/2}$ (y)	Abundance (%)	Daughter
^{14}C	5730	1.35×10^{-10}	^{14}N
^{40}K	1.25×10^{9}	0.0117	^{40}A
^{87}Rb	4.88×10^{10}	27.83	^{87}Sr
^{147}Sm	1.06×10^{11}	15.0	^{143}Nd
^{176}Lu	3.59×10^{10}	2.59	^{176}Hf
^{187}Re	4.30×10^{10}	62.60	^{187}Os

The general technique used in determining the age of a sample by radioactive dating is to measure the present abundance ratio of two isotopes, at least one of which is either radioactive or the stable end product of a radioactive decay, relative to the abundance ratio that is known (or assumed) to have existed at the time when the material was formed. Table 11-8 lists the present isotopic abundances of a few of the naturally occurring isolated radioisotopes used in dating.

^{14}C Dating An important example, used in dating archeological materials containing carbon such as bone and charcoal, measures the abundance ratio $^{14}C/^{12}C$. Radioactive ^{14}C is continuously produced in the atmosphere by the reaction $^{14}N(n, p)^{14}C$. The neutrons are produced by cosmic rays. ^{14}C is a β^- emitter that decays back to ^{14}N via the reaction

$$^{14}C \longrightarrow {}^{14}N + \beta^- + \bar{\nu}_e \tag{11-90}$$

with $t_{1/2} = 5730$ years.[27]

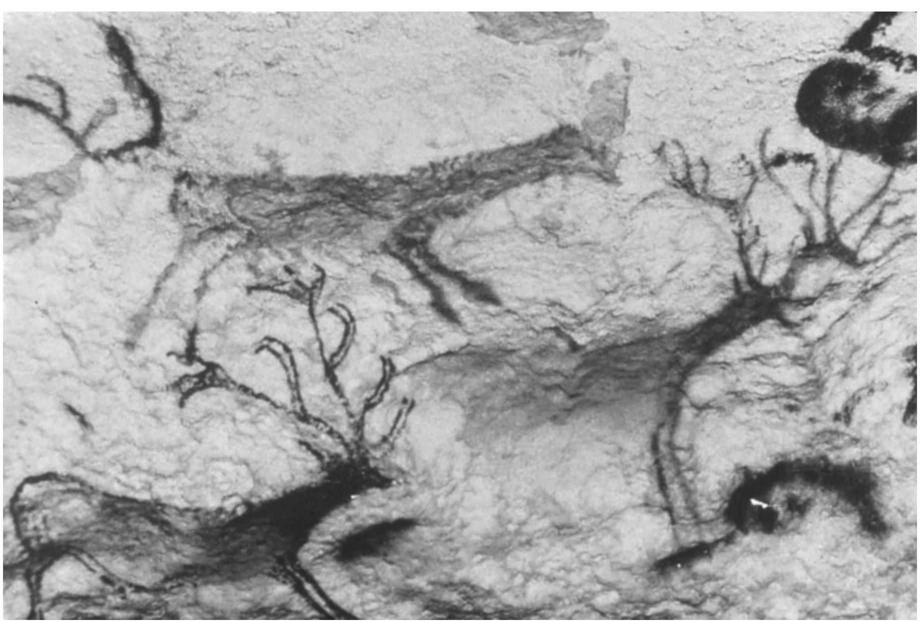

"Group of Stags" from the Lascaux Caves in France. Prehistoric paintings such as this are ^{14}C-dated, the oldest found so far having been painted 33,000 to 38,000 B.C., depending on the $^{14}C/^{12}C$ ratio used for that period. [*Art Resource.*]

The chemical behavior of ^{14}C atoms is the same as that of ordinary ^{12}C atoms. For example, atoms with ^{14}C nuclei combine with oxygen to form CO_2 molecules. Since living organisms continually exchange CO_2 with the atmosphere, the ratio of ^{14}C to ^{12}C in a living organism is the same as the equilibrium ratio in the atmosphere, which is presently about 1.35×10^{-12}. When an organism dies, it no longer absorbs ^{14}C from the atmosphere. The ratio $^{14}C/^{12}C$ in a dead sample continually decreases due to the radioactive decay of ^{14}C. A measurement of the decay rate per gram of carbon thus allows the calculation of the time of death of the organism, as illustrated by Example 11-28.

EXAMPLE 11-27 **^{14}C Decay Rate in Living Organisms** Calculate the decay rate of ^{14}C per gram of carbon in a living organism, assuming the ratio $^{14}C/^{12}C = 1.35 \times 10^{-12}$. The half-life of ^{14}C is 5730 years.

SOLUTION

1. Combining Equation 11-19 with Equation 11-22, the decay rate R can be written in terms of the half-life and the number of radioactive atoms N as

$$R = -\frac{dN}{dt} = \lambda N = \frac{0.693}{t_{1/2}} N$$

2. N is computed from the $^{14}C/^{12}C$ ratio by first computing the number of ^{12}C in a unit mass, e.g., in 1 g:

$$N_{^{12}C} = \frac{N_A}{M} = \frac{6.02 \times 10^{23} \text{ atoms/mol}}{12 \text{ g/mol}} = 5.02 \times 10^{22} \text{ nuclei/g}$$

3. The number N of ^{14}C nuclei per gram is then given by

$$N_{^{14}C} = 1.35 \times 10^{-12} N_{^{12}C} = (1.35 \times 10^{-12})(5.02 \times 10^{22}) = 6.78 \times 10^{10} \text{ nuclei/g}$$

4. The decay rate is then

$$R = \frac{(0.693)(6.78 \times 10^{10} \text{ g}^{-1})(60 \text{ s/min})}{(5730 \text{ y})(3.16 \times 10^{7} \text{ s/y})} = 15.6 \text{ decays/min} \cdot \text{g}$$

Remarks: *Thus, the decay rate for a living organism is 15.6 decays per minute per gram of carbon.*

EXAMPLE 11-28 **Age of a Bone Fragment** A bone fragment found in central Mexico was thought to be associated with the army of Hernán Cortés, who conquered the Aztecs in the early 1500s. The fragment contains 200 g of carbon and has a β-decay rate of 400 decays/min. Could the sample have come from a person who died during the 16th century?

SOLUTION

First we obtain a rough estimate. If the bone were from a living organism, we would expect the decay rate to be 200 g $\times$ 15.6 decays/min $\cdot$ g = 3120 decays/min.

Since 400/3120 is roughly $1/8 = 1/2^3$ (actually 1/7.8), the sample must have decayed for about 3 half-lives, or be about 3×5730 years old. To find the age more accurately, we note that after n half-lives, the decay rate has decreased by a factor of $(1/2)^n$. We therefore find n from

$$\left(\frac{1}{2}\right)^n = \frac{400}{3120}$$

or

$$2^n = \frac{3120}{400} = 7.8$$

$$n \ln 2 = \ln 7.8$$

$$n = \frac{\ln 7.8}{\ln 2} = 2.96$$

The age is therefore $t = nt_{1/2} = 2.96(5730 \text{ years}) = 16{,}980$ years. Thus, the bone fragment is much older than 500 years and cannot be related to Cortés's conquests. Instead, it places early humans in Mesoamerica at least 17,000 years ago.

Note that the calculation in Example 11-28 assumes that the ^{14}N concentration in the atmosphere and the cosmic ray intensity 17,000 years ago were essentially the same as they are today. Actually, neither has remained unchanged over that period. Accurate ^{14}C measurements must include corrections for (1) the variations of Earth's magnetic field, which affects the cosmic ray intensity, and (2) the changing composition of the atmosphere, which depends on global geological and chemical activity and on the average temperature of the atmosphere. For example, current evidence suggests that just prior to 9000 years ago, the ^{14}C/^{12}C ratio was about 1.5 times as large as the current value. The ratio has also been significantly altered over the past century by the burning of fossil fuels, which adds ^{14}C-free carbon to the atmosphere, and by atmospheric testing of hydrogen weapons, which added ^{14}C during the 1950s. Accelerator mass spectrometry, which was originally developed for just this purpose, makes possible determination of the ^{14}C/^{12}C ratio with sufficient accuracy to extend the applicability of ^{14}C dating back 50,000 years before the present with samples as small as a few milligrams. Calibration of the ratio for earlier periods requires cross-dating with other methods, such as U-Th dating.

Dating Ancient Rocks Starting with Equation 11-18, a useful relation can be derived for the age of a sample that initially contains N_0 radioactive parent nuclei that decay to a stable daughter with a half-life $t_{1/2}$. Assuming there are no daughter nuclei present initially, after a time t has elapsed, there will be N_P parent nuclei and N_D daughter nuclei in the sample. From Equation 11-18,

$$t = \frac{1}{\lambda}\ln\left(\frac{N_0}{N_P}\right) = \frac{t_{1/2}}{\ln 2}\ln\left(\frac{N_0}{N_P}\right) \qquad \textbf{11-91}$$

Since $N_P + N_D = N_0$ at any time, Equation 11-91 can be written as

$$t = \frac{t_{1/2}}{\ln 2}\ln\left(1 + \frac{N_D}{N_P}\right) \qquad \textbf{11-92}$$

where N_D/N_P is the isotopic ratio at age t.

Several isotopic abundance ratios are used as "rock clocks" for samples of geologic age. These include $^{238}U/^{206}Pb$, $^{87}Rb/^{87}Sr$, $^{40}K/^{40}Ar$, and the dual ratio $^{238}U/^{234}U/^{230}Th$. These have been used to determine the age of Earth rocks, Moon rocks, meteorites, and, by inference, the solar system itself. The oldest rocks on Earth have been dated at about 4.5×10^9 years. At that time the molten surface froze, fixing the isotopic ratios, which thereafter changed only as a result of decay. Surprisingly, perhaps, all meteorites turn out to be about the same age, 4.5×10^9 years, regardless of their composition or when they collided with Earth. This suggests that they originated in or are the debris of other bodies within the solar system that formed at the same time as Earth. This value for the age of Earth is supported by a number of independent ratio measurements, initially the relative abundances of ^{238}U and ^{235}U and the $^{238}U/^{206}Pb$ ratio and corroborated more recently by measurements of the $^{40}K/^{40}Ar$ and $^{87}Rb/^{87}Sr$ ratios.

EXAMPLE 11-29 **$^{87}Rb/^{87}Sr$ Dating** The $^{87}Rb/^{87}Sr$ ratio for a particular rock is found to be 40.0. How old is the rock?

SOLUTION

Note first that in Equation 11-92, the radioactive parent appears in the denominator of the ratio; therefore, in this case $N_D/N_P = 1/(^{87}Rb/^{87}Sr) = 1/40.0 = 0.025$. Substituting this value and the half-life of ^{87}Rb from Table 11-8 into Equation 11-92, we have

$$t = \frac{4.88 \times 10^{10}\text{ y}}{\ln 2}\ln(1 + 0.025) = \frac{4.88 \times 10^{10}\text{ y}}{0.693} \times 0.0247 = 1.74 \times 10^8\text{ y}$$

This is a young rock, considerably younger than the 4.5×10^9 y age of Earth.

Rocks found on Earth's surface have a range of ages from zero up to 3.7×10^9 years. None are older. In contrast, rocks brought back from the surface of the Moon by Apollo astronauts have ages ranging from 3.1 to 4.5×10^9 years; none are younger. The implications of these results from radioactive dating are (1) Earth surface rocks older than 3.7×10^9 years have weathered, eroded, and been recycled into other rocks or into the mantle and (2) the Moon's internal heat source (gravity and radioactivity) cooled sufficiently to solidify all its material and fix the initial isotopic ratios about 1.5×10^9 years after it was formed. The Earth's internal heat source has not yet reached that point.

Accelerator Mass Spectrometry

Originally developed to extend the usable time span and improve the accuracy of ^{14}C dating of archeological materials, accelerator mass spectrometry (AMS) is an ultrasensitive analytical technique in which the atoms of interest in a sample are counted directly rather than irradiating the sample with slow neutrons, then counting the gamma rays emitted by the radioactive daughter produced or measuring the radiations emitted by long-lived, naturally occurring radionuclides. To understand how AMS works, we will use its application to ^{14}C dating as an illustration. At the present time the $^{14}C/^{12}C$ ratio in living organic material is about 10^{-12}. Thus, a 1-g sample of carbon contains about 5×10^{10} ^{14}C atoms. Since the half-life of ^{14}C is 5730 y, a 1.0-g sample of 20,000-year-old charcoal would emit about one β^- per minute. To record 10,000 decays (the number needed for a statistical accuracy of 1 percent) would require counting for one week and involve only 2×10^{-6} of the ^{14}C atoms present in the sample, a very inefficient method.

Table 11-9 Radioisotopes measurable with AMS

Nuclide	Half-life (y)	Stable isobar	Sensitivity
^{3}H	12.3	^{3}He	10^{-14}
^{10}Be	1.5×10^{6}	^{10}B	10^{-15}
^{14}C	5.730×10^{3}	^{14}N	2×10^{-15}
^{26}Al	7.40×10^{5}	^{26}Mg	10^{-15}
^{36}Cl	3.01×10^{5}	^{36}S	2×10^{-15}
^{41}Ca	1.0×10^{5}	^{41}K	10^{-15}
^{129}I	1.6×10^{7}	^{129}Xe	10^{-14}

Mass spectrometry, which records *every* atom in the sample, provides a possible alternative (see Section 3-1). However, conventional mass spectrometers do not have the capability of measuring isotope ratios at the level of $^{14}C/^{12}C$ (or the other radioisotopes listed in Table 11-9) due to the presence of isobars and molecules with nearly the same mass. In the case of ^{14}C these include ^{14}N from residual air within the spectrometer and $^{12}CH_2$ and ^{13}CH, both from the sample itself or contamination. AMS works in part like a conventional mass spectrometer but reduces background due to mass ambiguities by taking advantage of the operational characteristics of medium-energy accelerators, particularly cyclotrons and tandem van de Graaffs. Using the latter as the basis of our discussion and referring to the photograph and diagram on page 518 and to Figure 11-66, the positive high-voltage terminal is in the middle of the accelerator with the two ends of the beam tube essentially at ground potential. The atoms of the sample are converted to negative ions in the ion source. The atoms of most elements can form stable negative ions, a notable exception being nitrogen. Thus, AMS immediately removes background due to ^{14}N. A bending magnet deflects the ions according to their radii of curvature. The negative ions are accelerated to the positive terminal, where a stripper removes several electrons, forming positive ions. If more than three electrons are removed, most molecules break apart. The ions are then accelerated further (to 50–100 MeV), emerging from the machine into another bending magnet, which effectively removes the molecular fragments that in general do not have the same radii of curvature as do the atomic ions. After passing through another 90° bending magnet that cleans the beam of any residual molecular fragments, the high-energy beam enters the detector, a so-called E-ΔE counting telescope (see

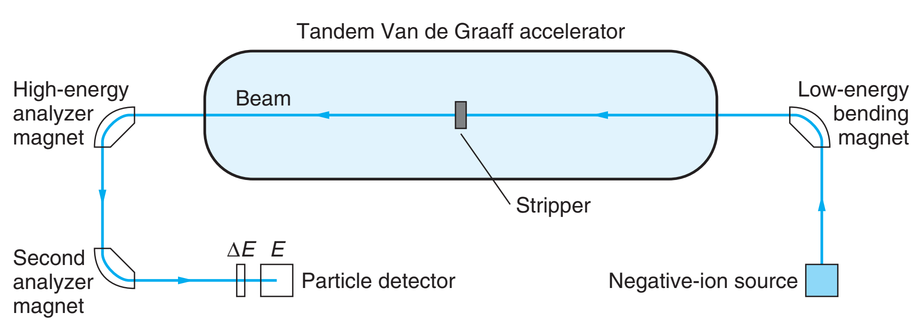

Figure 11-66 Schematic drawing of a tandem Van de Graaff accelerator configured as an accelerator mass spectrometer.

The perfectly preserved mummy of Ötzi the Iceman was found in the Tyrolean Alps in 1991. Accelerator mass spectrometry places his date of death between 3300 and 3200 years B.C. Recent (2003) measurements of oxygen isotopic ratios in his teeth and bones have pinpointed the area where he lived. [© *South Tyrol Museum of Archeology, Italy. www.iceman.it.*]

Figure 11-66). The very thin ΔE detector measures the energy loss by the atoms, which for particles with the same energy is approximately proportional to Z^2, thus rejecting atoms with a different atomic number than that of interest. The high-energy ions are then stopped in the E detector, which measures the energy of each one. The product $E \times \Delta E$ for each atom is approximately proportional to mZ^2. Thus, requiring sample masses of only a few milligrams, AMS measures the mass and atomic number of each atom, and it does so with very high precision and extremely low background.

Table 11-9 lists several long-lived radioisotopes that can be effectively assayed with AMS. For example, the technique has been used to time the migration of surface water into deep aquifers by measuring the concentration of ^{36}Cl, produced by cosmic ray bombardment of argon in the atmosphere. Using only a few strands, AMS ^{14}C-dated the famous Shroud of Turin as having been made in the Middle Ages, around 1300. Ötzi (the Iceman) discovered in 1991 in the Tyrolean Alps, was found to have lived during the late Neolithic age, about 5200 years ago. Some meteorites have been found to contain relatively short-lived ^{26}Al in excess of the concentration attributable to cosmic ray production, raising the intriguing question of its origin in the cosmos.

Particle-Induced X-ray Emission

An elemental analysis technique similar to neutron activation analysis (NAA), particle-induced x-ray emission (PIXE) involves bombarding the material of interest with low-energy (a few MeV) ions, such as protons or alpha particles. Coulomb interaction between the ions and the target atoms ionize the latter by ejecting K- or L-shell electrons. Since the interactions occur over atomic dimensions, the cross sections are quite high, as much as 1000 b for low-Z atoms, decreasing smoothly to about 1 b at $Z = 82$ (Pb). The vacancies produced are quickly filled by electrons from higher-energy shells, emitting K and L x rays or Auger electrons in the process that are characteristic of the elements in the target (see Section 4-4). Since the bombarding particles are relatively low energy, they do not penetrate far into matter, so the interactions occur near the surface. That fact, together with the low energy of the emitted x rays, 10 to 100 keV, dictates the use of thin samples. Figure 11-67*a* is a schematic of a typical PIXE experimental arrangement. The sensitivity of PIXE is comparable to NAA and has the advantage of being applicable to all elements above $Z = 20$, whereas NAA is restricted to those nuclides with sufficiently large thermal neutron absorption cross sections. The main disadvantage of PIXE is x-ray energy ambiguities. For example, the energy of the L_α x ray from Pb is 10.55 keV, while that of the K_α line of As is 10.54 keV. The resolution of the cooled Si(Li) detectors used for x rays is about 100 eV, insufficient to resolve the two lines. Figure 11-67*b* shows a typical PIXE spectrum.

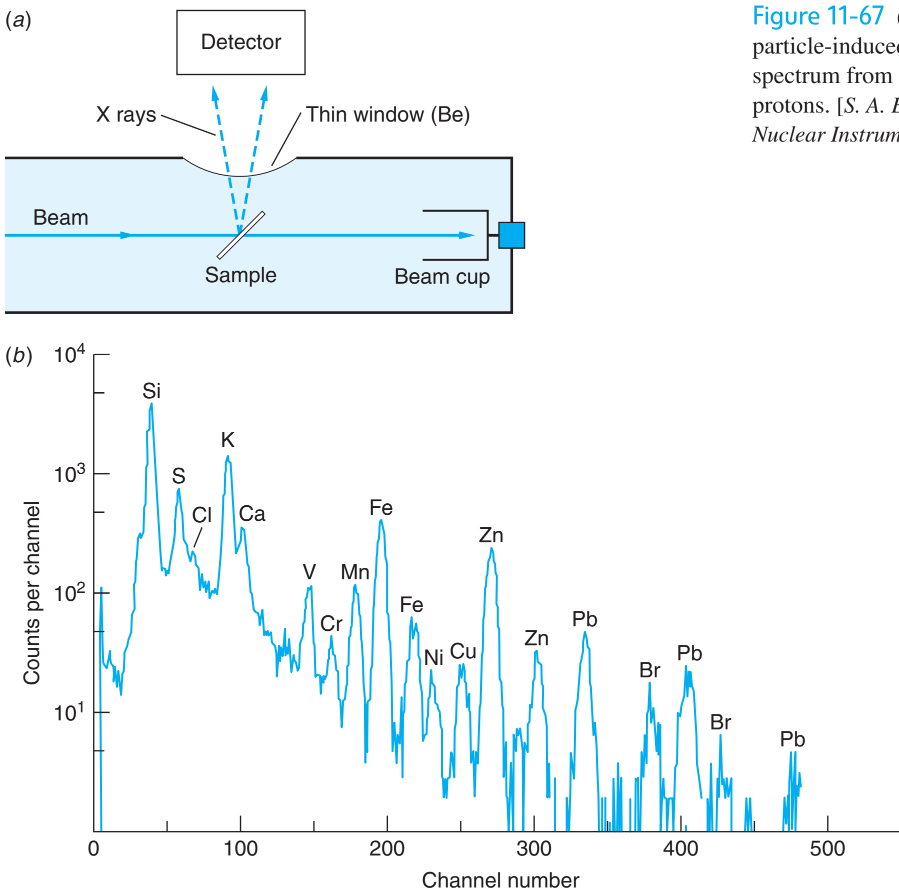

Figure 11-67 (*a*) Schematic drawing of a typical particle-induced x-ray emission system. (*b*) PIXE spectrum from an aerosol bombarded with 2-MeV protons. [*S. A. E. Johansson and T. B. Johansson, Nuclear Instruments and Methods, 137, 473, 1976.*]

Questions

20. If the $^{14}C/^{12}C$ ratio was 1.5 times larger than that used in Example 11-28, is the calculated age too large or too small? Explain.
21. Some meteorites are found to contain measurable amounts of ^{26}Al, whose $t_{1/2}$ is only 7.4×10^5 years. Devise a scenario that would account for its presence.
22. ^{40}Ar is a gas at ordinary temperatures. Explain why solid rocks can be accurately dated using the $^{40}K/^{40}Ar$ ratio in spite of that fact.
23. Explain why accelerator mass spectrometry can achieve reliable results using samples of only 1 mg.

More

The biological effects of ionizing radiation were largely unknown in the early days of atomic and nuclear physics. It took such things as the plight of the radium-watch dial painters, x-ray crystallographers with missing fingertips, and young cyclotron physicists with cataracts to focus scientific attention on the risks that attend exposure to ionizing radiation in the home, the workplace, and the environment. Questions of *Radiation Dosage*, its definition, origin, and effects, are discussed on the home page: www.whfreeman.com/tiplermodernphysics5e. See also Equations 11-93 through 11-95 here, as well as Tables 11-10 through 11-13.

Summary

TOPIC	RELEVANT EQUATIONS AND REMARKS	
1. The composition of the nuclei	Nuclei have Z protons, N neutrons, and mass number $A = Z + N$. Nuclei with the same Z but different N (and A) are called isotopes. The nucleons are Fermi-Dirac (spin 1/2) particles and both have intrinsic magnetic moments.	
2. Ground-state properties of nuclei		
Size and shape	The mean radius of the nuclear charge distribution is	
	$R = (1.07 \pm 0.02)A^{1/3}$ fm	**11-5**
	The radii thus vary from about 1 fm for the proton to about 10 fm for the heaviest nuclei. With few exceptions, nuclei are nearly spherical.	
Binding energy and mass	The binding energy of the nucleus is given by	
	$B_{\text{nuclear}} = ZM_{\text{H}}c^2 + Nm_nc^2 - M_Ac^2$	**11-11**
Magnetic moments	The moments of the proton and neutron are	
	$(\mu_p)_z = +2.79285\ \mu_N$	
	$(\mu_n)_z = -1.91304\ \mu_N$	
	where $\mu_N = e\hbar/2m_p$ is the nuclear magneton.	
3. Radioactivity	The decay rate R of radioactive nuclei is	
	$R = -\dfrac{dN}{dt} = \lambda N_0 e^{-\lambda t} = R_0 e^{-\lambda t}$	**11-19**
	where λ is the decay constant. N_0 and R_0 are the number of nuclei present and the decay rate at $t = 0$.	
Half-life	$t_{1/2} = \dfrac{\ln 2}{\lambda} = 0.693\tau$	**11-22**
	where $\tau = 1/\lambda$ is the mean life.	
Units	1 decay/s = 1 becquerel = 1 Bq	**11-23**
4. Alpha, beta, and gamma decay	These are the three most common forms of radioactive decay. Alpha particles are ^{4}He nuclei, beta particles are electrons and positrons, and gamma rays are very short wavelength electromagnetic radiation.	
5. The nuclear force	The nuclear force is	
	(*a*) About 10^2 stronger than the Coulomb force (*b*) Short-range (≈ 0 beyond 3 fm) (*c*) Charge independent (*d*) Saturated (*e*) Dependent on spin orientation	
	The nuclear force is considered to be an exchange force in which the attraction between a pair of nucleons is due to an exchange of virtual pions. The range R of the force, determined by the uncertainty principle, is	
	$R = c\,\Delta t = c\hbar/\Delta E = \hbar/mc$	**11-50**
	where m is the mass of the virtual pion.	

TOPIC	RELEVANT EQUATIONS AND REMARKS
6. The shell model	An independent particle model, similar to that used for assigning energy states to the atomic electrons, but one that makes use of a strong spin-orbit coupling for each nucleon accounts for the shell-like structure of the protons and neutrons. It explains the magic numbers 2, 8, 20, 28, 50, 82, and 126 in terms of the completion of the shells. Shell-model calculations are relatively successful in predicting nuclear spins and magnetic moments, particularly in the vicinity of closed shells.
7. Nuclear reactions	The Q value of a reaction X(x, y)Y determines if energy is released or must be supplied. Q is given by $$Q = (m_x + m_X - m_y - m_Y)c^2 \quad \textbf{11-58}$$
Cross section	The cross section σ measures the effective size of a nucleus for a particular nuclear reaction. $$\sigma = \frac{R}{I} \quad \textbf{11-62}$$ where R is the number of reactions per unit time per nucleus and I is the incident particle intensity.
8. Fission and fusion	Fission is the process by which heavy elements such as ^{235}U and ^{239}Pu capture a neutron and split into two medium-mass nuclei. Each event releases about 1 MeV/nucleon. Fusion is the reaction in which two light nuclei, such as ^{2}H and ^{3}H, fuse together to produce a heavier nucleus. Each event releases 1 to 4 MeV/nucleon.
9. Applications	The applications of nuclear reactions in medicine include the use of nuclear radiation in the treatment of diseases and the use of nuclear-based imaging techniques in diagnosis and research. Nuclear magnetic resonance imaging (MRI) is an alternative to x-ray imaging with the advantage that the RF photons involved produce little damage to biological tissue. Computer-assisted tomography using short-lived positron emitters (PET) provides rapid, three-dimensional images. Radioactive dating employs a number of naturally occurring radioisotopes to determine the age of rocks and artifacts. Accelerator mass spectrometry and neutron activation analysis are highly sensitive means of measuring the concentration of particular isotopes of nearly every element in the periodic table.

General References

The following general references are written at a level appropriate for the readers of this book.

Beyer, R. (ed.), *Foundations of Nuclear Physics*, Dover, New York, 1949. This paperback contains 13 original papers, eight in English—by Anderson, Chadwick, Cockroft and Walton, Fermi, Lawrence and Livingston, Rutherford (two papers), and Yukawa—the others are in German or French.

Biological Effects of Ionizing Radiation (*BEIR III*), National Academy of Sciences/National Research Council, Washington, D.C., 1988.

Das, A., and T. Ferbil, *Introduction to Nuclear and Particle Physics*, Wiley, New York, 1994.

Fermi, E., *Nuclear Physics*, rev. ed., University of Chicago Press, Chicago, 1974.

Frauenfelder, H., *The Mössbauer Effect*, W. A. Benjamin, New York, 1962.

Frauenfelder, H., and E. M. Henley, *Subatomic Physics*, 2d ed., Prentice-Hall, Englewood Cliffs, N.J., 1991.

Krane, K. S., *Introductory Nuclear Physics*, Wiley, New York, 1987.

Lilley, J., *Nuclear Physics: Principles and Applications*, Wiley, Chichester, UK, 2001.

Mayer, M., and J. H. D. Jensen, *Elementary Theory of Nuclear Shell Structure*, Wiley, New York, 1955.

Nero, A. V., Jr., *A Guidebook to Nuclear Reactors*, University of California Press, Berkeley, 1979.

Priest, J., *Energy: Principles, Problems, and Alternatives*, 5th ed., Kendall/Hunt, Dubuque, Iowa, 2000.

Segrè, E., *Nuclei and Particles,* 2d ed., Benjamin Cummings, Menlo Park, Calif., 1977.

Walecka, J. D., *Theoretical Nuclear and Subnuclear Physics*, 2d ed., Imperial College Press/World Scientific, London, 2004. Part 1 is appropriate reading for this chapter.

Notes

1. Antoine Henri Becquerel (1852–1908), French physicist. He held the scientific post at the Museum of Natural History in Paris that had been held by his father and grandfather before him, and his research on the fluorescence of potassium uranyl sulfate was a continuation of work that his father had begun. His discovery of radioactivity, which revolutionized existing theories of atomic structure, earned him a share of the 1903 Nobel Prize in Physics, together with Marie and Pierre Curie.

2. The phenomenon was named *radioactivity* by Marie Curie in 1898.

3. These accomplishments were of such importance to the development of nuclear physics that all four men were subsequently awarded the Nobel Prize, James Chadwick in 1935, Carl Anderson in 1936 (shared with Victor Hess, the discoverer of cosmic rays), and John Cockcroft and Ernest Walton in 1951.

4. The United States produced about 30 percent of the world's nuclear-generated electric power in 2005.

5. The term *tomography* is from the Greek *tomos*, meaning "slice," and *graphé*, meaning "picture." Thus, a tomograph is the pictorial representation of a slice through the object or body being studied.

6. Robert Hofstadter (1915–1990), American physicist. His electron-scattering measurements also revealed that the proton and neutron possessed internal structure, opening the way to a more fundamental understanding of the structure of matter. For his work he shared the 1961 Nobel Prize in Physics with Rudolf Mössbauer.

7. See, for example, Section 23-2 in P. A. Tipler and G. Mosca, *Physics for Scientists and Engineers*, 6th ed., W. H. Freeman and Co., New York, 2008.

8. See, for example, Section 26-2 in P. A. Tipler and G. Mosca, *Physics for Scientists and Engineers*, 6th ed., W. H. Freeman and Co., New York, 2008.

9. See P. A. Seeger, *Nuclear Physics*, **25**, 1 (1961).

10. The electric quadrupole moment of the nucleus, discussed earlier in this section, also causes hyperfine splitting, as do externally applied magnetic and electric fields. The effect of the reduced mass (isotope effect) mentioned in Chapter 4 is also considered a hyperfine effect.

11. Actually, the electron's magnetic moment deviates slightly from that predicted by the Dirac wave equation, one Bohr magneton. Quantum electrodynamics is able to account for the small deviation observed experimentally with an error of less than 1 part in 10^8, one of the most remarkable agreements between quantum theory and experiment in physics.

12. This statement requires a small qualification. An alternative to β^+ decay, discussed in Section 11-4, is electron capture, in which an orbital electron may be captured by the nucleus. The probability of its occurrence depends on the probability density of the electrons, which can be affected slightly by very high external pressures.

13. Leptons include the electrons and neutrinos that are emitted in β decay. (See Chapter 12.)

14. Rudolf Ludwig Mössbauer (b. 1929), German physicist. His discovery of the recoilless emission and absorption of gamma rays, made while he was a graduate student in Munich, made possible the verification (by R. V. Pound and G. A. Rebka in 1960) of the gravitational red shift predicted by general relativity. Mössbauer shared the 1961 Nobel Prize in Physics with Robert Hofstadter.

15. Note that this electrostatic potential corresponds to a force of nearly 60 N, or the weight of a 6-kg mass! It is acting not on 6 kg, however, but on only 1.67×10^{-27} kg.

16. Hideki Yukawa (1907–1981), Japanese physicist. His paper presenting the exchange meson theory of the nuclear force was his first publication. He was awarded the 1949 Nobel Prize in Physics for the discovery.

17. See, for example, Section 30-3 in P. A. Tipler and G. Mosca, *Physics for Scientists and Engineers*, 6th ed., W. H. Freeman and Co., New York, 2008.

18. Previously unknown particles had been observed in cosmic rays at about the same time that Yukawa proposed the meson exchange theory. He sent an article to the journal *Nature* in 1937 suggesting that they might be the mesons, but the journal rejected the article. Those particles were later found to be muons, a product of the decay of Yukawa's pi mesons.

19. Maria Goeppert-Mayer (1906–1972), German-American physicist, and Johannes Hans Daniel Jensen (1907–1973), German physicist. Goeppert-Mayer's antecedents for many generations had been university professors, while Jensen was the son of a gardener. They co-authored a famous (among physicists, at least) book explaining their nuclear-shell model and for that work shared the 1963 Nobel Prize in Physics with Eugene Wigner.

20. In *j-j* coupling the spin and orbital angular momentum of each particle add to give a total angular momentum **j** for that particle, and then **J** equals the sum of the individual *j* vectors. In L-S coupling the spins of all the particles and the orbital angular momenta of all the particles add to yield total **S** and total **L**, which then add to yield **J**.

21. This dependence, which occurs only for (n, γ) reactions with relatively low-energy neutrons, was first measured by Emilio Segrè in 1935.

22. The first such resonance was observed unexpectedly in the results of a neutron irradiation of silver conducted by Edoardo Amaldi and others on the morning of October 22, 1934. By 3:00 p.m. that day, Enrico Fermi had developed the correct explanation of the strange phenomenon. The paper describing the discovery was written that evening and delivered to the scientific journal *Ricerca Scientifica* the next morning, less than 24 hours after the discovery!

23. Otto Hahn (1879–1968), German physical chemist, and Fritz Stassmann (1902–1980), German chemist. Hahn recognized that uranium nuclei bombarded with neutrons were breaking apart but carefully avoided characterizing the event as fission since no such thing had been recorded before. He received the 1944 Nobel Prize in Chemistry for the discovery.

24. Actually, Fermi's reactor was the first *constructed* fission reactor. About 2 billion years ago several deposits of natural uranium located in what is now Gabon, West Africa, began chain reactions that continued for 150 million years at an average power of 100 kW before naturally shutting themselves off. The evidence that verified the discovery of the first of these, a fascinating example of scientific detective work, can be found in G. A. Cowan, "A Natural Fission Reactor," *Scientific American*, July 1976. The sites are being mined, and efforts to preserve one of the natural reactors as an international historic site are currently under way.

25. An elementary discussion of a magnetic bottle can be found in Section 26-2 in P. A. Tipler and G. Mosca, *Physics for Scientists and Engineers*, 6th ed., W. H. Freeman and Co., New York, 2008.

26. Godfrey Hounsfield (1919–2004), English engineer, and Allan Cormack (1924–1998), American physicist. They shared the 1979 Nobel Prize in Medicine for the invention of the CT scanner.

27. The radiocarbon-dating technique was developed by Willard F. Libby (1908–1980), an American chemist. He received the 1960 Nobel Prize in Chemistry for his work.

Problems

Level I

Section 11-1 The Composition of the Nucleus

11-1. What are the number of protons and the number of neutrons in each of the following isotopes? ^{18}F, ^{25}Na, ^{51}V, ^{84}Kr, ^{120}Te, ^{148}Dy, ^{175}W, and ^{222}Rn.

11-2. Electrons emitted in β decay have energies of the order of 1 MeV or smaller. Use this fact and the uncertainty principle to show that electrons cannot exist inside the nucleus.

11-3. The spin of the ground state of ^{6}Li, which constitutes 7.5 percent of natural lithium, is zero. Show that this value is not compatible with a model of the nucleus that consists of protons and electrons.

11-4. The magnetic moment of ^{14}N is 0.4035 μ_N. Show that this value is not compatible with a model of the nucleus that consists of protons and electrons.

11-5. Suppose that the deuteron really did consist of two protons and one electron. (It doesn't!) Compute the spin and magnetic moment of such a deuteron's ground state and compare the results with the values in Table 11-1.

Section 11-2 Ground-State Properties of Nuclei

11-6. Give the symbols for at least two isotopes and two isotones of each of the following nuclides: (*a*) ^{18}F, (*b*) ^{208}Pb, and (*c*) ^{120}Sn.

11-7. Give the symbols for at least two isobars and one isotope of each of the following nuclides: (*a*) ^{14}O, (*b*) ^{63}Ni, and (*c*) ^{236}Np.

11-8. Approximating the mass of a nucleus with mass number A as $A \times$ u and using Equation 11-3, compute the nuclear density in SI units.

11-9. Use the masses in the table in Appendix A to compute the total binding energy and the binding energy per nucleon of the following nuclides: (*a*) ^{9}Be, (*b*) ^{13}C, and (*c*) ^{57}Fe.

11-10. Use Equation 11-3 to compute the radii of the following nuclei: (*a*) ^{16}O, (*b*) ^{56}Fe, (*c*) ^{197}Au, and (*d*) ^{238}U.

11-11. Find the energy needed to remove a neutron from (*a*) ^{4}He, (*b*) ^{7}Li, and (*c*) ^{14}N.
11-12. Use the Weizsäcker formula to compute the mass of ^{23}Na. Compute the percent difference between the result and the value in the table in Appendix A.
11-13. Compute the "charge distribution radius" from Equation 11-5 and the "nuclear force radius" from Equation 11-7 for the following nuclides: (*a*) ^{16}O, (*b*) ^{63}Cu, and (*c*) ^{208}Pb.
11-14. ^{39}Ca and ^{39}K are a mirror pair, ^{39}Ca decaying into ^{39}K. Use Equations 11-1 and 11-2 to compute the radius of ^{40}Ca.

Section 11-3 Radioactivity

11-15. The counting rate from a radioactive source is 4000 counts per second at time $t = 0$. After 10 s, the counting rate is 1000 counts per second. (*a*) What is the half-life? (*b*) What is the counting rate after 20 s?
11-16. A certain source gives 2000 counts per second at time $t = 0$. Its half-life is 2 min. (*a*) What is the counting rate after 4 min? (*b*) After 6 min? (*c*) After 8 min?
11-17. A sample of a radioactive isotope is found to have an activity of 115.0 Bq immediately after it is pulled from the reactor that formed it. Its activity 2 h 15 min later is measured to be 85.2 Bq. (*a*) Calculate the decay constant and the half-life of the sample. (*b*) How many radioactive nuclei were there in the sample initially?
11-18. The half-life of radium is 1620 years. (*a*) Calculate the number of disintegrations per second of 1 g of radium and show that the disintegration rate is approximately 1 Ci. (*b*) Calculate the approximate energy of the α particle in the decay $^{226}\text{Ra} \rightarrow {}^{222}\text{Rn} + \alpha$, assuming the energy of recoil of the Rn nucleus is negligible. (Use the mass table of Appendix A.)
11-19. The counting rate from a radioactive source is 8000 counts per second at time $t = 0$. Ten minutes later the rate is 1000 counts per second. (*a*) What is the half-life? (*b*) What is the decay constant? (*c*) What was the counting rate after 1 minute?
11-20. The counting rate from a radioactive source is measured every minute. The resulting numbers of counts per second are 1000, 820, 673, 552, 453, 371, 305, 250, . . . (*a*) Plot the counting rate versus time and (*b*) use your graph to estimate the half-life. (*c*) What would be the approximate result of the next measurement after the 250 counts per second?
11-21. ^{62}Cu is produced at a constant rate [e.g., by the (γ, *n*) reaction on ^{63}Cu placed in a high-energy x-ray beam] and decays by β^+ decay with a half-life of about 10 min. How long does it take to produce 90 percent of the equilibrium value of ^{62}Cu?
11-22. The decay constant of ^{235}U is 9.8×10^{-10} y^{-1}. (*a*) Compute the half-life. (*b*) How many decays occur each second in a 1.0-μg sample of ^{235}U? (*c*) How many ^{235}U atoms will remain in the 1.0-μg sample after 10^6 years?
11-23. The decay constant of ^{22}Na is 0.266 y^{-1}. (*a*) Compute the half-life. (*b*) What is the activity of a sample containing 1.0 g of ^{22}Na? (*c*) What is the activity of the sample after 3.5 years have passed? (*d*) How many ^{22}Na atoms remain in the sample at the time?

Section 11-4 Alpha, Beta, and Gamma Decay

11-24. The stable isotope of sodium is ^{23}Na. What kind of radioactivity would you expect of (*a*) ^{22}Na and (*b*) ^{24}Na?
11-25. Using Figure 11-16, find the parameters *A* and *B* in Equation 11-30.
11-26. Make a diagram like Figure 11-18 for the $(4n + 1)$ decay chain that begins with ^{237}Np, a nuclide that is no longer present in nature. (Use Appendix A.)
11-27. Show that the α particle emitted in the decay of ^{232}Th carries away 4.01 MeV, or 98 percent, of the total decay energy.
11-28. ^{7}Be decays exclusively by electron capture to ^{7}Li with a half-life of 53.3 d. Would the characteristics of the decay be altered and, if so, how if (*a*) a sample of ^{7}Be were placed under very high pressure or (*b*) all four electrons were stripped from each ^{7}Be atom in the sample?
11-29. Compute the energy carried by the neutrino in the electron capture decay of ^{67}Ga to the ground state of ^{67}Zn.
11-30. Compute the maximum energy of the β^- particle emitted in the decay of ^{72}Zn.
11-31. In Example 11-13 we saw that ^{233}Np could decay by emitting an α particle. Show that decay by emission of a nucleon of either type is forbidden for this nuclide.

11-32. With the aid of Figures 11-19 and 11-20, list the energies of all of the possible γ rays that may be emitted by ^{223}Ra following the α decay of ^{227}Th.

11-33. ^{8}Be is very unusual among low-Z nuclides; it decays by emitting two α particles. Show why ^{8}Be is unstable toward α decay.

11-34. ^{80}Br can undergo all three types of β decay. (a) Write down the decay equation in each case. (b) Compute the decay energy for each case.

Section 11-5 The Nuclear Force

11-35. Assuming that the average separation between two protons in ^{12}C is equal to the nuclear diameter, compute the Coulomb force of repulsion and the gravitational force of attraction between the protons. If the nuclear potential seen by the protons is 50 MeV for separations up to 3 fm, compare the nuclear force to the other two forces.

11-36. Suppose the range of the nuclear force was 5 fm. Compute the mass (in MeV/c^2) of an exchange particle that might mediate such a force.

11-37. The repulsive force that results in the "hard core" of the nucleus might be due to the exchange of a particle, just as the strong attractive force is. Compute the mass of such an exchange particle if the range of the repulsive force equals about 0.25 fm, the radius of the core.

Section 11-6 The Shell Model

11-38. The nuclei listed below have filled j shells plus or minus one nucleon. (For example, $^{29}_{14}$Si has the $1d_{5/2}$ shell filled for both neutrons and protons, plus one neutron in the $2s_{5/2}$ shell.) Use the shell model to predict the orbital and total angular momentum of these nuclei:

$$^{29}_{14}\mathrm{Si} \quad ^{37}_{17}\mathrm{Cl} \quad ^{71}_{31}\mathrm{Ga} \quad ^{59}_{27}\mathrm{Co} \quad ^{73}_{32}\mathrm{Ge} \quad ^{33}_{16}\mathrm{S} \quad ^{87}_{38}\mathrm{Sr}$$

11-39. Use the shell model to predict the nuclear magnetic moments of the isotopes listed in Problem 11-38.

11-40. The atomic spectral lines of ^{14}N exhibit a hyperfine structure, indicating that the ground state is split into three closely spaced levels. What must be the spin of the ^{14}N ground state?

11-41. Which of the following nuclei have closed neutron shells: ^{36}S, ^{50}V, ^{50}Ca, ^{53}Mn, ^{61}Ni, ^{82}Ge, ^{88}Sr, ^{93}Ru, ^{94}Ru, ^{131}In, and ^{145}Eu?

11-42. Sketch diagrams like Figure 11-9 for the ground states of ^{3}H, ^{3}He, ^{14}N, ^{14}C, ^{15}N, ^{15}O, and ^{16}O.

11-43. Which of the following nuclei have closed proton shells: ^{3}He, ^{19}F, ^{12}C, ^{40}Ca, ^{50}Ti, ^{56}Fe, ^{60}Ni, ^{60}Cu, ^{90}Zr, ^{124}Sn, ^{166}Yb, and ^{204}Pb?

11-44. (a) Use Figure 11-35 to draw a diagram like Figure 11-9 for ^{13}N. (b) What value would you predict for the value of j? (c) What value would you predict for j for the first excited state? (d) Draw a diagram like Figure 11-9 for the first excited state. (Is there only one possible?)

11-45. Use Figure 11-35 to predict the values of j for the ground states of ^{30}Si, ^{37}Cl, ^{55}Co, ^{90}Zr, and ^{107}In.

Section 11-7 Nuclear Reactions

11-46. Using data from Appendix A, find the Q values for the following reactions: (a) $^{2}\mathrm{H} + {}^{2}\mathrm{H} \rightarrow {}^{3}\mathrm{H} + {}^{1}\mathrm{H} + Q$, ($b$) ^{3}He$(d,p)^{4}$He, and ($c$) $^{6}\mathrm{Li} + n \rightarrow {}^{3}\mathrm{H} + {}^{4}\mathrm{He} + Q$.

11-47. (a) Find the Q value for the reaction $^{3}\mathrm{H} + {}^{1}\mathrm{H} \rightarrow {}^{3}\mathrm{He} + n + Q$. ($b$) Find the threshold for this reaction if stationary ^{1}H nuclei are bombarded with ^{3}H nuclei from an accelerator. (c) Find the threshold for this reaction if stationary ^{3}H nuclei are bombarded with ^{1}H nuclei from an accelerator.

11-48. What is the compound nucleus for the reaction of deuterons on ^{14}N? What are the possible product nuclei and particles for this reaction?

11-49. Using data from Appendix A, compute the Q value for the reaction (a) ^{12}C$(\alpha,p)^{15}$N, and (b) ^{16}O$(p,d)^{17}$O.

11-50. The cross section for the reaction ^{75}As$(n, \gamma)^{76}$As is 4.5 b for thermal neutrons. A sample of natural As in the form of a crystal 1 cm $\times$ 2 cm that is 30 μm thick is exposed to a thermal neutron flux of 0.95×10^{13} neutrons/cm$^2 \cdot$ s. Compute the rate at which this reaction proceeds. (Natural arsenic is 100% ^{75}As. Its density is 5.73 g/cm^3.)

11-51. Write three different reactions that could produce the products (*a*) $n + {}^{23}\mathrm{Na}$, (*b*) $p + {}^{14}\mathrm{C}$, and (*c*) $d + {}^{31}\mathrm{P}$.
11-52. Write down the correct symbol for the particle or nuclide represented by the x in the following reactions: (*a*) ${}^{14}\mathrm{N}(n, p)\,x$; (*b*) ${}^{208}\mathrm{Pb}\,(n, x){}^{208}\mathrm{Pb}$; (*c*) $x(\alpha, p){}^{61}\mathrm{Cu}$; (*d*) ${}^{9}\mathrm{Be}(x, n){}^{12}\mathrm{C}$; (*e*) ${}^{16}\mathrm{O}(d, \alpha)x$; (*f*) ${}^{162}\mathrm{Dy}(\alpha, 6n)x$; (*g*) $x(d, n){}^{4}\mathrm{He}$; (*h*) ${}^{90}\mathrm{Zr}(d, x){}^{91}\mathrm{Zr}$.

Section 11-8 Fission and Fusion

11-53. A few minutes after the Big Bang the first fusion reaction occurred in the early universe. It was $n + p \rightarrow d + \gamma$. Compute the Q for this reaction.
11-54. Assuming an average energy release of 200 MeV per fission, calculate the number of fissions per second needed for a 500-MW reactor.
11-55. If the reproduction factor of a reactor is $k = 1.1$, find the number of generations needed for the power level to (*a*) double, (*b*) increase by a factor of 10, and (*c*) increase by a factor of 100. Find the time needed in each case if (*d*) there are no delayed neutrons, so the time between generations is 1 ms, and (*e*) there are delayed neutrons that make the average time between generations 100 ms.
11-56. Write down the several reactions possible when ${}^{235}\mathrm{U}$ captures a thermal neutron and $1n$, $2n$, $3n$, or $4n$ is produced.
11-57. Assuming an average energy release of 17.6 MeV/fusion, calculate the rate at which ${}^{2}\mathrm{H}$ must be supplied to a 500-MW fusion reactor.
11-58. From Figure 11-52, the cross section for the capture of 1.0-MeV neutrons by ${}^{238}\mathrm{U}$ is 0.02 b. A 5-gm sample of ${}^{238}\mathrm{U}$ is exposed to a total flux of 1.0-MeV neutrons of 5.0×10^{11} per m^2. Compute the number of ${}^{239}\mathrm{U}$ atoms produced.
11-59. Compute the total energy released in the following set of fusion reactions. This is the proton-proton cycle, the primary source of the sun's energy.

$$
\begin{aligned}
{}^{1}\mathrm{H} + {}^{1}\mathrm{H} &\longrightarrow {}^{2}\mathrm{H} + e^{+} + \nu_e \\
{}^{2}\mathrm{H} + {}^{1}\mathrm{H} &\longrightarrow {}^{3}\mathrm{He} + \gamma \\
{}^{3}\mathrm{He} + {}^{3}\mathrm{He} &\longrightarrow {}^{4}\mathrm{He} + 2{}^{1}\mathrm{H} + \gamma
\end{aligned}
$$

11-60. A particular nuclear power reactor operates at 1000 MWe (megawatts electric) with an overall efficiency in converting fission energy to electrical energy of 30 percent. What mass of ${}^{235}\mathrm{U}$ must fission in order for the power plant to operate for (*a*) one day, (*b*) one year? (*c*) If the energy were provided by burning coal instead of ${}^{235}\mathrm{U}$, what would be the answers to (*a*) and (*b*)? (Burning coal produces approximately 3.15×10^7 J/kg.)
11-61. (*a*) Assuming that the natural abundance of deuterium given in Appendix A is reflected in the formation of water molecules, compute the energy that would be released if all the deuterons in 1.0 m^3 of water were fused via the reaction ${}^{2}\mathrm{H} + {}^{1}\mathrm{H} \rightarrow {}^{3}\mathrm{He} + \gamma$. (*b*) Given that the world's 5.9×10^9 people used 3.58×10^{20} J in 1999, how long (in hours) would the result in part (*a*) have lasted a "typical" person?
11-62. Consider the possible fission reaction

$$n + {}^{235}_{92}\mathrm{U} \longrightarrow {}^{120}_{48}\mathrm{Cd} + {}^{112}_{44}\mathrm{Ru} + 3n$$

(*a*) Compute the energy released in the reaction. (*b*) Is this reaction likely to occur? Explain.

Section 11-9 Applications

11-63. A bone claimed to be 10,000 years old contains 15 g of carbon. What should the decay rate of ${}^{14}\mathrm{C}$ be for this bone?
11-64. A sample of animal bone unearthed at an archeological site is found to contain 175 g of carbon, and the decay rate of ${}^{14}\mathrm{C}$ in the sample is measured to be 8.1 Bq. How old is the bone?
11-65. The ${}^{87}\mathrm{Rb}/{}^{87}\mathrm{Sr}$ ratio for a particular rock is measured to be 36.5. How old is the rock?
11-66. In a PIXE experiment, an element with $A = 80$ forms 0.001 percent by weight of a thin foil whose mass is 0.35 mg/cm^2. The foil is bombarded with a 250 nA proton beam for 15 minutes. The cross section for exciting the L shell is 650 b. If the probability that the excited atom will emit an L x ray is 0.60 and the overall efficiency of the x-ray detector is 0.0035, how many counts will the detector record during the 15-minute bombardment?

11-67. The naturally occurring $A = 4n$ decay series begins with ^{232}Th and eventually ends on ^{208}Pb. (See Figure 11-18.) A particular rock is measured to contain 4.11 g of ^{232}Th and 0.88 g of ^{208}Pb. Compute the age of the rock.

11-68. Compute the resonance frequency of free protons in a magnetic field of (*a*) 0.5×10^{-4} T (approximate strength of Earth's field), (*b*) 0.25 T, and (*c*) 0.5 T.

11-69. A small piece of papyrus is to be ^{14}C-dated using AMS. During a 10-minute run with the system set to record ^{14}C, 1500 ions are counted. With the system set to transmit $^{12}C^{+3}$ ions, the beam current is 12 μA. (*a*) Compute the $^{14}C/^{12}C$ ratio, assuming both isotopes are transmitted with the same efficiency. (*b*) If the entire sample is consumed in 75 minutes, what was the mass of ^{12}C it contained? (Assume a constant consumption rate and an efficiency of 0.015. (*c*) How old is the sample?

11-70. A wooden spear found in the mountains of southeastern Spain was found to have ^{14}C activity of 2.05 disintegrations per minute per gram. How old is it? (The ^{14}C activity of live wood is 15.6 disintegrations per minute per gram.)

Level II

11-71. Using Equation 11-14 and the constants in Table 11-3, find the Z for which $dM/dZ = 0$, i.e., the minimum of curves like Figure 11-22*a* for (*a*) A = 27, (*b*) A = 65, and (*c*) A = 139. Do these calculations give the correct stable isobars ^{27}Al, ^{65}Cu, and ^{139}La?

11-72. An empirical expression for distance that α particles can travel in air, called the *range*, is $R(\text{cm}) = (0.31)E^{3/2}$ for E in MeV and $4 < E < 7$ MeV. (*a*) What is the range in air of a 5-MeV α particle? (*b*) Express this range in g/cm^2, using $\rho = 1.29 \times 10^{-3}$ g/cm^3 for air. (*c*) Assuming the range in g/cm^2 is the same as that of aluminum ($\rho = 2.70$ g/cm^3), find the range in aluminum in cm for a 5-MeV α particle.

11-73. Show that the average electrostatic energy of a proton-proton pair is about $6ke^2/5R$, where R is the separation of the pair and $k = 1/4\pi\epsilon_0$.

11-74. A sample of ^{114}Nd has a mass of 0.05394 kg and emits an average of 2.36 α particles per second. Determine the decay constant and the half-life.

11-75. A sample of radioactive material is found initially to have an activity of 115.0 decays/minute. After 4 d 5 h, its activity is measured to be 73.5 decays/minute. (*a*) Calculate the half-life of this material. (*b*) How long (after $t = 0$) will it take for the sample to reach an activity of 10.0 decays/minute? (*c*) How long after the time in (*b*) will it take for the activity to reach 2.5 decays/minute?

11-76. The half-life of ^{227}Th is 18.72 days. It decays by α emission to ^{223}Ra, an α emitter whose half-life is 11.43 days. A particular sample contains 10^6 atoms of ^{227}Th and no ^{223}Ra at time $t = 0$. (*a*) How many atoms of each type will be in the sample at $t = 15$ days? (*b*) At what time will the number of atoms of each type be equal?

11-77. The Mössbauer effect was discovered using the decay of the 0.12939-MeV second excited state of ^{191}Ir. The lifetime of this isomer is 0.13 ns. (*a*) Compute the width Γ of this level. (*b*) Compute the recoil energy of a free ^{191}Ir atom that emits the 0.12939-MeV photon. (*c*) Resonant (recoilless) absorption occurs when ^{191}Ir is bound into a lattice. If a Doppler shift equal to Γ destroys the resonance absorption, show that the Doppler velocity v necessary is given by

$$v \approx \frac{c\Gamma}{e}$$

11-78. ^{3}He and ^{3}H are a pair of mirror nuclei. Compute the difference in total binding energy between the two nuclides and compare the result to the electrostatic repulsion of the protons in ^{3}He. Let the protons be separated by the radius of the helium nucleus.

11-79. Use the masses in Appendix A to compute the energy necessary to separate a neutron from ^{47}Ca and ^{48}Ca. From those results determine a value for a_5 in the Weizsäcker formula (Equation 11-14) and compare it with the value in Table 11-3.

11-80. The centripetal force of a nucleus with $I \neq 0$ makes it more stable toward α decay. Use Figure 11-1*a* and a (classical) argument to show why this is the case.

11-81. (*a*) Calculate the radii of $^{141}_{56}$Ba and $^{92}_{36}$Kr from Equation 11-4. (*b*) Assume that after the fission of ^{235}U into ^{141}Ba and ^{92}Kr, the two nuclei are momentarily separated by a distance r equal to the sum of the radii found in (*a*), and calculate the electrostatic potential energy for these two nuclei at this separation. Compare your result with the measured fission energy of 175 MeV.

11-82. Consider a neutron of mass m moving with speed v_L and colliding head-on with a nucleus of mass M. (*a*) Show that the speed of the center of mass in the lab frame is $V = mv_L/(m + M)$. (*b*) What is the speed of the nucleus in the center-of-mass frame before the collision? After the collision? (*c*) What is the speed of the nucleus in the original lab frame after the collision? (*d*) Show that the energy of the nucleus after the collision is

$$\frac{1}{2}M(2V)^2 = \left[\frac{4mM}{(m+M)^2}\right]\frac{1}{2}mv_L^2$$

and use this to obtain Equation 11-82.

11-83. Suppose that the Van Dyck painting shown in the photographs on page 537 was irradiated with a thermal neutron flux of 10^{12} neutrons/cm$^2 \cdot$ s for 2 h. In terms of the numbers of manganese and phosphorus atoms initially present, determine the activity (*a*) 2 hours and (*b*) 2 days after the irradiation stopped. The (n, γ) cross section for ^{31}P is 0.180 b and for ^{55}Mn is 13.3 b. (Both isotopes are 100 percent of the naturally occurring elements.)

11-84. The total energy consumed in the United States in 1 y is about 7.0×10^{19} J. How many kilograms of ^{235}U would be needed to provide this amount of energy if we assume that 200 MeV of energy is released by each fissioning uranium nucleus, that 3 percent of the uranium atoms undergo fission, and that all of the energy-conversion mechanisms used are 25 percent efficient?

11-85. The rubidium isotope ^{87}Rb is a β emitter with a half-life of 4.9×10^{10} y that decays into ^{87}Sr. It is used to determine the age of rocks and fossils. Rocks containing the fossils of early animals contain a ratio of ^{87}Sr to ^{87}Rb of 0.010. Assuming that there were no ^{87}Sr present when the rocks were formed, calculate the age of these fossils.

11-86. In 1989, researchers claimed to have achieved fusion in an electrochemical cell at room temperature. They claimed a power output of 4 W from deuterium fusion reactions in the palladium electrode of their apparatus. (*a*) If the two most likely reactions are

$$^2\text{H} + {}^2\text{H} \longrightarrow {}^3\text{He} + n + 3.27\text{ MeV}$$

and

$$^2\text{H} + {}^2\text{H} \longrightarrow {}^3\text{H} + {}^1\text{H} + 4.03\text{ MeV}$$

with 50 percent of the reactions going by each branch, how many neutrons per second would we expect to be emitted in the generation of 4 W of power? (*b*) If 1/10th of these neutrons were absorbed by the body of an 80.0-kg worker near the device, and if each absorbed neutron carries an average energy of 0.5 MeV with an RBE of 4, to what radiation dose rate in rems per hour would this correspond? (*c*) How long would it take for a person to receive a total dose of 500 rems? (This is the dose that is usually lethal to half of those receiving it.)

11-87. Neutron activation analysis is used to study a small sample of automotive enamel found at the scene of a hit-and-run collision. The sample was exposed to a thermal neutron flux of 3.5×10^{12} neutrons/cm$^2 \cdot$ s for 2.0 minutes. Placed immediately in a gamma-ray detector, it was found to have an activity of 35 Bq due to ^{60}Co and 115 Bq due to ^{51}Ti. Compute the total amount of each metal in the original sample. (The cross section for ^{59}Co is 19 b; that for ^{50}Ti is 0.15 b.)

11-88. A fusion reactor using only deuterium for fuel would have the following two reactions taking place in it:

$$^2\text{H} + {}^2\text{H} \longrightarrow {}^3\text{He} + n + 3.27\text{ MeV}$$

and

$$^2\text{H} + {}^2\text{H} \longrightarrow {}^3\text{H} + {}^1\text{H} + 4.03\text{ MeV}$$

The ^{3}H produced in the second reaction reacts immediately with another ^{2}H to produce

$$^3\text{H} + {}^2\text{H} \longrightarrow {}^4\text{He} + n + 17.7\text{ MeV}$$

The ratio of ^{2}H to ^{1}H atoms in naturally occurring hydrogen is 1.5×10^{-4}. How much energy would be produced from 4 liters of water if all of the ^{2}H nuclei undergo fusion?

11-89. (*a*) Using the Compton-scattering result that the maximum change in wavelength is $\Delta\lambda = 2hc/Mc^2$ and the approximation $\Delta E \approx hc\,\Delta\lambda/\lambda^2$, show that for a photon to lose an amount of energy E_p to a proton, the energy of the photon must be at least $E = [(1/2)Mc^2E_p]^{1/2}$.

(b) Calculate the photon energy needed to produce a 5.7-MeV proton by Compton scattering. (c) Calculate the energy given a ^{14}N nucleus in a head-on collision with a 5.7-MeV neutron. (d) Calculate the photon energy needed to give a ^{14}N nucleus this energy by Compton scattering.

11-90. A photon of energy E is incident on a deuteron at rest. In the center-of-mass reference frame, both the photon and the deuteron have momentum p. Prove that the approximation $p \approx E/c$ is good by showing that the deuteron with this momentum has energy much less than E. If the binding energy of the deuteron is 2.22 MeV, what is the threshold energy in the lab for photodisintegration?

Level III

11-91. (a) Compute the binding-energy differences between the two nuclides of the mirror pairs (^{7}Li, ^{7}Be), (^{11}B, ^{11}C), and (^{15}N, ^{15}O). (b) From each value computed in (a), determine a value of the constant a_3 in Equation 11-14. Compare each value and their average with the value given in Table 11-3.

11-92. (a) Differentiate the Weizsäcker empirical mass formula with respect to Z, as in Problem 11-71, and show that the minima of the constant A curves that result, i.e., Z values for the most stable isotopes, are given by

$$Z = \frac{A}{2}\left[\frac{1 + \dfrac{(m_n - m_p)c^2}{4a_4}}{1 + \dfrac{a_3 A^{2/3}}{4a_4}}\right]$$

(a) Determine the atomic number for the most stable nuclides for $A = 29$, 59, 78, 119, and 140. (c) Compare the results in (b) with the data in Appendix A and discuss any differences.

11-93. (a) Use Figure 11-35 to make a diagram like Figure 11-9 for the ground state of ^{11}B. What do you predict for the value of j for this state? (b) The first excited state of ^{11}B involves excitation of a proton. Draw the diagram for this state and predict its j value. (c) The j value for the second excited state is 5/2. Draw a diagram of the nucleons like Figure 11-9 that could account for that value. (d) Repeat parts (a) and (b) for ^{17}O, where the excitation of the first excited state involves a neutron. (e) The j value for the second excited state of ^{17}O is 1/2. Draw a diagram like Figure 11-9 that would explain that value.

11-94. Approximately 2000 nuclides remain to be discovered between the proton and neutron driplines in Figure 11-15b. Consider those that lie on the energy parabola (see Figure 11-22a) for $A = 151$, whose only stable isotope is ^{151}Eu. (a) From the data in Appendix A, draw an accurate diagram of the $A = 151$ parabola showing known nuclides *and* those yet to be discovered between $Z = 50$ and $Z = 71$. (b) Determine where the edges of the driplines lie for $A = 151$, i.e., the lowest mass isotopes for which spontaneous proton or neutron emission becomes possible.

11-95. There are theoretical reasons to expect that a cluster of relatively long-lived nuclides will exist in the neighborhood of the doubly magic nucleus with $Z = 126$ and $N = 184$, the latter being the next magic number beyond 126 predicted by the shell model. (a) Compute the mass of this exotic nucleus using Equation 11-14. (b) Computing the necessary masses of the nearby nuclei, predict the decay modes that would be available to the doubly magic nucleus.

11-96. Assume that a neutron decays into a proton plus an electron without the emission of a neutrino. The energy shared by the proton and electron is then 0.782 MeV. In the rest frame of the neutron, the total momentum is zero, so the momentum of the proton must be equal and opposite that of the electron. This determines the relative energies of the two particles, but because the electron is relativistic, the exact calculation of these relative energies is somewhat difficult. (a) Assume that the kinetic energy of the electron is 0.782 MeV and calculate the momentum p of the electron in units of MeV/c. (*Hint:* Use Equation 2-32.) (b) From your result for (a), calculate the kinetic energy $p^2/2m_p$ of the proton. (c) Since the total energy of the electron plus proton is 0.782 MeV, the calculation in (b) gives a correction to the assumption that the energy of the electron is 0.782 MeV. What percentage of 0.782 MeV is this correction?

11-97. Radioactive nuclei with a decay constant of λ are produced in an accelerator at a constant rate R_p. The number of radioactive nuclei N then obeys the equation $dN/dt = R_p - \lambda N$. (*a*) If N is zero at $t = 0$, sketch N versus t for this situation. (*b*) The isotope ^{62}Cu is produced at a rate of 100 per second by placing ordinary copper (^{63}Cu) in a beam of high-energy photons. The reaction is

$$\gamma + {}^{63}\text{Cu} \longrightarrow {}^{62}\text{Cu} + n$$

^{62}Cu decays by β decay with a half-life of 10 minutes. After a time long enough so that $dN/dt \approx 0$, how many ^{62}Cu nuclei are there?

11-98. The $(4n + 3)$ decay chain begins with ^{235}U and ends on ^{207}Pb. (*a*) How many α decays are there in the chain? (*b*) How many β decays are there? (*c*) Compute the total energy released when one ^{235}U atom decays through the complete chain. (*d*) Assuming no energy escapes, determine the approximate temperature rise of 1 kg of ^{235}U metal over the period of 1 year.

11-99. Energy is generated in the Sun and other stars by fusion. One of the fusion cycles, the proton-proton cycle, consists of the following reactions:

$$^{1}\text{H} + {}^{1}\text{H} \longrightarrow {}^{2}\text{H} + \beta^{+} + \nu_e$$

$$^{1}\text{H} + {}^{2}\text{H} \longrightarrow {}^{3}\text{He} + \gamma$$

followed by either

$$^{3}\text{He} + {}^{3}\text{He} \longrightarrow {}^{4}\text{He} + {}^{1}\text{H} + {}^{1}\text{H}$$

or

$$^{1}\text{H} + {}^{3}\text{He} \longrightarrow {}^{4}\text{He} + \beta^{+} + \nu_e$$

(*a*) Show that the net effect of these reactions is

$$4\,{}^{1}\text{H} \longrightarrow {}^{4}\text{He} + 2\beta^{+} + 2\nu_e + \gamma$$

(*b*) Show that the rest mass energy of 24.7 MeV is released in this cycle, not counting the 2×0.511 MeV released when each positron meets an electron and is annihilated according to $e^{+} + e^{-} \rightarrow 2\gamma$. (*c*) The Sun radiates energy at the rate of about 4×10^{26} W. Assuming that this is due to the conversion of four protons into helium plus γ rays and neutrinos, which releases 26.7 MeV, what is the rate of proton consumption in the Sun? How long will the Sun last if it continues to radiate at its present level? (Assume that protons constitute about half the total mass of the Sun, which is about 2×10^{30} kg.)

11-100. The fusion reaction between ^{2}H and ^{3}H is

$$^{3}\text{H} + {}^{2}\text{H} \longrightarrow {}^{4}\text{He} + n + 17.7\text{ MeV}$$

Using the conservation of momentum and the given Q value, find the final energies of both the ^{4}He nucleus and the neutron, assuming that the initial momentum of the system is zero.

11-101. (*a*) A particular light-water ^{235}U-fueled reactor had a reproduction factor of 1.005 and an average neutron lifetime of 0.08 s. By what percentage will the rate of energy production by the reactor increase in 5 s? (*b*) By what fraction must the neutron flux in the reactor be reduced in order to reduce the reproduction factor to 1.000?

11-102. Compute the reproduction factor for uranium enriched to (*a*) 5 percent and (*b*) 95 percent in ^{235}U. Compute the corresponding fission rate doubling time in each case. Assuming no loss of neutrons and the release of 200 MeV/fission, at what rate will energy be produced in each case 1.0 s after the first fission occurs?

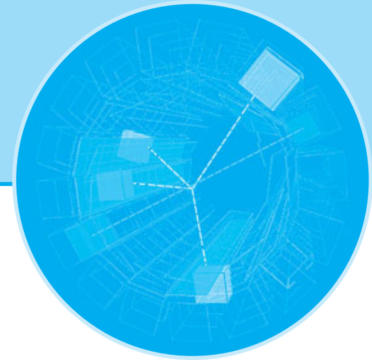

CHAPTER 12

Particle Physics

Notwithstanding the speculations of the ancient Greek natural philosopher Democritus (about 450 BC) and Dalton's atomic theory of matter (1808),[1] the story of particle physics really began with the discovery of the *electron* by Thomson in 1897 (see Section 3-1). That event was followed in 1913 by Rutherford's discovery of the atomic nucleus whose lightest example, that of hydrogen, he named the *proton* (see Section 4-2). As one moved upward through the periodic table of the elements, a dilemma arose, caused by the more-rapid increase of the atomic mass compared to that of the nuclear charge, even though both were presumably due to the protons bound together in the nucleus. That problem was solved in 1932 by Chadwick's discovery of the *neutron* (see Section 11-1). In the meantime Einstein had proposed (in 1905) that Planck's quantization of blackbody radiation was in fact a quite general property of the electromagnetic field (see Sections 3-2 and 3-3). Einstein's suggestion was not widely accepted until, over the next 20 years, Millikan's thorough experimental investigation of the photoelectric effect and Compton's discovery and explanation of the Compton effect provided incontrovertible evidence for the quantization of electromagnetic radiation, the field quantum being a particle we now call the *photon*. For a brief time, it was thought these four were the "elementary" particles from which all matter was formed. But then Anderson discovered the positron, or antielectron, later in 1932. Shortly thereafter, the muon, pion, and many other particles were discovered in searches that have intensified and continued down to the present.

During the past 50 years several nations and international consortia have constructed increasingly larger and more sophisticated particle accelerators capable of producing greater and greater energies with the goals of testing the predictions of current theories and searching for additional particles predicted by them. Initially, an important consideration in such complex experiments, which often involve hundreds of scientists from many nations, was the question of how to tell if a particle is truly elementary or composed of a combination of other particles. For example, both the proton and the neutron were once thought to be elementary, but probing with high-energy (short-wavelength) electron beams revealed that the nucleons have internal structure, just as do atoms and nuclei. Each of the nucleons was found to be a composite particle consisting of three, still more fundamental particles called *quarks*. Several hundred particles have at one time or another been considered to be elementary, but a series of

The construction of large particle accelerators in various countries has, over the years, been an impetus for developing bigger and better superconducting electromagnets. The LHC at CERN has 1232 large, superconducting dipole magnets. High-field, efficient superconducting magnets are used in applications ranging from medical diagnostic magnetic resonance imaging (MRI) systems to magnetically levitated (maglev) trains.

brilliant theoretical achievements over that same 50-year period vastly expanded our understanding of the "particle zoo." The culmination of these achievements is the *Standard Model*, which has been spectacularly successful in explaining and predicting the properties and interactions of particles by describing them in terms of a relatively small number of truly (for now, at least) elementary particles. Research at universities and at the giant accelerator laboratories around the world continues to strengthen our understanding of the structure of matter. In addition to the usual particle properties of mass, charge, and spin, research has unveiled new properties that have no classical analogs, some given whimsical names such as strangeness, charm, and color. Coincident with the construction of the large accelerators has been the development and deployment of larger and more sensitive particle detectors at the big machines and, for neutrinos, detectors deep underground, in the oceans, and buried in the polar ice cap.

In this chapter, we will first look at a few basic concepts that will enable us to classify and describe particles. We will then consider the fundamental interactions between particles and the conservation laws that apply to them. Central to our discussions will be the current theory of elementary particles, the Standard Model, in which all matter in nature—from the most exotic particles produced in the giant accelerator laboratories to ordinary grains of sand—is constructed from just three groups of elementary particles: leptons, quarks, and the particles that mediate interactions between them.

12-1 Basic Concepts

Antiparticles

The Positron In the same year that the neutron was discovered, the positron was discovered (and named) by Carl Anderson.[2] This particle has the same mass and intrinsic angular momentum as the electron but has positive charge; therefore, its intrinsic magnetic moment is parallel, rather than antiparallel, to its spin. It is the antiparticle of the electron and is represented by the symbol e^+, or sometimes in radioactive decay equations by β^+. The existence of the positron had been predicted by Dirac from his relativistic wave equation,[3] though there was some difficulty about the interpretation of this prediction. (See Section 2-4.)

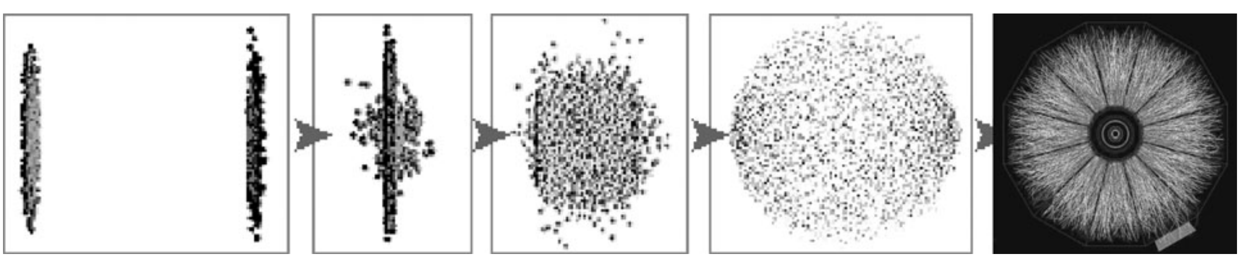

(*a*) (*b*) (*c*) (*d*) (*e*)

The Relativistic Heavy Ion Collider (RHIC) at Brookhaven National Laboratory began colliding gold nuclei (fully ionized gold atoms) late in 2000, with each of the ions moving at 99.99 percent of the speed of light. (*a*) through (*d*) are simulations of the accelerating Au nuclei at several stages. (*a*) Two Lorentz-contracted ions approach each other. (*b*) The collision "melts" the protons and neutrons and (*c*) for an instant releases the quarks and gluons from which the nucleons were formed. (*d*) From the enormous energy of the collision thousands more are created, creating in turn thousands of particles. (*e*) Computer construction of the tracks of the thousands of particles created in a single collision of two gold ions. [*Courtesy Brookhaven National Laboratory, STAR experiment.*]

Air view of the European Laboratory for Particle Physics (CERN) just outside of Geneva, Switzerland. The large circle shows the Large Hadron Collider (LHC) tunnel, which is 27 kilometers in circumference. The irregular dashed line is the border between France and Switzerland (in the foreground). The LHC occupies the tunnel formerly used by the Large Electron-Positron (LEP) collider, which was retired in 2000. The LHC began operations in 2008. [*CERN.*]

The energy of a relativistic particle is given by Equation 2-31:

$$E^2 = (pc)^2 + (mc^2)^2 \tag{2-31}$$

from which we can write

$$E = \pm[(pc)^2 + (mc^2)^2]^{1/2} \tag{12-1}$$

Though we can usually choose the plus sign and ignore the negative-energy solution with a "physical argument," the mathematics of the Dirac equation requires the existence of wave functions corresponding to these negative-energy states. Dirac postulated that all the negative-energy states were filled with electrons. Electrons in the negative-energy states would exert no net force on anything and thus would not be observable. Dirac invoked the exclusion principle to suggest that only holes in this "infinite sea" of negative-energy states would be observable. The holes would act as positive charges with positive energy. Anderson's discovery of a particle with mass identical to that of the electron but with positive charge seemed to indicate that this interpretation was reasonable, since the positron is produced simultaneously with an electron in pair production (see Figure 12-1).

Antiparticles The notion that we are immersed in an infinite sea of negative-energy electrons is an unsettling one, however. It was rendered unnecessary with the development of quantum electrodynamics (QED) by Feynman[4] and others in the late 1940s. The negative energy solutions of the Dirac equation were re-expressed as positive energy solutions of a *new* particle—the positron. And the need for the invisible "sea" of electrons with its mysterious "holes" vanished. However, Dirac's prediction of an anti-electron turned out to be farsighted. QED, whose predictions have been verified to the highest precision of any physical theory, requires that *every* particle must have a corresponding antiparticle with the same mass but opposite electric charge. For example, the theory predicts that protons and neutrons, which are both spin-1/2 particles whose wave functions are solutions of the Dirac equation, should have antiparticles.

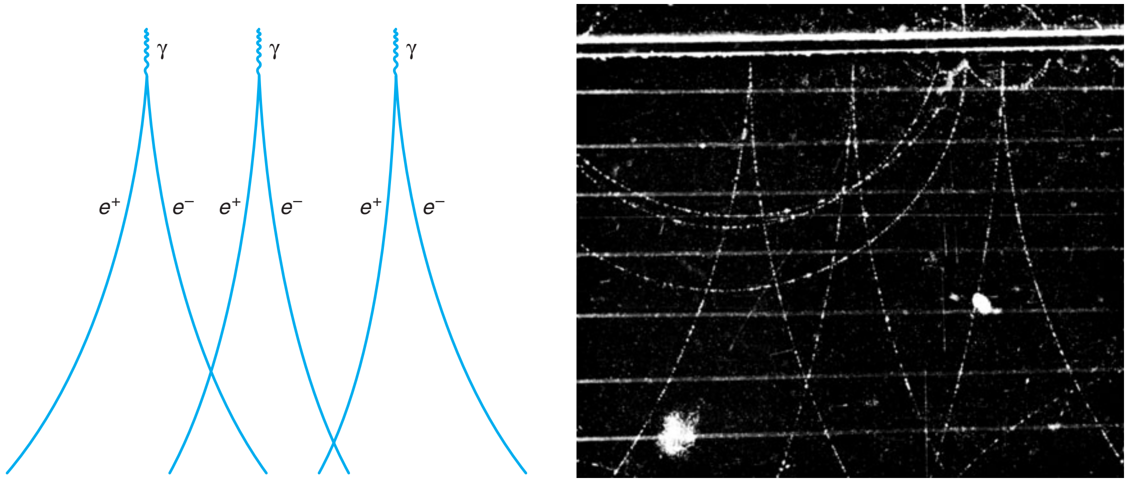

Figure 12-1 Tracks of electron-positron pairs produced by 300-MeV synchrotron x rays at the Lawrence Livermore Laboratory. The magnetic field in the chamber points out of the page. [*Photo courtesy of Lawrence Radiation Laboratory, University of California, Berkeley.*]

The creation of a proton-antiproton pair requires at least $2m_pc^2 = 1877$ MeV, which was not available except in cosmic rays until the development of high-energy accelerators in the 1950s. The antiproton (designated $\overline{p}$) was discovered by Segrè[5] and Chamberlain at Berkeley in 1955 using a beam of protons with kinetic energy 6.2-GeV from the Bevatron particle accelerator. (See Figure 12-2.) The antineutron ($\overline{n}$) (a particle with the same mass as the neutron but with a positive magnetic moment) was discovered two years later. (The standard notation for an antiparticle is the overbar; however, in many cases it is customary to specify the charge instead, as we did for the positron.)

Particles with integral spin, whose wave functions are not solutions of the Dirac equation, also have antiparticles. For example, those with zero spin, which are described by the Klein-Gordon relativistic wave equation (see Equation 11-52), include the pions, thought in the early days (circa 1940) to be the mediating exchange particle, or force carrier, of the nuclear force. In general, an antiparticle has exactly the same mass as the particle but with electric charge, *baryon number*, and *strangeness* (see Section 12-4) opposite in sign to that of the particle.

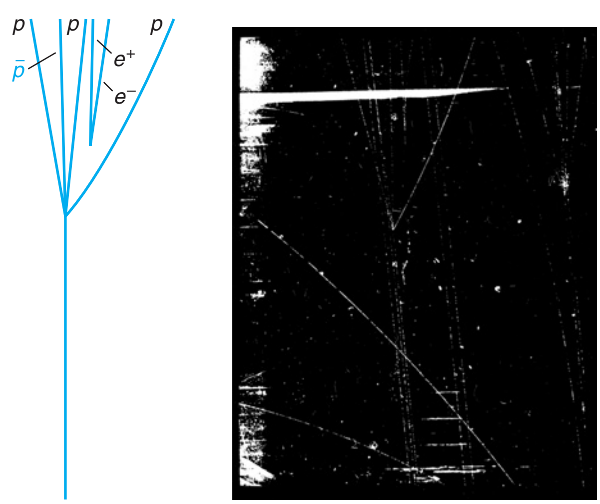

Figure 12-2 Bubble chamber tracks showing creation of proton-antiproton pair in the collision of an incident 25-GeV proton from the Brookhaven Alternating Gradient Synchrotron with a liquid hydrogen nucleus (stationary proton). The reaction is $p + p \rightarrow p + p + p + \overline{p}$. The energy necessary to create the pair is $2m_pc^2 = 1.877$ GeV in the center of mass system. A relativistic calculation in the laboratory frame shows that the beam protons must have at least $6m_pc^2 \approx 5.6$ GeV to reach the reaction threshold. [*Photo courtesy of R. Ehrlich.*]

The tunnel of the proton-antiproton collider at CERN. The same bending magnets and focusing can be used for protons or antiprotons moving in opposite directions. The rectangular box in the foreground is a focusing magnet; the next four boxes are bending magnets. [*CERN.*]

Although the positron is stable, it has only a short-term existence in our universe because of the large supply of electrons in matter. The fate of the positron is annihilation according to the reaction

$$e^+ + e^- \longrightarrow \gamma + \gamma \quad \text{or} \quad e^+ + e^- \longrightarrow \gamma + \gamma + \gamma \qquad \textbf{12-2}$$

Whether bound (as positronium—see Section 2-4) or unbound, annihilation occurs from S states (zero orbital angular momentum), the antiparallel spins ^1S state producing two quanta as on the left in Equation 12-2, the parallel spins ^3S state producing three photons. The fact that we call electrons *particles* and positrons *antiparticles* does not imply that positrons are less fundamental than electrons, but was initially merely an arbitrary choice reflecting the nature of our part of the universe. If our matter were made up of negative protons, positive electrons, and neutrons with positive magnetic moments, then particles such as positive protons, negative electrons, and neutrons with negative magnetic moments would suffer quick annihilation and would probably be called the antiparticles. Antihydrogen atoms (an antiproton and a positron) were first produced "hot" in the antiproton beam at the European Center for Nuclear Research (CERN) in 1995. Subsequently, the CERN ATHENA project has produced substantial amounts of "cold" (slow) antihydrogen and is conducting definitive comparisons of its physical properties with those of hydrogen. The cover of this book illustrates the annihilation of an antihydrogen atom recorded by the ATHENA project. The matter-antimatter asymmetry of the universe, that is, why our universe consists of matter with essentially no antimatter despite the prediction of QED and the symmetry of the relativistic wave equation, is a question we will return to later in this chapter and in Chapter 13.

EXAMPLE 12-1 Proton-Antiproton Annihilation A proton and an antiproton at rest annihilate according to the reaction (standard particle physics notation typically omits the + signs in reaction equations):

$$p\bar{p} \longrightarrow \gamma\gamma$$

Find the energies and wavelengths of the photons.

SOLUTION

Since the proton and the antiproton are at rest, conservation of momentum requires that the two photons created in their annihilation have equal and opposite momenta and therefore equal energies. Since the total energy on the left side of the reaction is $2m_pc^2$, the energy of each photon is

$$E_\gamma = m_pc^2 = 938 \text{ MeV}$$

The wavelength is

$$\lambda = \frac{c}{f} = \frac{hc}{hf} = \frac{hc}{E_\gamma} = \frac{1240 \text{ eV} \cdot \text{nm}}{9.38 \times 10^8 \text{ eV}} = 1.32 \times 10^{-15}\text{m} = 1.32 \text{ fm}$$

Feynman Diagrams

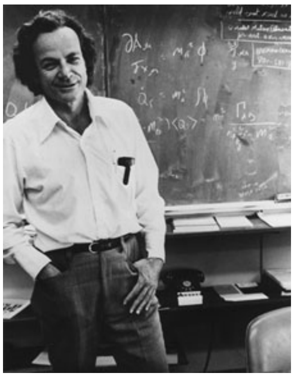

Richard Feynman, who called himself a "curious character," shared the 1965 Nobel Prize in Physics for his contributions to the development of quantum electrodynamics. [*American Institute of Physics, Emilio Segrè Visual Archives, Physics Today Collection.*]

As a part of quantum electrodynamics Feynman developed a wonderfully clear yet powerful technique for describing all electromagnetic phenomena. Like QED itself, the technique of *Feynman diagrams* is so good that it is used as a model by other quantum field theories, notably quantum chromodynamics (QCD), which we will discuss in Section 12-4. The detailed rules for drawing Feynman diagrams are directly related to the equations of QED and are beyond the scope of our discussions here; however, a brief description of a simplified version of the diagrams and a few basic rules will be ample for our use in illustrating the phenomena of interest in this chapter. (For a more complete discussion of Feynman diagrams refer to D. J. Griffith, Chapter 2, cited in the General References section.)

Feynman diagrams are spacetime diagrams, that is, *ct* versus *x* graphs, similar to those developed and used in Chapters 1 and 2. In particle physics Feynman diagrams are used to describe interactions at the level of quarks, leptons, and the mediators of the interactions and to compute lifetimes and cross sections for events. As noted in Figure 11-28, where a Feynman-like diagram was used to illustrate the early view of the π meson as the mediator of the nuclear force, the *ct* and *x* axes are normally not drawn. In this chapter, as in the earlier relativity chapters, time (*ct*) is positive upward. (Particle physicists often draw the diagrams with time flowing horizontally toward the right; there is no convention.) Particles are represented by straight lines with an arrow. A particle line whose arrow points backward in time is interpreted as the corresponding antiparticle moving forward in time. The arrows allow us to omit the overbars in the diagrams. The lines are symbolic and do *not* represent the particle trajectories. The rules for analyzing the diagrams, the details of which are beyond the scope of our discussions, force conservation of energy and momentum at each vertex. It is the *interactions* that we are interested in describing. Particles that are their own antiparticles, like the photon, have no arrows and are represented by wiggly or broken lines of various sorts. All electromagnetic phenomena can be represented by combinations of the process illustrated in Figure 12-3, called the *primitive vertex*. Interactions occur at the vertices. This diagram is read as follows: a moving charged particle enters, emits (or absorbs) a photon, and leaves. The primitive vertex is not itself a complete Feynman diagram, but rather the basic unit from which complete diagrams are constructed.

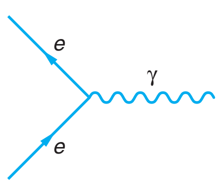

Figure 12-3 The primitive vertex of the Feynman diagram. The particle, shown as an electron, could be a proton or any other particle that feels the electromagnetic force. Note that the photon line has no arrow. The primitive vertex should be thought of as a "building block," combinations of which form complete Feynman diagrams.

Let's examine the Feynman diagrams for a few familiar events. In Figure 12-4*a*, two electrons enter, exchange a photon, and then leave. That is Coulomb repulsion of like charges.[6] Figure 12-4*b* represents Coulomb attraction of opposite charges. These serve to illustrate one more rule: Particle lines that both begin and end within the diagram are *virtual particles*, that is, like Yukawa's exchange pion in Section 11-5, they are not, indeed, cannot be observed in the laboratory. Note that a virtual particle need not have the same mass as the corresponding real particle; it is energy and momentum that are conserved at vertices, not mass. Only lines that enter or leave the diagram represent real, observable particles, and these do, of course, have the proper mass. The diagram makes clear why we say that the electromagnetic force is *mediated* by photons.

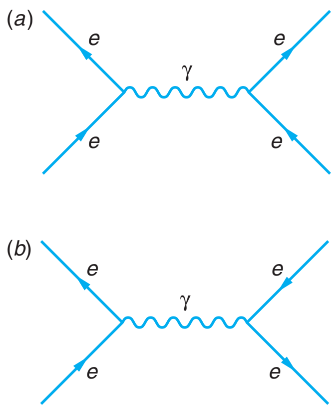

Figure 12-4 Feynman diagrams describing (*a*) Coulomb repulsion of charges of the same sign and (*b*) Coulomb attraction between charges of opposite signs.

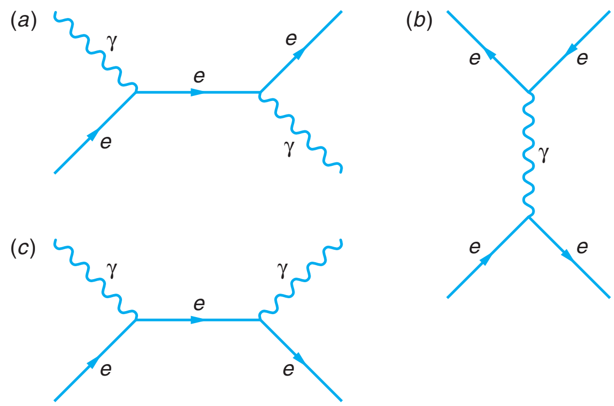

Figure 12-5 (*a*) The Compton effect. A photon enters and is absorbed by an electron, which then emits a photon and leaves. (Note that time, *ct*, is positive to the right in this diagram.) (*b*) At the lower vertex an electron and a positron enter and annihilate, producing a photon. At the upper vertex the photon creates a particle-antiparticle pair. (*c*) Another possible pair annihilation process.

Figure 12-5*a* illustrates Compton scattering. Figure 12-5*b* is another diagram that describes electron-positron scattering (Coulomb attraction) and includes both pair production (upper part) and pair annihilation (lower part). This points up the fact that there may be many diagrams representing any given reaction.[7] For example, Figure 12-5*c* is also a possible pair annihilation. With this introduction we will now use simple Feynman diagrams throughout the remainder of this chapter to visualize interactions that might otherwise be very difficult to understand.

EXAMPLE 12-2 Feynman Diagram of Particle-Antiparticle Creation In Section 2-4 we described the production of an electron-positron pair. Construct a Feynman diagram that illustrates this process.

SOLUTION

Consider the primitive vertex as an electron-photon interaction as below, left. Using the rules outlined above and noting that the now virtual electron exists for too short a time to be measured, we draw its line horizontal, i.e., with $\Delta(ct) = 0$. The positron interacts with a photon at the second primitive vertex. Together the two diagrams depict the creation of an electron-positron pair.

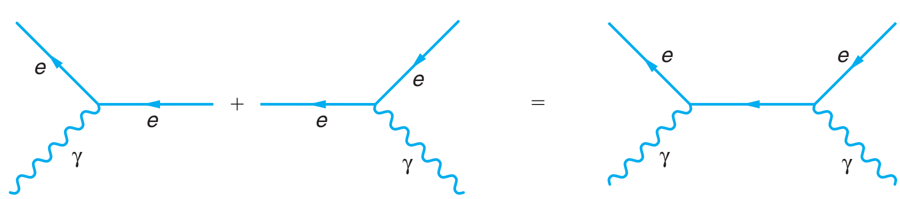

Other, so-called higher-order diagrams representing pair production are also possible. Can you draw one?

Questions

1. What problem might arise in using Dirac's filled infinite sea of negative energy states to explain the existence of particle-antiparticle pairs of pions, whose spins are zero?
2. Why do electron-positron pairs annihilate mainly from *S* states?

Leptons and Quarks

Since Thomson discovered the electron, theoretical and experimental research in particle physics has revealed the existence of 62 fundamental particles and antiparticles, fundamental in the sense that they have no internal structure, as far as we can tell with current technology. This is not to say that this is all that exist. In fact, an important task of CERN's Large Hadron Collider is to search for the predicted Higgs boson, which may be the key to explaining the origin of mass, and to test current theoretical predictions of supersymmetry (SUSY) that suggest the existence of a "superpartner" for each of the known fundamental particles (see Section 12-5).

Many particles with electric charge were first "seen" in the particle detectors of experimental searches. The existence of many electrically neutral particles was deduced indirectly by applying conservation laws, particularly energy and momentum, to interactions that included charged particles recorded by particle detectors. Still others, both charged and neutral, remain unseen directly or indirectly. These are the *quarks* and the force carriers that bind them together, the *gluons*. Nevertheless, we are confident of their existence because their properties and interactions are so successfully explained by the Standard Model of particle physics, which is second only to QED in the precision of its predictions. We will be discussing the Standard Model and its relation to the fundamental interactions and conservation laws throughout the rest of this chapter. In this section we will introduce the classifications of the quarks and leptons in *generations* (or *families*) and *flavors* and list a few of their physical properties. Once you are familiar with general characteristics, we will discuss their properties and interactions more thoroughly.

Leptons There are three generations of leptons,[8] each consisting of a charged lepton and its related neutrino, as shown in Table 12-1. The electron is the most familiar of the charged leptons and the only one that is stable. Each charged lepton has a distinct antiparticle. The Standard Model assigns each lepton a *weak isospin* T_z, the z component of a quantum-mechanical property represented by the vector $\mathbf{T}$ that is loosely analogous to spin (see Section 12-3). For each neutrino there is also an antineutrino, although at this point in time it is possible that the two are not distinct; that is, each neutrino may be its own antiparticle (a so-called Majorana neutrino), much as the photon is its own antiparticle. Investigating that possibility is an active area of current research. Unlike the quarks, as we will see, there are no lepton-lepton bound states. We also refer to leptons as having three flavors: electron, muon, and tau. We will use this terminology in Section 12-5 in a discussion of neutrino mass.

Quarks As with leptons, there are six quarks grouped into three generations. All have fractional electric charge and distinct antiparticles. As we will learn in the following sections, it is the quarks and antiquarks that bind together in a multitude of ways to form more than 200 particles, accounting for the vast majority of the visible mass of the universe. The bound states of the quarks and antiquarks are called *hadrons* (from

Table 12-1 The leptons

	Lepton l	Symbol	Charge (e)	Weak isospin T_z	Mass (MeV/c^2)	Lifetime (s)	Spin ($\hbar$)
1st generation	electron	e	-1	$-1/2$	0.5110	stable	1/2
	electron neutrino	ν_e	0	1/2	≤ 2.2 eV/c^2	stable	1/2
2nd generation	muon	μ	-1	$-1/2$	105.659	2.197×10^{-6}	1/2
	muon neutrino	ν_μ	0	1/2	≤ 3.5 eV/c^2	stable	1/2
3rd generation	tau	τ	-1	$-1/2$	1,784	3.3×10^{-13}	1/2
	tau neutrino	ν_τ	0	1/2	≤ 8.4 eV/c^2	stable	1/2

the Greek *hadros*, meaning "robust"). There are two subgroups of hadrons. Three-quark combinations are called *baryons* (from the Greek *barys*, meaning "heavy"), of which the proton and neutron are the two most common examples. Quark-antiquark pairs form the *mesons*. The term *meson*, derived from the Greek *mesos*, meaning "middle," was chosen because the first mesons discovered (the pions) had masses intermediate between those of the electron and the proton; however, many mesons heavier than the proton were subsequently discovered, so the name is no longer an indicator of the masses of these hadrons. For reasons we will discuss in Section 12-4, single, or "free" quarks have not been nor seem likely to be observed. The recently reported five-quark combination has not been independently confirmed. Table 12-2 records basic descriptions of the quarks.

Each quark in the table also has an additional property, analogous to electric charge, called *color*, or *color charge*. Color has three possible values: *red*, *blue*, and *green*. So, for example, there are three different u quarks: u_r, u_b, and u_g. The antiquarks have anticolor, just as they have opposite electric charge, so the three anti-u quarks are the $\bar{u}_{\bar{r}}$, $\bar{u}_{\bar{b}}$, and $\bar{u}_{\bar{g}}$. Of course, these terms have nothing to do with the usual meanings of the words *color*, *red*, *blue*, and *green*. They are simply labels that are used to describe a particular

Table 12-2 The quarks

	Quark (q)	Symbol	Charge (e)	Weak isospin T_z	Mass (MeV/c^2)	Spin ($\hbar$)	Baryon number
1st generation	up	u	2/3	1/2	336	1/2	1/3
	down	d	$-1/3$	$-1/2$	338	1/2	1/3
2nd generation	charm	c	2/3	1/2	1,500	1/2	1/3
	strange	s	$-1/3$	$-1/2$	540	1/2	1/3
3rd generation	top	t	2/3	1/2	170,900	1/2	1/3
	bottom	b	$-1/3$	$-1/2$	5,000	1/2	1/3

quantum-mechanical property of the particles, a choice that will turn out, perhaps unexpectedly, to be very convenient (see Section 12-4). Like electric charge, color charge is conserved. Quarks with $2e/3$ electric charge (see Table 12-2) are *up-type quarks* (up, charm, and top), and those with $-e/3$ are referred to as *down-type quarks* (down, strange, and bottom). As with the leptons, the Standard Model also assigns each quark a weak isospin T_z. The up-type quarks have $T_z = 1/2$; the down-type quarks have $T_z = -1/2$. Notice in Table 12-2 that each of the quark generations is an isospin doublet. The Standard Model provides for an equal number of lepton and quark generations, as you see are contained in Tables 12-1 and 12-2. We refer to the quarks as having six flavors; e.g., the down quark and antiquark are of the "down flavor." Altogether, Table 12-2 represents 36 quarks and antiquarks. Like the leptons, the quarks are all fermions.

12-2 Fundamental Interactions and the Force Carriers

All the different forces observed in nature, from ordinary friction to the tremendous forces involved in supernova explosions, can be understood in terms of the four basic interactions that occur among elementary particles. In order of decreasing strength, these are

1. The strong interaction
2. The electromagnetic interaction
3. The weak interaction
4. The gravitational interaction

Molecular forces and most of the everyday forces that we observe between macroscopic objects (for example, friction, contact forces, and forces exerted by springs and strings) are complex manifestations of the electromagnetic interaction, which occurs between all particles that carry electric charge. Although gravity, the interaction between all particles with mass, plays an important role in our lives, it is so weak compared with other forces that its role in the interactions between elementary particles is essentially negligible. The weak interaction acts between particles that carry *weak charge* and describes, among others, the interaction between electrons or positrons and nucleons that results in beta decay, which we discussed in Chapter 11. The strong interaction acts between particles that carry color charge and describes, for example, the force between nucleons that holds nuclei together. Some particles participate in all four interactions, whereas others participate in only some of them.

In 1979, S. L. Glashow, A. Salam, and S. Weinberg shared the Nobel Prize in Physics for development of the *electroweak theory*, successfully unifying theories of the electromagnetic and the weak interactions. This event, which came exactly 100 years after Maxwell had accomplished unification of the theories of electricity and magnetism, was a major advance toward achieving unification of the theoretical descriptions of the four basic interactions. Developing such a unified field theory has been a goal of physics for a long time, one that was vigorously sought without success by Einstein, among many others. As we will discuss in Section 12-4, the electroweak unification occurs only at high particle energies. Current efforts to unify the electroweak, strong, and gravitational interaction will be discussed in Section 12-5.

The term "strength" of the interactions refers specifically to the relative magnitudes of the dimensionless *coupling constants*[9] that multiply the fundamental space-dependent part of the potential energy function whose gradient determines the particular force.

The relative strengths stated in the paragraphs below and in Table 12-4 are only approximate as there is no unambiguous method of comparison, particularly for the weak interaction. As an example, the electric (Coulomb) potential energy of two charges is $U(r) = -(1/4\pi\epsilon_0)e^2/r$. The multiplier of the space-dependent function $1/r$ is made dimensionless by dividing both sides of the equation by the quantity $\hbar c$:

$$V(r) = U(r)/\hbar c = -\frac{e^2}{4\pi\epsilon_0 \hbar c}\frac{1}{r} \qquad \textbf{12-3}$$

where $V(r)$ is in m^{-1}. The quantity $(e^2/4\pi\epsilon_0\hbar c)$ you will recognize as the fine-structure constant $\alpha \approx 1/137$, first encountered in our discussion of Bohr's model of the hydrogen atom (see Section 4-3). The fine-structure constant is thus the coupling constant of the electromagnetic interaction. As we discovered in Chapter 4, energies resulting from this interaction are proportional to α^2 and characteristic dimensions (e.g., the Bohr radius a_0) are proportional to $1/\alpha$. (See Equations 4-32 and 4-33.) Moreover, the probability densities for atomic phenomena discussed in Chapter 7 are all directly dependent on the value of α. (See Equation 7-32.)

Just as Yukawa postulated the pion as the mediator, or carrier, of the force between nucleons (see Section 11-5), the Standard Model postulates one or more particles as the force carrier, or mediator, of each fundamental interaction. Each of these mediators, all of which the theory requires to be bosons, will be introduced in the following paragraphs, concerned with each of the interactions.

Strong Interaction

All hadrons interact via the strong interaction. Of the two subgroups of hadrons, baryons (the three-quark combinations) have 1/2-integral spins (1/2, 3/2, 5/2, etc.). Mesons (the two-quark combinations) have zero or integral spins. The range of the strong force is about 10^{-15} m, or one fm. (See Chapter 11.) The coupling constant α_s of the strong interaction is approximately 1, or about 10^2 larger than the fine-structure constant α of the electromagnetic force. Within the framework of the Standard Model, the strong force is due to color charge, analogous to the electromagnetic force being due to electric charge. The mediator of the strong force is the *gluon*. Like the quarks, the gluons carry color charge, but with a difference. Each quark carries one unit of one of the three color charges, but each gluon carries one unit of one of the three color charges *and* one unit of one of the three anticolor charges. Since there are nine possible combinations of r, b, and g with $\bar{r}$, $\bar{b}$, and $\bar{g}$, we expect nine different gluons; however, a technicality reduces that number to eight. One consequence of color-charged gluons is that the emission of a gluon by a quark can change the color (but not the flavor) of the quark. Another is that gluons can couple to other gluons (see Section 12-3). Since leptons don't carry color charge, they don't participate in the strong interaction. Note, too, that the photon, the electromagnetic interaction's counterpart to the gluon, does not carry electric charge.

The characteristic *interaction time* of the strong interaction is extremely short, only about 10^{-23} s, meaning that an event caused by this interaction "happens" in this length of time. Thus, if the probability is to be high that two particles will interact via the strong force by exchanging a virtual particle, the two must remain within the range of the force for at least 10^{-23} s. Similarly, particles that change into another particle or particles, that is, decay due to the action of the strong force, do so within about 10^{-23} s. This is about the time it takes light to travel a distance equal to the diameter of a nucleus.

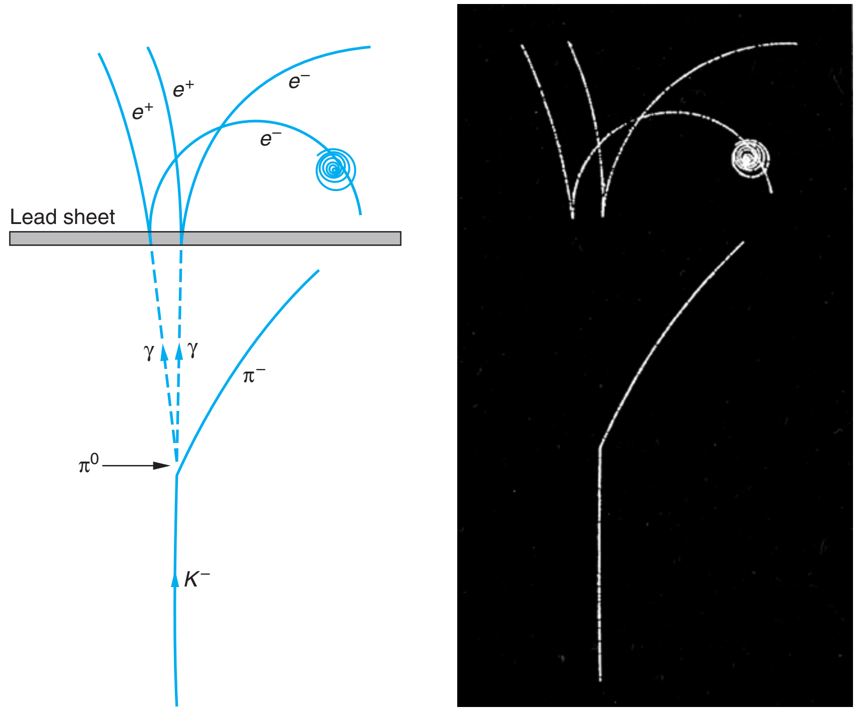

A negative kaon (K^-) enters a bubble chamber from the bottom and decays into a π^-, which moves off to the right, and a π^0, which immediately decays into two photons, whose paths are indicated by the dashed lines in the drawing. Each photon interacts in the lead sheet, producing an electron-positron pair. The spiral at the right is an electron that has been knocked out of an atom in the chamber. (Other, extraneous tracks have been removed from the photograph.)

Table 12-3 lists some of the properties of the hadrons that are stable against decay via the strong interaction, that is, those with lifetimes significantly longer than 10^{-23} s. Those that decay via the electromagnetic and weak interactions have much longer lifetimes, typically of the order of 10^{-18} s and 10^{-10} s, respectively. Note that all baryons ultimately decay to a proton. Note, too, that the baryons cluster into "charge multiplets" of about the same mass: the nucleons (n and p) of mass about 939 MeV, the Λ of mass about 1116 MeV, the Σ particles of mass about 1190 MeV, the Ξ particles of mass about 1315 MeV, and the Ω of mass 1672 MeV. The differences in masses within multiplets (such as between the neutron and proton) are due primarily to differences in the masses of the constituent quarks (see Section 12-4). The energy of the electromagnetic field also makes a contribution to the mass differences. There are six mesons in Table 12-3: three pions, two kaons, and the eta particle. The mesons also cluster into charge multiplets. As with the baryons, the mass differences within each multiplet are due primarily to the mass differences of the constituent quarks. Note that the mass of the π^+ is exactly equal to that of the π^-, as it must be since these particles are antiparticles of each other.

Being complex particles composed of other, more fundamental particles (quarks), the hadrons each have a ground state and a set of quantized excited states directly analogous to the allowed energy levels of atoms and nuclei, which are of course also complex particles composed of other, more fundamental particles. These excited hadron states usually decay via the strong interaction and thus have large energy widths, as

Table 12-3 Hadrons that are stable against decay via the strong interaction

Name	Symbol	Mass (MeV/c^2)	Spin ($\hbar$)	Charge (e)	Antiparticle	Mean lifetime(s)	Typical decay products†
Baryons							
Nucleon	p (proton) or N^+	938.3	1/2	+1	p^-	$>10^{32}$ y	
	n (neutron) or N^0	939.6	1/2	0	$\bar{n}$	930	$p + e^- + \bar{\nu}_e$
Lambda	Λ^0	1116	1/2	0	$\overline{\Lambda}^0$	2.5×10^{-10}	$p + \pi^-$
Sigma	Σ^+	1189	1/2	+1	$\overline{\Sigma}^-$	0.8×10^{-10}	$n + \pi^+$
	Σ^0	1193	1/2	0	$\overline{\Sigma}^0$	10^{-20}	$\Lambda^0 + \gamma$
	Σ^-	1197	1/2	−1	$\overline{\Sigma}^+$	1.7×10^{-10}	$n + \pi^-$
Xi*	Ξ^0	1315	1/2	0	$\overline{\Xi}^0$	3.0×10^{-10}	$\Lambda^0 + \pi^0$
	Ξ^-	1321	1/2	−1	$\overline{\Xi}^+$	1.7×10^{-10}	$\Lambda^0 + \pi^-$
Omega	Ω^-	1672	3/2	−1	Ω^+	1.3×10^{-10}	$\Xi^0 + \pi^-$
Charmed lambda	Λ_c^+	2285	1/2	+1	$\overline{\Lambda}_c^-$	1.8×10^{-13}	$p + K^- + \Lambda^+$
Mesons							
Pion	π^+	139.6	0	+1	π^-	2.6×10^{-8}	$\mu^+ + \nu_\mu$
	π^0	135	0	0	self	0.8×10^{-16}	$\gamma + \gamma$
	π^-	139.6	0	−1	π^+	2.6×10^{-8}	$\mu^- + \bar{\nu}_\mu$
Kaon	K^+	493.7	0	+1	K^-	1.24×10^{-8}	$\pi^+ + \pi^0$
	K^0	497.7	0	0	$\overline{K}^0$	0.88×10^{-10}	$\pi^+ + \pi^-$
						and 5.2×10^{-8}‡	$\pi^+ + e^- + \bar{\nu}_e$
Eta	η^0	549	0	0	self	2×10^{-19}	$\gamma + \gamma$

† Other decay modes also occur for most particles.

‡ The K^0 has two distinct lifetimes, sometimes referred to as K^0_{short} and K^0_{long}. All other particles have a unique lifetime.

* The Ξ particle is sometimes called the cascade.

required by the uncertainty principle ($\Delta E \approx \hbar/\Delta t$) and in contrast to the much slower atomic transitions and nuclear decays. Excited hadron states are usually observed as resonances in the cross section for scattering of one hadron on another and are therefore also called *resonance particles*. We describe resonance particles more thoroughly on the home page (see page 591).

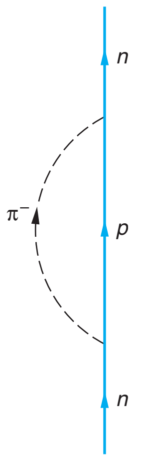

Figure 12-6 A neutron emits a virtual π^-. During the time Δt that the positive proton and the π^- exist, they can interact with other charged particles. After time Δt the π^- is reabsorbed by the proton.

Electromagnetic Interaction

This is the dominant interaction at scales larger than subatomic, the realm of the strong interaction, and smaller than astronomical, where the gravitational interaction rules. All particles that carry electric charge or have a magnetic moment participate in the electromagnetic interaction. In addition, neutral particles without magnetic moments may also participate in the interaction if the emission of virtual particles results in charged particles. A neutron emitting and reabsorbing a virtual π^- as shown in Figure 12-6 is an example of a neutral particle involved in an electromagnetic interaction. The range of the electromagnetic force is infinite, and its strength is about $1/137$ times that of the strong interaction, as we discussed earlier. Its characteristic interaction time is about 10^{-18} s. According to QED, the mediator of the electromagnetic force is the photon. In contrast to the gluon, the photon does not carry electric charge. Decays via the electromagnetic interaction generally result in the emission of one or more photons, although there are a few exceptions, e.g., $\pi^0 \longrightarrow e^+e^-$. Notice in Table 12-3 that the Σ^0, π^0, and η^0 decay via the electromagnetic interaction.

Weak Interaction

All quarks and leptons participate in the weak interaction. The range of the weak force is about 10^{-18} m or about 10^{-3} fm, considerably smaller than that of the strong force. Example 12-3 shows how the range of the weak force is determined. Its characteristic interaction time varies from about 10^{-16} s to about 10^{-10} s. No particular name is given to the source of the weak force, although it is occasionally called the *weak charge* or *flavor charge*, in analogy with electric charge. The strength of the weak interaction relative to the strong interaction is about 10^{-5}. The weak force is carried by three particles, the *charged weak force* by the W^+ and W^- (W for "weak") and the *neutral weak force* by the Z^0 (Z for "zero"). All three have spin 1 and thus are bosons. A very important aspect of the weak force is that interactions mediated by the $W^\pm$ turn one quark flavor into another. The weak interaction does not, however, change the lepton flavor. The mediation of three typical weak interactions, the scattering of a muon neutrino by an electron, the scattering of an electron neutrino and a muon, and the inverse beta decay of a proton are illustrated in Figure 12-7.

The need to transfer rapidly enormous volumes of data collected by detectors at the major particle physics laboratories throughout the world to the thousands of collaborating scientists in many countries led to the development of the World Wide Web at CERN.

The mediators of the weak interaction were all discovered in 1983 by C. Rubbia and a large international team of co-workers after a long search using the $p\overline{p}$ collider

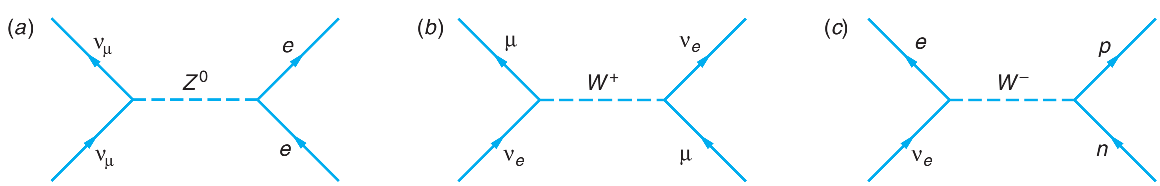

Figure 12-7 (a) The scattering of a muon neutrino from an electron involves the exchange of a Z^0. Such an exchange is called a *neutral current* interaction. The interaction does not convert the electron into a muon neutrino. (b) The scattering of an electron neutrino from a muon may also occur via a neutral current interaction as in (a), but a *charged current* interaction in which a charged W is exchanged is also possible, and both would contribute to the cross section. Measuring the cross sections thus provides a means of testing the standard model. (c) Inverse beta decay also proceeds via a *charged current* interaction.

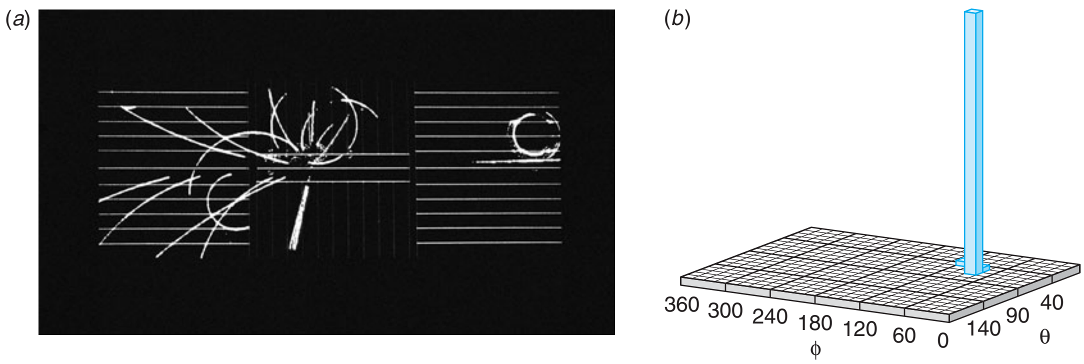

Figure 12-8 (*a*) The production and subsequent decay of one of the first W bosons ever detected was recorded by the UA1 detector at the CERN Sp$\bar{p}$S proton-antiproton collider. A $p\bar{p}$ collision occurs at the center. A W^+ is produced, which decays by $W^+ \rightarrow \tau^+ + \nu_\tau$. The tau decays into charged particles clearly seen as the thicker pencil-jet in the central detector directed nearly vertically downward. Conservation of energy and momentum for all particle tracks produced yields results consistent with a missing ν_τ from the decay. [*CERN*.] (*b*) The UA1's energy detectors surrounding the beam pipe recorded the energetic τ^+ and its angular position relative to the decay event. Energy is plotted vertically upward.

at CERN[10] that was specifically designed for the task. (See Figures 12-8 and 12-9.) The Z^0 is the second-heaviest elementary particle known, with a mass of 91 GeV/c^2 or nearly 100 times that of the proton. The $W^\pm$, with masses of 80 GeV/c^2, are the next heaviest.

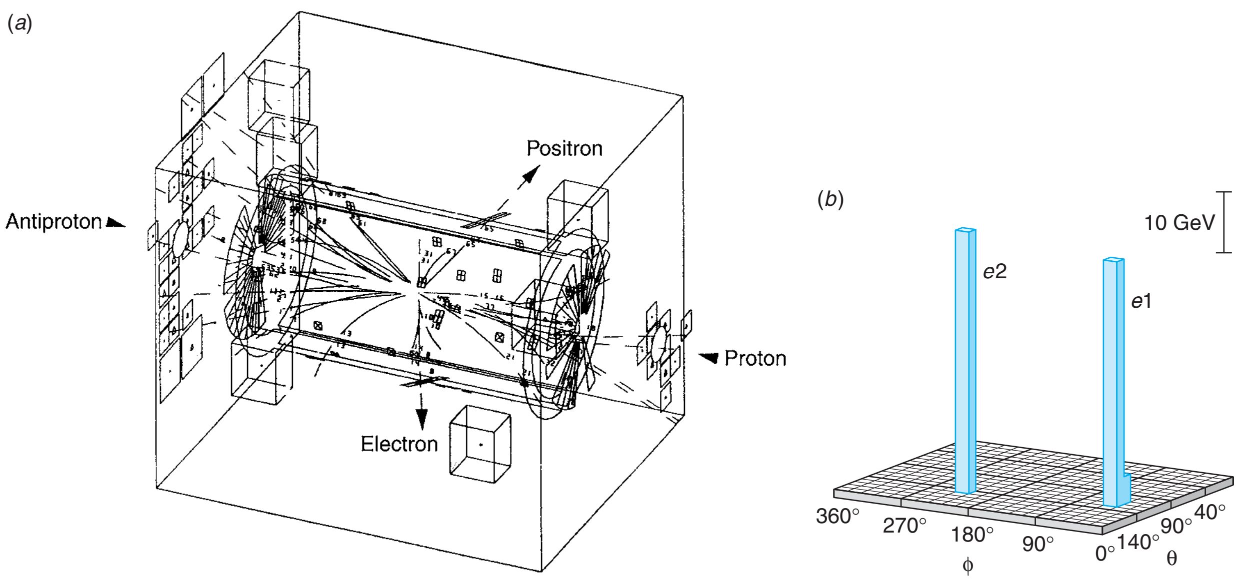

Figure 12-9 (*a*) This computer reconstruction of the CERN UA1 detector shows the first Z^0 decay ever recorded, obtained by Rubbia's group in 1983. Millions more such events have since been seen. [CERN Courier, ***33***, *4 (1993)*.] (*b*) The energy plot of the electron-positron pair from the $Z^0 \rightarrow e^+ + e^-$ decay. Energy, plotted vertically, is measured by individual detectors that "wrap around" the central cylinder of the UA1. The angular locations of the recorded electron and positron are measured relative to the position of the Z^0. Graphs like this are called "Lego plots."

EXAMPLE 12-3 Range of the Weak Interaction The mass of the Z^0 has been accurately measured to be 91.16 GeV$/c^2$. What range does that value imply for the neutral current weak interaction mediated by the Z^0?

SOLUTION

1. The range, the distance R traveled in time $t = \hbar/\Delta E$ by a particle moving at about c, is given by Equation 11-50:

$$R = \frac{\hbar}{mc} = \frac{\hbar c}{mc^2}$$

2. Substituting the mass of the Z^0 into this expression for R gives

$$R = \frac{(1.055 \times 10^{-34}\ \text{J}\cdot\text{s})(3.00 \times 10^{8}\ \text{m/s})}{(91.16\ \text{GeV}/c^2)(1.60 \times 10^{-10}\ \text{J/GeV})}$$
$$= 2.17 \times 10^{-18}\ \text{m} = 2.17 \times 10^{-3}\ \text{fm}$$

3. An alternate calculation of R:

$$R = \frac{(197.3\ \text{eV}\cdot\text{nm})}{(91.16\ \text{GeV})(10^{7}\ \text{eV/GeV})(10^{9}\ \text{nm/m})}$$
$$= 2.17 \times 10^{-3}\ \text{fm}$$

Gravitational Interaction

All particles participate in the gravitational interaction, but this interaction is so weak as to be unimportant in the discussion of elementary particles. As we have seen previously, its strength relative to the strong interactions is about 10^{-38}. The interaction has infinite range, with the force decreasing as $1/r^2$, as does the electrostatic force. The mediating particle for this force is the *graviton*, which is expected to be uncharged, massless, and have spin 2. This particle has not yet been observed, nor does the experimental capability to do so yet exist. Experiments with the objective of detecting gravity waves are currently under way. (See Section 2-5.) The gravitational interaction is produced by mass, which is the "gravitational charge" corresponding to the color charge, electric charge, and weak charge of the strong, electromagnetic, and weak interactions, respectively. Table 12-4 summarizes the characteristics of the four fundamental interactions.

Table 12-4 Characteristics of the fundamental interactions

Interaction	Force carrier	Mass (GeV$/c^2$)	Spin ($\hbar$)	Source	Particles carrying charge	Range (m)	Interaction time (s)	Coupling constant
Strong	gluon	0	1	color charge	q, g	10^{-15}	10^{-23}	$\alpha_s \approx 1$
Electromagnetic	photon	0	1	electric charge	q, e, μ, τ, $W^{\pm}$	∞	10^{-18}	$\alpha = 1/137$
Weak	$W^{\pm}$, Z^0	80, 91	1, 1	weak charge	q, e, μ, τ, $W^{\pm}$, Z^0	10^{-18}	10^{-16} to 10^{-10}	$\alpha_w \approx 10^{-5}$
Gravity	graviton	0	2	mass	q, e, μ, τ, ν, $W^{\pm}$, Z^0	∞	?	$\alpha_g \approx 10^{-38}$

EXPLORING

A Further Comment About Interaction Strengths

At the beginning of this section we defined the strengths of the interactions in terms of the coupling constants, relating their approximate values to the most familiar one, which is the fine-structure constant $\alpha = e^2/4\pi\epsilon_0\hbar c$. In QED the electric charge

$$e = \sqrt{4\pi\epsilon_0\hbar c\alpha} \propto \sqrt{\alpha}$$

is the amplitude of the coupling of the photon (the mediating boson) to the electron (the particle). Thus, the probability of events involving that coupling, such as the Compton effect, illustrated in Figure 12-5(a), is proportional to $e^2 \propto \alpha$.

The time-independent solution to the Klein-Gordon equation (Equation 11-52) can also be interpreted as the static potential $U(r)$ of the field of a point charge represented by the exchange particles. We then have

$$U(r) = \frac{Ae^{-r/R}}{r} \qquad \textbf{12-4}$$

where A is a constant of integration and $R = \hbar/mc$ is both the range of the force and the Compton wavelength $\lambda_c/2\pi$ of the mediating boson. For the electromagnetic interaction the range R is infinite and $U(r)$ becomes

$$U(r) = \frac{A}{r} \qquad \textbf{12-5}$$

Recalling from classical electromagnetism that the electrostatic potential of a point charge q is $U(r) = q/4\pi\epsilon_0 r$, we see that the constant A in Equation 12-5 plays the same role as the charge. In this manner a coupling constant proportional to A^2, just as $\alpha \propto e^2$, can be obtained for each of the interactions, albeit not without some difficulty. Doing so for the strong and weak interactions involves mathematics beyond the scope of our discussions, but as we will see in Section 12-4, this use of QED as a model is a powerful aid in understanding both the weak and the strong interaction. The coupling constants and other characteristics of the four interactions are given in Table 12-4.

One last comment before we leave this topic: The coupling constants are not actually constants. Again, this can be most clearly illustrated using the electromagnetic interaction. Consider a positive point charge q embedded in a dielectric as shown in Figure 12-10*a*. The charge q polarizes the nearby molecules of the dielectric. As a result, the charge q is partially screened by the negative ends of the polarized molecules and the electric field of q at a distance r away is correspondingly reduced. Thus, the value measured for q is the effective charge q_{eff}, which depends on how far from q the measurement is made, where q_{eff} is given by

$$q_{\text{eff}} = \frac{q}{\epsilon} \qquad \textbf{12-6}$$

and ϵ is the dielectric constant of the material, which you remember is a measure of how difficult it is to polarize the material. Only by measuring very close to q, roughly speaking within the molecular equilibrium separation r_0 (closer than the closest molecule so that there is no screening), will you actually measure the value q. This is shown in Figure 12-10*b*. Notice also that (1) measurements made at large values of r yield q/ϵ, not q, and (2) the value of q_{eff} *increases* for very small values of r.

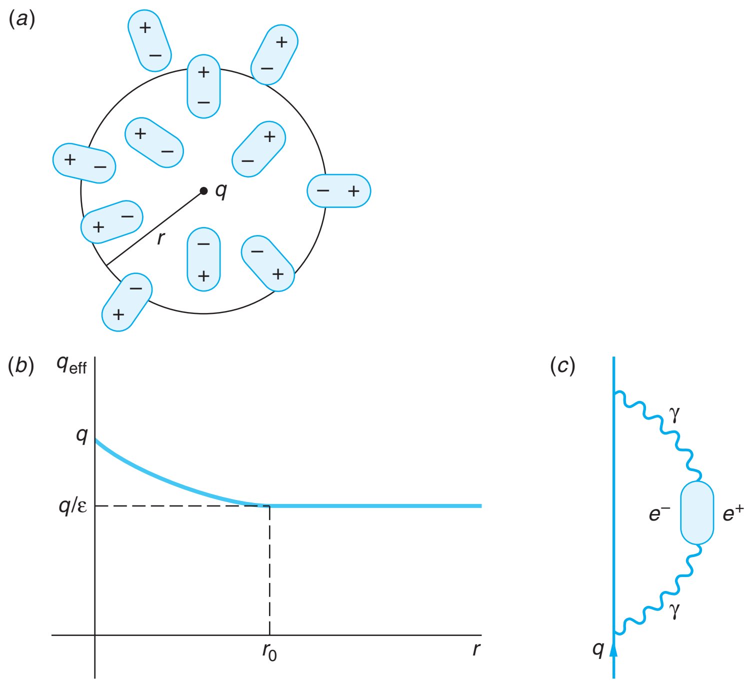

Figure 12-10 (*a*) A positive charge *q* placed in a dielectric material polarizes the dielectric by orienting the nearby molecules with their negative ends closest to *q*. An observer at some distance *r* from *q* sees a reduced electric field because of the screen of negative charges. (*b*) The value q_{eff} is measured for the charge. At small distances, those less than the equilibrium separation r_0 of the molecules of the dielectric, the value of q_{eff} approaches the value of *q*. (*c*) The vacuum also polarizes like a dielectric due to production of virtual electron-positron pairs by virtual photons. The effect is to increase the value of the fine-structure constant at very short interaction distances.

The production and absorption of virtual particles in QED results in the vacuum behaving like a dielectric. The positive charge *q* (or any charge) is continually emitting and absorbing virtual photons. Some of the photons occasionally create electron-positron pairs, which then annihilate, as the Feynman diagram in Figure 12-10*c* illustrates. The virtual electron and positron are attracted and repelled, respectively, by *q*, resulting in *vacuum polarization*, which partially screens *q*, just as it was screened when embedded in the dielectric. And just as in the dielectric, the full value of the charge *q* is not seen, or measured, until you get inside the screen. In vacuum polarization the role of the equilibrium separation r_0 is played by the Compton wavelength of the electron $\lambda_c = h/mc = 2.43 \times 10^{-12}$ m. Thus, even in a vacuum the "actual" value of *q* can only be measured at distances closer than about 2.43×10^{-12} m. What we measure experimentally and refer to as "the charge of the electron" is actually the completely screened effective charge. Thus, the fine-structure constant α, which is proportional to the square of the electric charge, will *increase* at very small distances from *q*.

A corresponding discussion can be given for the weak and strong interactions, but there are significant differences. The photon, which mediates the electromagnetic interaction, does not carry electric charge. However, the $W^{\pm}$ and Z^0, which mediate the weak interaction, have mass and carry weak charge. (The $W^{\pm}$ also carry electric charge.) The gluons, which mediate the strong force, carry color charge. This latter difference results in an important characteristic of the strong force called *quark confinement*, which we will discuss further in Section 12-4.

Questions

3. How are baryons and mesons similar? How are they different?
4. What properties do all leptons have in common?
5. The mass of the muon is nearly equal to that of the pion. How do these particles differ?
6. The bonding of the electrons to nuclei to form atoms is an example of the electromagnetic interaction. Use the interaction's properties to explain why the dimensions of atoms are of the order of 10^{-10} m.
7. Describe a way the world would be different if electrons felt the strong interaction.
8. What might be the "technicality" that results in there being eight gluons instead of the expected nine?

EXAMPLE 12-4 Neutron Decay The free neutron decays via the weak interaction with a half-life of 10.4 min according to the reaction

$$n \longrightarrow p + e^- + \overline{\nu}_e$$

Use a Feynman diagram to illustrate the details of this decay.

SOLUTION

Since this decay involves a change in the charge of the hadron, the mediating boson is a W^-. The W^- then decays to the e^- and $\overline{\nu}_e$. The Feynman diagram describing these events is therefore as shown below, where particles shown moving backward in time are to be interpreted as the corresponding antiparticle moving forward in time. Notice that, as mentioned earlier, the charged weak interaction changes the quark flavor.

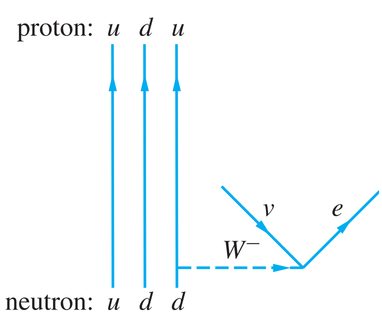

In words, this diagram is read like this: A d quark in the neutron emits a W^-, changing (decaying) to a u quark, thus changing the neutron into a proton. The W^- then decays to an e^- and an $\overline{\nu}_e$.

Remarks: *The mediating boson could also be a W^+. What would the diagram look like in that case?*

EXAMPLE 12-5 Estimate of Cross Section for Strong Interaction Obtain a rough estimate for the cross section of a typical strong interaction scattering of two hadrons, such as pions by protons or protons by protons.

SOLUTION

1. The cross section σ for an interaction or reaction is given approximately by the area of a circle whose radius is the range of the interaction. (See Section 11-7.) For the strong interaction we can write, therefore, that

$$\sigma_S = \pi R_S^2$$

2. From Example 11-15 we found the range of the strong interaction R_S to be about 10^{-15} m. Therefore, σ_S is equal to

$$\sigma_S = \pi(10^{-15}\text{ m})^2$$
$$= 3.1 \times 10^{-30}\text{ m}^2 = 31\text{ mb}$$

Remarks: *The cross section, as noted in Section 11-7, is actually dependent on the collision energy, but typical values are of the order of tens of millibarns, in agreement with our approximation.*

12-3 Conservation Laws and Symmetries

One of the maxims of nature, sometimes referred to as the *totalitarian principle*, is "anything that can happen does happen." If a conceivable decay or reaction does *not* occur, then there must be a reason. The reason is usually expressed in terms of a conservation law. You are already familiar with several such laws. The *conservation of energy* rules out the decay of any particle for which the total mass of the decay products would be greater than the initial mass of the particle before decay. The *conservation of linear momentum* requires that when an electron and positron annihilate, two photons (at least) must be emitted. *Angular momentum* must also be conserved in a reaction or decay. A fourth conservation law that restricts the possible particle decays and reactions is that of *electric charge*. The net electric charge before a decay or reaction must equal the net charge after the decay or reaction.

Every conservation law is a consequence of a particular symmetry in the laws of physics that govern the universe. This is a paraphrased statement of a theorem proven in 1918 by Emmy Noether[11] for conjugate variables in classical mechanics. For instance, the laws of physics are symmetric (i.e., invariant) with respect to translations in time. That means they work the same today as they have in the past. Noether's theorem relates this particular invariance of the physical laws to the conservation of energy. The fact that the physical laws are symmetric under translations in space leads to the conservation of linear momentum. If a system is symmetric to rotations about a point, then the angular momentum is conserved. The conservation of electric charge is a consequence of the invariance of the laws of electrodynamics under a gauge (i.e., scale) transformation.

There is a quantum theory analog of Noether's theorem; however, as was the case in classical physics, the conservation law is often discovered empirically before the symmetry that is its origin is identified. For example, Herman von Helmholtz set forth the law of conservation of energy primarily on the basis of James Joules's experiments long before Emmy Noether had proven her theorem. This is also the situation today in particle physics. Most of the conservation laws discussed in this section are empirical discoveries since no symmetry has yet been identified that provides their foundation. We will point out a few of these as we proceed.

Baryon Number

In Section 11-4 we mentioned two conservation laws in our discussion of radioactive decay: conservation of nucleon number and of lepton number. We now need to state these more explicitly. The first is a special case of the following more general law:

The baryon number is conserved.

All baryons have baryon quantum number $B = +1$, all antibaryons have $B = -1$, and all other particles are assigned $B = 0$. Conservation of baryon number requires that the total B for all particles before a decay or reaction occurs must be equal to that for all particles afterward. As an example of baryon conservation, consider the production of the antiproton in Figure 12-2 again. The reaction is

$$pp \longrightarrow ppp\bar{p} \qquad \textbf{12-7}$$

The total baryon number before the reaction is $B = +1 + 1 = +2$. That after the reaction is $B = +1 + 1 + 1 - 1 = +2$. Thus, conservation of B requires that three protons appear on the right side of Equation 12-7; that is, the production of an antiproton is always accompanied by the production of a proton. Conservation of baryon number together with the conservation of energy implies that the least massive baryon, the proton, must be stable. Whether that is in fact true is currently an active experimental question among particle physicists. There is no known symmetry requiring conservation of baryon number. There are several conceivable proton decay modes, all involving the proton decaying to a lepton and a meson, both of which have $B = 0$. To date, nonconservation of baryon number has never been observed. Current experiments place the lower limit of the proton lifetime at about 10^{32} years. We will return to this matter later in this chapter.

Lepton Number

In the original version of the Standard Model neutrinos have no mass and are polarized. Experiments had shown that neutrinos were left-handed; that is, their spin direction was antiparallel to their momentum, and antineutrinos were right-handed, their spin being parallel to their momentum (see Figure 12-11*a*). In the Standard Model mass arises from interaction with the Higgs boson. That interaction also changes right-handedness to left-handedness and vice versa, so the fact that neutrinos were always detected as left-handed meant that, like the photon, they did not interact with the Higgs and therefore had no mass. This in turn means that lepton number is conserved in the weak interactions and conservation of leptons applies independently to each of the three flavors.

The lepton number for each flavor of leptons is independently conserved.

The lepton quantum number for the electron and the electron neutrino is $L_e = +1$ and that for the positron and electron antineutrino is $L_e = -1$. All other particles, including the other leptons, have $L_e = 0$. In a similar fashion the lepton quantum numbers L_μ are assigned for the muon generation and L_τ for the tau generation. To see how conservation of lepton number works, consider the following decays:

$$p \longrightarrow \pi^0 e^+ \qquad \textbf{12-8}$$

$$\mu^+ \longrightarrow e^+ \nu_e \bar{\nu}_\mu \qquad \textbf{12-9}\boldsymbol{a}$$

$$\mu^+ \longrightarrow e^+ \gamma \qquad \textbf{12-9}\boldsymbol{b}$$

$$n \longrightarrow pe^- \bar{\nu}_e \qquad \textbf{12-10}$$

The decay shown in Equation 12-8 (one of the conceivable proton decay modes) would conserve energy, charge, angular momentum, and linear momentum, but it has not been observed. It conserves neither baryon number B nor lepton number L_e. The decay of the μ^+, given by Equation 12-9a, results in both an electron neutrino and a muon antineutrino. The μ^+ has $L_\mu = -1$ and $L_e = 0$. The decay products also have $L_\mu = -1$ (the ν_μ) and $L_e = -1 + 1 = 0$ (the e^+ and ν_e). The μ^+ decay given in Equation 12-9b had been searched for by many groups without success for many years. Its absence was the first indicator that L_e and L_μ were independently conserved. Equation 12-10, the decay of the neutron, conserves both B and L_e. Conservation of lepton number implies that the neutrino emitted in the beta decay of a free neutron is an electron antineutrino.

However, during the past several years experiments at the Sudbury Neutrino Observatory and Super-Kamiokande have shown that neutrinos do in fact have mass and oscillate, albeit slowly, from one flavor to another as they travel. This discovery was the first experimental evidence that the Standard Model is an approximation of a more comprehensive, unknown theory. We will speculate briefly on what that theory might be in Section 12-5, but for our discussion here the implications are considerable. Since neutrinos have mass, their speeds are less than c. This implies that a left-handed neutrino can become a right-handed neutrino with respect to an observer and vice versa. Since we know of no fundamental symmetry that requires conservation of leptons, if lepton number is not conserved, then we have no way to distinguish between neutrinos and antineutrinos; the neutrino may be a Majorana particle, as was alluded to in Section 12-1. A number of theoretical extensions of the Standard Model have been suggested to deal with this problem, but as yet there is no clear solution. With this caveat in mind, we will for the remainder of this section use the lepton and baryon conservation laws stated above and defer discussion of the possible consequences of their violation until Section 12-5.

EXAMPLE 12-6 Conservation Laws What conservation laws (if any) are violated by the following reactions?

(a) $n \longrightarrow p\pi^-$ (b) $\Lambda^0 \longrightarrow \bar{p}\pi^+$ (c) $\pi^- \longrightarrow \mu^-\bar{\nu}_\mu$

SOLUTION

(a) There are no leptons in this decay, so there is no problem with the conservation of lepton number. The net charge is zero before and after the decay, so charge is conserved. Also, the baryon number is $+1$ before and after the decay. However, the rest energy of the proton (938.3 MeV) plus that of the pion (139.6 MeV) is greater than the rest energy of the neutron (939.6 MeV). Thus, this decay violates the conservation of energy.

(b) Again, there are no leptons involved, and the net charge is zero before and after the decay. Also, the rest energy of the Λ^0 (1116 MeV) is greater than the rest energy of the antiproton (938.3 MeV) plus that of the pion (139.6 MeV), thus energy is conserved with the loss in rest energy equaling the gain in kinetic energy of the decay products. However, this decay does not conserve baryon number, which is $+1$ for the Λ^0, -1 for the antiproton, and 0 for the pion.

(c) There are no baryons involved, so conservation of baryon number is not a problem. The net charge is -1 before and after the decay, so charge is conserved. Also, the rest energy of the π^- (139.6 MeV) is greater than that of the μ^- (105.7 MeV) and the $\bar{\nu}_\mu$, so energy is conserved, the difference appearing as kinetic energy of the muon and neutrino. Finally, $L_\mu = 0$ on the left side and $L_\mu = 1 - 1 = 0$ on the right side, therefore lepton number is also conserved. This is the reaction by which the π^- decays.

More

Each conservation law results from a particular symmetry in the laws that govern the physical universe. Since it is not necessarily obvious under what mathematical operations the laws of physics will be symmetric, on a pragmatic level it is fair to ask, quantum mechanically, *When Is a Physical Quantity Conserved?* We provide an answer to this question on the home page: www.whfreeman.com/tiplermodernphysics5e. See also Equations 12-11 through 12-22 and Note 12 here, as well as Example 12-7.

More Conservation Laws

The quantum numbers and corresponding conservation laws of the hadrons described in this section arise logically from combinations of so-called *internal quantum numbers* of the quarks. These are listed in Table 12-5. They are the electric charge Q, baryon number B, strangeness S, charm C, bottom B', and top T. As we have noted above, electric charge and baryon number are conserved in all interactions. Strangeness, charm, bottom, and top are conserved in the strong and electromagnetic interactions but are not conserved in the weak interaction.

Strangeness There are some conservation laws that are not universal but apply only to certain kinds of interactions. In particular, there are quantities that are conserved in decays and reactions that occur via the strong interaction but not in decays or reactions that occur via the weak interaction. This is somewhat analogous to the selection rules discussed in atomic transitions. For example, the selection rule $\Delta\ell = \pm 1$ holds for electric dipole transitions from one atomic state to another. An atom in a state with $\ell = 2$ cannot decay to a lower energy state with $\ell = 0$ via electric dipole radiation because of this selection rule, but it can decay via an electric quadrupole transition, which is generally much slower than electric dipole transitions. One of the particularly important quantities conserved in strong interactions is *strangeness*. This quantity was introduced by M. Gell-Mann[13] and K. Nishijima in 1952 to explain the seemingly strange behavior of the heavy baryons and mesons.

Table 12-5 Internal quantum numbers of the quarks

Quark	Q	B	U	D	C	S	T	B'
u	2/3	1/3	1	0	0	0	0	0
d	−1/3	1/3	0	−1	0	0	0	0
c	2/3	1/3	0	0	1	0	0	0
s	−1/3	1/3	0	0	0	−1	0	0
t	2/3	1/3	0	0	0	0	1	0
b	−1/3	1/3	0	0	0	0	0	−1

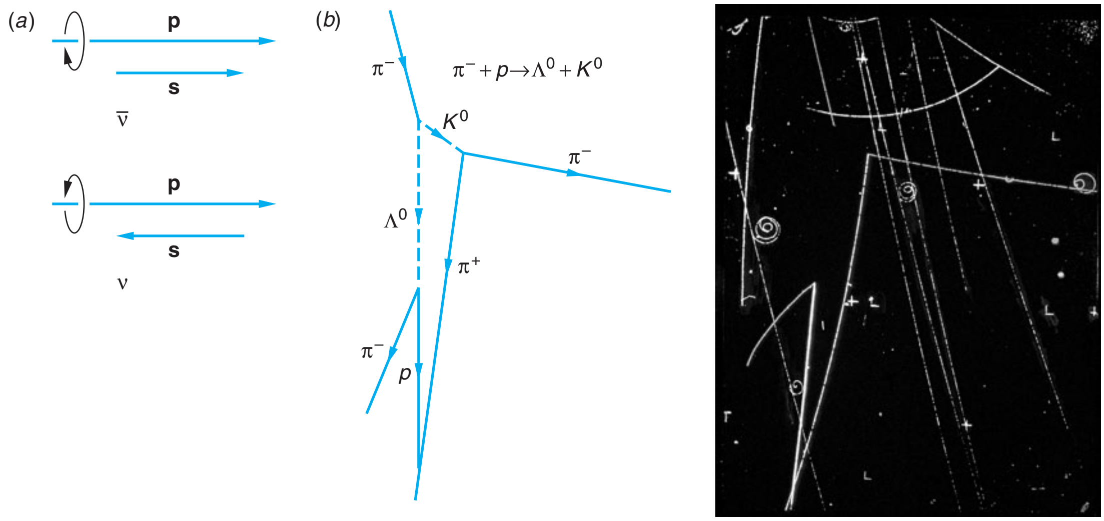

Figure 12-11 (*a*) The spin of antineutrinos is parallel to their momentum. The spin of neutrinos is antiparallel to their momentum. Described in terms of *helicity* $= m_s/s$ with the z axis in the direction of **p**, antineutrinos have helicity $+1$ and neutrinos have helicity -1. (*b*) An early photograph of bubble chamber tracks at the Lawrence Berkeley Laboratory, showing the production, represented by Equation 12-23, and decay of two strange particles, the K^0 and the Λ^0. These neutral particles are identified by the tracks of their decay particles. The lambda particle was so named because of the similarity of the tracks of its decay particles and the Greek letter Λ. The incident π^- meson had energy of 1 GeV. [*(b) Lawrence Berkeley Laboratory/Photo Researchers.*]

Consider the reaction in which a high-energy π^- interacts with a proton,

$$p\pi^- \longrightarrow \Lambda^0 K^0 \qquad \textbf{12-23}$$

shown in Figure 12-11*b*. The cross section for this reaction is large, as would be expected since it takes place via the strong interaction (see Example 12-5). However, the decay times for both Λ^0 and K^0 are of the order of 10^{-10} s, which is characteristic of the weak interaction. When first discovered, their unexpectedly long lifetimes were very strange, so these and other particles showing similar behavior were called *strange particles*. An early success of the quark model was the explanation of these unexpectedly long lifetimes. As an example, the Λ^0 is a *uds* quark combination, which corresponds to a particular set of the internal quark quantum numbers. If no lighter (i.e., lower-energy) hadron with that exact set of quantum numbers exists, then decay via the strong or electromagnetic interaction is not possible. Decay can only occur via the much slower weak interaction.

These particles are always produced in pairs and never singly, even when all other conservation laws are met. This behavior is described by assigning to them a new quantum number called *strangeness*. The strangeness of the ordinary hadrons—the nucleons and pions—was arbitrarily chosen to be zero. The strangeness of the K^0 was arbitrarily chosen to be $+1$. Therefore, the strangeness of the Λ^0 particle must be -1 so that strangeness is conserved in the reaction of Equation 12-23. The strangeness of other particles could then be assigned by looking at their various reactions and decays. In reactions and decays that occur via the strong and electromagnetic interactions, strangeness is conserved. In those that occur via the weak interaction, strangeness is not conserved but can only change by ±1.

Isospin As pointed out earlier, a striking feature of the hadrons is that they cluster into *charge multiplets*, groups of particles with nearly the same mass, such as the multiplet consisting of the proton ($p = uud$) and neutron ($n = udd$). Within each multiplet all of the particles have the same spin, parity (see below), baryon number, strangeness, charm, and bottom but differ in their electric charges. In addition, we learned in Section 11-5 that the strong (nuclear) force is independent of electric charge. Were it not for the masses of the quarks and the electromagnetic interaction, the masses of the particles in a given charge multiplet would be the same. We are thus led to the view that the members of the multiplet are simply different charge states of the same particle. The "splitting" of particle mass states is analogous to the splitting of atomic energy states due to the spin-orbit interaction. (See Section 7-5.) Because of the analogy with isotopes (atoms with the same Z but slightly different masses) and with the splitting of different spin states, the term *isospin* is used to describe this multiplicity. The isospin $\mathbf{I}$ is treated as a vector in a three-dimensional "charge space," just as the orbital angular momentum $\mathbf{L}$ is a vector in real space. The component of $\mathbf{I}$ in the "z direction" is called I_3 and is quantized, just as the z components of the orbital and intrinsic angular momenta of atomic electrons are quantized. Similarly, there are $(2I + 1)$ different I_3 states. The charge q on a particle is related to its value of I_3 by

$$q = eQ = e\left(I_3 + \frac{B + S}{2}\right) \qquad \textbf{12-24}$$

where Q is the charge quantum number. The value of I of the nucleon is $1/2$, with the two possible values $I_3 = +1/2$ for the proton and $I_3 = -1/2$ for the neutron. The isospin I is also $1/2$ for the xi doublet and 0 for the lambda and omega singlets. It is 1 for the Σ triplet (with $I_3 = +1$ for Σ^+, 0 for Σ^0, and -1 for Σ^-). In the case of the mesons, the pion isospin triplet has $I = 1$, the kaon doublet $I = 1/2$, and the eta singlet $I = 0$. The rules for combining isospin are the same as those for combining real spin or angular momentum. If only the strong interaction is present, then I_{op} and H_{op} commute and $\mathbf{I}$ is conserved. Decays and reactions in which the total isospin of the system is not conserved do not proceed via the strong interaction.

Hypercharge Four of the quantum numbers that we have discussed thus far turn out to be related to one another. These are strangeness, charge, isospin, and baryon number. The relation is

$$S = 2(Q - I_3) - B \qquad \textbf{12-25}$$

Strangeness is now used less frequently than a simpler quantity called *hypercharge* Y, which is defined as

$$Y \equiv B + S + C + B' + T \qquad \textbf{12-26}$$

With the aid of Equation 12-25 the hypercharge quantum number Y is then given by

$$Y = S + B = 2(Q - I_3) \qquad \textbf{12-27}$$

Stated simply, the hypercharge is twice the average charge of a given multiplet. For example, the average charge of the nucleon multiplet is $(1e + 0)/2 = (1/2)e$. Thus, for the nucleon, $Y = 1$, as given by Equation 12-27. Since baryon number is strictly conserved and strangeness is conserved only in strong interactions, hypercharge, too, is conserved only in strong interactions. Since $\Delta S = \pm 1$ or 0 in weak interactions,

Table 12-6 Some quantum numbers of the hadrons that are stable against decay via the strong interaction

Particle	Spin ($\hbar$)	I	I_3	B	S	Y
p	1/2	1/2	+1/2	1	0	1
n	1/2	1/2	−1/2	1	0	1
Λ^0	1/2	0	0	1	−1	0
Σ^+	1/2	1	+1	1	−1	0
Σ^0	1/2	1	0	1	−1	0
Σ^-	1/2	1	−1	1	−1	0
Ξ^0	1/2	1/2	+1/2	1	−2	−1
$\Xi-$	1/2	1/2	−1/2	1	−2	−1
$\Omega-$	3/2	0	0	1	−3	−2
π^+	0	1	+1	0	0	0
π^0	0	1	0	0	0	0
π^-	0	1	−1	0	0	0
K^+	0	1/2	+1/2	0	+1	+1
K^0	0	1/2	−1/2	0	+1	+1
η^0	0	0	0	0	0	0

changes in hypercharge are similarly restricted to $\Delta Y = \pm 1$ or 0. Table 12-6 lists the values of these additional quantum numbers for those hadrons that are stable against decay via the strong interaction. Note that, if it were not for the conservation of strangeness or hypercharge in the strong interaction, all the baryons except the nucleons would decay via the strong interaction and live only for about 10^{-23} s.

The singlet, doublet, and triplet charge multiplets discussed above are clearly represented in graphs of Y versus I_3. Studies of the regularities apparent in such graphs (see Figure 12-12) were instrumental in the development of the quark model of fundamental particles to be discussed in Section 12-4. The regularities are analogous to those observed in the multiplet structure of atomic energy states that ultimately led to the understanding of atomic structure.

The conservation laws and the properties of charge Q, lepton number L, baryon number B, and strangeness S give us some insight into the relation between particles and their antiparticles. A particle and its antiparticle must have opposite signs for the values of each of these properties. Any particle that has a nonzero value for any of these properties will therefore have a distinct antiparticle. The photon, graviton, and the π^0 have $Q = 0$, $L = 0$, $B = 0$, and $S = 0$ and are therefore in some sense their own antiparticles. The π^+ and π^- mesons are somewhat special because they have charge but have zero values for L, B, and S. They are therefore antiparticles of each other, but since there is no conservation law for mesons, it is impossible to say which is the particle and which is the antiparticle.

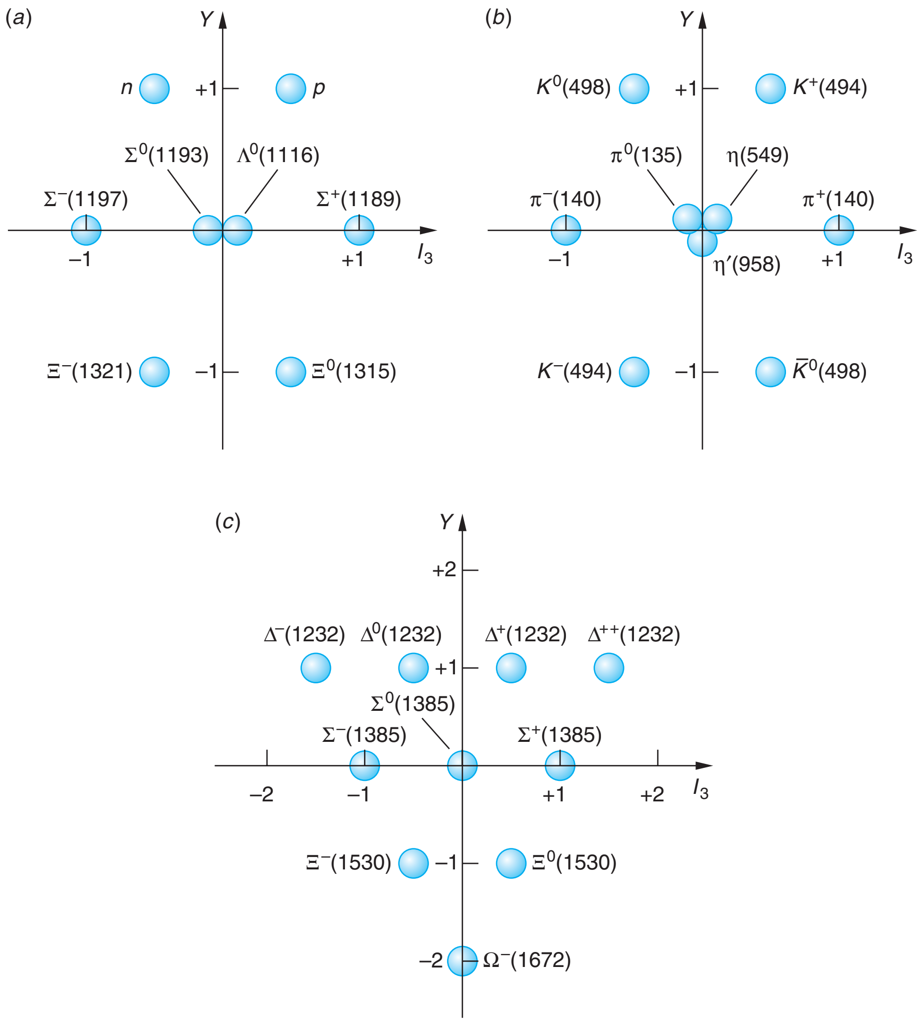

Figure 12-12 Graphs of hypercharge Y vs. the I_3 component of the isospin. (*a*) Baryons with spin 1/2. (*b*) Mesons with spin 0. (*c*) Baryons with spin 3/2. Except for the Ω^-, these are resonance particles, as discussed in Section 12-3 and on the home page. Masses in parentheses are in MeV/c^2. Notice in each case that particles of like charge lie along downward-sloping diagonals and particles of like hypercharge (and strangeness) lie along horizontal lines.

EXAMPLE 12-8 Applying the Conservation Laws State whether the following decays can occur via the strong interaction, via the electromagnetic interaction, via the weak interaction, or not at all:

(*a*) $\Sigma^+ \longrightarrow p\,\pi^0$ (*b*) $\Sigma^0 \longrightarrow \Lambda^0\gamma$ (*c*) $\Xi^0 \longrightarrow n\pi^0$

SOLUTION

We first note that the mass of each decaying particle is greater than that of the decay products, so there is no problem with energy conservation in any of the decays. In addition, there are no leptons involved in any of the decays, and charge and baryon number are both conserved in all the decays.

(*a*) From Figure 12-12, we can see that the hypercharge of the Σ^+ is 0, whereas the hypercharge of the proton is $+1$ and that of the pion is 0. This decay is possible via the weak interaction but not the strong interaction. It is, in fact, one of the decay modes of the Σ^+ particle, with a lifetime of the order of 10^{-10} s.

(*b*) Since the hypercharge of both the Σ^0 and Λ^0 is 0, this decay can proceed via the electromagnetic interaction. It is the dominant mode of decay of the Σ^0 particle, with a lifetime of about 10^{-20} s.

(*c*) The hypercharge of the Ξ^0 is -1, whereas that of the neutron is $+1$ and that of the pion is 0. Since hypercharge cannot change by 2 in a decay or reaction, this decay cannot occur.

Questions

9. How can you tell if a decay proceeds via the strong, electromagnetic, or weak interactions?
10. Can the strangeness or hypercharge of a new particle be determined even if the number of particles in the multiplet is unknown? How or why not?

Parity The *parity* of a nucleus or particle is defined in the same way as for an atom. (See Section 6-5.) The parity operation reflects the space variables in the coordinate origin. If the parity operator acting on the wave function changes the sign of the wave function, the parity is said to be odd, or -1. If the wave function does not change sign, the parity is even, or $+1$. The parity quantum number P is different from the other quantum numbers we have been considering. It can have only the values $+1$ or -1. If the value of the parity of a system changes, the new value is -1 times the old value. Parity is therefore a multiplicative property rather than an additive property like baryon number, strangeness, or hypercharge. The parity of an atomic wave function is related to the orbital angular momentum by $P = (-1)^{\ell}$. The parity is odd or even depending on whether ℓ is odd or even. In our discussion of radiation from atoms, we saw that the parity of an atom can change just as the angular momentum of the atom changes when the atom emits light. For electric dipole transitions, $\Delta\ell = \pm 1$, so the parity and angular momentum quantum numbers always change. However, if the complete system, including the photon, is considered, the total angular momentum and the total parity do not change in atomic transitions; that is, parity is conserved in electromagnetic interactions. Parity is also conserved in the strong interaction.

Until 1956 it was assumed that parity is conserved in all nuclear reactions and radioactive decays. In that year, T. D. Lee and C. N. Yang suggested that parity might not be conserved in weak interactions. This suggestion grew out of attempts to understand the peculiar behavior of what were then known as the τ and θ mesons. These particles were identical in every way except that the θ meson decayed into two pions with positive parity, whereas the τ decayed into three pions with negative parity. (Each elementary particle can be assigned an intrinsic parity. That of the pion is negative.) The τ-θ puzzle was this: Are there two different particles with all properties identical except parity, or is it possible that parity is not conserved in some reactions? After careful study Lee and Yang found that all the experimental evidence for parity conservation pertained to strong or electromagnetic interactions and not for weak interactions. They suggested that the nonconservation of parity could be observed experimentally by measuring the angular distribution of electrons emitted in β decay of nuclei that have their spins aligned. Such an experiment was performed in December 1956 by a group led by C. S. Wu and E. Ambler. The results confirmed Lee and Yang's predictions, for which they received the Nobel Prize in Physics in 1957. The τ and θ mesons are a single particle, now known as the K^0 meson, which has two distinct modes of decay. The significance of the K^0 decay will be discussed further in the TCP Invariance section below.

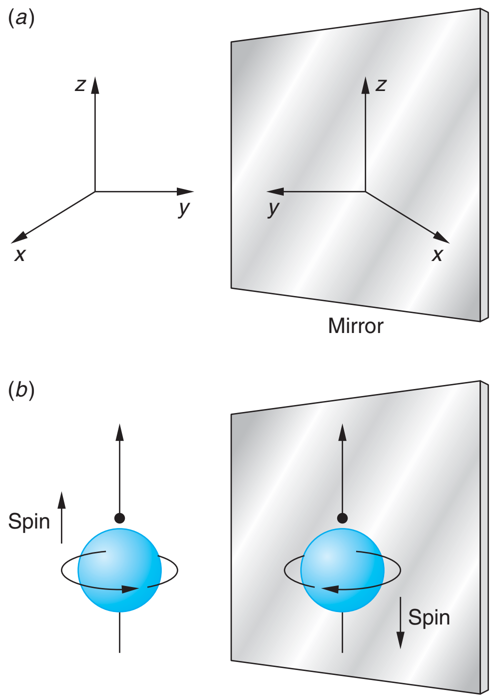

Figure 12-13 (*a*) The mirror image of a right-handed coordinate system ($\mathbf{x} \times \mathbf{y}$ in the $\mathbf{z}$ direction) is a left-handed coordinate system ($\mathbf{x} \times \mathbf{y}$ in the $-\mathbf{z}$ direction). No combination of translation and rotation can change a right-handed coordinate system into a left-handed system. (*b*) Spinning nucleus emitting an electron in the direction of its spin. In the mirror, the image nucleus is emitting the electron in the direction opposite to its spin because the mirror reverses the direction of the spin vector.

The conservation of parity essentially means that a process described by the coordinates x, y, and z appears the same if described by the coordinates $x' = -x$, $y' = -y$, and $z' = -z$. The system x, y, z is called a *right-handed coordinate system* because $\mathbf{x} \times \mathbf{y}$ is in the $+\mathbf{z}$ direction. Similarly, the system x', y', z' is called a *left-handed coordinate system* because $\mathbf{x'} \times \mathbf{y'}$ is in the negative $\mathbf{z'}$ direction. No rotation can change a right-handed coordinate system into a left-handed one, but reflection in a mirror does, as shown in Figure 12-13*a*. We can thus state the law of conservation of parity in more physical terms: If parity is conserved, the mirror image of a process cannot be distinguished from the process itself. Figure 12-13*b* shows a spinning nucleus emitting an electron in the direction of its spin. In the mirror, the nucleus appears to be emitting the electron in the direction opposite to that of its spin. If parity is conserved in β decay, the chance of emission in the direction of the nuclear spin must equal the chance of emission in the opposite direction; i.e., there can be no preferred direction. Whether or not one direction is actually preferred in β decay is usually not observable because the nuclear spins are randomly oriented. Wu and Ambler aligned the nuclei in ^{60}Co by placing their sample in a magnetic field at a very low temperature (about 0.01 K). They found that more particles were emitted opposite to the spin of the nucleus than in the direction of the spin, indicating that parity is not conserved in weak interactions. Table 12-7 summarizes the conservation laws discussed in this section.

TCP Invariance It is a property of any relativistic quantum theory in which signal speeds cannot exceed the vacuum speed of light, that the combined operations of *P*arity ($\mathbf{r} \rightarrow -\mathbf{r}$), *T*ime reversal ($t \rightarrow -t$), and *C*harge conjugation (particle $\rightarrow$ antiparticle) leave any wave function unchanged:

$$TCP\,\Psi(\mathbf{r}, t) = +1\,\Psi(\mathbf{r}, t) \quad \text{or} \quad TCP = +1 \qquad \textbf{12-28}$$

Table 12-7 Conserved quantities in fundamental particle interactions

	Interaction		
Conserved quantity	Strong	Electromagnetic	Weak
Energy			
Momentum			
Charge (Q)	Yes	Yes	Yes
Baryon number (B)			
Lepton number (L)			
Isospin (I)	Yes	No	No ($\Delta I = \pm1, 0$)
Hypercharge (Y)	Yes	Yes	No ($\Delta Y = \pm1, 0$)
Strangeness (S)	Yes	Yes	No ($\Delta S = \pm1, 0$)
Parity (P)	Yes	Yes	No

It makes no difference in what order the operations are performed. Invariance under these combined operations requires that particles and their antiparticles have the same masses and lifetimes. It was long thought that the invariance under the combined operations was the result of invariance of physical laws under each of the operations independently, i.e., $T = +1$, $P = +1$, and $C = +1$.

However, as we described in the previous section, it was discovered that parity was not conserved in weak interactions. For the weak interaction the parity operation yields $P = -1$. That immediately implies that one of the other operations must not be conserved in the weak interaction. Lee and Yang's solution to the $\tau - \theta$ puzzle revealed that there are two K^0 mesons (kaons) with nearly identical masses but very different decay modes and lifetimes. The K^0_S (S for "short") decays to two pions with a lifetime of about 0.9×10^{-10} s. The K^0_L (L for "long") decays to three pions with a lifetime of about 0.5×10^{-7} s. (See Table 12-3.)

Then in 1964 J. H. Christenson and his collaborators showed that in about 1 of every 1000 decays, the K^0_L also decayed into just two pions. This result means that for the K^0_L decay, the combined operation $CP = -1$ because the two-pion final system has $CP = +1$ and the three-pion final system has $CP = -1$.

The implications of this result are enormous and continue to be a focus of intense theoretical and experimental research. For example, within the framework of the Standard Model, CP violation requires that there be three generations of quarks and, correspondingly, the very large number of hadrons that can be assembled from them. The observed matter-antimatter asymmetry in the universe also requires CP violation. If $TCP = +1$ and $CP = -1$, $T = -1$ also, which establishes an absolute direction for the flow of time.

Questions

11. Suppose a new uncharged meson is discovered. What condition is necessary for it to have a distinct antiparticle?
12. How might Table 12-7 be different if strangeness were not conserved in interactions between hadrons?

More

Particles and excited states of particles that decay via the strong interaction have mean lives of only 10^{-23} s or so, not nearly long enough to be tracked by a particle detector. Such particles are instead detected by measuring resonances in the scattering cross sections in a way analogous to J. Franck and G. Hertz's detection of the first excited state of the Hg atom by measuring the resonances in the electron scattering from Hg atoms. Many fundamental particles have been found in this way, as is described on the home page (www.whfreeman.com/tiplermodernphysics5e), *Resonances and Excited States*, which also includes a partial list of meson and baryon resonances. See also Figures 12-14 through 12-16, Table 12-8, Equations 12-29 through 12-31, and Examples 12-9 and 12-10 here.

12-4 The Standard Model

The Standard Model is currently (since 1978) the accepted theory of elementary particle physics. It includes the *quark model* of particle structure that had been developed earlier, the unified theory of electromagnetic and weak interactions called the *electroweak theory*, and the strong-interaction analog of quantum electrodynamics called *quantum chromodynamics* (QCD). It has been remarkably though not totally successful in explaining the characteristics of fundamental particles and the interactions between them and is second only to QED in the accuracy of its predictions. In our discussions thus far in this chapter we have had occasion to allude to a number of specific features of the Standard Model. In this section we will consider the three of its constituents noted above in further detail. Since the complexity of the Standard Model's mathematical detail is beyond the level of this book, our discussion will be largely qualitative and conceptual.

Searches for experimental support for the Standard Model led to the development of many new types of particle detectors. Several have found applications beyond particle physics, one example being BGO crystal detectors, used in medical diagnostic PET scanners (see Figure 11-65).

Quark Model of the Hadrons

The Eightfold Way The construction of large high-energy particle accelerators beginning in the 1950s made possible the production of a flood of previously unseen hadrons.[14] Among the many attempts at understanding and classifying the jumble of hadrons, the most successful scheme is known as the *eightfold way*.[15] It was suggested independently by Gell-Mann and Y. Ne'eman in 1961 and subsequently justified by the Standard Model. In this scheme, hadrons that make up the charge multiplets were arranged in groups, called *supermultiplets*, in which each member had the same intrinsic spin and parity, J^P, where J is the intrinsic spin and P is the parity. Three of Gell-Mann's supermultiplets are shown in Figure 12-12: (*a*) the eight lightest baryons, called the *baryon octet*; (*b*) the eight lightest mesons, the *meson octet* (actually a *nonet*); and (*c*) the next 10 heavier baryons, the *baryon decuplet*. Figure 12-17 shows the energies of the baryon octet in a diagram analogous to the fine-structure splitting of atomic states. The energy splittings between the isospin multiplets (from 78 to 176 MeV) are about 20 times the splitting within the multiplets. There are no completed baryon supermultiplets beyond the octet and decuplet, although there are several partially completed ones. The known mesons complete six nonets. Note that there is also an *antibaryon* octet, decuplet, etc., but for the mesons their antiparticles are members of the same nonet. Gell-Mann's accomplishment is the elementary

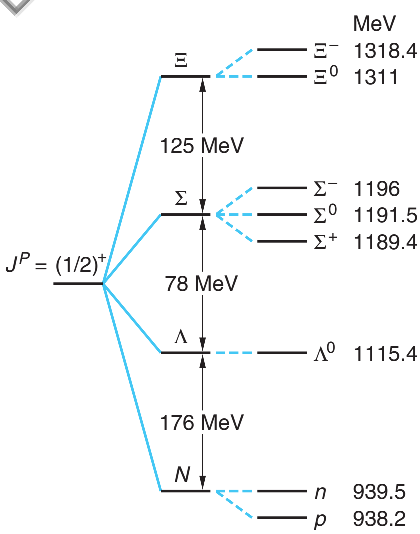

Figure 12-17 The energy-level diagram of the baryon octet, the supermultiplet of the hadronically stable $J^P = (1/2)^+$ baryons. In the absence of any interactions, all these particles should have the same mass. The different numbers of s quarks splits the mass state into four states, corresponding to the nucleon (N), lambda (Λ), sigma (Σ), and xi (Ξ) particles. The different quark masses and the weaker electromagnetic interaction further splits the particles into the N doublet, Σ triplet, and Ξ doublet.

particle analog of Mendeleev's development of the periodic table of the chemical elements, which was first published in 1869, nearly 100 years earlier, far in advance of the theoretical foundation for the periodic table provided by atomic theory and quantum mechanics.

The eightfold way is based on part of a mathematical theory known as the theory of continuous groups that was developed by the Norwegian mathematician S. Lie, among others. The simplest Lie group is known as SU(2), for *s*pecial *u*nitary group of 2×2 matrices. A special condition on the 2×2 arrays reduces the number of components from 4 to 3. The three independent components of these arrays correspond to the three components of angular momentum (or isospin). As we have seen previously, the various possible values of angular momentum J have corresponding states that occur in multiplets having 1, 2, 3, 4, . . ., $(2J + 1)$ elements, which we describe as having angular momentum of $0, 1/2, 1, 3/2, \ldots \hbar$ units. The next higher Lie group is known as SU(3), for *s*pecial *u*nitary group of 3×3 arrays. Again, a special condition reduces the number of components from 9 to 8 (hence the name *eightfold way*). The eight quantities in the application of SU(3) group theory to hadrons consist of the three components of isospin, the hypercharge, and four that are yet to be named. Without going into the details of group theory, we will merely state that the SU(3) group leads to multiplets of 1, 3, 8, 10, . . . elements. Rather than assigning a single number to these multiplets analogous to the angular momentum quantum number of SU(2), it is more useful to make two-dimensional diagrams called *weight diagrams*, which are the geometric patterns of points, triangles, and hexagons shown in Figure 12-18. In the application of SU(3) to particle theory, the axes are Y and I_3, as in Figure 12-12.

In the plot of Y versus I_3 for the $J^P = 3/2^+$ baryons (the decuplet shown in Figure 12-12*c*), neither the Ξ nor the Ω^- had been discovered prior to 1961. Note that the difference in rest energy between each line of the decuplet is about 140 MeV. A constant energy difference between successive multiplets in the decuplet is predicted by SU(3) theory. The prediction of the Ω^- particle by Gell-Mann in 1961 and its discovery in 1964 with just the mass and spin Gell-Mann had predicted was one of the spectacular successes of the pre–Standard Model eightfold way. Note that the Ω^- is the only particle in the decuplet that is not a resonance particle. The mass of the Ω^- is just small enough that energy conservation prevents it from decaying via a strangeness-conserving strong interaction such as $\Omega^- \to \Xi^0 + K^-$.

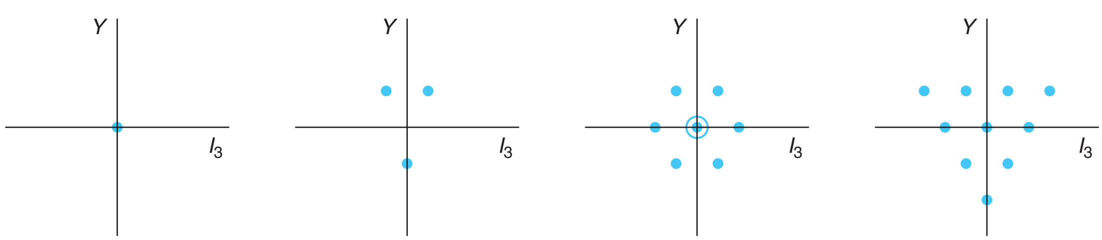

Figure 12-18 Weight diagrams occurring in SU(3) group theory. The circle and dot at the origin in the hexagon indicate two particles at the origin, making this pattern an octet.

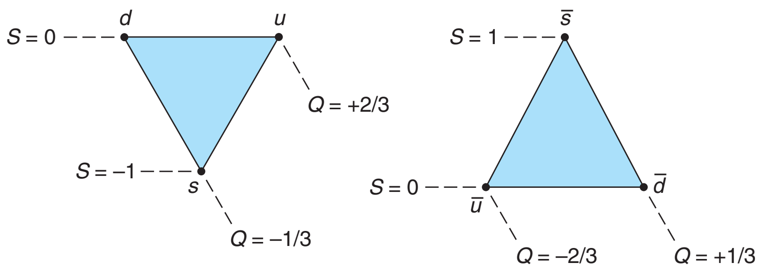

Figure 12-19 The SU(3) weight diagrams (Y vs. I_3) for the three light quarks and their antiquarks. As in the supermultiplet diagrams of the eightfold way, the downward-sloping lines are constant charge and the horizontal lines are constant strangeness.

Murray Gell-Mann, who proposed the existence of strangeness, developed the classification system for hadrons [SU(3)] and postulated the existence of fractionally charged particles, which he called quarks. He won the Nobel Prize in Physics in 1969. [*American Institute of Physics, Neils Bohr Library.*]

Other supermultiplets can be formed from the unstable baryons and mesons, but there are no observed groups of three particles corresponding to the triplet allowed by SU(3) theory, illustrated second from the left in Figure 12-18. This fact and the absence of a *reason* for the supermultiplets of the eightfold way led Gell-Mann and G. Zweig in 1964 to independently propose that all hadrons are composed of even more fundamental constituents called quarks.[16] Their proposal is the basis of the quark model, arguably the most important advance in our understanding of elementary particles.

In the original quark model, quarks came in three types labeled u, d, and s (for *u*p, *d*own, and *s*trange). Later discoveries, as we have seen, added three more quarks, labeled c, b, and t for *c*harm, *b*ottom, and *t*op. Recall that the charge of the u quark is $2e/3$ and that of the d and s quarks is $-e/3$. Each quark has $B = 1/3$. Each quark has spin 1/2. The strangeness of the u and d quark is 0 and that of the s quark is -1. Each quark has an antiquark with the opposite electric charge, baryon number, and strangeness. The three types up, down, and strange form the triangular SU(3) weight diagram of Figure 12-18, as shown in detail in Figure 12-19. The properties of the quarks are listed in Table 12-2. The basic assertion of the quark model is that all baryons consist of three quarks (or three antiquarks for antiparticles), whereas mesons consist of a quark and an antiquark. The mesons thus have baryon number $B = 0$, as required. The proton consists of the combination *uud* and the neutron *udd*. Baryons with a strangeness $S = -1$ contain one s quark. All the particles listed in Table 12-3 can be constructed from the three original quarks and the corresponding three antiquarks.[17]

A great success of the quark model was that all of the allowed combinations of the three quarks and quark-antiquark pairs resulted in known hadrons. Strong evidence for the existence of quarks inside the nucleons is provided by high-energy scattering experiments called *deep inelastic scattering*. In these experiments, a nucleon is bombarded with electrons or muons of energies from 15 to 200 GeV. Analyses of particles scattered at large angles indicate the presence within the nucleon of spin-1/2 particles of sizes much smaller than that of the nucleon. These experiments are analogous to Rutherford's scattering of α particles by atoms in which the presence of a tiny nucleus in the atom was inferred from the large-angle scattering of the α particles.

Table 12-9 Properties of three-quark combinations

Combination	Spin ($\hbar$)	Charge (e)	Baryon number	Strangeness	Hypercharge	I_3
uuu	3/2	+2	1	0	+1	+3/2
uud	1/2, 3/2	+1	1	0	+1	+1/2
udd	1/2, 3/2	0	1	0	+1	−1/2
uus	1/2, 3/2	+1	1	−1	0	+1
uss	1/2, 3/2	0	1	−2	−1	+1/2
uds	1/2, 3/2	0	1	−1	0	0
ddd	3/2	−1	1	0	+1	−3/2
dds	1/2, 3/2	−1	1	−1	0	−1
dss	1/2, 3/2	−1	1	−2	−1	−1/2
sss	3/2	−1	1	−3	−2	0

Since the conservation laws represented by the several quantum numbers in Table 12-5 are additive, it is simply a matter of arithmetic to determine the properties of the hadrons. For example, a particle formed by the combination *uds* can have a spin of either 1/2 or 3/2, charge equal to $+2/3 - 1/3 - 1/3 = 0$, and baryon number $B = 1/3 + 1/3 + 1/3 = 1$. Table 12-9 lists the possible three-quark combinations (baryons), and Table 12-10 lists the possible quark-antiquark combinations (mesons).

Table 12-10 Properties of quark-antiquark combinations for three quarks

Combination	Spin ($\hbar$)	Charge (e)	Baryon number	Strangeness	Hypercharge	I_3
$u\bar{u}$	0, 1	0	0	0	0	0
$u\bar{d}$	0, 1	+1	0	0	0	+1
$u\bar{s}$	0, 1	+1	0	+1	+1	+1/2
$d\bar{u}$	0, 1	−1	0	0	0	−1
$d\bar{d}$	0, 1	0	0	0	0	0
$d\bar{s}$	0, 1	0	0	+1	+1	−1/2
$s\bar{u}$	0, 1	−1	0	−1	−1	−1/2
$s\bar{d}$	0, 1	0	0	−1	−1	+1/2
$s\bar{s}$	0, 1	0	0	0	0	0

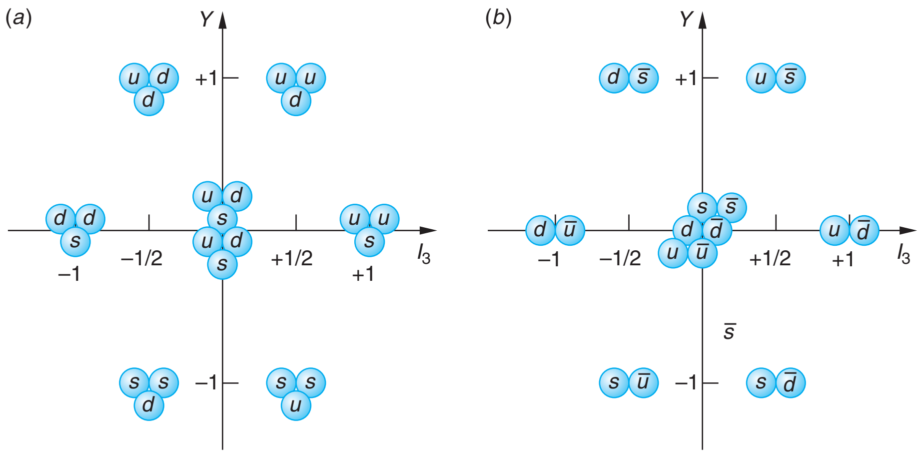

Figure 12-20 (*a*) The graph of Y vs. I_3 for the spin-1/2 three-quark combinations—the baryon octet. (*b*) The graph of Y vs. I_3 for the quark-antiquark combinations that form the lightest meson nonet.

The eight spin-1/2 baryons make up the baryon octet of Figure 12-12*a*. The three quarks of which each member is composed are shown in Figure 12-20*a*. Notice that Table 12-10 lists *nine* quark-antiquark combinations, rather than eight, as given by the eightfold way. The ninth meson identified by the quark model as a part of this group, the η', had already been found but had been thought to be a singlet in the eightfold way. Figure 12-20*b* shows the quark-antiquark composition of the first of the several meson nonets, the one illustrated in Figure 12-12*b*.

EXPLORING
Where Does the Proton Get Its Spin?

In the quark model of the hadrons the proton consists of two up quarks and a down quark, *uud*. The electric charge and quantum numbers of the proton, as with the neutron and other composite particles, are correctly given by summing the corresponding quantities for the constituent quarks. For example, the proton's charge is $+(2/3)e + (2/3)e - (1/3)e = +1e$, and its spin is the $+1/2\hbar$ combination of the three spin $1/2\hbar$ quarks. However, a series of deep inelastic scattering experiments of electrons and muons on protons have yielded a surprising result. Begun in 1987 at CERN and continued up to the present there and at Brookhaven National Laboratory (Relativistic Heavy Ion Collider, RHIC) and the Thomas Jefferson National Accelerator Facility, the experiments consist of scattering extremely high-energy (= very short wavelength) muons or electrons whose spins are polarized from protons and ^{3}He nuclei whose spins are also polarized. Measuring the exit angles and energies of the scattered particles is a rich source of information concerning the spin structure of both the proton and the neutron. Surprisingly, the experimental results indicate that the spins of the three constituent, or "valence," quarks account for only 20 to 30 percent of the proton's spin! The experiments show that the spins of the *u* quarks are aligned parallel with the proton's spin, but this is not true for the spin of the *d* quark, which is as one would expect it to be. These results suggest that the orbital angular momentum of the valence quarks and perhaps the spins of the gluons and the "sea" quarks make a significant contribution to the nucleon spin. Aptly called "the proton spin crisis," the results have underscored that our understanding of nucleon structure and quantum chromodynamics (QCD) is incomplete in some important respects.

Nor does the spin crisis stop there. The results also show that the "sea" of virtual quark-antiquark pairs that surround the valence quarks (just as virtual pions surround the nucleons themselves in the nucleus) is strongly polarized with its collective spin direction *opposite* to the proton's net spin. Even more mysterious, the "sea" turns out to contain a significant number of strange (s) quarks. As one scientist put it, there is no simple "gee whiz" explanation for the spin crisis. Several theories have been advanced to account for the discovery, but thus far none have been successful. The spin crisis is currently the focus of vigorous experimental and theoretical research.

EXAMPLE 12-11 Predicting the Properties of Particles What are the properties of the particles made up of the following quarks: (a) $u\bar{d}$, (b) $\bar{u}d$, (c) dds, and (d) uss?

SOLUTION

(a) Since $u\bar{d}$ is a quark-antiquark combination, it has baryon number 0 and is therefore a meson. There is no strange quark here, so the strangeness of the meson is zero. The charge of the up quark is $+2/3e$ and that of the anti-down quark is $+1/3e$, so the charge of the meson is $+1e$. This is the quark combination of the π^+ meson.

(b) The particle $\bar{u}d$ is also a meson with zero strangeness. Its electric charge is $-2/3e + (-1/3e) = -1e$. This is the quark combination of the π^- meson.

(c) The particle dds is a baryon with strangeness -1 since it contains one strange quark. Its electric charge is $-1/3e - 1/3e - 1/3e = -1e$. This is the quark combination for the Σ^- particle.

(d) The particle uss is a baryon with strangeness -2. Its electric charge is $+2/3e - 1/3e - 1/3e = 0$. This is the quark combination for the Ξ^0 particle.

Color In Section 12-1 we briefly introduced the concept of the color charge of the quarks. In this section we will extend that discussion to include some important quark and hadron properties related to color. The quark model as described thus far in Section 12-4, essentially that developed over the decade following the introduction of Gell-Mann's quark hypothesis, contained two significant problems: despite numerous experimental searches, no free quarks had been found, and the model's construction of baryons was inconsistent with the Pauli exclusion principle. For example, the $\Delta^{++}(1232)$ has spin 3/2 and thus contains three u quarks (fermions) with exactly the same set of quantum numbers.

The solution to the exclusion-principle dilemma came from O. W. Greenberg, who postulated that each quark flavor (u, d, and s) came in three *colors* in addition to their other properties. The color charge of a quark has three possible values: *r*ed, *b*lue, and *g*reen. Thus, a blue quark would have blueness $+1$, redness 0, and greenness 0, and its antiquark would have blueness -1, and so on. The terms "color" and "color charge" are, of course, simply labels to describe a quark property analogous to electric charge and are in no way related to the usual meanings of the words. The use of the three primary colors for this purpose did, however, provide a very simple rule to ensure that the exclusion principle was obeyed:

All particles that occur in nature are colorless.

The term "colorless" means that either

1. The total amount of color (i.e., the sum of the color quantum numbers) is zero, or
2. There are equal amounts of all three colors present (in analogy with the combining of the three primary colors to produce white).

Thus, for example, the three up quarks that compose the $\Delta^{++}(1232)$ are one each of u_r, u_b, and u_g.

The J/ψ Puzzle The solution provided by color seemed an artificial one, as did the explanation for seeing no free quarks described in the next subsection, but strong support for the model came late in 1974 from an unexpected quarter. Two groups independently discovered a new meson. The first, S. Ting and his co-workers at Brookhaven, called it the J, while the second group, B. Richter and his co-workers at SLAC,[18] called it the ψ. Now referred to as the J/ψ, the new meson had three times the mass of the proton and a lifetime of 10^{-20} s, extraordinarily long for a strongly interacting particle. The exceptionally long lifetime pointed to new physics,[19] and within months after its discovery it was recognized that the J/ψ was composed of a fourth quark and its antiquark. The fourth quark, which had been proposed by S. Glashow and others for compelling theoretical reasons some years earlier so as to make equal numbers of quarks and leptons (before the discovery of the τ and ν_τ), is called the *c*harm quark and $J/\psi = (c\bar{c})$.[20] Discovery of the first charm baryon, the Λ_C^+, is shown in Figure 12-21. Figure 12-22

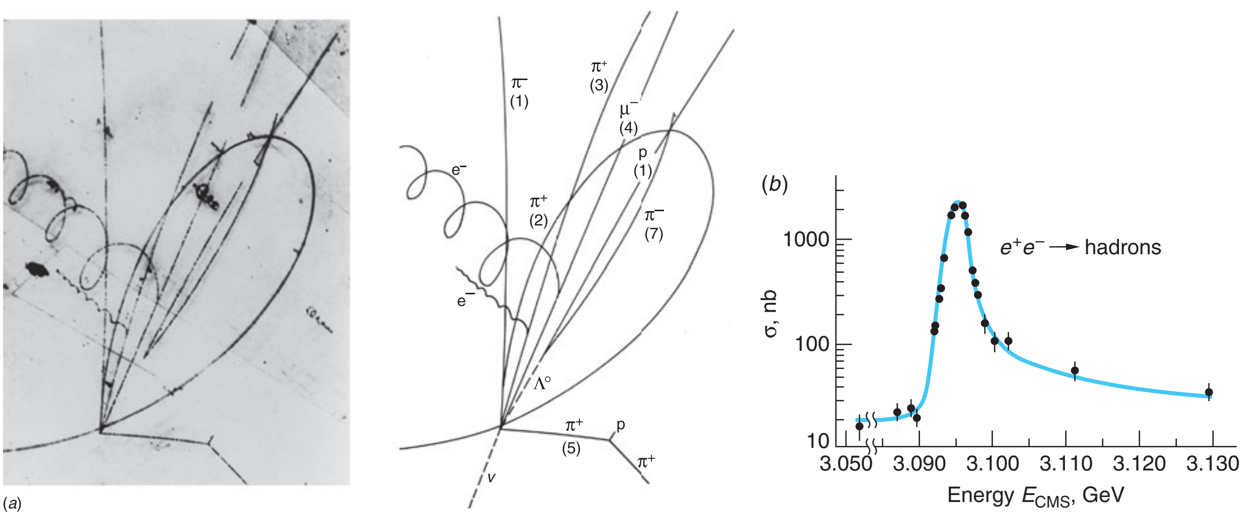

Figure 12-21 (*a*) Discovery of the first charm baryon, the Λ_c^+. The reaction is $\nu_\mu + p \rightarrow \Lambda_c^+ + \mu^- + \pi^+ + \pi^-$. The charm baryon decays via $\Lambda_c^+ \rightarrow \Lambda^0 + \pi^+$ too soon to leave a track, but the subsequent decay of the Λ^0 is easily seen. [*Brookhaven National Laboratory.*] (*b*) A portion of the experimental data obtained by B. Richter and his co-workers at SLAC showing the J/ψ resonance.

shows some supermultiplets formed with four quarks. This discovery made two nicely symmetric sets of four leptons (e, ν_e, μ, ν_μ) and four quarks (u, d, s, c) and, of course, their antiparticles. Then in 1975 a new lepton was found! The new lepton, the τ, presumably had an associated neutrino, the ν_τ, and the numerical symmetry of the generations of particles was again upset. But within two years a new heavy meson, the upsilon Υ, was discovered and quickly recognized as being composed of a fifth quark-antiquark pair. The fifth quark is called the *b*ottom (or sometimes *b*eauty) quark, and $\Upsilon = (b\bar{b})$. The theory then predicts a sixth quark, called, as you might guess, the *t*op (or *t*ruth) quark. The t quark was found in 1995 by two groups at Fermilab, thus restoring Glashow's symmetry of fundamental quarks and leptons and completing the new periodic table of the constituents of fundamental particles. (See Figure 12-23.) At 176 MeV/c^2, the t quark is the most massive fundamental particle that has been discovered. There are substantial theoretical and experimental reasons to believe that there are no more quarks or leptons to be found. (See Figure 12-24.) Table 12-5 lists the up, down, strangeness, charm, top, and bottom internal quantum numbers for the six flavors of quarks and their antiquarks.

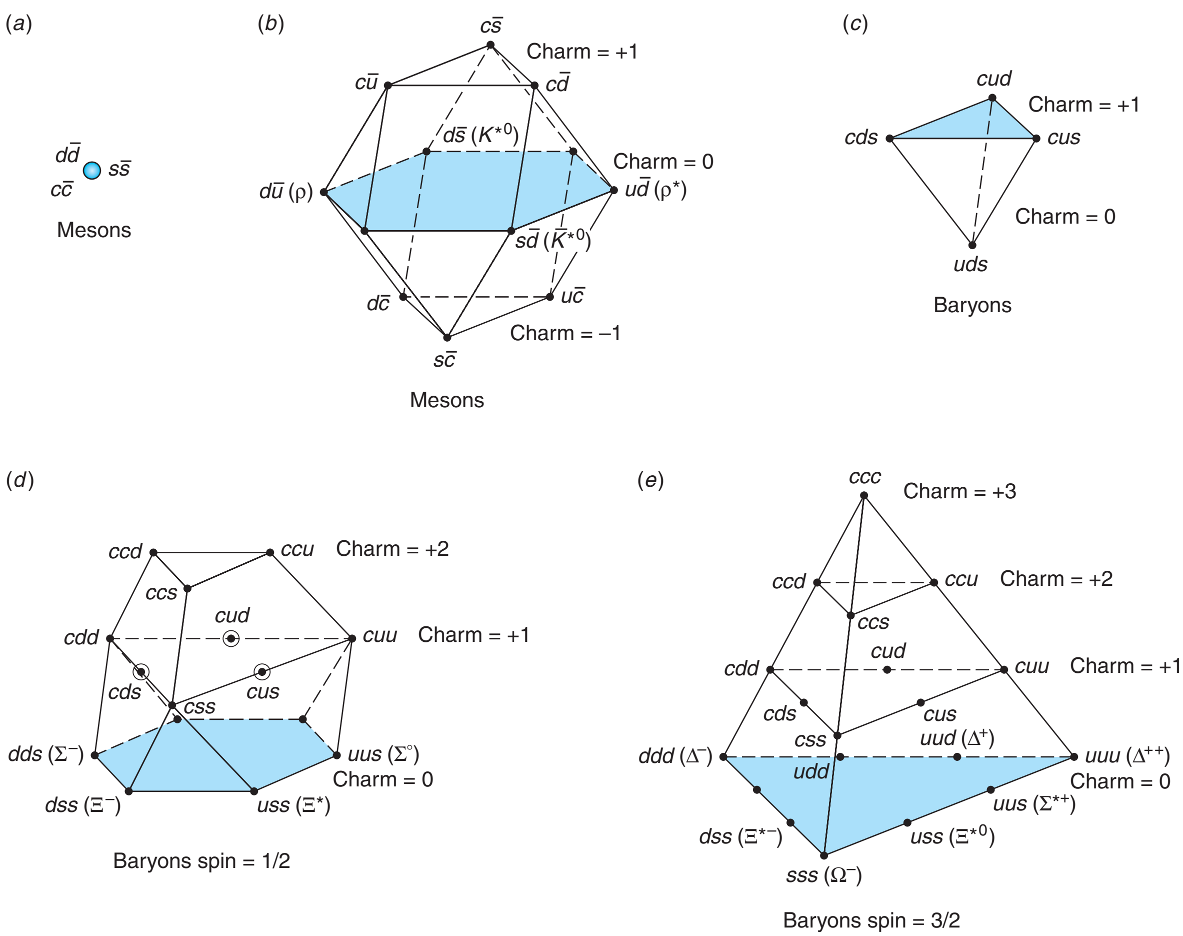

Figure 12-22 Supermultiplets formed from u, d, s, and c quarks. The circles indicate that there are two particles with the same quark composition and different energies.

Charge	First generation	Second generation	Third generation
		Quarks	
+2/3	u_r u_b u_g	c_r c_b c_g	t_r t_b t_g
−1/3	d_r d_b d_g	s_r s_b s_g	b_r b_b b_g
		Leptons	
−1	e	μ	τ
0	ν_e	ν_μ	ν_τ

Figure 12-23 Periodic table of elementary particle constituents.

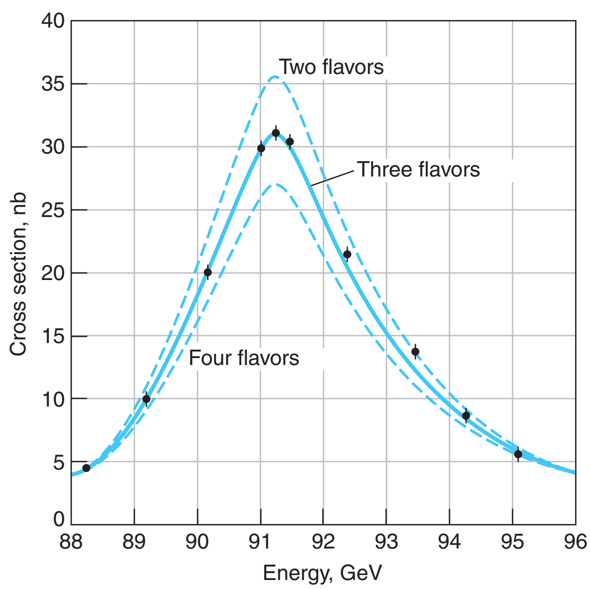

Figure 12-24 Both the shape and height of Z^0 resonance are theoretically related to the number of flavors of the leptons and quarks. As that number increases, the maximum cross section decreases and the energy width (at half the maximum height) becomes larger. Current measurements, shown by the black circles, are fully consistent with three flavors, or generations, excluding both two and four.

Quantum Chromodynamics

Quantum chromodynamics (QCD) is the modern theory that describes the strong interaction between quarks and gluons. It is directly analogous to quantum electrodynamics (QED), which so successfully accounts for the electromagnetic interaction. Indeed, QCD was modeled on QED. As stated earlier, the particle (boson) that mediates the strong quark-quark interaction is the gluon and the fundamental process (analogous

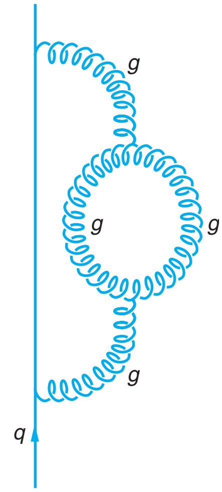

Figure 12-26 Feynman diagram of a quark emitting a gluon, which then creates two gluons that recombine, the resulting gluon being absorbed by the quark.

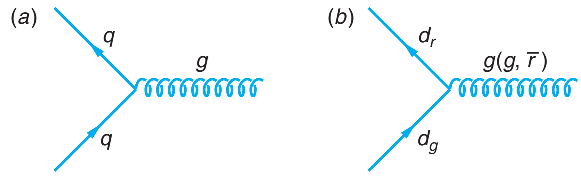

Figure 12-25 (*a*) The fundamental vertex of QCD, in which a quark emits a virtual gluon. (*b*) Since gluons carry a color and an anticolor, the emission of the gluon may also change the color of the quark.

to $e \longrightarrow e + \gamma$ shown in Figure 12-4) is illustrated by the Feynman diagram in Figure 12-25*a*. The gluons are the QCD analog of the photon in QED. Like photons, they are massless and have spin 1; however, there is one crucial difference between the two particles. The gluons carry color charge, whereas the photon is electrically neutral. In fact, the gluons are bicolored, carrying one unit of a color charge and one of an anticolor charge and hence are not color neutral. Thus, in the process $q \longrightarrow q + g$ the quark may change color (but not flavor), as shown in Figure 12-25*b*. Since the gluons carry net color charge, they can also interact with each other via the strong interaction *and* they form an octet in the SU(3) group theory representation, just as do the mesons.[21] This means that, in addition to the increase in the strong interaction coupling constant α_s at very short distances analogous to the vacuum polarization in QED discussed in Section 12-2 and shown in Figure 12-10, there are also gluon-gluon loops, as shown in Figure 12-26. The effect of such gluon loops is to, in a sense, dilute the strong force and decrease the value of the strong interaction coupling constant α_s at extremely short distances ($\lesssim 10^{-18}$ m). As it turns out, this latter effect predominates at very small quark separations. As a pair of quarks move extremely close to each other, their coupling decreases, a condition called *asymptotic freedom*. The result is that inside the nucleon, the quarks move more or less as free particles, a phenomenon that has been confirmed by electron deep scattering experiments. Indeed, hundreds of experiments have confirmed the property of asymptotic freedom.

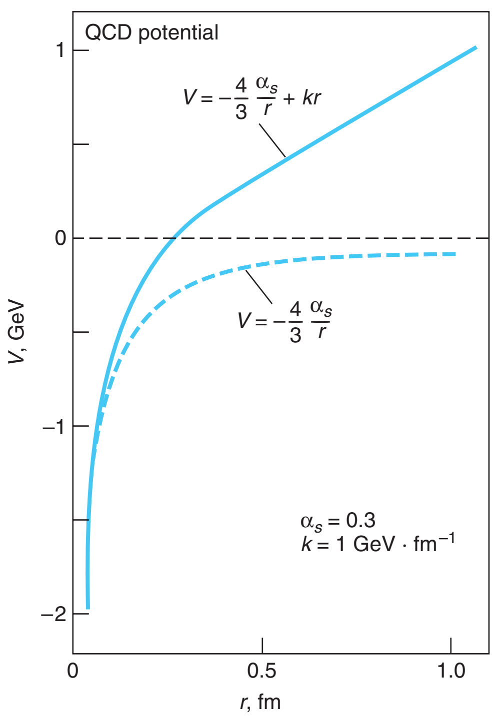

Figure 12-27 The potential seen by quarks in QCD. In this diagram the strong coupling constant $\alpha_s = 0.3$ and $k = 1$ GeV/fm in Equation 12-29.

One of the possible potential functions for the strong interaction has the approximate form

$$V_{\text{QCD}}(r) = -\frac{4\alpha_S}{3r} + kr \qquad \textbf{12-32}$$

It has been reasonably well tested experimentally at short distances. Notice that V_{QCD} increases indefinitely with r (see Figure 12-27), that is, the strong force at large r, $F_{\text{QCD}} = -\nabla V_{\text{QCD}} =$ constant, rather than going to zero, as do the Coulomb and gravitational forces. The result is to prevent the quarks from getting too far apart, effectively containing them inside the hadrons, a phenomenon called *quark confinement*. This is the QCD explanation for why free quarks have not yet been found. When a large amount of energy is added to a quark system such as a nucleon, a quark-antiquark pair is created and the original quarks remain confined within the original system. This is the origin of the virtual pions that were postulated by the Yukawa model of the nuclear force as the mediator of that interaction. (See Figure 12-28.)

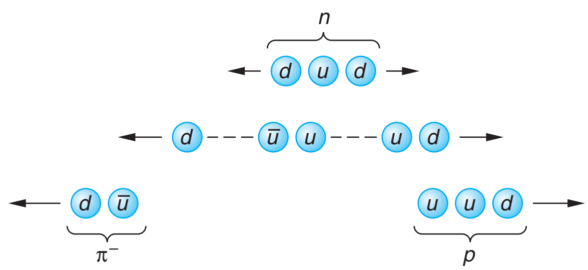

Figure 12-28 Shown is one possible illustration of quark confinement. If energy is added to remove a d quark from a neutron, a $(\bar{u}, u)$ pair is created. The $\bar{u}$ and one of the d quarks combine to form a π^-, while the u from the pair and the original u and d combine to produce a proton and no free quark appears.

During particle decays and interactions quarks transform into one another. For example, the β^-decay of the neutron given by Equation 11-38 proceeds according to the quark model in which a d quark turns into a u quark, as illustrated by Example 12-4. All baryons eventually decay in one or more steps to the lightest (lowest-energy) baryon, the proton. The decay of the proton is prohibited by conservation of energy and baryon number, but searches for proton decay are continuing. Example 12-12 illustrates the decay of another baryon, the Λ^0.

Questions

13. How can you tell whether a particle is a meson or a baryon by looking at its quark content?
14. Are there any quark-antiquark combinations that result in nonintegral electric charge?
15. What experimental evidence exists to support the assertion that natural particles are colorless?

EXAMPLE 12-12 Decay of Λ^0 Draw a Feynman diagram that shows the quarks involved in the decay of the Λ^0, which goes according to

$$\Lambda^0 \longrightarrow pe^-\bar{\nu}_e$$

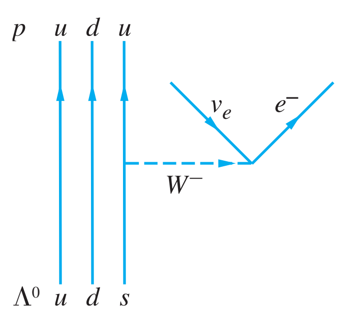

SOLUTION

From Table 12-10 we see that the Λ^0 is composed of a u quark, a d quark, and an s quark. The proton consists of two u quarks and a d quark. The decay results from the weak interaction, the s quark decaying to a u quark and a W^-. Note that strangeness is not conserved in the weak interaction that transforms the s quark into the u quark.

Table 12-11 Quark composition of selected particles

Baryons	Quarks	Mesons	Quarks
p	uud	π^+	$u\bar{d}$
n	udd	π^-	$\bar{u}d$
Λ^0	uds	K^+	$u\bar{s}$
Δ^{++}	uuu	K^0	$d\bar{s}$
Σ^+	uus	$\bar{K}^0$	$s\bar{d}$
Σ^0	uds	K^-	$s\bar{u}$
Σ^-	dds	J/ψ	$c\bar{c}$
Ξ^0	uss	D^+	$c\bar{d}$
Ξ^-	dss	D^0	$c\bar{u}$
Ω^-	sss	D_s^+	$c\bar{s}$
Λ_c^+	udc	B^+	$u\bar{b}$
Σ_c^{++}	uuc	$\bar{B}^0$	$d\bar{b}$
Σ_c^+	udc	B^0	$d\bar{b}$
Ξ_c^+	usc	B^-	$\bar{u}b$


(*a*)


(*b*)


(*c*)

Figure 12-29 The plastic strip in (*a*) has left-right symmetry. Increased vertical force on the ends of the strip breaks the symmetry, causing the strip to take one or the other of the positions (*b*) or (*c*), neither of which has left-right symmetry.

The Electroweak Theory

In the *electroweak theory*, the electromagnetic and weak interactions are considered to be two different manifestations of a more fundamental electroweak interaction. At very high energies ($\gg 100$ GeV), the electroweak interaction is mediated by four bosons. From symmetry considerations, these would be a triplet consisting of W^+, W^0, and W^-, all of equal mass, and a singlet boson B^0 of some other mass. Neither the W^0 nor the B^0 would be observed directly, but one linear combination of the W^0 and the B^0 would be the Z^0, and another would be the photon. At ordinary energies, the symmetry is spontaneously broken.

By "spontaneously broken symmetry" we mean the following: the Hamiltonian H_{op} retains the complete symmetry, but the ground state computed from that H_{op} does not, or, as we say, the symmetry is broken. For example, magnetism in solids arises due to interaction of the spins of the atoms of the crystal lattice. For a ferromagnet, such as iron, the H_{op} describing that interaction is invariant under rotation, but in the ground state magnetic domains are spontaneously formed in the sample. The spin direction changes from domain to domain but is the same inside each domain. A domain is certainly not invariant to a rotation of the spins. Thus, the ground state spontaneously breaks the rotational symmetry. (To further help you visualize what "spontaneously broken symmetry" means, think of a small plastic strip, like a short ruler, gripped at the ends between your thumb and index finger. As you squeeze, the strip will snap into a curve to one side or the other, breaking the original left-right symmetry. See Figure 12-29.)

The broken symmetry in the electroweak interaction leads to the separation of the electromagnetic interaction mediated by the photon and the weak interaction mediated by the W^+, W^-, and Z^0 particles. The fact that the photon is massless and that the W and Z particles have masses of the order of 100 GeV$/c^2$ shows that the symmetry assumed in the electroweak theory does not exist at lower energies. The symmetry-breaking agent is called a *Higgs field*, which requires a new boson, the *Higgs boson*, whose rest energy is expected to be of the order of 1 TeV (1 TeV = 10^{12} eV). According to the Standard Model, it is by interacting with the Higgs field that particles acquire their masses. The Higgs boson has not yet been observed. Calculations show that Higgs bosons (if they exist) should be produced in a head-on collision between protons of energies of the order of 20 TeV. While such energies are not available with existing accelerators, the Large Hadron Collider, which began operation at CERN in 2008, will be able to reach and exceed that energy by accelerating beams of a variety of nuclei. Searching for the Higgs boson is a primary goal for the LHC.

The Standard Model—A Summary

The *Standard Model* is the theoretical model of elementary particles and their interactions. It is based on a combination of the quark model, electroweak theory, and quantum chromodynamics. In this model, the fundamental particles are the leptons and quarks, each of which comes in three generations, as shown in Tables 12-1 and 12-2. The force carriers are the photon, the $W^\pm$ and Z^0 particles, and eight types of gluons. The leptons and quarks are all spin-1/2 fermions, which obey the Pauli exclusion principle. The force carriers are integral-spin bosons, which do not obey the Pauli exclusion principle. Every force in nature is due to one of the four basic interactions: strong, electromagnetic, weak, and gravitational. A particle experiences one of the basic interactions if it carries a charge associated with that interaction. Electric charge is the familiar charge that you have studied previously. It is carried by the quarks and charged leptons. Weak charge, also called flavor charge, is carried by leptons and quarks. The charge associated with the strong interaction is called color charge and is carried by quarks and gluons but not by leptons. The charge associated with the gravitational force is mass. It is important to note that the photon, which mediates the electromagnetic interaction, does not carry electric charge. The $W^\pm$ and Z^0 particles, which mediate the weak interaction, do carry weak charge, and the gluons, which mediate the strong interaction, carry color charge. This latter fact is related to the confinement of quarks.

All matter is made up of leptons and quarks. There are no known composite particles consisting of leptons bound together by the weak force. Leptons exist only as isolated particles. Hadrons (baryons and mesons) are composite particles consisting of quarks bound together by the color charge. A result of the QCD theory is that only color-neutral combinations of quarks are allowed. Three quarks of different colors can combine to form color-neutral baryons, such as the neutron and proton. Mesons contain a quark and an antiquark and are also color neutral. Excited states of hadrons are considered to be different particles. For example, the Δ^{++} particle is produced by $\pi^+ p \rightarrow \Delta^{++}$. The Δ^{++} must have the exact same set of internal quantum numbers as the $\pi^+ p$: $B = 1, C = S = T = B' = 0$, which from Equations 12-26 and 12-27 means $Y = 1$ and $I_3 = 3/2$. The three u quarks can be in the same spin state in the Δ^{++} without violating the exclusion principle because they have different colors.

The strong interaction can manifest itself in two ways: the fundamental, or color, interaction and the *residual strong interaction*. The fundamental interaction is responsible for the force exerted by one quark on another and is mediated by gluons.

The residual strong interaction is responsible for the force between color-neutral nucleons, such as the neutron and proton. This force is due to the residual strong interactions between the color-charged quarks that make up the nucleons and can be viewed as being mediated by the exchange of mesons. The residual strong interaction between color-neutral nucleons is analogous to the residual electromagnetic interaction between neutral atoms that bind them together to form molecules.

For each particle there is an antiparticle. A particle and its antiparticle have identical mass and spin but opposite electric charge. For leptons, the leptons numbers L_e, L_μ, and L_τ of the antiparticles are the negatives of the corresponding numbers for the particles. For example, the lepton number for the electron is $L_e = +1$ and that for the positron is $L_e = -1$. For hadrons, the baryon number, strangeness, charm, topness, and bottomness are the sums of those quantities for the quarks that make up the hadron. The number for each antiparticle is the negative of the number for the corresponding particle. For example, the lambda particle Λ^0, which is made up of the uds quarks, has $B = 1$ and $S = -1$, whereas its antiparticle, $\overline{\Lambda}^0$, which is made up of the $\overline{uds}$ quarks, has $B = -1$ and $S = +1$. Particles such as the photon γ and the Z^0 that have zero electric charge, $B = 0$, $L = 0$, $S = 0$ and zero charm, top, and bottom, are each their own antiparticle. Note that the K^0 meson ($d\bar{s}$) has a zero value for all of these quantities except strangeness, which is $+1$. Its antiparticle, the $\overline{K}^0$ meson ($\bar{d}s$), has strangeness -1, which makes it distinct from the K^0. The π^+ ($u\bar{d}$) and π^-($\bar{u}d$) have electric charge but zero values for L, B, and S. They are antiparticles of each other, but since there is no conservation law for mesons, it is impossible to say which is the particle and which is the antiparticle. Similarly, the W^+ and W^- are antiparticles of each other. Table 12-11 lists the quark compositions of several particles.

EXAMPLE 12-13 Decay of the Ω^- The Ω^- decays according to the equation

$$\Omega^- \longrightarrow \Lambda^0 + K^-$$

and the resulting Λ^0 and K^- usually decay according to

$$\Lambda^0 \longrightarrow p + \pi^- \quad \text{and} \quad K^- \longrightarrow \mu^- + \bar{\nu}_\mu$$

Write each of these reactions in terms of quarks.

SOLUTION

Using Table 12-11, the Ω^- decay is given by

$$sss \longrightarrow uds + s\bar{u}$$

in which an s is changed to a d and a $u\bar{u}$ pair is created. The Ω^0 and K^- decay according to, for the Λ^0,

$$uds \longrightarrow uud + \bar{u}d$$

where again an s is changed to a d and a $u\bar{u}$ pair is created, and for the K^- meson,

$$s\bar{u} \longrightarrow \mu^- + \bar{\nu}_\mu$$

where the s and u annihilate, producing a W^-, which decays to the leptons.

12-5 Beyond the Standard Model

Grand Unification Theories

At the beginning of Section 12-4 we noted that the Standard Model of particle physics, while correctly accounting for a wide range of observations, has left a number of fundamental questions unanswered. Of premier importance among these are why nature requires four interactions rather than one and why their strengths and properties should be so different. The successful unification of the electromagnetic and weak interactions into the electroweak theory discussed earlier has led to a number of efforts to include the strong interaction and, ultimately, the gravitational interaction into a single, so-called *grand unification theory*, or GUT.[22] As in the electroweak theory, the different strengths at energies well below the rest energies of the mediating bosons would be accounted for by spontaneous symmetry breaking. GUTs also explain the equality of the electron and proton charges.

A central feature of current GUTs is that the coupling constants of all four interactions approach the same value, approximately that of the fine-structure constant α, at some very high energy. It is a remarkable experimental observation that the measured values of the coupling constants do appear to be tending toward a common value. Unfortunately, extrapolation to the common point must be made over an extraordinarily large energy range, that point of common value being at about 10^{16} GeV, compared with about 10^4 GeV that can be reached with the largest existing accelerator, the LHC at CERN. (See Figure 12-30.) To assume that nature has no surprises or new physics to await us somewhere in that colossal energy range ignores the lessons of history.

Supersymmetry (SUSY)

A number of GUTs include a proposed new symmetry in addition to the symmetries we have discussed. Called *supersymmetry* (with the acronym SUSY), it assigns to each elementary particle a *superpartner*. The superpartner is in every way identical to the particle except for its spin. The leptons and quarks, both spin-1/2 fermions, have

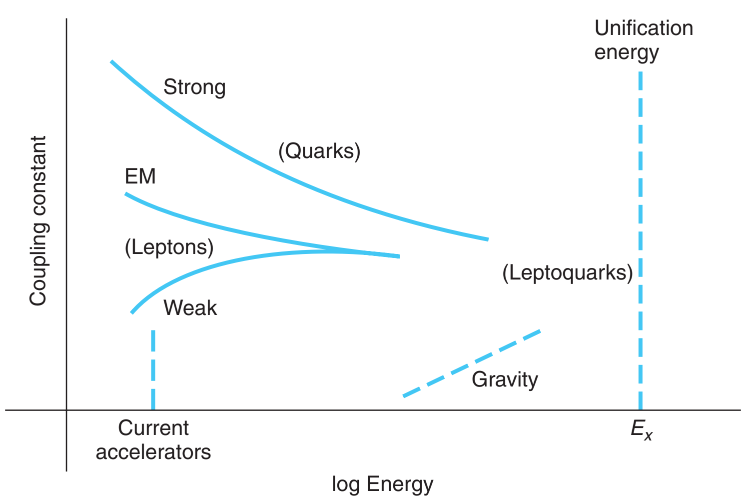

Figure 12-30 The coupling constants of the four interactions appear to be approaching a common value at some energy in the range 10^{16} to 10^{18} GeV. Since the largest existing accelerator, the Large Hadron Collider at CERN, can reach only about 14 TeV, the extrapolation to the unification energy E_x is highly uncertain.

Table 12-12 Elementary particle and their superpartners

Particle	Symbol	Spin	Superpartner	Symbol	Spin
Quark	q	1/2	Squark	q	0
Electron	e	1/2	Selectron	e	0
Muon	μ	1/2	Smuon	μ	0
Tau	τ	1/2	Stau	τ	0
W	W	1	Wino	W	1/2
Z	Z	1	Zino	Z	1/2
Photon	γ	1	Photino	γ	1/2
Gluon	g	1	Gluino	g	1/2
Higgs	H	0	Higgsino	H	1/2

superpartners with spin 0. The spin-1 bosons have spin-1/2 superpartners. The superpartners of the fermions are given the same names with a prefix *s*; e.g., the electron's superpartner is the selectron. The superpartners of the bosons have the same names with a suffix *ino* added (sort of), e.g., the gluon's superpartner is the gluino. The particles and their superpartners are listed in Table 12-12.

Exact supersymmetry would equate the masses of the particles and their superpartners. However, this is apparently not true in nature or the superpartners would have been detected long ago. So SUSY is modified to account for that absence by postulating that the mass of the lightest superpartner would be very large indeed, of the order of the masses of the $W^{\pm}$ and the Z^0 bosons. Doing so ultimately predicts the GUT unification energy in the vicinity of the current extrapolated projections, predicts the proton lifetime in agreement with current experimental limits, and keeps the GUT unification coupling constant in line with current extrapolations. An important goal of the Large Hadron Collider is to test predictions of supersymmetry.

SUSY is also a component of current theories designed to include gravity within GUTs. These are the *string* and *superstring theories*. String theories replace pointlike elementary particles with tiny, quantized strings and require 10 or more dimensions. Their purpose is to surmount current theoretical problems in quantizing gravity. Currently, particle physicists are sharply devided over string theories, some heralding them as the "theory of everything," others dismissing them as "not even wrong." As of this date, there is no experimental evidence supporting any of the string theories.

Proton Decay

In GUTs the quarks and leptons are states of one particle, the leptoquark, and occur symmetrically in the same multiplet. This would account for why there are equal numbers of quark and lepton flavors and also lead to the prediction that each type of particle can be changed into the other. If that is the case, then baryon number is no longer a conserved quantity and the proton should not be stable. Current versions of GUTs place the lifetime of the proton at about 10^{30} to 10^{33} years, the long lifetime being the result of the large energy at which unification of the interactions occurs.

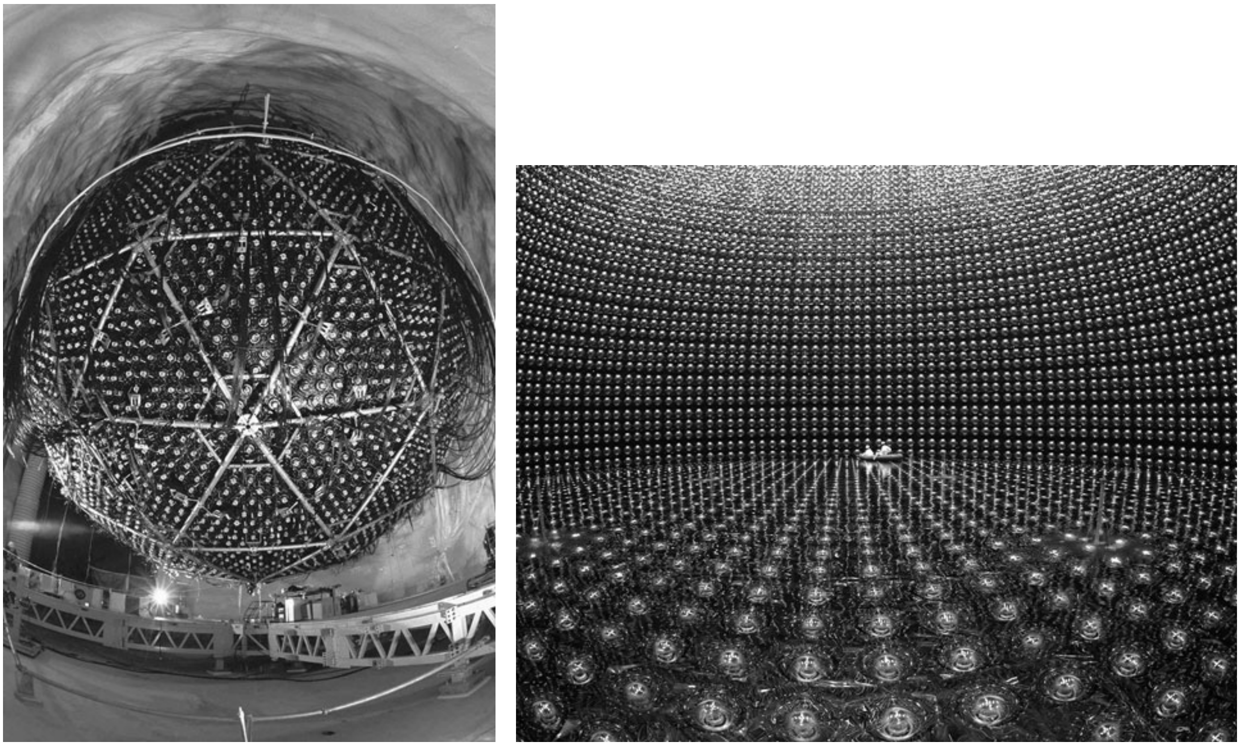

(*a*) (*b*)

The Sudbury Neutrino Observatory (SNO) in Canada and the Super-Kamiokande (Super-K) neutrino detector in Japan collected data on neutrino interactions that confirmed neutrino oscillations. (*a*) The SNO neutrino detector is a spherical acrylic vessel 12 m in diameter and contains 1000 metric tons of ultrapure heavy water (D_2O) located 2000 m below ground. Čherenkov light produced by neutrino reactions in the water is viewed by 9456 photomultipliers, each 20 cm in diameter. (*b*) The Super-K neutrino detector, a cylindrical structure 41 m tall and 39 m in diameter, contains 45,000 metric tons of pure water (H_2O) viewed by 11,200 photomultipliers. [*(a) Courtesy of Sudbury Neutrino Observatory; (b) courtesy of Kamioka Observatory, University of Tokyo.*]

Current experiments have placed the lower limit on the proton lifetime at about 10^{32} years; to date, no proton decays have been detected. Searches for proton decay, such as that at Super-Kamiokande, generally involve monitoring very large volumes of pure water, watching for one of the several possible proton decay "signatures"; e.g., $p \rightarrow \pi^0 e^+$ or $p \rightarrow \pi^+ \bar{\nu}_e$. The nonconservation of baryon number in the early universe when energies were very high provides an explanation of a major cosmological problem, namely, why the present universe has many more baryons than antibaryons.

Lepton numbers would no longer be conserved at the unification energy, and currently forbidden reactions such as $\mu^- \rightarrow e^- + \gamma$ and $\mu^+ \rightarrow e^+ + e^+ + e^-$ would be allowed. Experimental searches have been made, but no lepton-number-nonconserving events have been found.

Massive Neutrinos

From the time Pauli first suggested their existence in 1930, neutrinos were thought to have zero mass. Then, based on Bahcall's theoretical calculation of the solar neutrino flux and Davis's remarkable measurement[23] of the flux at only about 30 percent of Bahcall's prediction, the *solar neutrino problem* emerged (see Section 11-8). Its recent solution through the detection of neutrino oscillations by the Sudbury Neutrino

Observatory (SNO) and Super-Kamiokande (Super-K) experiments gives support to GUTs since most GUTs require that neutrinos have mass. The theories predict their mass to be given approximately by

$$m_\nu \approx \frac{M_{eW}^2}{M_x} \qquad \textbf{12-33}$$

where M_{eW} is a characteristic mass of the electroweak interaction, roughly 10^2 GeV/c^2, and M_x is the unification mass $E_x/c^2 \approx 10^{16}$ GeV/c^2 (see Figure 12-30). Nearly all GUTs project M_x values of this order of magnitude, which in turn means that all neutrinos would have m_ν less than about 1 eV. The theories also predict $m(\nu_e) \ll m(\nu_\mu) \ll m(\nu_\tau)$. The impact of massive neutrinos on both the solar neutrino problem described briefly in Chapter 11 and the universe's "missing energy" (or "missing mass") problem discussed in Chapter 13 is substantial. S. Mikheyev, A. Smirnov, and L. Wolfenstein proposed a solution to the solar neutrino problem in particular in which an ν_e can oscillate to a ν_μ or ν_τ while propagating through the Sun's mass. For this complex process, called the *MSW effect*, to occur, the neutrino wave functions $\psi(\nu_e)$, $\psi(\nu_\mu)$, and $\psi(\nu_\tau)$ must each consist of superpositions of the three mass states. Similar processes can be described for neutrinos moving through space and the atmosphere. (See Exploring, Neutrino Oscillations and Mass.) The relative phases of the mass states may change for two reasons. (1) In passing through the solar matter (electrons and protons), the three mass states scatter differently; hence their relative phases change. (2) While propagating through space and the atmosphere, the mass states move at different speeds, which also results in a change in the relative phase. The phase changes result in interference of the neutrino matter waves, and as a consequence a neutrino emitted in the Sun as a ν_e may oscillate to a ν_μ or ν_τ before reaching Earth and therefore not be detected by experiments searching for electron neutrinos. Experimental evidence supporting the existence of oscillations was provided by the SNO and Super-K measurements.

Magnetic Monopoles

Magnetic monopoles, first suggested by Dirac in 1929, are also proposed by GUTs. Dirac showed that their existence in relativistic quantum mechanics leads to the quantization of both the electric charge e and the magnetic charge q_m. The magnetic charge of a monopole would be

$$q_m = n\frac{\hbar c}{2e} \quad \text{for } n = 1, 2, 3, \ldots \qquad \textbf{12-34}$$

It is important to note that $q_m^2/\hbar c \approx \hbar c/e^2 \propto 1/\alpha$. In the unified theories the quantization of electric charge occurs naturally in units of e, and magnetic monopoles of charge q_m and mass M_m are then predicted. The predicted values of M_m are very large, about 10^{16} GeV/c^2, far beyond the energy achievable in any accelerator. Cosmic ray searches for monopoles place an upper limit on their flux at about 10^{-15} cm^{-2} s^{-1} per unit solid angle. Coincidentally, this value corresponds approximately to the maximum flux that could exist in the Milky Way without having long since destroyed the galactic magnetic field. As of this writing, only a single possible observation of a magnetic monopole has been reported in the literature, by B. Cabrera in 1982. This observation is inconsistent with current limits.

Quantum Gravity

The addition of quantum gravity to grand unified theories is a formidable task. Called *superstring theories* because of their basic view of fundamental particles as strings rather than points, perhaps the most promising of the current versions is based on a 10-dimensional universe (nine space and one time dimension) in which six of the space dimensions have been collapsed or curled up on themselves. The string "lengths" are much shorter than can be measured, about 10^{-35} m. Besides the inclusion of quantum gravity, superstring theories also produce the *gauge theories*[24] with the correct mediating bosons; however, although they are the subject of considerable interest to theoretical physicists, there is as yet no experimental support for these theories, and it is not clear to what extent, if any, they represent physical reality.

Many questions are still unanswered. For example, do the quarks have internal structure? What is the origin of isospin? There is some indication that hadrons are surrounded by a "sea" of virtual quark-antiquark pairs. What is their role? Is the fractional charge of the quarks related to color? Investigating these problems experimentally will require new, higher-energy accelerators and more advanced detectors than currently exist anywhere in the world. Obviously, there is much to be done.

EXPLORING
Neutrino Oscillations and Mass

Quantum mechanics requires that, if neutrinos oscillate from one type, or flavor, to another, then they must have mass, whether they originate in the Sun, the atmosphere, a nuclear power reactor, an accelerator, or somewhere else in the cosmos. While the detailed justification of this requirement is beyond the scope of our discussions, an outline of why this must be true is presented here. The relationship between neutrino (flavor) wave functions and the mass eigenfunctions is given by

$$\psi_\alpha = \sum_i U^*_{\alpha i}\,\psi_i \qquad \psi_i = \sum_\alpha U_{\alpha i}\,\psi_\alpha \tag{12-35}$$

where ψ_α are the wave functions of the neutrino flavors ($\alpha = \nu_e, \nu_\mu, \nu_\tau$), ψ_i are the mass eigenfunctions ($i = \nu_1, \nu_2, \nu_3$), and $U_{\alpha i}$ (and its complex conjugate) is a function that describes the extent to which mixing of the flavors or masses occurs, i.e., the phases of the oscillations. Note that, if there were no oscillations, $U_{\alpha i} = 1$ and the ψ_α would equal the mass eigenfunction for ν_α; however, the experiments noted above show that $U_{\alpha i} \neq 1$. The states with different mass eigenfunctions propagate at different speeds, the less massive moving faster than the more massive ones. Since the mass eigenfunctions are combinations of neutrino (flavor) wave functions, the difference in speeds results in interference between the neutrino waves in each mass eigenfunction. When, eventually, constructive interference occurs, one neutrino flavor has changed into another.

The mass eigenfunctions are plane wave solutions of the time-dependent Schrödinger equation. (See Equation 6-7.)

$$\psi_i(x, t) = e^{i(px - Et)/\hbar} \tag{12-36}$$

The dependence of the energy on the mass is given by Equation 2-31 and the extremely relativistic approximation of Equation 2-36

$$E = \sqrt{(pc)^2 + (mc^2)^2} \qquad \textbf{2-31}$$

written as

$$E = (pc)\left[1 + \frac{(mc^2)^2}{(pc)^2}\right]^{1/2}$$

Since for each of the neutrinos under discussion the total energy $E \gg mc^2$, the binomial expansion allows us to write

$$E \approx pc + \frac{(mc^2)^2}{2pc} + \ldots \qquad \textbf{12-37}$$

After time t moving at $v \approx c$, the neutrino has traveled a distance $x \approx ct = L$ and the mass wave functions become

$$\psi_i(L) = e^{-\frac{iL}{\hbar c}\frac{(mc^2)^2}{2E}}\psi_i(0) \qquad \textbf{12-38}$$

and the probability that a neutrino of flavor α at $t = 0$ will be observed to have changed or oscillated to flavor β is given by

$$P_{\alpha\rightarrow\beta} = |\psi_\beta\psi_\alpha|^2 = \left|\sum_i U^*_{\alpha i}U_{\beta i}e^{-\frac{iL}{\hbar c}\frac{(mc^2)^2}{2E}}\right|^2 \qquad \textbf{12-39}$$

If we confine our attention to the two-neutrino case (the three-neutrino case is more complex to describe), Equation 12-39 becomes (after some work!)

$$P_{\alpha\rightarrow\beta,\,\alpha\neq\beta} = \sin^2 2\theta\,\sin^2\!\left(1.267\frac{\Delta m^2 L}{E}\frac{\text{GeV}}{\text{eV}^2\text{km}}\right) \qquad \textbf{12-40}$$

where θ is the neutrino mixing angle and Δm is the difference in the masses of the two neutrinos. Although Equation 12-40 applies to a two-neutrino world, its is a decent approximation for the $\nu_\mu \leftrightarrow \nu_\tau$ oscillations in the atmosphere since electron neutrinos do not contribute significantly in this case. It is also reasonable for solar electron neutrinos oscillating to superpositions of ν_μ and ν_τ.

From Equation 12-40 we now can see why flavor-changing neutrinos must have mass. Since experiments show that $P_{\alpha\rightarrow\beta} \neq 0$ and measure for solar neutrinos $\theta(\nu_e, \nu_\mu) = 33.9°\ (\neq 0)$ and for atmospheric neutrinos $\theta(\nu_\mu, \nu_\tau) = 45°$, then in both cases $\Delta m^2 \neq 0$. Thus, *neutrinos have mass*. The current values of Δm^2 are

$$\Delta m^2_{\text{solar}} = 8.0 \times 10^{-5}\ \text{eV}^2$$

$$\Delta m^2_{\text{atmo}} = 2.4 \times 10^{-3}\ \text{eV}^2$$

More

GUTs aren't the only avenue being actively explored by physicists in search of a deeper understanding of the structure of matter than we now have. The so-called *Theories of Everything* that seek to account for all of physics within a single theoretical construct are highly speculative, and none yet have any experimental support. On the home page at www.whfreeman.com/tiplermodernphysics5/e.

Summary

TOPIC	RELEVANT EQUATIONS AND REMARKS
1. Particles and antiparticles	Each fundamental particle found in nature has an antiparticle; some are distinct, e.g., the electron and positron; some are the antiparticles of themselves, e.g., the photon.
Feynman diagrams	These are spacetime diagrams that provide a useful way of visualizing interactions between particles—for example, Coulomb repulsion of like charges.
Leptons and quarks	All visible matter is made of two types of elementary particles, leptons and quarks, each consisting of three generations.
2. Fundamental interactions Force carriers	1. Strong interaction—gluons 2. Electromagnetic interaction—photons 3. Weak interaction—$W^{\pm}$, Z^0 4. Gravitational interaction—graviton
Interaction "strengths"	This term refers to the magnitudes of the dimensionless coupling constants that multiply the space-dependent part of the potential energy functions.
3. Conservation laws and symmetries	Every symmetry of the particle Hamiltonians leads to a conservation law and vice versa (Noether's theorem). Energy, momentum, electric charge, and angular momentum are conserved in all interactions. Some quantities are conserved in some interactions but not in others. For example, isospin is conserved in the strong interaction but not in the weak interaction.
4. Standard Model	The Standard Model seeks to explain all matter in terms of the interactions among three types of elementary particles: quarks, leptons, and force carriers.
Color	All quarks and gluons have color charge with one of three possible values: red, blue, and green. The exclusion principle requires that all particles that occur in nature are colorless.
QCD	The potential function of the strong interaction has the approximate form $V_{\text{QCD}}(r) = -\frac{4\alpha_s}{3r} + kr$ **12-32**
5. Beyond the standard model	Grand unification theories (GUTs) attempt to unify all four basic interactions mathematically. While thus far unsuccessful, some predict, among other things, proton decay, magnetic monopoles, and massive neutrinos. The latter has been verified by experiments.

General References

The following general references are written at a level appropriate for the readers of this book.

Das, A., and T. Ferbel, *Introduction to Nuclear and Particle Physics*, Wiley, New York, 1994.

Eisberg, R., and R. Resnick, *Quantum Physics,* 2d ed., Wiley, New York, 1985.

Frauenfelder, H., and E. M. Henley, *Subatomic Physics,* 2d ed., Prentice Hall, Englewood Cliffs, N.J., 1991.

Fritzch, H., *Elementary Particles,* World Scientific, Singapore, 2005.

Griffiths, D. J., *Introduction to Elementary Particles*, Prentice Hall, New York, 1987.

Martin, B. R., and G. Shaw, *Particle Physics*, 2d ed., Wiley, New York, 1997.

Rubbia, C., and M. Jacob, "The Z^0," *American Scientist*, **78,** 502 (1990).

Veltman, M., *Facts and Mysteries in Elementary Particle Physics*, World Scientific, London, 2003.

Williams, W. S. C., *Nuclear and Particle Physics*, Oxford, New York, 1997.

Notes

1. The word *atom* comes from the Greek word *atomos*, meaning indivisible, which was coined by the philosopher Democritus, a contemporary of Socrates, about 2400 years ago. In addition to suggesting that matter consisted of a variety of tiny atoms, he also suggested that the Milky Way was made of a large number of individual stars and that the Moon had mountains and valleys just like Earth.

2. Carl David Anderson (1905–1991), Swedish-American physicist. His discovery of the positron in cosmic ray cloud chamber tracks was followed three years later by his discovery of the muon in cloud chamber tracks recorded on Pikes Peak in Colorado. The former earned him a share of the 1936 Nobel Prize in Physics.

3. The Dirac equation for particles with $1/2$-integral spin, like the electron, is the relativistic analog of the Schrödinger equation; however, it is not obtained by operator substitution into Equation 2-31 since the resulting wave function does not include the effects of spin.

4. Richard Phillips Feynman (1918–1988), American physicist who described himself as a "curious character." An almost legendary figure among physicists in the United States, he was one of many who worked on the Manhattan Project at Los Alamos during World War II, where he also became an accomplished safecracker. An excellent bongo drummer and a passable artist, he shared the 1965 Nobel Prize in Physics with Julian Schwinger and Sin-itiro Tomonaga, all of whom independently contributed to the development of quantum electrodynamics. His books *Surely You're Joking, Mr. Feynman!* and *What Do You Care What People Think?* provide delightful insights into his life.

5. Emilio Gino Segrè (1905–1989), Italian-American physicist. A lifelong friend and colleague of Fermi, Segrè shared the 1959 Nobel Prize in Physics with Owen Chamberlain, a member of his Berkeley research group, for the discovery of the antiproton. Of greater interest to most people might be his discovery of technetium ($Z = 43$), the first chemical element to be artificially created. The isomeric state of the isotope of technetium, ^{99}Tc, is by far the most widely used radioisotope in medical diagnosis, treatment, and research.

6. This process is called Møller scattering in QED.

7. In fact, an infinite number. The contribution that each possible diagram makes to the total process decreases sharply as the number of vertices increases, so complex diagrams may typically be ignored.

8. The name *lepton*, which means "light particle," was originally selected to reflect the small mass of these particles relative to that of the hadrons; however, the τ (discovered by M. Perl in 1975) has a mass nearly twice that of the proton, so the name is no longer an indicator of the mass of these particles.

9. The reason for making the coupling constants dimensionless is so all observers will measure comparable values, independent of the units they may have used.

10. Carlo Rubbia (b. 1934), Italian physicist. He shared the 1984 Nobel Prize in Physics with Simon van der Meer for their contributions to the discovery of the $W^{\pm}$ and Z^0.

11. Emmy A. Noether (1882–1935), German mathematician. Dismissed from her position at Göttigen by the Nazi regime, she came to the United States in 1933. Her obituary in the *New York Times* was written by Einstein.

12. Operators, like H_{op}, that result in real (i.e., observable) values are called *Hermitian* operators. They obey the rule

$$\int a(x)F_{\text{op}}b(x)\,dx = \int b(x)F^*_{\text{op}}a(x)\,dx$$

13. Murray Gell-Mann (b. 1929), American physicist. He received the 1969 Nobel Prize in Physics for this and other work on fundamental particles and their interactions.

14. The rate of discovery became so large that one physicist quipped that "by 1990 all physicists would be famous because there would be a particle named for each physicist" ($\approx$30,000). Most "discoveries" turned out to be spurious.

15. From a saying attributed to the Buddha: "Now this, O monks, is the noble truth of the way that leads to the cessation of pain: this is the noble *Eightfold Way*: namely, right views, right intention, right speech, right action, right living, right effort, right mindfulness, and right concentration."

16. The name "quark" was suggested to Gell-Mann by a quotation from *Finnegans Wake*, by James Joyce: "Three quarks for Muster Mark." Joyce did not tell us and the context does not make clear exactly what a quark is.

17. The correct quark combinations of hadrons are not always obvious because of the symmetry requirements on the total wave function. For example, the π^0 meson is represented by a linear combination of $u\bar{u}$ and $d\bar{d}$

18. Samuel Chao Chung Ting (b. 1936), American physicist, and Burton Richter (b. 1931), American physicist, shared the 1976 Nobel Prize in Physics for this important discovery.

19. One physicist put the long lifetime of the J/ψ in biological terms by comparing it with someone coming upon a remote mountain village where the average age of the inhabitants was 70,000 years. That would be a definite indication of new biology.

20. Particle physicists call the discovery of the J/ψ the "November revolution," referring to the enormous support of the quark model that its November 1974 publication provided.

21. They form nine combinations, just like the mesons, but for the gluons the ninth combination is really a singlet and hence is independent.

22. Since no theory of quantum gravity complementing QED and QCD exists, current efforts to develop GUTs include only the strong and electroweak interactions.

23. Raymond Davis, Jr. (1914–2006), American physicist, and John Bahcall (1934–2005) American physicist. Davis's measurements won him a share of the 2002 Nobel Prize in Physics.

24. Theories in which the interaction is determined by the invariance of the theory (i.e., its mathematical equations) under particular transformations are called *gauge theories*. For example, classical electrodynamics is a gauge theory (although not usually referred to as such), as are QED and QCD. Historically, interactions were "figured out" by clever physicists on the basis of experimental evidence. A bit of a surprise, Schrödinger's wave mechanics is not a gauge theory.

Problems

Level I

Section 12-1 Basic Concepts

12-1. Two pions at rest annihilate according to the reaction $\pi^+ + \pi^- \rightarrow \gamma + \gamma$. (*a*) Why must the energies of the two gamma rays be equal? (*b*) Find the energy of each gamma ray. (*c*) Find the wavelength of each gamma ray.

12-2. Find the minimum energy of the photon needed for the following reactions: (*a*) $\gamma \rightarrow \Lambda^+ + \pi^-$, (*b*) $\gamma \rightarrow p + \overline{p}$, and (*c*) $\gamma \rightarrow \mu^- + \mu^+$.

12-3. Draw two different Feynman diagrams for each of the following events: (*a*) $e^+ + e^- \rightarrow e^+ + e^-$; (*b*) $\gamma + e^- \rightarrow \gamma + e^-$.

12-4. Draw a Feynman diagram illustrating each of the following scattering events: (*a*) electron-electron, (*b*) electron-positron, and (*c*) Compton effect.

12-5. Find (*a*) the energy of the electron, (*b*) the energy of the ^{32}S nucleus, and (*c*) the momentum of each in the decay $^{32}\text{P} \rightarrow {}^{32}\text{S} + e^-$, assuming no neutrino in the final state ($n \rightarrow p + e^-$). (The rest mass of ^{32}P is 31.973762 u.)

12-6. The fate of an antiproton is usually annihilation via the reaction $p + \overline{p} \rightarrow \gamma + \gamma$. Assume that the proton and antiproton annihilate at rest. (*a*) Why must there be two photons rather than just one? (*b*) What is the energy of each photon? (*c*) What is the wavelength of each photon? (*d*) What is the frequency of each photon?

12-7. Figure 12-2 shows the production of the first antiproton. It was produced by the reaction $p + p \rightarrow p + p + p + \overline{p}$ and required a minimum kinetic energy of 5.6 GeV. (The proton beam energy was actually 25 GeV.) Less energy would be required by either of the following reactions. Why is neither of them a possible alternative? Justify your answer.

(*a*) $p + p \longrightarrow p + e^- + e^+ + \overline{p}$ (*b*) $p + p \longrightarrow p + \overline{p}$

12-8. Positronium is a bound state of an electron and a positron (see Section 2-4). Its lifetime expressed in natural units used by particle physicists ($\hbar = c = 1$) is $\tau = 2/m\alpha^5$, where m = electron mass and α = the fine-structure constant. Use dimensional analysis (*a*) to include $\hbar$ and c in the expression for τ and (*b*) to compute the value of τ.

Section 12-2 Fundamental Interactions and the Force Carriers

12-9. Name the interaction responsible for each of the following decays:

(*a*) $n \longrightarrow p + e^- + \overline{\nu}_e$

(*b*) $\pi^0 \longrightarrow \gamma + \gamma$

(*c*) $\Delta^+ \longrightarrow \pi^0 + p$

(*d*) $\pi^+ \longrightarrow \mu^+ + \nu_\mu$

12-10. Which of the following decays—$\pi^0 \rightarrow \gamma + \gamma$ or $\pi^- \rightarrow \mu^- + \overline{\nu}_\mu$—would you expect to have the longer lifetime? Why?

12-11. Of the reactions below, which are allowed to proceed via the weak interaction and which are forbidden? Justify your answer.

(*a*) $K^+ \longrightarrow \pi^0 + \mu^+ + \nu_\mu$

(*b*) $p + e^- + \nu_e \longrightarrow e^- + \pi^+ + p$

(*c*) $\Lambda^0 \longrightarrow \pi^+ + e^- + \overline{\nu}_e$

(*d*) $p + \nu_\mu \longrightarrow \mu^+ + n$

12-12. Which of the four fundamental interactions is most likely responsible for the following reactions?

(*a*) ^{16}O (excited state) $\longrightarrow$ ^{16}O (ground state) $+ \gamma$

(*b*) $\nu_e + e \longrightarrow \nu_e + e$

(*c*) $p + \overline{p} \longrightarrow \gamma + \gamma$

(*d*) $p + \overline{\nu}_e \longrightarrow n + e^+$

(*e*) $\pi^0 + p \longrightarrow \pi^0 + p$

(*f*) $^3\text{H} \longrightarrow {}^3\text{He} + e^- + \overline{\nu}_e$

12-13. Using the information concerning the neutrinos from SN1987A, including Figure 12-31, compute an upper limit to the mass of the electron neutrino.

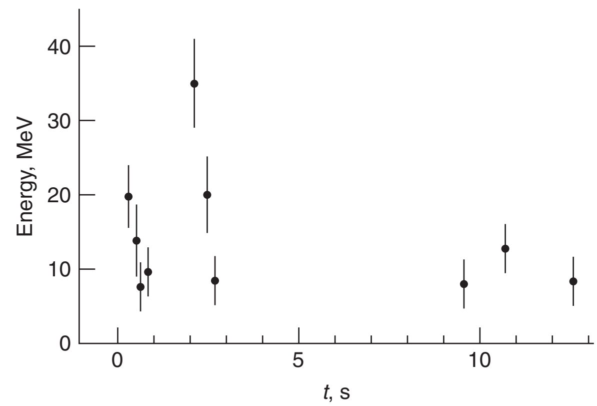

Figure 12-31 Problem 12-13. Electron antineutrino energy versus arrival time in the Kamiokande detector in Japan for antineutrinos emitted by the supernova 1987A. The spread in arrival times (about 13 s) permits a calculation of an upper limit to the mass of the $\overline{\nu}_e$.

12-14. The rest energies of the Σ^+ and Σ^- are slightly different, but those of the π^+ and π^- are exactly the same. Explain this difference in behavior.

12-15. Draw Feynman diagrams of the following decays:

(*a*) $\mu^+ \longrightarrow e^+ + \nu_e + \overline{\nu}_\mu$

(*b*) $\pi^- \longrightarrow \mu^- + \overline{\nu}_\mu$

(*c*) $\tau^- \longrightarrow \mu^- + \overline{\nu}_\mu + \nu_\tau$

Section 12-3 Conservation Laws and Symmetries

12-16. What is the uncertainty in the rest energies of the following particles?

(*a*) $\Lambda(1670)$, (*b*) $\Sigma(2030)$, (*c*) $\Delta(1232)$.

12-17. State which of the decays or reactions that follow violate one or more of the conservation laws, and give the law or laws violated in each case.

(*a*) $p \longrightarrow n + e^+ + \overline{\nu}_e$

(*b*) $n \longrightarrow p + \pi^-$

(*c*) $e^+ + e^- \longrightarrow \gamma$

(*d*) $p + \overline{p} \longrightarrow \gamma + \gamma$

(*e*) $\nu_e + p \longrightarrow n + e^+$

(*f*) $p \longrightarrow \pi^+ + e^+ + e^-$

12-18. Determine the change in strangeness in each reaction that follows, and state whether the reaction can proceed via the strong interaction, the electromagnetic interaction, the weak interaction, or not at all:

(*a*) $\Omega^- \longrightarrow \Xi^0 + \pi^-$

(*b*) $\Xi^0 \longrightarrow p + \pi^- + \pi^0$

(*c*) $\Lambda^0 \longrightarrow p + \pi^-$

12-19. Determine the change in strangeness for each decay, and state whether the decay can proceed via the strong interaction, the electromagnetic interaction, the weak interaction, or not at all: (*a*) $\Omega^- \longrightarrow \Lambda^0 + \overline{\nu}_e + e^-$, (*b*) $\Sigma^+ \longrightarrow p + \pi^0$, and (*c*) $\Sigma^0 \longrightarrow \Lambda^0 + \gamma$

12-20. The rules for determining the isospin of two or more particles are the same as those for combining angular momentum. For example, since $T = 1/2$ for nucleons, the combination of two nucleons can have either $T = 1$ or $T = 0$ or may be a mixture of these isospin states. Since $T_3 = +1/2$ for the proton, the combination $p + p$ has $T_3 = +1$ and therefore must have $T = 1$. Find T_3 and the possible values of T for the following:
(*a*) $n + n$
(*b*) $n + p$
(*c*) $\pi^+ + p$
(*d*) $\pi^- + n$
(*e*) $\pi^+ + n$

12-21. Which of the following decays are allowed and which are forbidden? If the decay is allowed, state which interaction is responsible. If it is forbidden, state which conservation law its occurrence would violate.
(*a*) $\pi^- \longrightarrow e^- + \gamma$
(*b*) $\pi^0 \longrightarrow e^- + e^+ + \nu_e + \overline{\nu}_e$
(*c*) $\pi^+ \longrightarrow e^- + e^+ + \mu^+ + \nu_\mu$
(*d*) $\Lambda^0 \longrightarrow \pi^+ + \pi^-$
(*e*) $n \longrightarrow p + e^- + \overline{\nu}_e$

12-22. For each of the following particles, write down two possible decays that satisfy all conservation laws: (*a*) Ω^-, (*b*) Σ^+, (*c*) Λ^0, (*d*) π^0, and (*e*) K^+.

12-23. Consider the following reactions:

$$K^- + p \longrightarrow K^0 + K^+ + \Omega^-$$

followed by

$$\Omega^- \longrightarrow \Xi^0 + \pi^-$$

Given that $B = 1$ for the proton and $B = 0$ for mesons and that baryon number is conserved, determine the baryon number of the Ω^- and the Ξ^0.

12-24. Which of the following decays and reactions conserve strangeness?
(*a*) $\overline{p} + p \longrightarrow \gamma + \gamma$
(*b*) $\Xi^- \longrightarrow \pi^- + \Lambda^0$
(*c*) $\Sigma^+ \longrightarrow \Lambda^0 + \pi^+$
(*d*) $\pi^- + p \longrightarrow \pi^- + \Sigma^+$
(*e*) $\Omega^- \longrightarrow \Xi^- + \pi^0$

Section 12-4 The Standard Model

12-25. Find the baryon number, charge, isospin, and strangeness for the following quark combinations and identify the corresponding hadron: (*a*) *uud*, (*b*) *udd*, (*c*) *uuu*, (*d*) *uss*, (*e*) *dss*, (*f*) *suu*, and (*g*) *sdd*.

12-26. Find the baryon number, charge, isospin, and strangeness for the following quark combinations and identify the corresponding hadron (the charge and strangeness of the antiquarks are the negatives of those of the corresponding quarks, as with any other particle-antiparticle pair): (*a*) $u\overline{d}$, (*b*) $\overline{u}d$, (*c*) $u\overline{s}$, (*d*) $s\overline{s}$, and (*e*) $\overline{d}s$

12-27. Draw two Feynman diagrams that represent the decay of the antibottom quark.

12-28. Some quark combinations can exist in two or more isospin states, with each state corresponding to a different hadron. One such combination is *uds*. (*a*) What is the value of I_3 for this combination? (*b*) What are the possible values of total isospin I for this combination? (*c*) Find the baryon number, charge, and strangeness of this combination, and identify the hadron corresponding to each isospin state.

12-29. The Δ^{++} particle is a baryon that decays via the strong interaction. Its strangeness, charm, topness, and bottomness are all zero. What combination of quarks gives a particle with these properties?

12-30. Compute the approximate range of a weak interaction mediated by a W^+.

12-31. One mode of weak decay of the $\overline{K}^0$ is

$$\overline{K}^0 \longrightarrow \pi^+ + \mu^- + \overline{\nu}_\mu$$

Showing the quark content of the particles, draw the Feynman diagram of this so-called semi-leptonic decay.

12-32. The Λ^0 undergoes a weak decay as follows: $\Lambda^0 \rightarrow p + \pi^-$. Showing the quark content of the particles, draw the Feynman diagram of this so-called nonleptonic decay.

12-33. Show that the neutron cannot undergo the weak decay shown for the Λ^0 in Problem 12-32.

12-34. The decay of the Λ^0 shown in Problem 12-32 can also proceed via the strong interaction. Showing the quark content of the particles, draw the Feynman diagram that illustrates the strong decay of the Λ^0.

12-35. The $X^0(1193)$ can be produced by the reaction $K^- + p \rightarrow \pi^0 + X^0$. (*a*) Determine the baryon, strangeness, charm, and bottom quantum numbers of the $X^0(1193)$. (*b*) From your answer to (*a*), what is the quark content of the $X^0(1193)$?

12-36. Find a possible combination of quarks that gives the correct values for electric charge, baryon number, and strangeness for (*a*) K^+ and (*b*) K^0.

12-37. The D^+ meson has strangeness 0, but it has charm of $+1$. (*a*) What is a possible quark combination that will give the correct properties for this particle? (*b*) Repeat (*a*) for the D^- meson, which is the antiparticle of the D^+.

12-38. The lifetime of the Σ^0 is 6×10^{-20} s. The lifetime of the Σ^+ is 0.8×10^{-10} s and that of the Σ^- is 1.48×10^{-10} s, nearly twice as long. How can these differences in lifetimes between members of the same isospin multiplet be explained?

Section 12-5 Beyond the Standard Model

12-39. Grand unification theories predict that the proton is unstable. If that turns out to be true, why does it mean that baryon number is not conserved? If leptons and quarks are interchangeable at the unification energy, does this mean that there is a new, conserved "leptoquark number"?

12-40. GUTs predict a lifetime of about 10^{32} y for the proton. If that is the case, how many protons will decay each year in the world's oceans? (Assume the average depth of the oceans to be 1 km and that they cover 75 percent of Earth's surface.)

12-41. Protons might decay via a number of different modes. What conservation laws are violated by the following possibilities?

(*a*) $p \longrightarrow e^+ + \Lambda^0 + \nu_e$

(*b*) $p \longrightarrow \pi^+ + \gamma$

(*c*) $p \longrightarrow \pi^+ + K^0$

Level II

12-42. Find a possible quark combination for the following particles: (*a*) $\overline{n}$, (*b*) Ξ^0, (*c*) Σ^+, (*d*) Ω^-, and (*e*) Ξ^-.

12-43. State the properties of the particles made up of the following quarks: (*a*) ddd, (*b*) $u\overline{c}$, (*c*) $u\overline{b}$, and (*d*) $\overline{s}\overline{s}\overline{s}$.

12-44. Show that the Z^0 cannot decay into two identical zero-spin particles.

12-45. Consider the following decay chain:

$$\begin{aligned}
\Xi^0 &\longrightarrow \Lambda^0 + \pi^0 \\
\Lambda^0 &\longrightarrow p + \pi^- \\
\pi^0 &\longrightarrow \gamma + \gamma \\
\pi^- &\longrightarrow \mu^- + \overline{\nu}_\mu \\
\mu^- &\longrightarrow e^- + \overline{\nu}_e + \nu_\mu
\end{aligned}$$

(*a*) Are all the final products shown stable? If not, finish the decay chain. (*b*) Write the overall decay reaction for Ξ^0 to the final products. (*c*) Check the overall decay reaction for the conservation of electric charge, baryon number, lepton number, and strangeness. (*d*) In the first step of the chain, could the Λ^0 have been a Σ^0?

12-46. There are six hadrons with quantum numbers (Q,U,S,C,B) = (2,1,0,1,0); (0,1,−2,1,0); (0,0,1,0,−1); (0,−1,1,0,0); (0,1,−1,1,0); (−1,1,−3,0,0). Determine the quark content of each hadron.

12-47. Show that the following decays conserve all lepton numbers:

(*a*) $\mu^+ \longrightarrow e^+ + \nu_e + \bar{\nu}_\mu$

(*b*) $\tau^- \longrightarrow \mu^- + \nu_\mu + \nu_\tau$

(*c*) $n \longrightarrow p + e^- + \bar{\nu}_e$

(*d*) $\tau^- \longrightarrow \mu^- + \nu_\mu$

12-48. A π^0 with energy 850 MeV decays in flight via the reaction $\pi^0 \rightarrow \gamma + \gamma$. Compute the angles made by the momenta of the gammas with the original direction of the π^0.

12-49. Test the following decays for violation of the conservation of energy, electric charge, baryon number, and lepton number:

(*a*) $\Lambda^0 \longrightarrow p + \pi^-$

(*b*) $\Sigma^- \longrightarrow n + p^-$

(*c*) $\mu^- \longrightarrow e^- + \bar{\nu}_e + \nu_\mu$

Assume that linear and angular momentum are conserved. State which conservation laws (if any) are violated in each decay.

12-50. Consider the following decay chain:

$$\begin{aligned}
\Omega^- &\longrightarrow \Xi^0 + \pi^- \\
\Xi^0 &\longrightarrow \Sigma^+ + e^- + \bar{\nu}_e \\
\pi^- &\longrightarrow \mu^- + \bar{\nu}_\mu \\
\Sigma^+ &\longrightarrow n + \pi^+ \\
\pi^+ &\longrightarrow \mu^+ + \nu_\mu \\
\mu^+ &\longrightarrow e^+ + \nu_e + \bar{\nu}_\mu \\
\mu^- &\longrightarrow e^- + \bar{\nu}_e + \nu_\mu
\end{aligned}$$

(*a*) Are all the final products shown stable? If not, finish the decay chain. (*b*) Write the overall decay reaction for Ω^- to the final products. (*c*) Check the overall decay reaction for the conservation of electric charge, baryon number, lepton number, and strangeness.

Level III

12-51. The mass of the hydrogen atom is smaller than the sum of the masses of the proton and the electron, the difference being the binding energy. The mass of the π^+ is 139.6 MeV/c^2; however, the masses of the quarks of which it is composed are only a few MeV/c^2. How can that be explained?

12-52. (*a*) Calculate the total kinetic energy of the decay products for the decay $\Lambda^0 \rightarrow p + \pi^-$. Assume the Λ^0 is initially at rest. (*b*) Find the ratio of the kinetic energy of the pion to the kinetic energy of the proton. (*c*) Find the kinetic energies of the proton and the pion for this decay.

12-53. A Σ^0 particle at rest decays into a Λ^0 plus a photon. (*a*) What is the total energy of the decay products? (*b*) Assuming that the kinetic energy of the Λ^0 is negligible compared with the energy of the photon, calculate the approximate momentum of the photon. (*c*) Use your result for (*b*) to calculate the kinetic energy of the Λ^0. (*d*) Use your result for (*c*) to obtain a better estimate of the momentum and the energy of the photon.

12-54. In this problem, you will calculate the difference in the time of arrival of two neutrinos of different energy from a supernova that is 170,000 light-years away. Let the energies of the neutrinos be $E_1 = 20$ MeV and $E_2 = 5$ MeV, and assume that the mass of a neutrino is 2.2 eV/c^2. Because their total energy is so much greater than their rest energy, the neutrinos have speeds that are very nearly equal to c and energies that are approximately $E \approx pc$. (*a*) If t_1 and t_2 are the times it takes for neutrinos of speeds u_1 and u_2 to travel a distance x, show that

$$\Delta t = t_2 - t_1 = x\frac{u_1 - u_2}{u_1 u_2} \approx \frac{x\,\Delta u}{c^2}$$

(b) The speed of a neutrino of mass m_0 and total energy E can be found from Equation 2-10. Show that when $E \gg m_0c^2$, the speed u is given by

$$\frac{u}{c} \approx 1 - \frac{1}{2}\left(\frac{m_0c^2}{E}\right)^2$$

(c) Use the result for (b) to calculate $u_1 - u_2$ for the energies and mass given, and calculate Δt from the result (a) for $x = 170{,}000\ c \cdot \mathrm{y}$. ($d$) Repeat the calculation in (c) using $m_0c^2 = 40$ eV for the rest energy of a neutrino.

12-55. There are three possible decay modes for the τ^-. (a) Draw the Feynman diagrams for each mode. (b) Which mode is the most probable? Explain why.

12-56. In a large accelerator, such as the Large Hadron Collider at CERN, the momentum of a proton in a circular orbit of radius R is given by $\mathbf{p} = 0.3\ R\mathbf{B}$ GeV$/c$, where $\mathbf{B}$ is the magnetic field. Derive this expression.

CHAPTER 13

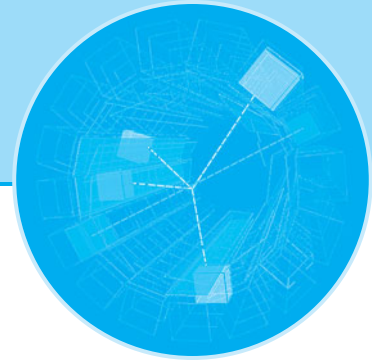

Astrophysics and Cosmology

Physics is an experimental science. The formulation and acceptance of our current understanding of the physical world, from Newton's laws and Maxwell's equations to relativity theory and quantum mechanics, are based on countless experimental observations. In this chapter, we look outward from Earth into the cosmos and apply the principles and techniques of physics first to the composition and evolution of stars, a branch of physics called *astrophysics*, and then to the large scale structure and evolution of the universe, a field called *cosmology*. In doing so the scale of our discussions expands from the nanometer and femtometer dimensions of the molecules, atoms, and nuclei to the light-year and parsec dimensions of galaxies and space, a span of more than 40 orders of magnitude.

When observing stars and galaxies, astrophysicists and cosmologists are limited to examining the electromagnetic radiation and occasional particles emitted at times past that happen to have traveled to the vicinity of Earth so as to arrive at the moment of observation. The information thus gained, together with the fundamental assumption that the laws of physics discovered here on Earth are also valid throughout the universe, forms the basis for their work. During most of history, the instrument used for studying the cosmos was the human eye. Though well adapted to life on Earth, the eye is a relatively poor instrument for the scientific examination of the sky because it stores information for only a small fraction of a second before transmitting it to the brain for analysis, is sensitive to a very limited portion of the electromagnetic spectrum, and has limited resolution and light-gathering capacity. Today, most of our information about the distant universe is received through telescopes.

13-1 The Sun

As we look outward from Earth and beyond the Moon, the most obvious object in the sky is, of course, the Sun. It is important to us for several reasons. First, the light that reaches us from the Sun is responsible for life on Earth. It sustains a comfortable average temperature on Earth's surface and is the ultimate source of virtually all of our energy. Since the Sun contains nearly all of the mass of the solar system, it also provides the gravitational force that binds our planet to the system. But most important for our purposes in this section, the Sun is the only star of the 100 billion or so in the Milky Way that is close enough for us to examine its surface in detail. The others are so far away that they appear only as point sources when viewed by even the largest telescopes. (The very recent exceptions are Alpha Orionis—Betelgeuse—which has been imaged by the Hubble Space Telescope, and Altar, which has been imaged by long-baseline interferometry.) What we learn from studies of our star not only provides a more complete understanding of the processes taking place in it, but surely applies to other stars as well.

The Surface and Atmosphere of the Sun

We can see only the thin outer layer of the Sun, the *photosphere*, which emits the light that makes the Sun visible. The photosphere is generally considered to be the surface of the Sun. The energy per second per square meter that arrives from the Sun at the top of Earth's atmosphere is called the *solar irradiance* or the *solar constant* f. It has been measured to be

$$f = 1.365 \times 10^3 \text{ W/m}^2 \qquad \textbf{13-1}$$

The corresponding quantity for stars other than the Sun is called the *radiant flux*, as we shall see in Section 13-2. Using the solar constant, the Earth-Sun distance of 1 astronomical unit (AU) = 1.496×10^8 km, and conservation of energy, we can calculate the *luminosity* L, which is the total power radiated by the Sun or by any star. The area A of a sphere of 1 AU radius is

$$A = 4\pi r^2 = 4\pi(1.496 \times 10^{11})^2 \text{ m}^2$$

At that radius, each square meter receives energy from the Sun at the rate given by the solar constant. Therefore, the Sun's luminosity $L_\odot$ is given by

$$L_\odot = Af = 4\pi(1.496 \times 10^{11} \text{ m})^2(1.365 \times 10^3 \text{ W/m}^2)$$

$$L_\odot = 3.84 \times 10^{26} \text{ W} \qquad \textbf{13-2}$$

This is truly enormous power. If we could put a 1000-MW electricity-generating plant on each square meter of Earth's surface, all of them combined would only produce 0.1 percent of the power produced by the Sun.

If we assume that the Sun radiates as a blackbody, we can use the luminosity of the Sun along with its radius (6.96×10^8 m) to calculate the effective temperature at the surface of the Sun from the Stefan-Boltzmann law. It states that the power per unit area R (= intensity) radiated by a blackbody in thermal equilibrium is proportional to the fourth power of its surface temperature:

$$R = \sigma T^4 \qquad \textbf{3-4}$$

where Stefan's constant $\sigma = 5.67 \times 10^{-8}$ W/m$^2 \cdot$ K^4 and T is the absolute temperature. If the radius of the Sun is $R_\odot$, the intensity radiated at the surface of the Sun is

$$R = \frac{L_\odot}{4\pi R_\odot^2} \qquad \textbf{13-3}$$

Take care not to confuse the intensity R with the solar radius $R_\odot$. The effective temperature T_e for the surface of the Sun is defined as the temperature for which the intensity radiated satisfies the Stefan-Boltzmann law for a blackbody:

$$R = \frac{L_\odot}{4\pi R_\odot^2} = \sigma T_e^4$$

Solving for T_e, we obtain

$$T_e = \left(\frac{R}{\sigma}\right)^{1/4} = \left(\frac{L_\odot}{4\pi\sigma R_\odot^2}\right)^{1/4} \qquad \textbf{13-4}$$

EXAMPLE 13-1 The Temperature of the Sun's Photosphere Use the Stefan-Boltzmann law to calculate the effective temperature of the photosphere.

SOLUTION

Using $L_\odot = 3.84 \times 10^{26}$ W from Equation 13-2 in Equation 13-4, we have

$$T_e = \left(\frac{L_\odot}{4\pi\sigma R_\odot^2}\right)^{1/4} = \left[\frac{3.84 \times 10^{26}\ \text{W}}{4\pi(5.67 \times 10^{-8}\ \text{W/m}^2\cdot\text{K}^4)(6.96 \times 10^8\ \text{m})^2}\right]^{1/4}$$

$$= 5780\ \text{K}$$

The intensity of solar radiation has been measured at wavelengths ranging from about 10^{-13} m in the gamma-ray region to nearly 10 m in the radio region, a range accounting for over 99 percent of the Sun's emitted power. Over much of this span, the solar spectrum is quite well predicted by Planck's law of blackbody radiation (see Chapter 3) with $T = 5800$ K, as shown in Figure 13-1. The distribution peaks in about the middle (yellow) region of the visible spectrum. This agreement between the measured and theoretical spectra is very constant and is one of the characteristics of the *quiet Sun*.

If we examine the edge of the solar disk, called the *limb*, we see that it is sharply demarcated and darker than the rest of the Sun. From the sharpness of the limb, we conclude from the following reasoning that the photosphere is very thin. Atmospheric turbulence during daylight limits the angular resolution of optical telescopes to about 1 arc second (1/3600 of a degree). At the distance of the Sun, this corresponds to about 700 km. As we look at the Sun, the angle over

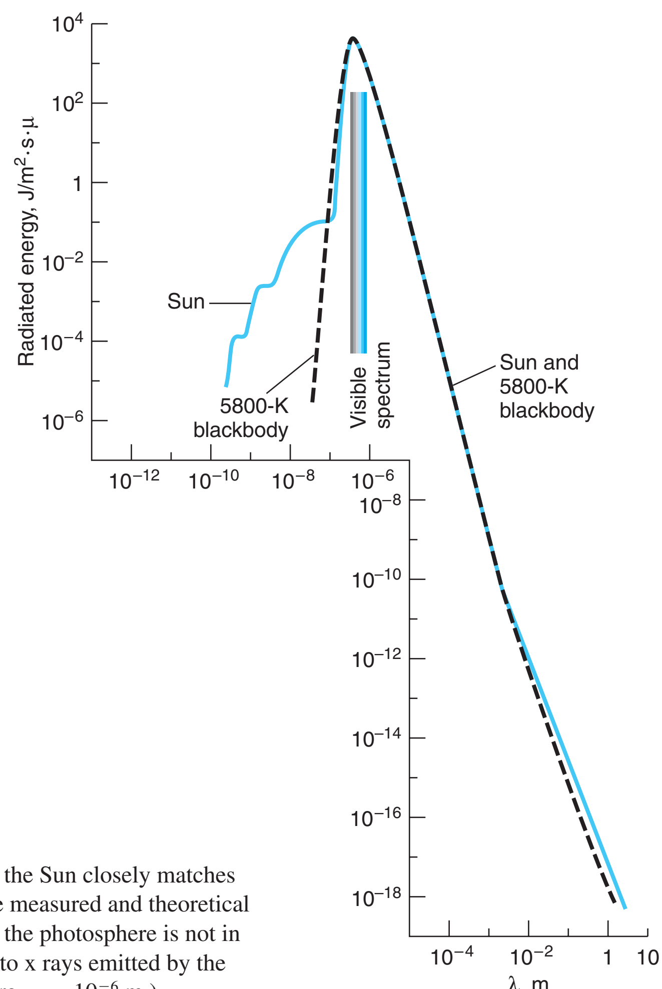

Figure 13-1 The spectral distribution of energy emitted by the Sun closely matches that of a blackbody at 5800 K. The discrepancy between the measured and theoretical curves in the region illustrated is due mainly to the fact that the photosphere is not in thermal equilibrium. The hump at short wavelengths is due to x rays emitted by the corona, which is at a much higher temperature. (In this figure $\mu = 10^{-6}$ m.)

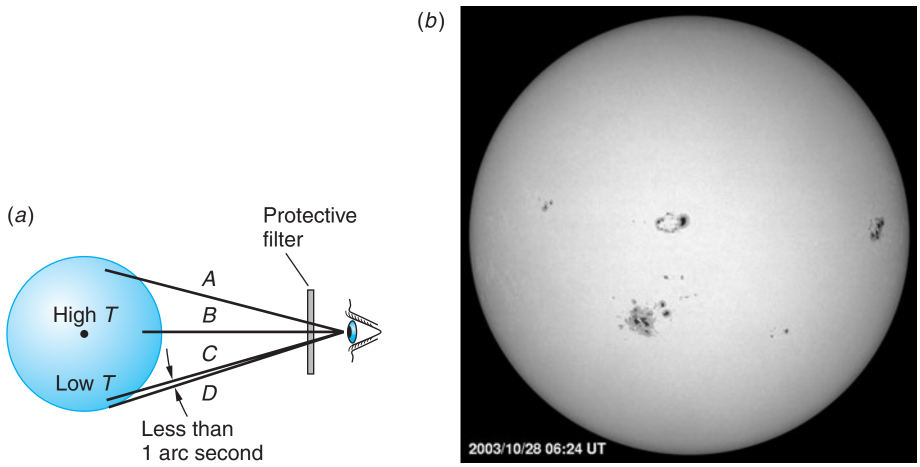

Figure 13-2 (*a*) Two sight lines of equal optical path length, *A* and *B*. Along *B* the observer sees deeper (= hotter = brighter) into the Sun than along *A*; therefore, path *B* looks brighter than path *A*, so the limb looks darker than the disk of the Sun. For paths *C* and *D*, the angle over which the gas of the photosphere changes from transparent to opaque is smaller than we can resolve, so the limb looks sharp. (*b*) A full disk image taken in the visible spectrum or white light at the National Solar Observatory/Sacramento Peak, New Mexico, on October 28, 2003. This image shows sunspot groups and evidence of limb darkening. [*SOHO (ESA & NASA).*]

which the gas of the photosphere changes from rarified and transparent to optically dense and opaque is smaller than we can resolve. Therefore, the photosphere must be less than 700 km thick, which is only about 0.1 percent of the solar radius.

The relatively dark appearance of the limb tells us about the temperature gradient in the Sun's atmosphere. Figure 13-2 shows two paths, *A* and *B*, for viewing the Sun. Because the photosphere is more transparent when viewed at normal incidence than when viewed at a grazing angle, the light traveling along path *B* originates deeper in the Sun than light traveling along path *A*. Since the interior is hotter than the outer layers, the light traveling path *B* originates in a hotter (brighter) part of the Sun than light traveling path *A*. Thus, the light from the limb appears less intense, hence darker (cooler). By measuring the change in brightness from path *A* to path *B*, we can determine the temperature gradient in the photosphere. It is shown in the left portion of Figure 13-3. Notice in the right portion of Figure 13-3 that the temperature begins to rise sharply, accompanying the transition from the Sun's surface, the photosphere, into the solar atmosphere.

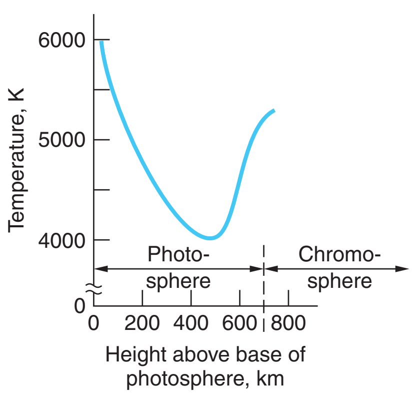

Figure 13-3 The temperature of the Sun decreases from the base of the photosphere outward to a minimum at about 500 km, then increases rather rapidly to about 15,000 K in the chromosphere.

Outside the photosphere are two layers of the Sun's atmosphere that are not generally seen because of the brightness of the photosphere. The inner most of the two layers of the solar atmosphere, the *chromosphere*, is visible for a few seconds just before totality during a solar eclipse. Under high resolution, the chromosphere resembles a field of burning grass, although each burning "blade" is about 700 km thick and 7000 to 10000 km high and lasts for only 5 to 15 minutes. Spectral examination indicates that the temperature of the chromosphere increases with distance above the photosphere, averaging about 15,000 K (Figure 13-4).

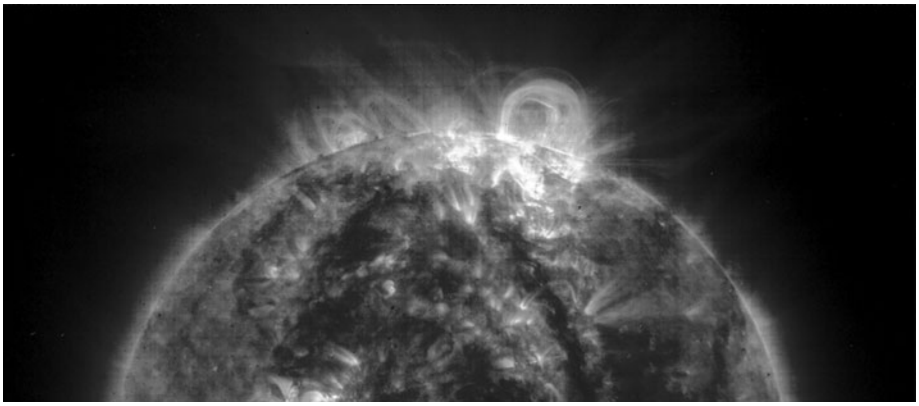

Figure 13-4 This ultraviolet image shows a loop in the magnetic field, seen circling back toward the Sun, trapping hot gas in the chromosphere. [*SOHO (ESA & NASA).*]

When the totality of the eclipse blocks out the chromosphere, the outer layer of the Sun's atmosphere, the *corona*, becomes visible. It is decidedly nonuniform in thickness, consisting of faint white streamers extending 2 to 3 solar diameters into space. The temperature of the corona is approximately 2,000,000 K. Radiation from the corona would overpower that from the 5800 K photosphere, except for the fact that the gas of the corona is so rarified that the total energy it emits is minuscule compared to that of the photosphere. It does, however, account for the relatively high intensity of x rays emitted by the Sun, which shows up in Figure 13-1 as a deviation from the spectral distribution of the blackbody at short wavelengths. It is thought that the extreme temperatures in the corona are produced by acoustic waves generated in the Sun's interior that build into shock waves in the corona. These shock waves heat the gases of the Sun's outer atmosphere and give the particles so much energy that even the Sun's enormous gravity cannot confine them. These high-energy particles, mostly protons and electrons, stream outward from the corona continuously. They form the *solar wind* that pervades the entire solar system.

The Sun's Interior

We cannot see through the photosphere into the interior of the Sun. Consequently, our understanding of the processes there is purely theoretical. With the single exception of solar neutrinos, no radiation or particles originating in the interior reach us directly. To understand the principle features of the current theory, we need first to determine the Sun's mass, as we can do easily with the aid of Newton's law of universal gravitation and the second law of motion. The result is that the Sun's mass $M_\odot = 1.99 \times 10^{30}$ kg.

For simplicity, theoretical models usually consider the Sun to be a nonrotating star in hydrostatic equilibrium. This means that the outward pressure at any point, which is presumed to be due to energy conversion processes occurring in the Sun's interior, is exactly balanced by the inward pressure of gravity. Although the mean density of the Sun (1.4 g/cm^3) is not much different from that of Earth (5.5 g/cm^3), the enormous pressures that exist in the solar interior substantially exceed those that correspond to the electrodynamic forces that bind the electrons to the nuclei. Thus, the matter in the interior of the Sun—and certainly within the *core*, the central region in which temperatures are high enough to allow hydrogen fusion—must surely be in the plasma (ionized) state.

EXAMPLE 13-2 **Hydrogen in the Sun's Core** Show that neutral hydrogen is unlikely to exist in the Sun's interior.

SOLUTION

The pressure at the center of the Sun P_c is of the order $P_c = \mu g$, where

$$\mu = \text{mass/unit surface area} \approx \left(\frac{M_\odot}{R_\odot^2}\right)$$

and

$$g = \frac{1}{2}G\left(\frac{M_\odot}{R_\odot^2}\right)$$

is the average acceleration due to gravity in the Sun. The pressure turns out to be about 10^{15} N/m^2. This is the pressure pushing on the surface of a hydrogen atom near the Sun's center. The resistance to this gravitational pressure would come from the Coulomb force tending to hold the atom together. That pressure is given by the Coulomb attraction between the proton and electron per unit surface area of the atom. Using the Bohr radius a_0 for hydrogen, we have

$$\frac{F}{A} = \frac{ke^2/a_0^2}{4\pi a_0^2} = \frac{ke^2}{4\pi a_0^4} = \frac{(9 \times 10^9 \text{ N}\cdot\text{m}^2/\text{C}^2)(1.6 \times 10^{-19}\text{ C})^2}{4\pi(0.5 \times 10^{-10}\text{ m})^4} = 2.9 \times 10^{12}\text{ N/m}^2$$

Thus, the gravitational pressure in the Sun's interior, at least near the center, exceeds that tending to hold the hydrogen atoms together by a factor of about 1000—making it unlikely that neutral hydrogen atoms could exist there.

Remarks: *Given the Sun's density, even the particles in the depths of the core are still relatively far apart, so that the plasma behaves much like an ideal gas. This allows calculation of the core temperature from the ideal-gas law. It is found to be about 1.5×10^7 K.*

The Source of the Sun's Energy

Using the value for the luminosity of the Sun that we computed earlier, Lord Kelvin was the first to point out that the present energy content of the Sun as calculated from thermodynamics would be radiated away in about 3×10^7 years. Since life has existed on Earth for approximately 100 times that long, we can conclude that the Sun has been radiating at close to its present luminosity for at least 3×10^9 years. Therefore, the Sun must have a supply of energy far larger than that represented by gravitational potential energy, the hot plasma, and the observed radiation field. The source of the Sun's energy is nuclear fusion.

Current theory proposes that, as the young Sun contracted, its temperature rose. To understand why the Sun contracted and why that caused its temperature to rise, we start with Newton's law of universal gravitation.

$$F_{\text{grav}} = G\frac{Mm}{R^2}$$

where F_{grav} is the attractive gravitational force between the masses M and m which are separated by a distance R, and G is the constant of gravitation.. Notice that, as R becomes smaller, F_{grav} becomes larger, which means that the masses M and m move toward one another with increasing acceleration. Conservation of energy requires that the resulting increase in kinetic energy must come from somewhere. That "somewhere" is the gravitational potential energy U_{grav} of the masses in their original positions; U_{grav} must decrease correspondingly. How might this account for the energy emitted by the Sun (and other stars)? A star is a huge ball of gas. The gas atoms near the surface feel the gravitational force attracting them toward the inner atoms of the star's core. The core atoms feel that force, too, but they are also attracted in the opposite direction by the gas atoms near the surface on the other side; hence, the core atoms don't move. (See Figure 13-5.) However, the entire surface of the star accelerates toward the core—the star undergoes gravitational contraction. The increasing kinetic energy of the accelerated atoms (heat) increases the star's temperature, radiating energy into space.

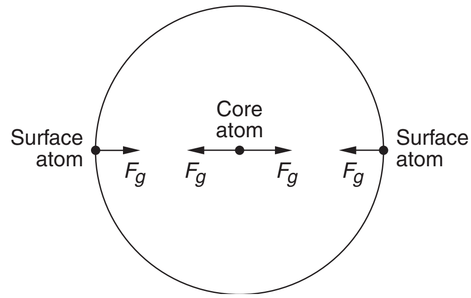

Figure 13-5 Atoms in the outer areas of stars feel a net gravitational force directed toward the core. The net gravitational force on the atoms in the core is essentially zero. In the absence of an outward-directed pressure, the star collapses.

Eventually the temperature of the core reached about 1.5×10^7 K, which is high enough for the hydrogen nuclei (protons) in the plasma to have sufficient energy on the average (about 1 keV) to fuse into helium nuclei. This reaction, actually a chain of reactions, was first proposed by H. A. Bethe[1] and is referred to as the *proton-proton cycle*. The first reaction in the chain is

$$^1\text{H} + {}^1\text{H} \longrightarrow {}^2\text{H} + e^+ + \nu_e + 0.42 \text{ MeV} \qquad \textbf{13-5}$$

Due to the height of the Coulomb barrier the probability for this reaction is very low except for those protons in the high-energy tail of the Maxwell-Boltzmann distribution. Fusion is possible only because of quantum mechanical tunneling. This sets a limit on the rate at which the Sun can produce energy and thus ensures a long lifetime for the Sun and similar stars. This limit is sometimes called the "bottleneck" of the solar fusion cycle. Once ^{2}H (deuterium) is formed via Equation 13-5, the following reaction becomes very probable:

$$^2\text{H} + {}^1\text{H} \longrightarrow {}^3\text{He} + \gamma + 5.49 \text{ MeV} \qquad \textbf{13-6}$$

It is followed by

$$^3\text{He} + {}^3\text{He} \longrightarrow {}^4\text{He} + 2\,{}^1\text{H} + \gamma + 12.86 \text{ MeV} \qquad \textbf{13-7}$$

This process by which hydrogen nuclei are "burned" to helium nuclei is shown schematically in Figure 13-6*a*. There are other possible reactions for converting ^{1}H to ^{4}He, all of which have the same net Q value. Their rates, however, differ depending on the composition and temperature of the Sun's interior. The most important of these is the CNO (carbon-nitrogen-oxygen) cycle, which accounts for about 1.5 percent of the total solar luminosity. The CNO cycle is very temperature dependent and is the dominant H-fusion cycle for stars slightly more massive than the Sun.

The neutrinos produced in the proton-proton cycle escape from the core, providing our only means for direct observation of the Sun's interior. The measured luminosity $L_\odot$ and the known total Q value of the proton-proton cycle enable a calculation of the total reaction rate. In addition, the alternative reactions for ^{3}He have different neutrino energy spectra, thus providing a way of determining the relative contributions of each reaction and gaining further information about the composition and temperature of the core. The neutrino flux arriving at Earth from all reactions in the proton-proton fusion cycle determined by John Bahcall's[2] definitive theoretical analysis of the solar neutrino spectrum based on the standard solar model is shown in Figure 13-6*b*.

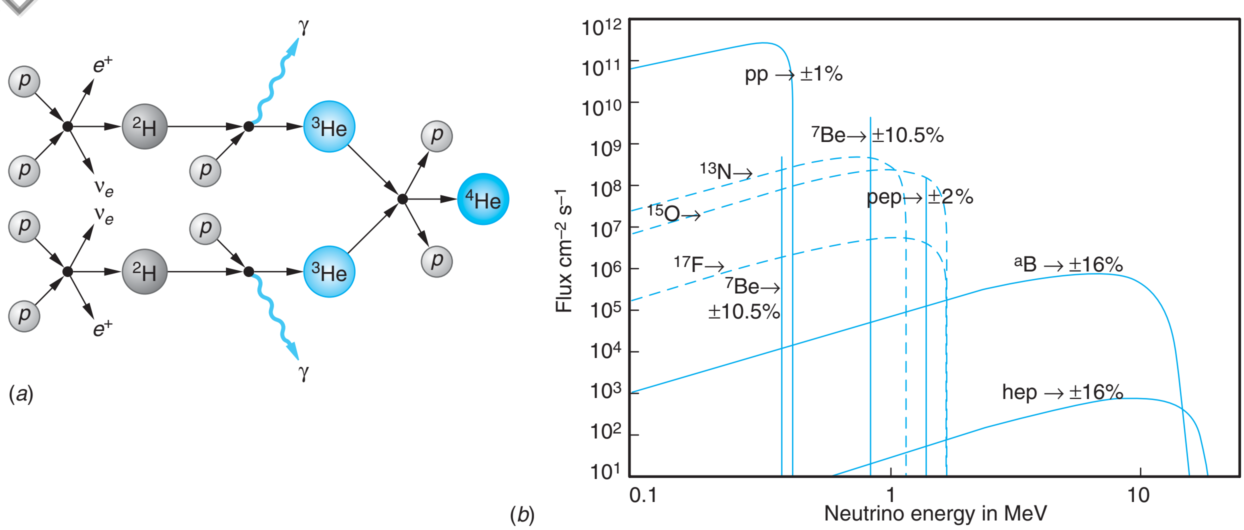

Figure 13-6 (*a*) The proton-proton cycle is the primary source of the Sun's energy. The neutrino created in the initial step escapes from the core. The net energy produced, including that released from orbital electron binding and e^-e^+ annihilation, is about 26.7 MeV per ^{4}He produced. (*b*) Neutrino flux at Earth predicted by the standard solar model. Neutrinos produced in the *p-p* cycle are shown by solid lines; those produced in the CNO cycle are shown by dotted lines. [*J. Bahcall and A. Serenilli, ApJ,* **621**, *L85 (2005).*]

For those neutrinos resulting from the $^8\text{B} + p \rightarrow {}^8\text{Be}^* + \text{e}^+ + \nu_e$ reaction (Table 13-1) the predicted intensity is 8.1 ± 1.3 *S*olar *N*eutrino *U*nits (1 SNU = 1 event per 10^{36} target atoms per second). However, experiments conducted by Ray Davis and his co-workers over more than 30 years using a chlorine radiochemical detector located deep inside a gold mine in South Dakota which was sensitive primarily to the ^{8}B-produced neutrinos[3] found the measured rate at which solar neutrinos from this reaction arrive at Earth to be 2.56 ± 0.16 SNU, only about 32 percent of the expected rate. Subsequently, experiments sensitive to other reactions in the *p-p* cycle performed at six other laboratories around the world confirmed this discrepancy. This discrepancy is referred to as the *solar-neutrino problem*. Davis shared the 2002 Nobel Prize in Physics for this discovery.

The discrepancy between the theoretical prediction of the standard solar model and the experimental results presented a very serious problem for both astrophysics and particle physics. In the words of John Bahcall, whose calculations provided the solar model prediction:

> Is the solar neutrino problem caused by unknown properties of neutrinos or by a lack of understanding of the interior of the Sun? In other words, is this a case of new physics or faulty astrophysics?

It turned out to be a case of "new physics." As was described in Section 12-5, the recent discovery of neutrino oscillations that enables neutrinos of one flavor to change into neutrinos of another flavor, means that electron neutrinos emitted in the Sun's *p-p* fusion cycle may oscillate to muon or tau neutrinos during their trip from the Sun to Earth. Davis's neutrino telescope was sensitive only to electron neutrinos. This accounts for the discrepancy and also, according to the Standard Model of particle physics, requires that neutrinos have a nonzero mass.

Table 13-1 Proton-proton nuclear fusion cycle

	Reaction	% of events	ν energy (MeV)
1.	$p + p \longrightarrow {}^2\text{H} + e^+ + \nu_e$	99.96	≤ 0.423
	or		
	$p + e^- + p \longrightarrow {}^2\text{H} + \nu_e$	0.04	1.445
2.	${}^2\text{H} + p \longrightarrow {}^3\text{He} + \gamma$	100	
3.	${}^3\text{He} + {}^3\text{He} \longrightarrow {}^4\text{He} + 2p$	85	
	or		
	${}^3\text{He} + {}^4\text{He} \longrightarrow {}^7\text{Be} + \gamma$	15	
4.	${}^7\text{Be} + e^- \longrightarrow {}^7\text{Li} + \nu_e$	15	0.863 (90%)
			0.385 (10%)
5.	${}^7\text{Li} + p \longrightarrow 2\,{}^4\text{He}$		
	or		
	${}^7\text{Be} + p \longrightarrow {}^8\text{B} + \gamma$	0.02	
6.	${}^8\text{B} \longrightarrow {}^8\text{Be}^* + e^+ + \nu_e$		<15
7.	${}^8\text{Be}^* \longrightarrow 2\,{}^4\text{He}$		
	or		
	${}^3\text{He} + p \longrightarrow {}^4\text{He} + e^+ + \nu_e$	0.00003	<18.8

Source: Data from J. Bahcall, *Phys. Rev. C*, **56**, 3391 (1997).

The Active Sun

In addition to the relatively stable phenomena that we have discussed, the Sun exhibits a number of transient phenomena, most of which are associated with its magnetism. We noted earlier that the solar interior must be primarily a plasma composed of protons and electrons. The Sun rotates with different angular velocities at different latitudes. At any given latitude, it probably has different angular velocities at different distances from the spin axis as well. The complex motions resulting from this differential rotation and from the rise and fall of charged particles in the convection zone between the core and the photosphere are probably the source of the Sun's chaotic magnetic field structure (Figure 13-7). This transient structure may have localized magnetic field strengths exceeding 1 T on occasion.

The transient structure is superimposed onto a general average magnetic field of about 10^{-4} T, roughly twice Earth's average magnetic field. The origin of this general field is not known, except that it is not a remnant of the Sun's formation, since a primeval field would likely have decayed away by now. Its presence poses formidable problems for any theoretical solar model. Not only must the model explain the origin of the general field, but it must also account for the fact that its polarity reverses every 11 years, in step with the *sunspot cycle*.

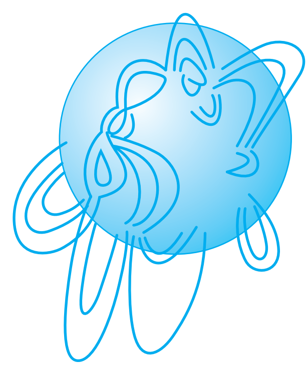

Figure 13-7 The field lines that describe the Sun's magnetic field structure at any given time are derived from ground-based measurements, e.g., Zeeman effect and the transport of charged matter. The high-intensity, chaotic structure is superimposed onto a constant general magnetic field of about 10^{-4} T.

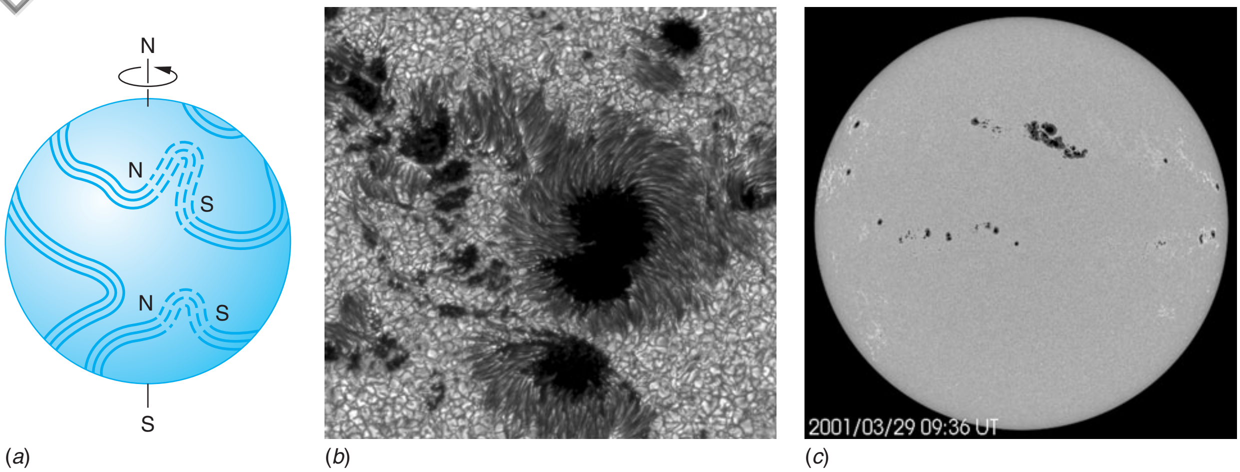

Figure 13-8 (*a*) Magnetic flux lines are distorted by the Sun's differential rotation and pushed up out of the surface by motion in the convection zone. (*b*) A sunspot occurs where a bundle of field lines leaves and reenters the surface. The areas where they leave and return to the surface become sunspots. This very large spot on this part of the Sun's surface is about 20 arc seconds in diameter. The granular appearance of the Sun's surface is very apparent. Sunspot activity on 29 March 2001. [(*b*) *Institute for Solar Physics of the Royal Swedish Academy of Sciences*. (*c*) *SOHO (ESA & NASA)*.]

Sunspots, dark blemishes on the solar disk, were first reported in pretelescope times and were observed by Galileo in 1610. They originate in the following way, according to one of the current models: As shown in Figure 13-8, the Sun's magnetic field lines are distorted into bundles or tubes by the Sun's differential rotation. Occasionally vertical movements in the convection zone may push a bundle through the surface. The area where it leaves the surface and the area where it returns to the surface become the sunspots. They appear darker than the adjacent photosphere, which means that they are cooler, typically around 3800 K. One of the pair of spots will have a magnetic north pole, the other a south pole. If the bundle of field lines does not protrude completely through the photosphere, only a single sunspot is formed.

The number of spots per year varies regularly from about 20 to about 150 in a cycle of 11 years, as can be seen in Figure 13-9. Early in each new cycle, the sunspots form at a latitude of about 30°. As the Sun progresses through its 11-year cycle, the spots form progressively closer to the equator. There is an additional cyclical variation in the annual number of sunspots with a period of about 100 years that is also apparent in Figure 13-9. Currently, the theoretical explanation for these regularities, while in agreement with some features of the observations, is not complete.

Solar flares are violent, stormlike phenomena that appear to be associated with the large magnetic fields in the vicinity of sunspots. There is, however, no generally accepted model to explain them. Solar flares erupt explosively, ejecting particles and emitting radiation ranging from the x-ray through the radio regions of the spectrum. They last anywhere from a few minutes to a few hours and can have temperatures as high as 5×10^6 K. The particles ejected by solar flares reach Earth within a day or so and often produce auroras as they accelerate in Earth's magnetic field. Solar flares can disrupt some types of radio transmissions, and on rare occasions can generate surges in high-voltage transmission lines. A flare that happened to be directed toward Earth in 1996 caused, among other things, the failure of a communications satellite.

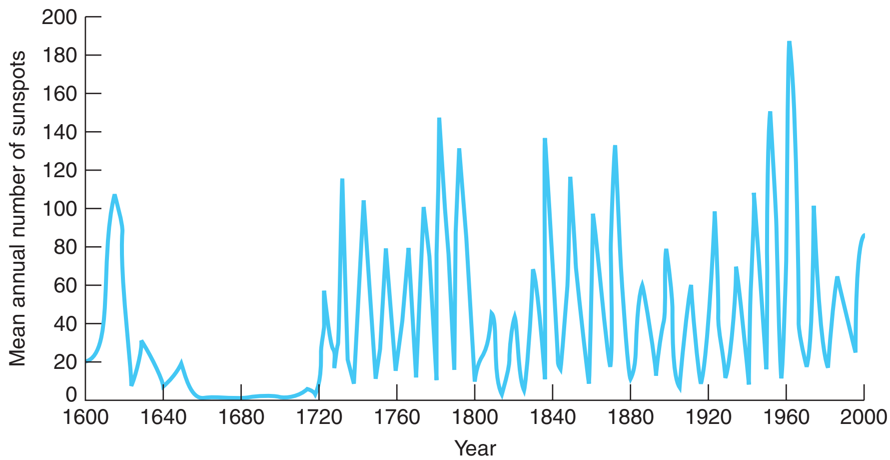

Figure 13-9 The number of sunspots that occur each year has varied regularly on an 11-year cycle for more than 270 years. The unexplained absence of spots between about 1650 and 1700, referred to as the Maunder minimum, approximately coincides with a period of unusually low temperatures in Europe referred to as the "Little Ice Age." Whether there exists a causal connection between the two phenomena is a matter of scientific debate. Sunspot cycle 23 began in 1996 and ended in 2007. (Counting the cycles began in 1775.) Sunspot activity is next expected to peak in 2011–2012.

Two other transient solar phenomena related to sunspots are plages and filaments. *Plages* are bright (hotter) areas adjacent to the dark sunspots. The evolution of plages suggests that they are areas of increased mass density, resulting perhaps from the movement of the magnetic field bundles generated from the sunspots. *Filaments* are dark, thin lines that seem to thread their way across the disk, sometimes for thousands of kilometers. They do not lie on the surface but extend out into space, sometimes more than 100,000 kilometers, in graceful loops and swirls. Filaments that are seen projecting into space at the Sun's edge are called *prominences*. They may erupt and disappear quickly or persist for several weeks. While prominences appear closely related to the shape of the magnetic field, as with other transient features, there is as yet no model that fully accounts for them.

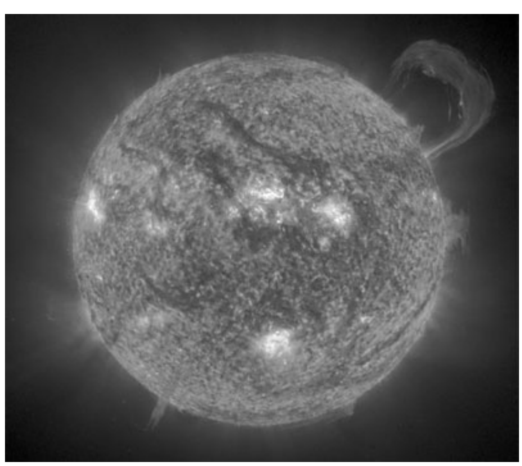

The huge handle-shaped prominence shown on the upper right was photographed in 304 Å [30.4 nm] light on 14 September 1999. It consists of charged particles confined by the magnetic field of the sun. [*SOHO (ESA & NASA)*.]

EXPLORING
Is There Life Elsewhere?

We are certainly not the first to ask that question. The Greek philosophers beginning with Thales and continuing through Plato and his student Aristotle thought and wondered about the structure of the heavens and the mysteries they might contain. Many scientists in the nineteenth century assumed that the other planets of the solar system, particularly Mars and Venus, were inhabited. In the twentieth century the term *Martian* became synonymous with "beings from outer space." An entire movie and television genre has flourished based on time travel, spaceships, aliens from outer space, and a plethora of weird science—pseudoscience.

The real issue, however, is much more serious: Is life "out there" possible? The answer is surely, Yes. Consider: With the development and evolution of telescopes we have learned that the motions of stars and galaxies obey the same laws of physics that have been discovered on Earth. Our location is in no way special. The physical processes that occur on Earth occur throughout the universe. All of the chemical elements discovered in our studies of the near and distant universe also occur on Earth. The relativistic and quantum physics we have developed works in the cosmos, too. So, then, must our biology—an application of physics and chemistry—work throughout the universe. On Earth we have learned that life-forms can survive and prosper in seemingly hostile environments. Sea animals thrive in the scalding hot water and enormous pressures of the deep ocean volcanic vents. Other organisms live in the rocks of deep mines and in the permanent ice of the Antarctic. Other creatures have been discovered that use sulfur in their metabolism, rather than oxygen. And the complex organic molecules that are the building blocks of life as we know it have been found in meteorites and identified in interstellar gas clouds. Thus, it would appear that the development of life elsewhere in the Galaxy and the universe may not be all that unusual.

If intelligent life has developed elsewhere, where is it and how do we find it? Since 1995 new technology and techniques have led to the indirect discovery (e.g., via stellar motion perturbations) of 229 extrasolar planets (called *exoplanets*) orbiting 194 relatively nearby stars (as of April 2007). While most of the discovered planets are hot and large, Neptune to Jupiter in size, at least two are cool and about 5 times Earth's mass orbiting a faint star in the Milky Way's central bulge. As of now, only one exoplanet has been imaged directly. If intelligent life on these planets (or the millions of others that must exist throughout the universe) are sending electromagnetic signals into space, as we are, detecting those signals could provide the first clue that we are not the only intelligent life that has existed in the universe. Listening for those signals is the objective of the Search for Extraterrestrial Intelligence (SETI) project. Look for SETI online to learn more.

13-2 The Stars

On clear, dark nights, we can see about 6000 stars without the aid of telescopes. The sight is incredibly beautiful and must surely have been just as awesome to our forebears. A cursory glance at the night sky reveals the following features: the distribution of stars is not uniform, the stars do not all have the same brightness, and there is a dim irregular band of light bisecting the sky. In this section, we will investigate these features.

The hazy band of light that stretches across the entire sky is the Milky Way. With the aid of a small telescope or even binoculars, the band is resolved into a mass of individual stars. It is part of a huge Galaxy[4] containing an estimated 10^{11} stars that are bound together gravitationally in our region of the universe. Most of the stars visible to the unaided eye seen in any direction are simply those members of the Galaxy close enough to Earth to be individually resolved by the eye.

Constellations Chance groupings in the celestial pattern, usually among the brighter individual stars, are called *constellations*. Ancient peoples associated them with persons, gods, and objects from their histories, religions, and myths, probably as mnemonic devices. The constellations, as well as several prominent stars, have always had practical uses. For centuries, seafarers have used the Pole Star (in the northern hemisphere) and the Southern Cross (in the southern hemisphere) as aids in navigation. In ancient Egypt the pharaoh's advisors learned to predict the life-sustaining annual flooding of the Nile by watching for the first appearance of the bright star Sirius[5] above the horizon in the early spring. Today, 88 constellations (see Figure 13-10 for some of them) are used by astronomers to identify sections of the sky. For example, the center of the Milky Way is said to be "in Sagittarius," meaning it is in the direction of the constellation Sagittarius. (The center of the Galaxy is actually more than 10 times farther from the Sun than are the stars that form that constellation.)

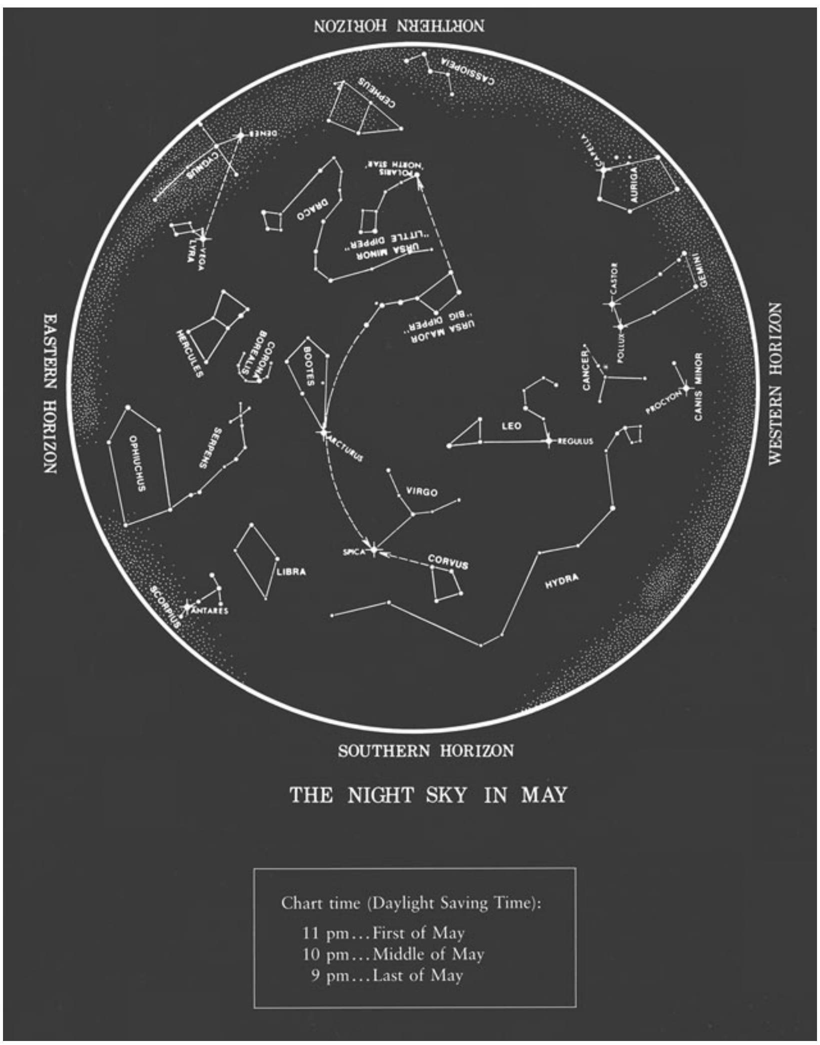

Figure 13-10 Star chart of the sky as it appears on a spring evening at latitude 40° north, showing many of the constellations visible. During the night, the entire pattern revolves about 120° about Polaris, the Pole Star. To use the chart, hold it (or a copy) in front of you with the S (south) at the bottom while you face south. Match the lower half to the stars that you see. Then rotate the chart, putting the W at the bottom, face west and again match the lower half to the stars you see, and so on. [*R. A. Freedman and W. J. Kaufmann III, Universe, 8e (New York: W. H. Freeman and Co., 2008), p. S-6.*]

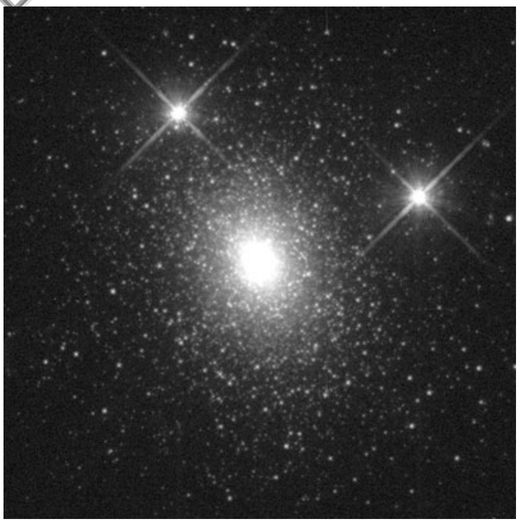

Globular cluster G1 in galaxy M31 contains more than 300,000 stars. G1 orbits the Andromeda galaxy, the nearest large spiral to Earth. The two bright stars with "spikes" are in the Milky Way. [*Michael Rich, Kenneth Mighell, and James D. Neill (Columbia University), and Wendy Freedman (Carnegie Observatories), and NASA.*]

Stellar Populations One characteristic of our Galaxy is that certain regions of it have many more stars than other nearby regions. Such concentrations are called *star clusters*. There are two types of star clusters. *Galactic clusters*, also called *open clusters*, may contain from about 20 to several hundred stars. All stars in galactic clusters appear to have very similar compositions, as inferred from studies of their optical spectra. About 70 percent of their mass is hydrogen, another 28 percent or so is helium, and 2 to 3 percent consists of elements heavier than helium. Stars with this characteristic composition, like our Sun, are referred to as *population I stars*. *Globular clusters* may consist of 10^3 to 10^6 stars in a compact, roughly spherical group. Their concentrations of elements heavier than helium are all very similar and much lower than that of population I stars, typically 0.1 to 0.01 percent. These are called *population II stars*. One such cluster, photographed by the Hubble Space Telescope, is shown in the photo at the left.

Population I stars are thought to be current generation stars that formed after the gas and dust that exists between these stars had been enriched by the products of ancient fusion reactions in the early universe. The lower concentration of heavier elements in the population II stars suggests that they are of a previous generation, hence older than those of population I. The fact that they are found in regions of space where there is little dust or gas tends to support that interpretation.

Classification of Stars Stars are grouped into classes based primarily on the spectral lines each emits and absorbs. That different stars have different spectra was discovered nearly 200 years ago by Joseph Fraunhofer who also measured numerous absorption lines in the solar spectrum. Over the years, advances in spectroscopy, instrumentation, and atomic theory enabled astrophysicists Edward Pickering and Annie Jump Cannon[6] to rearrange systematically the earlier classification scheme into a temperature sequence. Stars are grouped according to temperature categories (or spectral types) ranging from hot blue, so-called O stars, to cool red, so-called M stars. The seven categories are: O B A F G K M. Generations of students have memorized the classifications by using the phrase "Oh Be A Fine Girl/Guy, Kiss Me." Table 13-2 lists some of their important characteristics. Cannon also added ten subdivisions (0 to 9) within each category to provide for finer distinctions between the stars in each group. For example, B0 stars are hotter (called *early type*) than B9 stars (called *late type*). The physical basis for the distinction between the groups and early/late types lies in the quantum mechanical details of the spectra and the atomic electron excitations and ionizations of the elements comprising each star. Improved observational techniques and analytical methods have led to a number of additional classifications including several for hot blue emission stars and classes L, T, and Y for cool red and brown dwarfs.

Stellar Magnitudes The Greek astronomer Hipparchus[7] devised the first classification of stars based on how bright each appeared. Called *apparent magnitude* and represented with the letter m, the values he assigned ranged from $m = 1$ for the brightest stars to $m = 6$ for the dimmest visible to his eye. (The telescope had not yet been invented.) As time passed and technology was developed and improved, astronomers extended and refined the apparent magnitude scale. The modern definition of the

Table 13-2 Characteristics of star categories

Spectral type	Important characteristics
O	Hottest blue-white stars; helium absorption lines
B	Hot blue-white stars; helium and hydrogen absorption lines
A	White stars; hydrogen and calcium absorption lines
F	Yellow-white stars; calcium and some metal absorption lines
G	Yellow stars; solar-type spectra with calcium and iron absorption lines (The Sun is a G2 star.)
K	Cool orange stars; strong metal absorption lines
M	Coolest red stars; strong metal absorption lines

apparent magnitude scale is that a difference of 5 in the value of m corresponds to a factor of 100 in brightness; that is, a difference of 1 in the value of m between two stars means the *ratio* of their respective brightness is $100^{1/5} = 2.51$. Thus, star A with $m = 2$ is 2.51 times brighter than star B with $m = 3$, $2.51 \times 2.51 = 6.31$ times brighter than star C with $m = 4$, and so on. (Note that smaller m-values mean brighter, larger m-values mean dimmer.) Modern technology enables scientists to measure apparent magnitude with an accuracy of ± 0.01 and has vastly extended the range of m-values. For example, the brightest star in the sky, the Sun, has $m = -26.81$ and the faintest objects that can be observed have about $m = 29$.

Of course, apparent magnitudes are not the whole story. Two stars with the same luminosity, but located at different distances from us will have different m-values, the furthest away being the dimmer and, therefore, having the larger m-value. So we define a new, more basic quantity, the *absolute magnitude* M, in terms of the *radiant flux* F which includes both the star's luminosity L and its distance R from Earth (see Section 13-1). The radiant flux F is defined as

$$F = \frac{L}{4\pi R^2} \qquad \textbf{13-8}$$

Recall that $4\pi R^2$ is the surface area of a sphere of radius R and has SI units of meter squared (m^2). The units of radiant flux are then $J/s \cdot m^2$. Using Equation 13-8, the absolute magnitude M of a star is defined as being equal to the apparent magnitude the star would have, *if* it were located at a distance of 10 parsecs (pc; see Section 13-3) from Earth. Using the expression for the radiant flux and the definitions for the apparent and absolute magnitudes, one can eventually obtain the expression below connecting F, m, M, and R:

$$100^{(m-M)/5} = \frac{F_{10\text{ pc}}}{F} = \left(\frac{R}{10\text{ pc}}\right)^2 \qquad \textbf{13-9}$$

where R is the actual distance between the star and Earth (measured in pc).

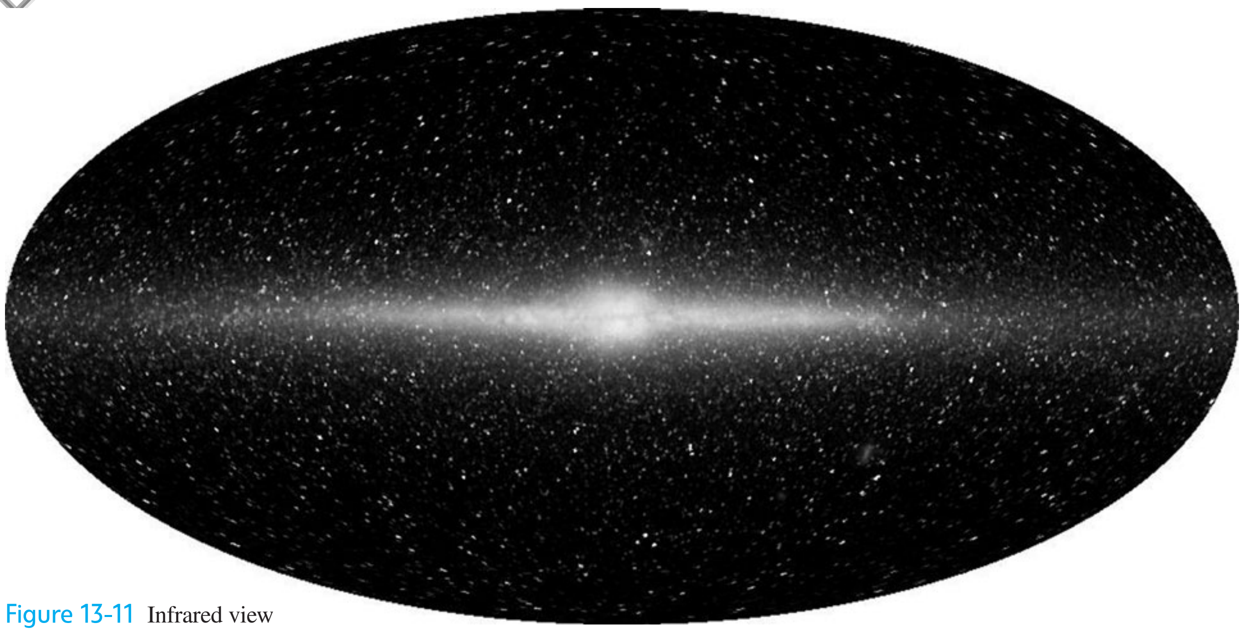

Figure 13-11 Infrared view of the Milky Way taken by the COBE satellite showing the disk and the central bulge. [*The COBE Project, DIRBE/NASA.*]

The Structure of the Milky Way

Figure 13-11 is a map of the Milky Way viewed from the location of the Sun. The size and shape of the Galaxy are not at all obvious in the picture—hardly surprising from the perspective of an observer inside the Galaxy itself.[8] However, painstaking counts of the number of stars per unit volume in various directions have revealed that the Milky Way is basically a huge disk. Up until the early 1900s, astronomers thought that the Sun was located at the disk's center. The true size and shape of the Galaxy (Figure 13-12) were deduced by H. Shapley[9] through a brilliant analysis of the distribution of globular clusters. He discovered that 200 or so globular clusters are distributed approximately spherically in space and proposed that the center of that distribution coincided with the center of our Galaxy. That center lies about 28,000 $c \cdot y$ (8 kpc; see Equation 13-12) from the Sun, which is approximately one-third of the way out from the center. The Milky Way is roughly $1.63 \times 10^5\ c \cdot y$ in diameter. It has been said that Shapley dethroned the Sun from the center of the Galaxy in much the same way that Copernicus had dethroned Earth from the center of the universe.

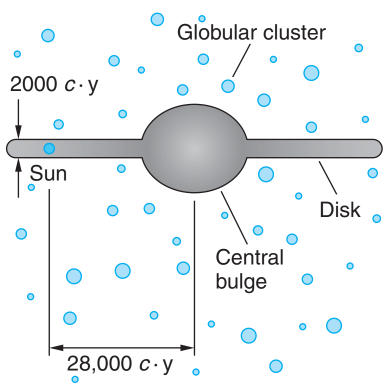

Figure 13-12 A diagram of the presently accepted structure of the Milky Way based on the work of Harlow Shapley. The Milky Way is brighter in the summer night sky in the northern hemisphere than in the winter because the summer night sky looks toward the center of the Galaxy, while the winter night sky is toward its outer edge.

Following Shapley's work, astronomers studying other nearby galaxies with the aid of new, high-resolution telescopes found that the distribution of stars within those systems, many of which had open spiral structures such as shown in Figure 13-24*b* (page 655), depends in part upon the ages and compositions of the stars, with open clusters being found mainly in the arms of the spirals. Making the reasonable assumption that such distribution patterns would also hold for the Milky Way and with meticulous measurements of the distances to about 200 galactic clusters, astronomers have identified three spiral arms and a bar associated with the central bulge for the Milky Way. Thus, if we could look down on the Milky Way from the Galactic north pole, it would look much like Figure 13-13*a*.

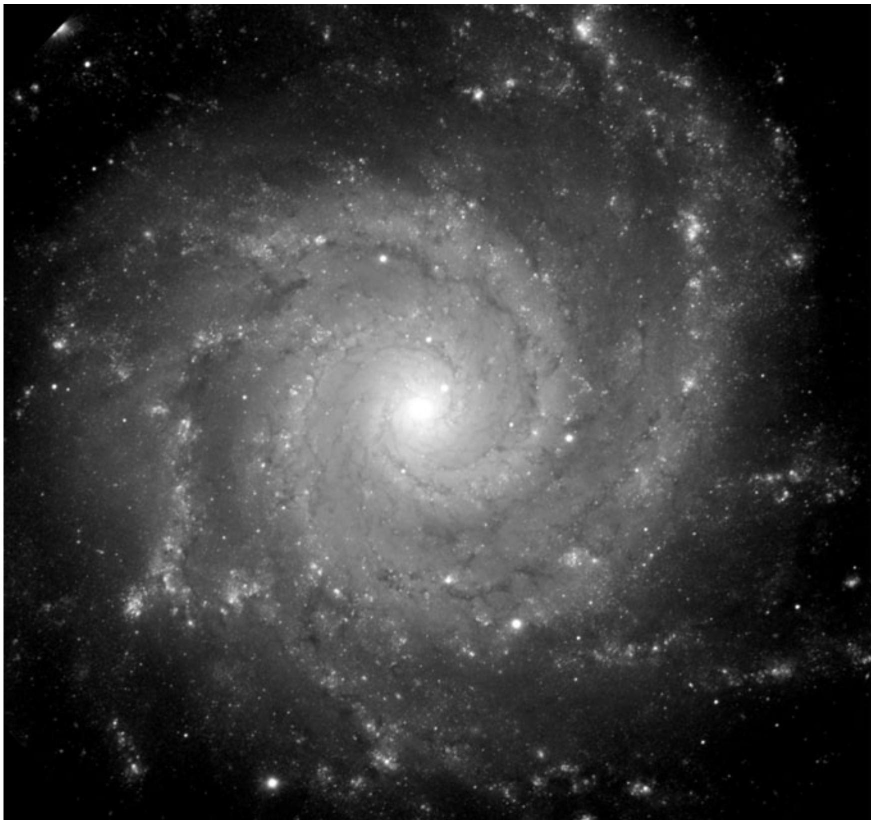

(*a*)

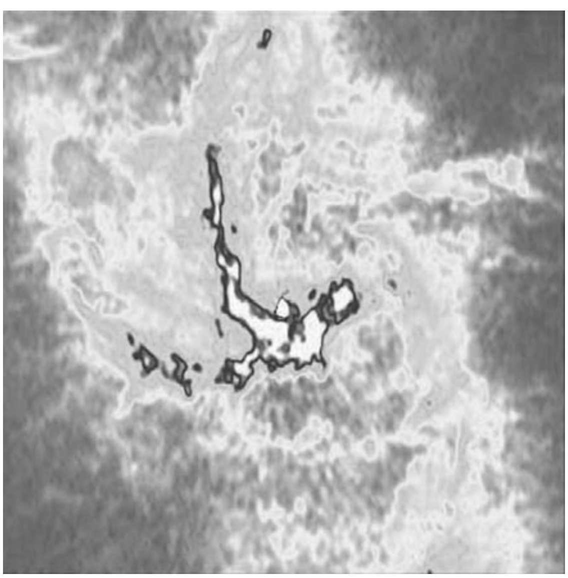

(*b*)

Figure 13-13 (*a*) The combination of observations in the visible and radio regions of the spectrum reveal a spiral structure with a faint bar for the Milky Way. To an observer looking down on the Galaxy from about 1 million parsecs, the Milky Way might look something like this. The Sun is 28,000 $c \cdot$ y from the center in one of the spiral arms. (*b*) Viewed from Earth, the center of the Galaxy is obscured by clouds of dust and gas that prevent most visible light from reaching us; however, it contains several areas of strong radio emission, the strongest of which is Sagittarius A*, a compact radio source that appears to dominate the large-scale motion of the galactic center. This radio image (taken at 6 cm wavelength) is of the inner 8 $c \cdot$ y of the Milky Way. The dark spot at the very center is Sagittarius A, which is very likely a huge black hole (see Section 13-5). This image was made using the Very Large Array, a radio frequency interferometer made of 27 synchronized antennae with an effective diameter of about 40 km, located in New Mexico. Its resolution is better than that of the best ground-based optical telescopes by about a factor of five. [*(a) Gemini Observatory-GMOS Team. (b) HST Astronomy Imaging Workbench/Farhad Yusef-Sadeh/ Northwestern University.*]

EXPLORING
The Celestial Sphere

Copernicus's refined heliocentric model of the solar system and its subsequent verification by observations laid to rest for all time the geocentric model of Aristotle and Ptolemy. However, we still use one feature of the latter. Putting aside the motions of the planets and a few interplanetary space probes, our observations of the stars and specification of their locations in the sky are normally referred to a coordinate system centered on Earth, not the Sun. The distances to the stars are so great that the stars appear to us to be fixed relative to one another and collectively form the surface of a huge sphere—the *celestial sphere*—with Earth at its center.

The celestial sphere rotates regularly each night from east to west, its axis of rotation coinciding with Earth's rotational axis and its north and south poles oriented in the same way as Earth's poles. The locations of the stars on the celestial sphere, like towns on a road map and points on the surface of Earth, are specified with two coordinates. For locations on Earth the coordinates are called *latitude* and *longitude*. The former specifies how many degrees north or south of the equator (which is defined as zero degrees, 0° latitude) the point is located; the latter tells how many degrees west of zero degrees longitude the point lays. The longitude line (also called a meridian) that passes through Greenwich, United Kingdom, is defined as 0°. (See Figure 13-14*a*.)

Since there are 360° around Earth and our planet rotates on its axis once every 24 hours (1440 min), longitude is often expressed in time units (hours) rather than angle units (degrees or radians).

$$\frac{1440\text{ min}}{360\text{ deg}} = 4.0\frac{\text{min}}{\text{deg}}$$

For example, Orlando, Florida, is located at 28.4° N latitude, 81.3° W longitude. In time units 81.3° W longitude is

$$81.3\text{ deg} \times 4.0\text{ min/deg} = 325.2\text{ min} = 5.42\text{ h}$$

Thus, Orlando is 5.42 hours west of (i.e., earlier than) Greenwich.

On the celestial sphere the locations of stars are described in an exactly analogous way. The analog of longitude on the celestial sphere is *right ascension*.[10] It is represented by the lower case Greek letter α. Right ascension is measured in hours, rather than degrees, from zero up to 24 as on Earth. The analog of latitude is *declination*, represented by the lower case Greek letter δ. Declination is measured in degrees north (+) or south (−) of the celestial equator. (See Figure 13-14*b*.)

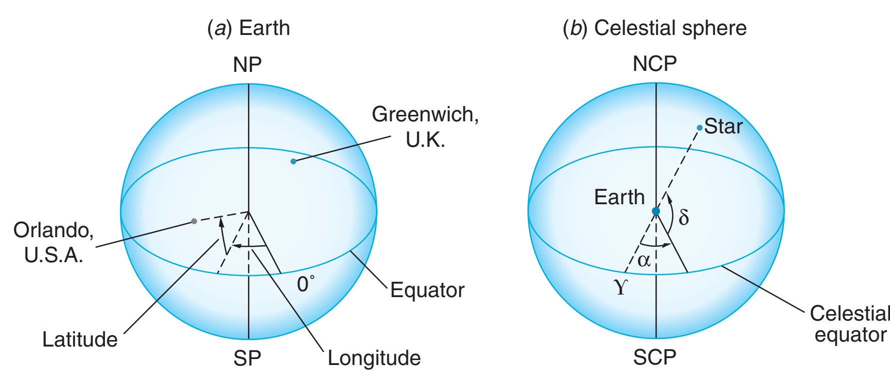

Figure 13-14 (*a*) Diagrammatic definition of longitude and latitude on Earth. (*b*) Corresponding definition of right ascension α and declination δ on the celestial sphere. ϒ marks the celestial sphere analog of Earth's 0° longitude, the meridian through Greenwich, United Kingdom.

Choosing the analog of the Greenwich meridian, i.e., the 0° longitude, for the celestial sphere requires a bit of explanation. Since Earth rotates on its axis from west toward east, the stars fixed on the celestial sphere continually move across the sky from east toward west. Also, Earth orbits the Sun once every 365.26 days. This means that while Earth rotates on its axis once each 24 hours, it also advances along its orbit around the Sun slightly less than 1° during that 24-hour period. To bring the Sun directly over the same meridian as on the day before, Earth must rotate very nearly 361°; however, doing the same thing with a star on the celestial sphere requires only a 360° rotation, because the distances to the stars are vastly greater than Earth's daily motion in its orbit. As we noted above, 1° corresponds to 4.0 minutes, so a given star rises in the east each night 4.0 minutes earlier than it did the night before, as a result of Earth's orbital motion around the Sun.

In addition to the nightly advance of star rise, there is a gradual change in the orientation of the celestial sphere that varies with the seasons. This change is due to the fact that Earth's rotational axis is tilted at about 23.5° with respect to the plane of our orbit around the Sun. This means that over the course of one year as viewed from Earth, the Sun follows a path, called the *ecliptic*, on the celestial sphere that ranges from 23.5° north to 23.5° south of the celestial equator. Thus, the ecliptic intersects 0° declination twice each year (Figure 13-15), once on about March 20, the *vernal* (or *spring*) *equinox*, and again on about September 23, the *autumnal equinox*. The Sun reaches its maximum north declination of 23.5° N on about June 21, the *summer solstice* and its maximum south declination of 23.5° S on about December 21, the *winter solstice*[11] (see Figure 13-15).

By international agreement, the point at which the Sun's path projected against the celestial sphere (the ecliptic) crosses the celestial equator (0° declination) in the spring, the vernal equinox, is defined as zero hours (and 0°) right ascension. On the celestial sphere the vernal equinox is designated with the Greek capital letter Υ (see Figure 13-14*b*). There are a number of other small motions of Earth that affect the appearance of the celestial sphere over very long periods of time, e.g., the slow wander of Earth's poles; however, those are beyond the scope of our discussions in this chapter.

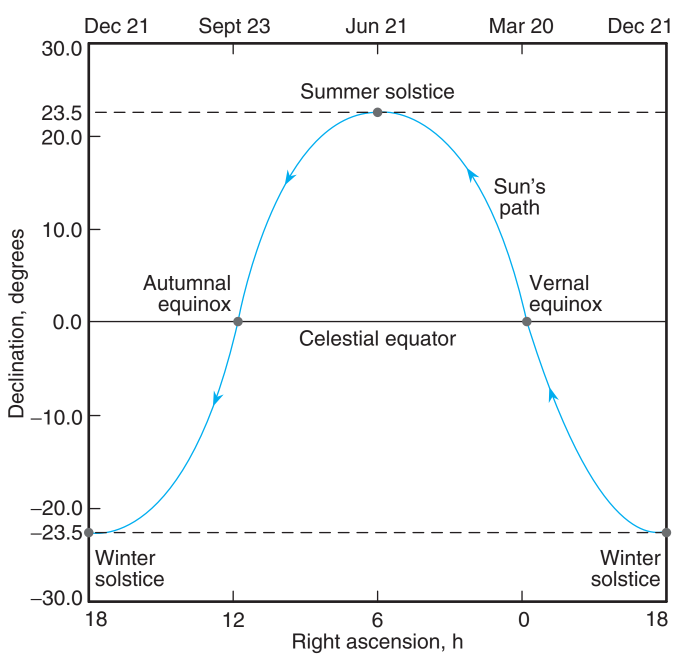

Figure 13-15 The Sun's path as projected onto the celestial sphere.

The Mass (and Missing Mass) of the Milky Way

Using the Doppler effect, J. Oort and B. Lindblad first demonstrated in 1926 that the Galaxy is rotating. The Sun is apparently moving in a circular orbit at a speed of about 2.5×10^5 m/s toward the constellation Cygnus. Assuming that the Sun's speed is constant, we can compute the time for the Sun to complete one revolution around the center of the Milky Way (a "Sun year") and the mass of the Galaxy. Since the Sun is 28,000 $c \cdot y$ from the galactic center, a Sun year is 2.1×10^8 Earth years. (See Problem 13-4.)

EXAMPLE 13-3 The Mass of the Galaxy Calculate an approximate value for the mass of the Galaxy. Include in the calculation the mass that lies inside the Sun's orbit in the Milky Way.

SOLUTION

1. Using Newton's law of gravitation, where the gravitational force acting on the solar mass $M_\odot$ by the mass of the Galaxy M_G is given by:
$$F = G\frac{M_\odot M_G}{R^2}$$

2. This gravitational force provides the centripetal force that holds the Sun in its galactic orbit of radius R. Thus,
$$\frac{GM_\odot M_G}{R^2} = \frac{M_\odot v^2}{R}$$

3. Solving for M_G gives:
$$M_G = \frac{Rv^2}{G}$$

4. Substituting values for the Sun's orbital radius R and speed v and for the universal gravitational constant G gives:
$$M_G = \frac{(28{,}000\ c \cdot \text{y})(9.46 \times 10^{15}\ \text{m}/c \cdot \text{y})(2.5 \times 10^5\ \text{m/s})^2}{6.67 \times 10^{-11}\ \text{Nm}^2/\text{kg}^2}$$
$$= 2.48 \times 10^{41}\ \text{kg}$$

Remarks: *Thus, if the Sun's mass is a representative average for the stars of the Milky Way, the Galaxy contains about* 1.3×10^{11} *stars.*

A problem arises in that, if we add together the masses of all of the visible stars in the Galaxy, including those beyond the Sun's orbit, plus all of the dust and gas clouds, we can account for only about 4 percent of the gravitational mass necessary to hold the Galaxy together. This discrepancy is referred to as the *missing mass* or *dark matter problem*. It exists for all galaxies and, indeed, for the universe itself. The first hint of the problem came in 1933. Based on his studies of the motions of the galaxies in the Coma Cluster of galaxies (see Section 13-6), F. Zwicky found that the mass of the cluster, estimated from the brightness and number of galaxies it contained, was too small by a factor of about 400 to account for the observed motions. He inferred that there must be some kind of unseen gravitational mass in the cluster—dark matter. Various solutions to the problem, such as black holes and dark matter, are under intense investigation and debate. Possible dark matter candidates include massive neutrinos and *w*eakly *i*nteracting *m*assive *p*articles (called WIMPs). Among the WIMP candidates (out of many suggested possibilities) are *axions* and *neutralinos*, hypothetical elementary particles that many astrophysicists and cosmologists think may be the best choices. Although it is now certain that neutrinos have mass, they probably do not contribute significantly to solution of the dark matter problem because, being relativistic, they don't clump together into clouds like cold interstellar hydrogen does.

Axions were postulated more than 30 years ago as part of an elegant theoretical solution to a problem with quantum chromodynamics, namely that QCD predicted a large electric dipole moment for the neutron (that experiments show it does not have). The axion resulted from the breaking of a symmetry (see Section 12-4) in the theory that explained the absence of an electric dipole moment for the neutron. As proposed the axion would have no electric charge and interact only minimally with ordinary matter. As a contributor to the solution of the dark matter problem, its value may be limited, since recent experiments place an upper limit to its mass, if it exists, of 10^{-6} eV$/c^2$.

The neutralino is considered by many astrophysicists and cosmologists as perhaps the best candidate to solve the dark matter problem. The neutralinos (there may be four of them) are the mass eigenstates that result from the quantum mixing of the supersymmetry partners of the W, Z, and Higgs bosons, the Wino, Zino, and Higgsino (see Table 12-11). One of the neutralinos may be the lightest possible supersymmetric particle and would, therefore, be stable. In some cosmological models it was produced copiously in the early universe and, with no decay channel available, it may have a relic abundance that could account for the dark matter. The lightest neutralinos mass is estimated at 10 to 10^4 GeV$/c^2$. (The proton mass is 0.938 GeV$/c^2$.) It would couple to other particles only via the weak interaction, so its behavior would be similar to that of the neutrino in that it would not be directly observable in existing detectors at the big accelerators. A significant portion of the experimental runs of the Large Hadron Collider will be searches for supersymmetry particles, including the energy/momentum discrepancy signature of the neutralinos.

13-3 The Evolution of Stars

While no universally accepted theory of stellar formation exists, it is generally agreed that stars are formed from massive clouds of dust and gas that exist throughout space. At some point in the swirling cloud, gravitational attraction begins to cause aggregations of matter to collect. These contract further due to gravity, attracting still more matter to them and eventually—if the cloud has sufficient mass—increasing the temperature to that necessary to initiate fusion as was described earlier, and a star is born.

In this section, we discuss how stars evolve once they have been formed. Two characteristics of stars are important for this discussion, the luminosity L and the effective temperature T_e. The effective temperature of a star is difficult to measure. It is usually inferred from a comparison of the spectral distribution of its radiation with that of a blackbody or from measurements of the absorption lines of hydrogen and helium in the atmosphere of the star.

The luminosity is the total power radiated by the star. It is determined from the radiant flux F of the star at Earth (remember, called the solar constant f for the Sun) and the distance r from Earth to the star (see Equation 13-2):

$$L = 4\pi r^2 F \qquad \textbf{13-10}$$

Determining the distance to a star is generally a very difficult task. For stars that are relatively close, the distance can be determined from the apparent motion of the star in the sky due to the motion of Earth around the Sun. During one complete revolution

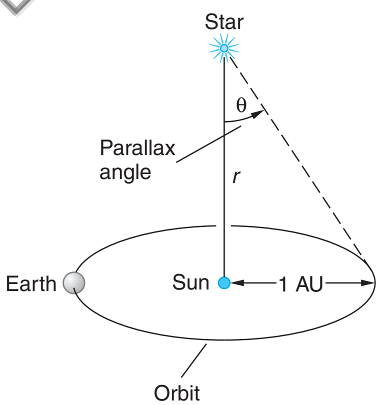

Figure 13-16 The parallax method of finding distances to nearby stars. A parsec is the distance r for which the parallax angle θ subtended by 1 AU is 1 arc second.

of Earth, a star appears to move in an ellipse of angular radius θ along the major axis called the *parallax angle* as shown in Figure 13-16. The parallax angle is given by

$$\theta = \frac{1\ \text{AU}}{r} \tag{13-11}$$

Astronomical distances are measured in parsecs or light-years. One parsec (pc) is that distance at which 1 AU subtends an angle of 1 arc second (1″), which equals 1/3600 of a degree. Setting $\theta = 1''$ in Equation 13-11, we obtain

$$1\ \text{parsec} = \frac{1\ \text{AU}}{1''} \times \frac{3600''}{1^\circ} \times \frac{180^\circ}{\pi\ \text{rad}} = 2.60 \times 10^5\ \text{AU} \tag{13-12}$$

Using 1 AU $= 1.496 \times 10^{11}$ m and $1\ c \cdot y = 9.461 \times 10^{15}$ m, we can express the parsec in terms of meters or light-years:

$$1\ \text{pc} = 3.086 \times 10^{16}\ \text{m} = 3.26\ c \cdot \text{y} \tag{13-13}$$

EXAMPLE 13-4 Distance to Proxima Centauri Proxima Centauri is the star closest to the Sun. By measuring the maximum apparent change in the direction to Proxima Centauri between two observations made six months apart, the parallax angle is found to be 0.77233″. How far is it to Proxima Centauri? (Proxima Centauri's location: R. A. $14^h29^m43^s$, Dec. 16°41′58″.)

SOLUTION

Since 1 AU/1″ = 1 parsec, we have for $\theta = 0.77233''$,

$$r = \frac{1\ \text{AU}}{\theta} = \frac{1\ \text{AU}}{0.77233''} = \frac{1\ \text{AU}}{1''}\,\frac{1''}{0.77233''} = 1\ \text{pc} \times \frac{1''}{0.77233''} = 1.2948\ \text{pc}$$

$$= 4.22\ c \cdot \text{y}$$

Parallax angles as small as 0.001″ can be measured, which means that the parallax method of Example 13-4 can be used to measure stellar distances from the Sun out to about 1 kpc. Since it is about 8 kpc to the center of the Galaxy, the method can be used for only about 10,000 stars that are relatively close to the Sun and, thus, in the Milky Way. For the rest, the parallax angle is immeasurably small. In other situations, more indirect measurements of distance are necessary. One involves complex analyses of intensity variations over time for particular types of pulsating stars (Cepheid variables) found primarily in star clusters. Distances to clusters as far away as about 29 Mpc have been measured by this method. Supernovae (see Section 13-4) provide several methods for determining distances to the galaxies in which they are located. The most important of these makes use of the similarity of the light curves, that is, the emitted light intensity versus time, of so-called Type Ia supernovae. Such measurements enable calculations of the distances to supernovae that are accurate to within about 5 percent and recently provided the crucial evidence that the expansion of the universe is accelerating.

Hertzsprung-Russell Diagram The various states of stars can be conveniently displayed by plotting the luminosity L versus the effective temperature T_e. The result is called the *Hertzsprung-Russell (H-R) diagram*. Figure 13-17*a* shows an H-R diagram for some stars of representative masses. The large majority of stars on an H-R diagram fall in the broad central band called the *main sequence*. Main sequence stars are normal in that they are homogeneous mixtures, except in the core, they have essentially the same chemical composition, and they are fusing hydrogen into helium via one or another of the nuclear reactions discussed earlier. Stars expand as they leave the main sequence. For that reason, stars in the main sequence are often called *main sequence dwarfs*. Between 80 and 90 percent of all stars are on the main sequence.

The location of a star along the main sequence in the H-R diagram depends on its luminosity, which is primarily dependent on the mass of the star. The masses of stars range from about 0.08 $M_\odot$ to about 60 $M_\odot$, where $M_\odot$ is the mass of the Sun. Gaseous objects with less than about 0.08 $M_\odot$ do not have enough gravity for their central cores to be compressed sufficiently to generate the temperature necessary to sustain the nuclear fusion reactions needed for energy emission. Objects with masses greater than 60 $M_\odot$ would generate such enormous internal temperatures that the outward radiation pressure would exceed the gravity-generated inward pressure. Such a system would be very unstable, if indeed it could form at all.

Evaluation of the masses of binary stars has shown that the luminosity of a star is approximately proportional to the fourth power of its mass:

$$L \propto M^4 \qquad \textbf{13-14}$$

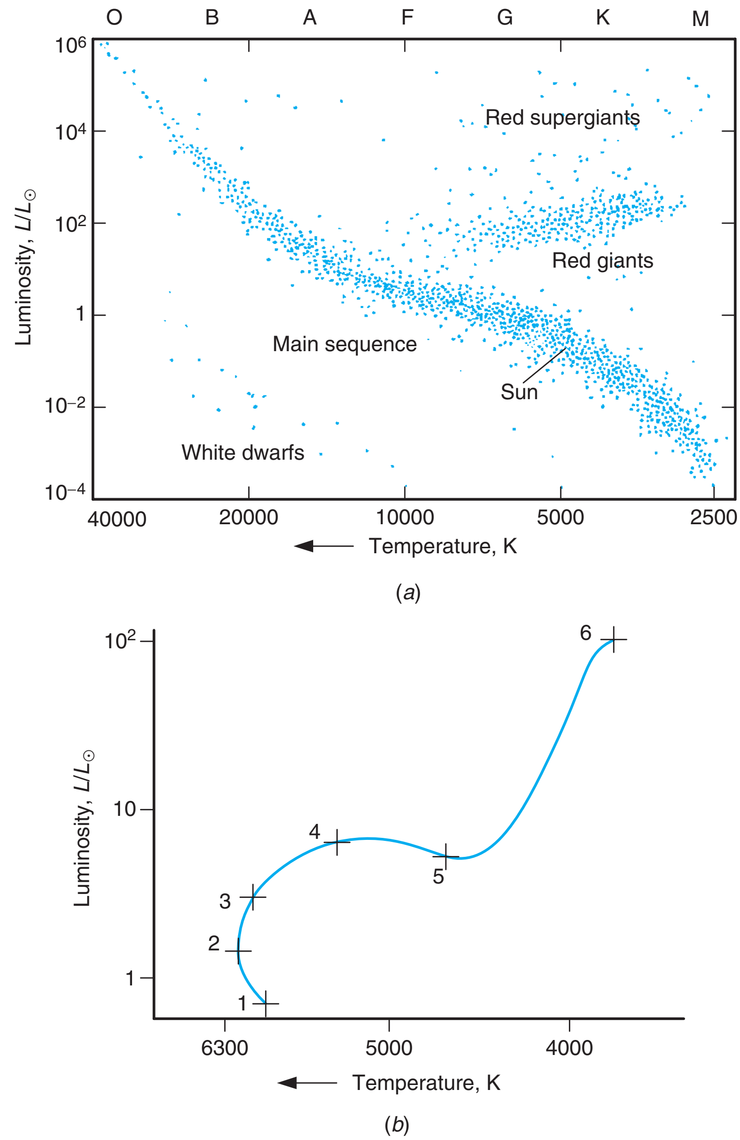

Figure 13-17 (a) The Hertzsprung-Russell (H-R) diagram for stars in the solar neighborhood. Most stars (80 to 90 percent) fall on the main sequence. Stars in the lower right end of the main sequence are cool and dim, those in the upper left are hot and bright. (*b*) The Sun's evolutionary track from the time it entered the main sequence at point 1. The Sun is currently between points 1 and 2. It will leave the main sequence at point 4. The time between successive points is approximately 10^9 years.

The lifetime of a star t_L is proportional to the total available energy, which is proportional to the star's mass ($E = Mc^2$), and inversely proportional to the rate of energy emission, which is the luminosity:

$$t_L = \frac{E}{L} \propto \frac{Mc^2}{M^4} \propto M^{-3} \qquad \textbf{13-15}$$

Thus, more massive stars burn their hydrogen more quickly than do less massive stars. Thus, a star with twice the Sun's mass would be expected to have a lifetime only 1/8 as long as that of the Sun. (Equation 13-15 doesn't work for very small or very large stars because the luminosity-mass relationship of Equation 13-14 is only an average result. The exponent in Equation 13-15 is larger in magnitude for very small stars and smaller for very large stars.)

Considerations of energy balance for stars on the main sequence lead to the approximate proportionality of the radius and the mass, as can be demonstrated using the data in Table 13-3 (see Problem 13-6):

$$R \propto M \qquad \textbf{13-16}$$

Combining this with Equation 13-4, which relates the effective temperature to the luminosity per unit area, we can relate the effective temperature to the mass of the star:

$$T_e = \left(\frac{L}{4\pi R^2 \sigma}\right)^{1/4} \propto \left(\frac{M^4}{M^2}\right)^{1/4} \propto M^{1/2} \qquad \textbf{13-17}$$

Thus, stars with larger masses have higher effective temperatures and, hence, higher luminosities than those with lower masses. It is on the basis of Equations 13-15 and 13-17 that the stellar masses were plotted on the H-R diagram in Figure 13-17*a*. Table 13-3 lists properties of stars by spectral type. The following values for the Sun's characteristics will enable calculation of numerical values for the corresponding characteristics of individual stars: $L_\odot = 3.83 \times 10^{26}$ J/s; $R_\odot = 6.96 \times 10^8$ m; $M_\odot = 1.99 \times 10^{30}$ kg.

As the star ages, it consumes its primary fuel, hydrogen. What happens to it as the hydrogen supply in the core becomes exhausted depends on its initial mass. Low-mass and high-mass stars follow somewhat different evolutionary paths. In either case, however, the fundamental processes involved are successive nuclear reactions fueled by the product of the previous cycle. Thus, after the hydrogen in the core has fused to helium, the star must begin fusing helium in a cycle that eventually forms carbon.

Table 13-3 Selected properties of stars

Spectral type	Surface temperature (K)	$L/L_\odot$	$R/R_\odot$	$M/M_\odot$
O5	44,500	790,000	15	60
B0	30,000	52,000	8	18
A0	9,520	54	3	3
F0	7,200	6	2	2
G0	6,030	1.5	1.1	1.1
Sun (G2)	5,800	1.0	1.0	1.0
K0	5,300	0.4	0.8	0.8
M0	3,900	0.08	0.6	0.5
M8	2,600	0.001	0.17	0.06

Before this can occur, the core must heat up still further to the 10^8 K necessary to initiate helium fusion. The chain of events involved in this process is complex and beyond the scope of this book. However, its result for low-mass stars is that the radius (and therefore the surface area) increases while luminosity remains nearly constant. Thus, the intensity (luminosity per unit area) and, consequently, the effective temperature decrease and the radiation emitted shifts to longer wavelengths as the star expands to become a *red subgiant*. The photosphere rapidly becomes more transparent as T_e and the density ρ decrease, increasing the luminosity and effectively limiting the decrease in temperature. The star is then a *red giant*. The track of a typical evolving low mass star such as the Sun is shown on the H-R diagram in Figure 13-17*b*.

Helium ignition results in the star again increasing its effective temperature and moving to the *horizontal branch*. When the helium in the core is exhausted, the star begins fusing carbon and ascends the red giant branch again, becoming a *red supergiant*. Betelgeuse, the bright star in the shoulder of the constellation Orion, is a red supergiant. Its density is about 1.5×10^{-5} kg/m^3, a hundred thousand times less than the air we breathe! What happens after this is not completely clear. Through a combination of events that includes the loss of considerable mass, perhaps including the ejection of an expanding shell of gas (called a *planetary nebula*), such as that shown in Figure 13-18, the star may become a white dwarf, slowly cooling toward thermal equilibrium with the universe. We will discuss white dwarfs further in Section 13-5.

High mass stars—those with masses greater than about $6M_\odot$—evolve much more quickly than low-mass ones, as predicted by Equation 13-15. In addition, they have sufficient initial mass to generate gravitationally the high pressures and temperatures necessary to ignite the fusion reactions with oxygen, neon, and then silicon to produce, ultimately, iron. These reactions occur with phenomenal speed and lead to catastrophic events that will be discussed in the next section. An extremely massive star, such as Betelgeuse, may become a supernova via core collapse (see Section 13-4).

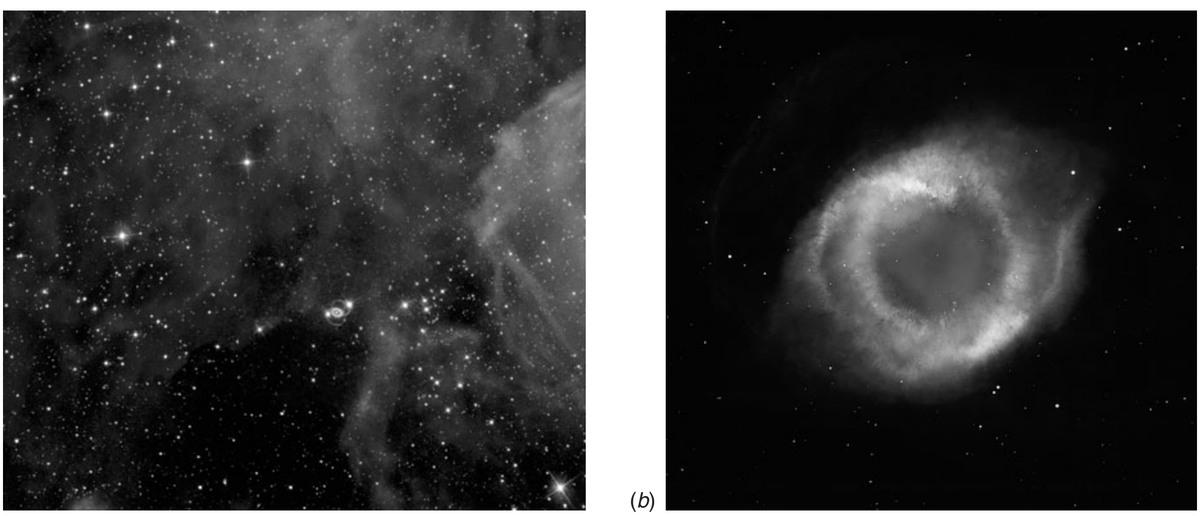

(*a*) (*b*)

Figure 13-18 The nebula 30 Doradus (*a*), also known as the Tarantula nebula, is believed to be older than nebula NGC 7293 (*b*), also known as the Helix nebula. The Tarantula nebula's rapidly expanding gas cloud consequently shows a greater degree of diffusion. Located in the Large Magellanic Cloud, the Tarantula contains one of the most massive stars known, as well as supernova SN1987A, the very bright star slightly below the center (of the left-hand photo). Ultraviolet radiation from stars heats the gas of a nebulae, causing it to radiate. [*(a) The Hubble Heritage Team (AURA/STScI/NASA). (b) NASA, NOAO, ESA, the Hubble Helix Nebula Team, M. Meixner (STScI), and T.A. Rector (NRAO).*]

13-4 Cataclysmic Events

Huge explosions and other sorts of cataclysmic events are a natural part of the life cycle of stars. Stars formed in swirling clouds of gas move along the H-R diagram, incorporating such occurrences into their evolution and forming in the process the elements needed to form new stars. Why these cataclysmic events occur is the subject of this section.

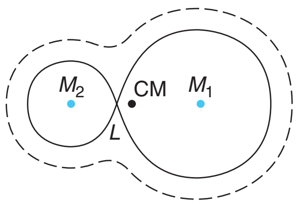

Figure 13-19 Cross sections of two gravitational equipotential surfaces for stars M_1 and M_2. The point labeled L is one of five Lagrangian points where the net gravitational potential is an extremum (a saddle point in this case) and the net force is zero.

Novae

More than half of all stars are members of *binary pairs* or even larger associations. These stars orbit their common center of mass as the group moves with the rotation of the Galaxy. The periods of binaries vary from a few hours for those with the companions very close to each other to millions of years for those with the companions separated by thousands of astronomical units. Here, we are interested in close binaries.

A complete analysis of the interactions between the two stars forming a close binary is beyond the scope of this book, but a qualitative explanation will suffice. Consider a binary whose stars of masses M_1 and M_2 rotate about their common center of mass in circular orbits. An observer at rest in the rotating system experiences a net force that is the sum of the gravitational forces due to the two stars and the pseudoforces due to the rotation. Figure 13-19 shows an equipotential surface about a binary pair. It is easy to visualize that there is a point along the line joining the centers of the two stars where the net potential is a minimum. At this point, the net force due to the combined effects of the rotation and the gravitational attraction by the masses M_1 and M_2 is zero. This point is a *Lagrangian point*. The three-dimensional equipotential surface that includes the Lagrangian point L forms an envelope around each star called the *Roche lobe*.[12]

Now consider what happens when, through natural evolution, one of the stars, say M_1, begins expanding and fills its Roche lobe. The photosphere of the star feels a vacuum outside the surface, the outward pressure at any point being balanced by gravity. But at the Lagrangian point there is no gravity. Thus, material from M_1 pours through the Langrangian point into the Roche lobe of M_2. Once inside it is gravitationally attracted toward M_2. Since the system is rotating, the material from M_1 doesn't simply move directly toward M_2 but, because of the Coriolis effect, forms a spiraling *accretion disk* (Figure 13-20).

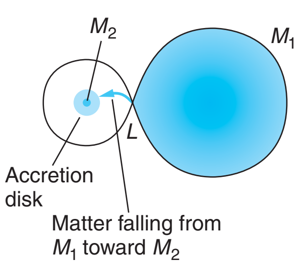

Figure 13-20 Material from M_1 pouring through the Lagrangian point into the Roche lobe of M_2 forms an accretion disk in M_2's equatorial plane. Material arriving later hits the disk, generating a high-temperature impact area. This causes novae to flicker irregularly.

If M_2 is a normal star, nothing of great consequence occurs, but if it is a white dwarf, then cataclysmic events called *novae* can occur. We will mention two possibilities. Material flowing through the Lagrangian point into the accretion disk is stored there until some instability occurs in the disk that results in the dumping of material onto the surface of the white dwarf. The impact heats the surface, causing a sudden luminosity increase by a factor of 10 to 100. Such events recur at intervals of a few weeks for *dwarf novae* to hundreds or thousands of years for *recurrent novae*. Between these sudden bursts in intensity, the novae flicker as described in the caption of Figure 13-20.

For *classical novae*, which eject substantial material into space and can brighten by a factor of a million within a few days, astrophysicists suggest that the sudden dumping of material from the accretion disk onto the hot surface may result in the buildup of sufficient hydrogen to initiate a thermonuclear explosion. After the blast the system returns to a more quiescent state, pending the accumulation of more hydrogen in the disk. The theoretical problems involved in explaining such an event are formidable, however, and no general agreement on the mechanism exists.

Supernovae

A *supernova*—the catastrophic explosion of an entire star—is, perhaps surprisingly, somewhat more clearly understood than the nova. Supernovae are classified as Type I or Type II mainly on the basis of their spectra (Figure 13-21). The spectra of *Type I* supernovae do not contain hydrogen lines, indicating that they are devoid of hydrogen, or nearly so. In contrast, *Type II* supernovae exhibit strong hydrogen lines. Type I supernovae are further divided into Type Ia, which show a strong line of singly ionized Si at 615 nm, Type Ib whose spectra include strong He lines, and Type Ic whose spectra do not include He lines. Recalling that H and He are in that order the most abundant elements in the universe, these spectral differences indicated that there are significant differences in the progenitors of the Type I and Type II supernovae. Type II supernovae are subdivided into two groups based on the shape of their light intensity versus time curves following peak brightness. The light curves of Type II-L supernovae decline *l*inearly with time; the light curves of Type II-P exhibit an intermediate *p*lateau lasting 30 days or more before the intensity decline resumes.

Supernovae are not just big novae. Their origin is completely different. In Section 13-3, we saw what occurs in a star as it uses up the hydrogen in the core and begins moving off the main sequence of the H-R diagram. The star begins to fuse helium, then carbon. If it were a low-mass star, it would have insufficient gravitational energy to ignite the fusion of heavier nuclei in quantity. For massive stars, however, the situation is different. Type Ia supernovae originate in binary systems where one star is a massive white dwarf rich in carbon and oxygen (see Section 13-5). An expanding companion that fills its Roche lobe may dump a huge amount of gas directly onto the dwarf's surface, increasing the gravitational pressure in the core. If the pressure increases the core temperature enough to trigger carbon fusion, a runaway fusion reaction results, producing a massive thermonuclear explosion—a huge "carbon bomb." Depending on the characteristics of the particular binary, it may be possible that Type Ib and Type Ic supernovae result from gravitational core collapse. Type I supernovae occur among population II stars. (Don't be confused by the apparent inconsistency in nomenclature.) As noted earlier, Type Ia supernovae all have very similar maximum intensities and light curves which makes it possible for them to be identified even at very large distances, enabling them to be used as "standard candles" by astronomers. It is these features that have made it possible for astronomers to measure much greater distances to host galaxies than was previously possible.

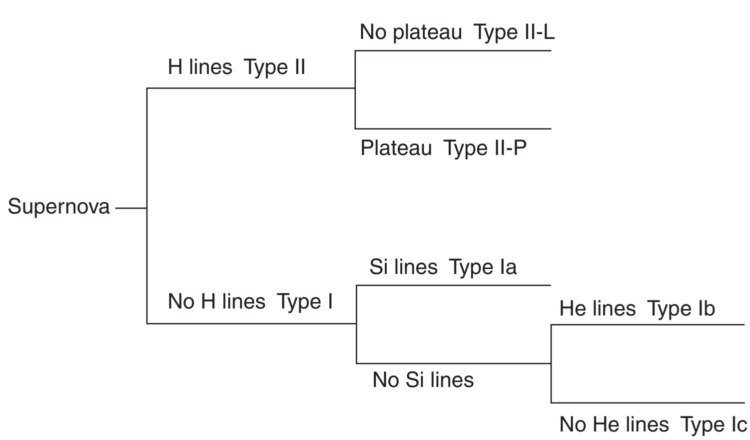

Figure 13-21 Schematic of the classifications of supernovae. Type I subgroups are based on their spectra at maximum brightness. Type II subgroups are based on the existence or absence of a plateau in the light curve.

If a star's mass is greater than about $8M_\odot$, evolution toward a Type II supernova proceeds approximately as follows. Gravity is strong enough to continue to draw mass from the middle layers into the core as the core uses up fuel. The increasing temperatures, exceeding 10^8 K, are sufficient to ignite fusion in neon and silicon ultimately producing iron. As we saw in Chapter 11, the specific binding energy of iron is the highest in the periodic table. Fusing elements above iron doesn't emit energy, it absorbs energy. Thus, when the core has been fused to iron, there is nowhere else to go via thermonuclear reactions. With no counteracting outward pressure from nuclear reactions, gravitational contraction continues even more rapidly and the core consequently continues to heat up until it exceeds 10^9 K. At that point, the radiation within the star is intense and iron nuclei undergo photodisintegration into helium and neutrons, absorbing energy from the core and accelerating the gravitational collapse:

$$^{56}_{26}\text{Fe} \longrightarrow 13\,^{4}_{2}\text{He} + 4n \qquad \textbf{13-18}$$

The helium nuclei then begin to photodisintegrate, absorbing enormous amounts of energy to overcome the nuclear binding energy of helium:

$$^{4}_{2}\text{He} \longrightarrow 2p + 2n \qquad \textbf{13-19}$$

The core is now in gravitational free fall, compressing the electrons and protons into neutrons via inverse beta decay:

$$p + e^- \longrightarrow n + \nu_e \qquad \textbf{13-20}$$

What happens next to the core is a matter of intense theoretical conjecture that we will explore further in Section 13-5.

What happens to the envelope of the star—the material outside the core—although unclear theoretically, is certainly apparent visually. The entire envelope is blown away in an incredibly massive explosion. This is a Type II supernova. Supernovae are extremely rare, but scientists were fortunate enough to observe one in 1987 only 170,000 $c \cdot$y away in the Large Magellanic Cloud, a small irregular galaxy that is a companion to the Milky Way. Called SN1987A (see Figure 13-18 and the photo at the left), it was the first to occur close enough to be visible to the unaided eye since 1604, when both Kepler and Galileo saw one. Two others were recorded earlier, in 1006 and 1054, the latter documented by Chinese astronomers and still visible as the Crab Nebula. Several others have been observed with telescopes. As a result of the enormous number of nuclear reactions and decays initiated by the supernova, the radiation emitted in the explosion is accompanied by a flood of neutrinos. Neutrinos emitted by SN1987A were detected by the Kamiokande neutrino observatory, bringing with them information about the core-collapse model of supernovae and a hint of the nonzero neutrino mass (see Problem 12-13).

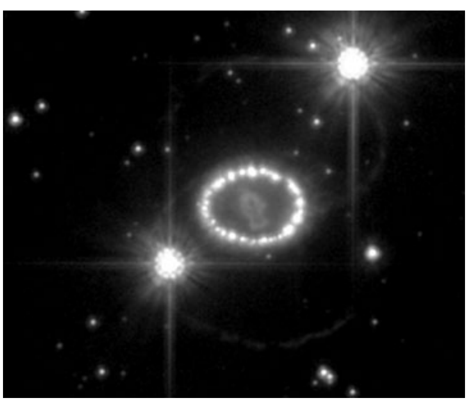

Supernova 1987A developed a set of rings some weeks after it was first seen. The rings are likely caused by a beam of high-energy radiation or particles sweeping across the gas. The source of the beam may be a previously unseen companion of the star that exploded. This Hubble Space Telescope photo was made with hydrogen Balmer alpha light. [*NASA, ESA, P. Challis and R. Kirshner (Harvard-Smithsonian Center for Astrophysics).*]

At its peak light output, a supernova typically shines more brightly than the entire galaxy in which it is located. The spectra of supernovae reveal the presence of elements throughout the entire periodic table. This indicates that some of the energy removed from the core following the production of iron is used to produce elements of even higher atomic numbers. The supernova ejects some of this material into space, where it eventually contributes to the formation of a new generation of stars and their planets via condensation. Such events undoubtedly preceded the birth of the Sun and the formation of Earth. We are, as has been said before, "made of the stuff of stars."

13-5 Final States of Stars

The cataclysmic events that occur near the end of the life of a star lead to one of only three possible final states: a white dwarf, a neutron star, or a black hole. The mass of the star, particularly that of the core, appears to be the primary factor in determining the final state.

White Dwarfs

Stars whose masses are less than about $6M_\odot$ follow an evolutionary track on the H-R diagram that takes them through one or more periods of substantial mass loss from the outer layers of gas. How this occurs is not clear, but the ejected mass, which is heated to a glowing planetary nebula by the hot core, leaves behind a *white dwarf*, a term used because many, though by no means all, are literally white hot. Its mass is typically about $1M_\odot$ and its radius of the order of 10^7 m, which is about the same as the radius of Earth. Thus, the density of a typical white dwarf is about 5×10^5 g/cm^3 compared to Earth's average density of about 5.5 g/cm^3. A coin the size of a penny made from white dwarf material would have a mass of over 200 kg, one the size of a Euro over 400 kg.

Thermonuclear reactions have ceased in the white dwarf, leaving it with a core consisting primarily of carbon and oxygen, so there is no outward pressure due to them from within the star. The star therefore collapses because of the inward gravitational pressure until the exclusion principle prevents the atomic electrons from coming any closer together. This effect is similar to the exclusion-principle repulsion between atoms in a molecule that we discussed in Chapter 9. It results in an outward pressure that is larger even than the thermal pressure of the hot core. It is this *electron degeneracy pressure* that supports the white dwarf. When the outward electron degeneracy pressure equals the inward pressure due to gravity, the star stops contracting.

Explicit derivation of the expression for the electron degeneracy pressure leads to a nonrelativistic relation between the dwarf's radius R and mass M:

$$R = (3.1 \times 10^{17}\ \mathrm{m \cdot kg^{1/3}})\left(\frac{Z}{A}\right)^{5/3} M^{-1/3} \qquad \textbf{13-21}$$

where Z is the atomic number and A is the atomic mass number of the material of the star. Note the interesting result that the larger the mass, the smaller the radius, a consequence of the gravitational contraction that was discussed earlier. For example, a white dwarf with a mass of $1M_\odot$ will have a radius smaller than one with a mass of $0.5M_\odot$! Equation 13-21 raises the interesting question of whether, when the electrons become relativistic, the mass might become large enough for the radius of the dwarf to shrink to zero. Although Equation 13-21 does not formally allow that possibility until M approaches infinity, S. Chandrasekhar[13] derived the corresponding relativistic relation and found that the radius would go to zero when the mass reached about $1.4M_\odot$. This quantity is called the *Chandrasekhar limit*. Its validity is strongly supported by the fact that the masses of all white dwarfs that have been measured are less than that value.

A lone white dwarf continually radiates heat to space and, without a nuclear furnace, slowly cools and dims. When it is no longer visible, it has become a *black dwarf*. It continues to cool toward thermal equilibrium with the universe. It is not likely that any white dwarfs have yet reached this final stage. However, if the white dwarf is a part of a binary, then in addition to the possibility of a nova described earlier, mass may flow from the companion directly onto the surface of the white dwarf. When the degenerate electron pressure can no longer support the white dwarf (at the Chandrasekhar limit), the star implodes, suddenly raising the core temperature and

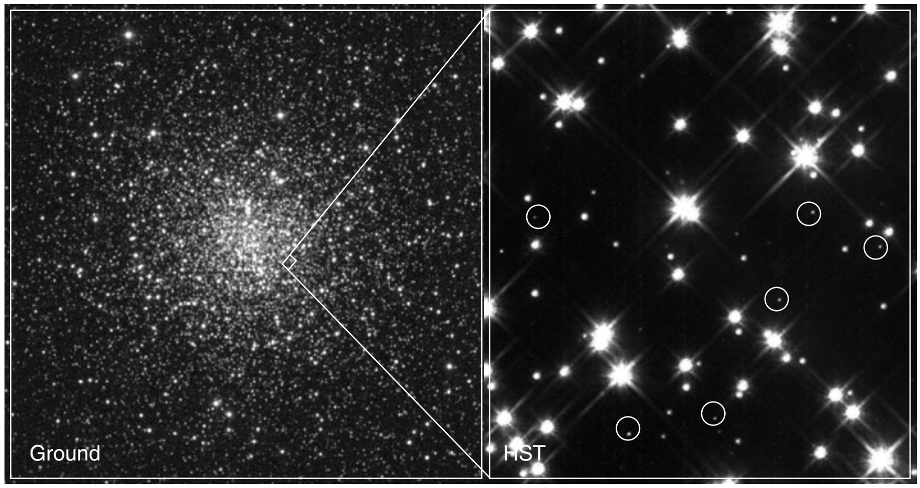

White dwarfs identified by the Hubble Space Telescope in M4, the globular cluster closest to Earth (7000 $c \cdot$ y). M4 contains more than 100,000 stars. [*(left) Kitt Peak National Observatory 0.9-meter telescope, National Optical Astronomy Observatories; courtesy M. Bolte (University of California, Santa Cruz). (right) Harvey Richer (University of British Columbia, Vancouver, Canada) and NASA.*]

detonating fusion in the carbon/oxygen core. The sudden energy release causes the white dwarf to explode as a Type Ia supernova. The common mass limit, 1.4 $M_\odot$, at which the white dwarfs explode, is a major factor in the resulting similarity of the Type Ia supernovae light curves that enables their use as a luminosity standard for measuring astronomical distances. Following the supernova explosion, about half of the residual core of the star is iron.

Neutron Stars

In the discussion of supernovae, we saw that the enormous pressures developed in the core forced inverse beta decay to occur, converting the core into neutrons. If the mass of the core following the explosion is greater than the Chandrasekhar limit, what happens? We can get an idea by considering the neutrons to be an ideal gas of fermions and derive a nonrelativistic expression for the mass-radius relation analogous to Equation 13-21. The result is

$$R = (1.6 \times 10^{14}\ \mathrm{m \cdot kg^{1/3}})M^{-1/3} \qquad \textbf{13-22}$$

where M is the mass in kilograms and R is the radius of the core in meters. Such a star is called a *neutron star*, since the envelope was blown away in the supernova and all that is left is the core consisting of neutrons. For $M = 1.0M_\odot$, Equation 13-22 yields the radius $R = 1.27 \times 10^4$ m $= 12.7$ km.

The density of the neutron star is about 1.2×10^{14} g/cm^3. This is only slightly less than the density of the neutron itself, which is about 4×10^{14} g/cm^3. Thus, we can conclude that the gravitational pressure of the neutron star is balanced by the repulsive component (due to the exclusion principle) of the strong nuclear force between the neutrons. As you might guess from our earlier discussion, gravity can overcome even this resisting pressure. The mass corresponding to the gravity at which that occurs would be the maximum mass possible for a neutron star, a mass analogous to the Chandrasekhar limit for white dwarfs. Current theory puts the maximum mass of a neutron star between 1.7 $M_\odot$ and $3M_\odot$. The few neutron stars that have been tentatively identified and measured all have masses below this limit.

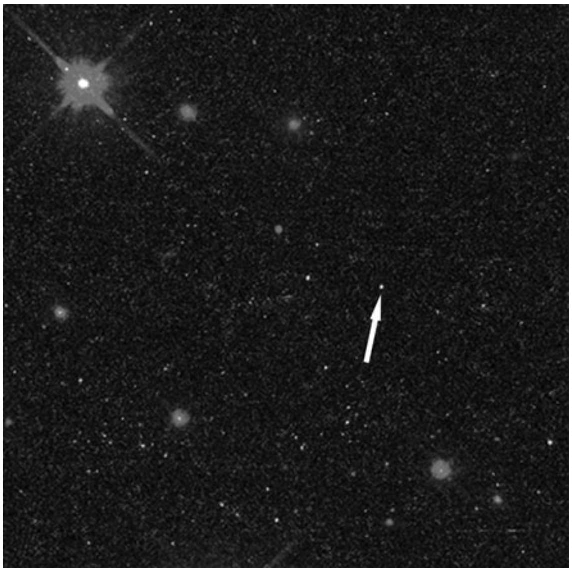

A lone neutron star, the first seen in visible light, is very hot (about 650,000 K at the surface) and may be no larger than 28 km in diameter. [*Fred Walter (State University of New York at Stony Brook) and NASA.*]

Regularly pulsing radio sources, called *pulsars*, discovered in 1967 in nebulae such as the Crab Nebula that are remnants of supernovae, are thought to be neutron stars. Current theory suggests that the radiation is emitted as the result of charged particles emitted by the neutron star that are accelerated along the star's magnetic field lines as a consequence of the star's rapid rotation as illustrated in Figure 13-22.

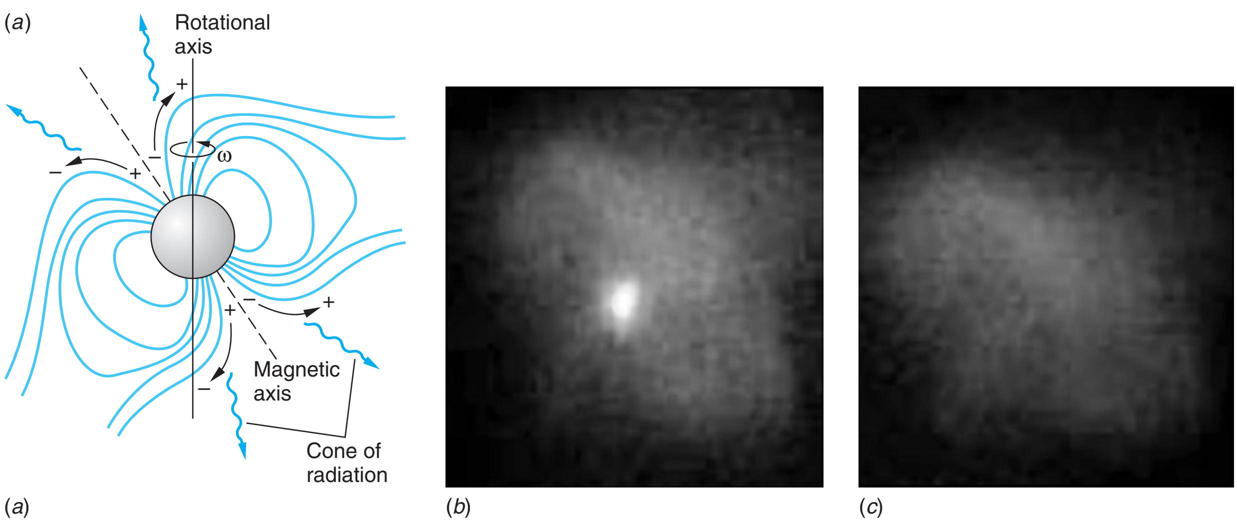

Figure 13-22 (*a*) The neutron star acquires much of the original star's angular momentum and magnetic field, causing it to rotate rapidly while dragging along a distorted magnetosphere. Accelerated charged particles radiate in a cone about the rotating magnetic axis like a cosmic lighthouse. (*b*) The pulsar in the Crab Nebula. As the cone of radiation swings to face Earth, light emitted from accelerated electrons becomes visible (the bright spot in the image). (*c*) A fraction of a second later, the pulsar has turned and this light is no longer directed toward Earth. Currently rotating about 30 times a second, the pulsar has a period that is increasing by about 10^{-5} s per year. [*(b) and (c) Harvard/Smithsonian Center for Astrophysics.*]

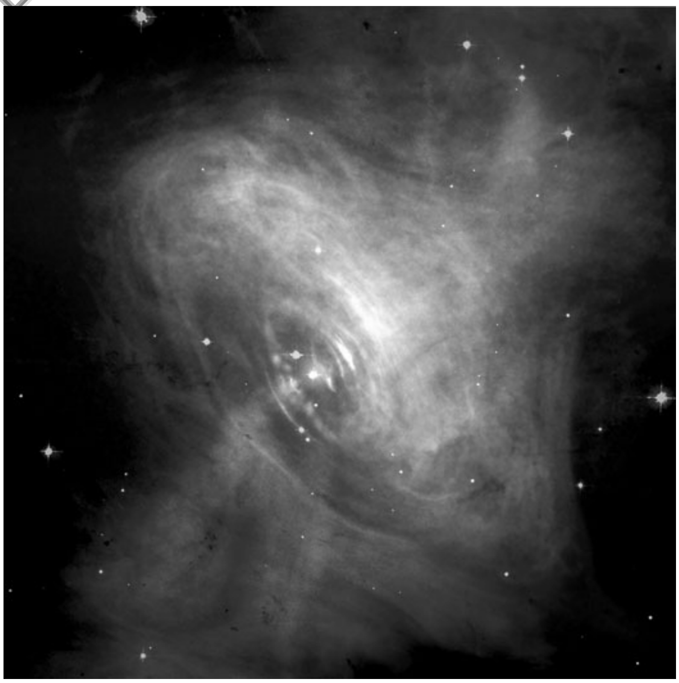

This composite image of the Crab Nebula was made from an x-ray image recorded by the Chandra X-Ray Observatory and an optical image from the Hubble Space Telescope. The inner ring is about 1 $c \cdot$y across. [*Credits for X-ray Image: NASA/CXC/ASU/J. Hester et al. Credits for Optical Image: NASA/HST/ASU/J. Hester et al.*]

The Crab pulsar also corresponds to an optical variable as illustrated in Figures 13-22*b* and *c*. It emits energy at an incredible 3×10^{31} W. Its period is equally incredible, 0.033 seconds, one of the shortest known. As it emits energy into space, the neutron star also slowly cools, approaching thermal equilibrium with the universe.

Black Holes

What happens when the mass of the remaining core of a supernova exceeds the $1.7M_\odot$ to $3M_\odot$ upper limit for the formation of a neutron star? The velocity necessary for an object with mass to escape from an object of mass M is found by equating the gravitational potential energy at the surface of M to the kinetic energy necessary to escape. This results in the escape velocity

$$v_e = \left(\frac{2GM}{R}\right)^{1/2} \qquad \textbf{13-23}$$

For a neutron star with $M = 1.0M_\odot$, $v_e = 1.3 \times 10^8$ m/s, more than 40 percent of the speed of light. If there were no relativistic and quantum mechanical effects, the escape velocity would equal c when

$$R_S = \frac{2GM}{c^2} \qquad \textbf{13-24}$$

where R_S is called the *Schwarzschild radius*. Thus, if an incipient neutron star is so massive that its radius is less than R_S, no object with mass can escape from its surface. In addition, radiation of wavelength λ_0 emitted at some distance R from mass M is shifted to a longer wavelength λ according to the *gravitational redshift* described in Section 2-5; the ratio is given by

$$\frac{\lambda}{\lambda_0} = \left(1 - \frac{v_e^2}{c^2}\right)^{-1/2} = \left(1 - \frac{2GM}{c^2 R}\right)^{-1/2} = \left(1 - \frac{R_S}{R}\right)^{-1/2} \qquad \textbf{13-25}$$

If R shrinks to the Schwarzschild radius, then λ approaches infinity and the energy $(E = hf = hc/\lambda)$ approaches zero. Thus, if R is less than R_S, no energy can escape the surface as radiation, either. Such an object is called a *black hole*, because it neither emits nor reflects radiation or mass and, hence, appears absolutely black.[14]

The radius of a black hole with a mass of $1M_\odot$, if there is such an object, would be only about 3 km. Many astrophysicists currently believe that a massive black hole is located at the center of the Milky Way and may account for a very small part of the "missing mass" of the Galaxy. During the past decade astronomers at the Max Planck Institute (Germany) have tracked about a dozen individual stars (of more than 300) orbiting an unseen object at Sagittarius A*, a radio source near the center of the Milky Way (see Figure 13-13). One of these, for example, is called S2. Determining S2's orbital period to be 15.2 y enabled calculation of the mass of the unseen object to

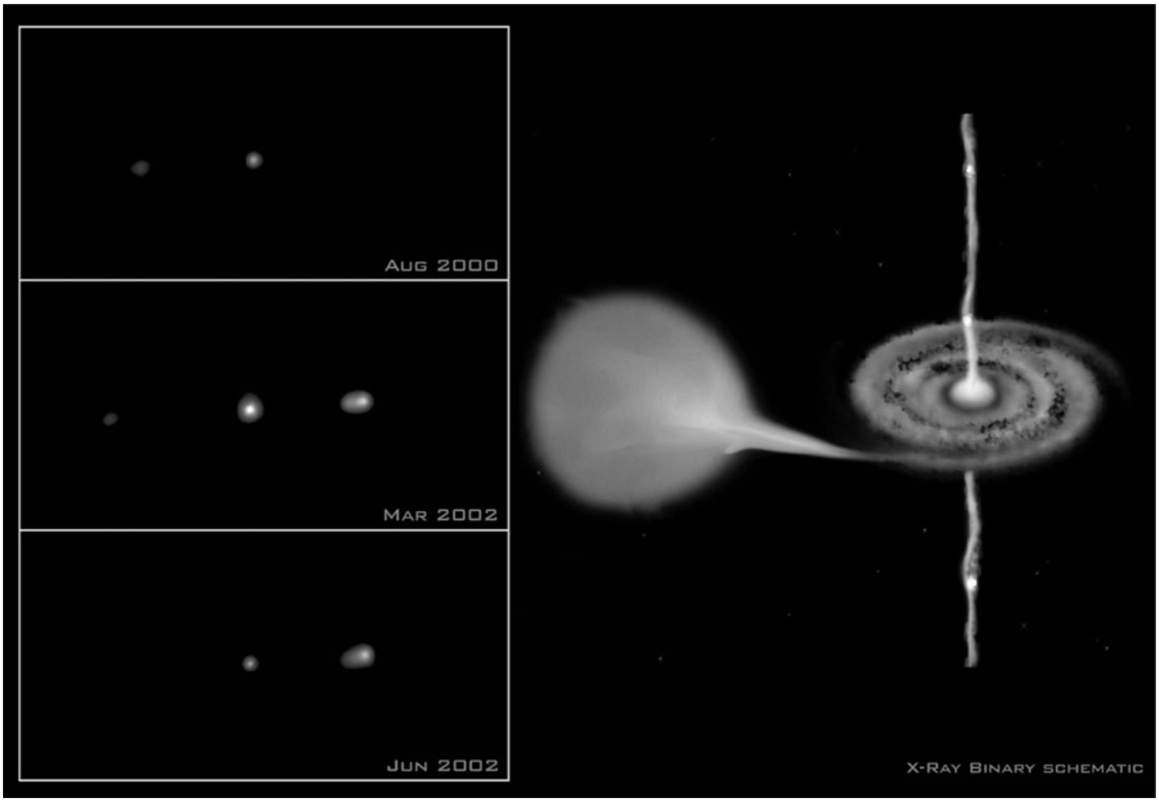

The series of Chandra X-Ray Observatory images on the left show jets of high-energy particles being produced near a black hole in a binary system, first on the left (top image), then on the right (middle image). The jets are moving away from each other at about 0.5 *c*. In the lower image the left jet has disappeared. The schematic on the right illustrates how the jets originate. The black hole draws mass from the normal companion, then intense electromagnetic forces in the accretion disk expel the jets of high-energy particles. [*Left: X-ray (NASA/CXC); Right: Illustration (CXC/M.Weiss).*]

be about $3 \times 10^6\ M_\odot$. S2's orbital speed of approximately 4×10^6 m/s "confines" the unseen mass of Sagittarius A* to such a small volume that there can be little doubt that it is an enormous black hole. Unlike white dwarfs and neutron stars, black holes are not cooling toward thermal equilibrium with the universe.

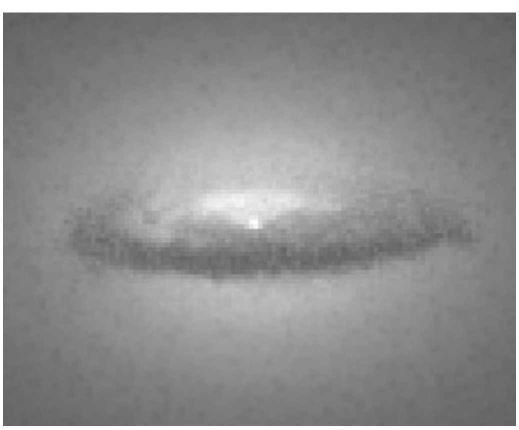

Black hole in the center of galaxy NGC 7052. The disk is 3700 $c \cdot y$ in diameter. The black hole, whose mass is about 300 million solar masses, will swallow the disk in a few billion years. [*Roeland P. van der Marel (STScI), Frank C. van den Bosch (Univ. of Washington), and NASA.*]

Gamma-Ray Bursts

Flashes of gamma rays (and x rays) that occur about once a day at apparently random locations in the sky were discovered by Vela military satellites in 1967. They are short, lasting from less than a second to as long as a few minutes. During the burst they are by far the brightest gamma-ray sources in the sky, their fluxes exceeding those of the brightest steady sources, such as the Sun and the Crab Nebula, by a factor of a 1000 or more. Their brief lifetime makes it difficult to attempt to identify the bursts with individual stars or galaxies because of the inherent delay in processing the burst information and re-aiming the large telescopes. With a bit of good fortune, that problem was first solved in 1997 when the Dutch/Italian BeppoSAX satellite detector discovered an x-ray afterglow following burst GRB970228.[15] Then in 1999 burst GRB990510 was seen simultaneously by the Compton Gamma Ray Observatory and BeppoSAX satellites within the field of view of the Very Large Telescope (VLT) in Chile, the largest telescope in the southern hemisphere. The subsequent x-ray, optical, and radio wavelength afterglows told astronomers what to look for and, since then, many bursts have been studied more thoroughly via their afterglows, some lasting for several months.

Since that time the all-sky surveys of the Burst and Transient Source Experiment (BATSE) and Swift satellites have recorded more than 8000 gamma-ray bursts distributed isotropically over the sky (see the photo below). The uniform distribution of the GRBs across the sky is strong evidence that they occur in the distant universe, since only at great distances does the cosmos appear uniform. The VLT measured the redshift z of GBR990510 to be 1.61 implying a recession speed that places the source about halfway to the edge of the visible universe. The origin of the bursts and the mechanism for the enormous energy release implied by the gamma-ray flux are not yet clear. As of this writing approximately 100 afterglows have been located and for most of these a host galaxy has been identified. The GRBs in many cases appear to be the result of the supernova collapse of very large stars becoming neutron stars or black holes. This is an area of active current research.

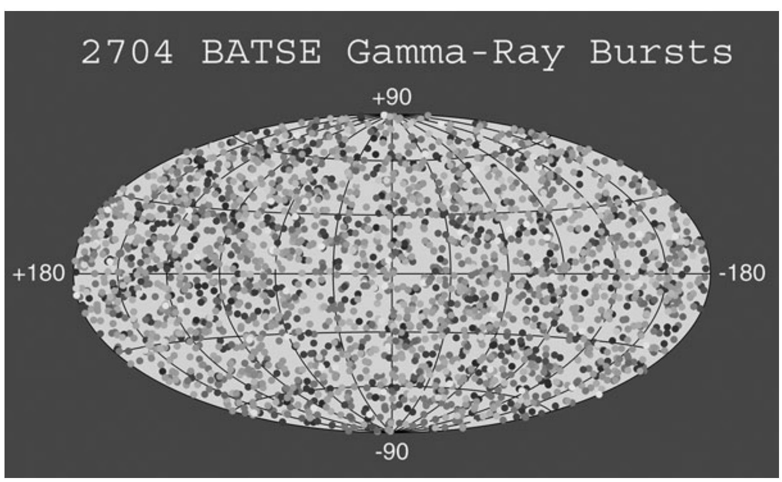

This map shows the locations of more than 2700 gamma-ray bursts recorded by BATSE aboard the Compton Gamma-Ray Observatory during its 9 years of operation. The projection is in galactic coordinates, the plane of the Milky Way being the horizontal line through the middle of the figure. The burst locations are color-coded based on the integrated energy over the duration of the burst. [*Image courtesy of the BATSE team, http://gammaray.nsstc.nasa.gov.*]

13-6 Galaxies

In Section 13-2 we saw that the Milky Way is shaped like a spiral disk with a central bulge located about 28,000 $c \cdot y$ from the Sun. The disk is surrounded by a roughly spherical "halo" of globular clusters made up mostly of population II stars, which are also part of our Galaxy. We will now look at some of the characteristics of galaxies.

Material Between the Stars

"Holes in the sky"—regions where no stars are seen—have been observed since the early days of astronomy and were assumed to be empty space. However, studies of open clusters about 70 years ago led to the discovery of a more or less continuous distribution of tiny dust particles, called *interstellar dust*, between the stars. Consisting of solid specks of silicates and carbides averaging only a few hundred nanometers in diameter (approximately matching the wavelength of visible light), the interstellar dust both absorbs and scatters some of the starlight striking it. Thus, dust in the interstellar medium (ISM) dims starlight coming toward Earth and, since blue light scatters more efficiently than red light, starlight is reddened on its trip to us, just as sunlight is reddened at sunset. Although the dust seems to pervade the entire Galaxy, the concentrations are very low and its total mass makes only a very small contribution to the total mass of the ISM. The vacuum in interstellar space is far better than the best obtainable in the laboratory.

The ISM consists primarily of hydrogen and helium. Hydrogen as atomic hydrogen, ionized hydrogen (protons), and hydrogen molecules (H_2) makes up about 70 percent of the mass of the ISM. Atomic helium is most of the rest, while the carbide and silicate dust contribute only a few percent of the ISM's total mass. Spectroscopic studies of binaries reveal some absorption lines that are not Doppler-shifted. In 1904, J. F. Hartmann reasoned correctly, although not to universal acceptance, that the unshifted lines result from absorption of light from the binary by an intervening gas cloud, rather than by gas in the atmosphere of the star. Though still difficult to demonstrate conclusively in all cases, the existence of interstellar gas clouds is now generally accepted. As a result of temperature variations in the early universe and the subsequent continuous action of gravity, huge clouds of primarily hydrogen have formed throughout the ISM. They range in mass from about 1 to 1000 times the mass of the Sun and have temperatures of about 30 to 150 K. At these temperatures the hydrogen atoms in the clouds are in their ground states.

Even though the atoms are in their ground states, it is possible to see the clouds as a result of the hyperfine splitting of the hydrogen ground state due to the spins (i.e., magnetic moments) of the electrons and protons. If the spins of the electron and the proton in a particular atom are antiparallel, the atom's ground state energy is very slightly lower that it would be if the spins were parallel. (See Section 7-4 and Figure 13-23.) The energy difference between the two states is so small, 5.9×10^{-6} eV, that a collision with another atom or a dust grain can result in the atom absorbing enough energy to "flip" the electron's spin into the parallel configuration. Once the electron's spin is flipped, the atom has only two ways to return to the ground state: it can have another collision

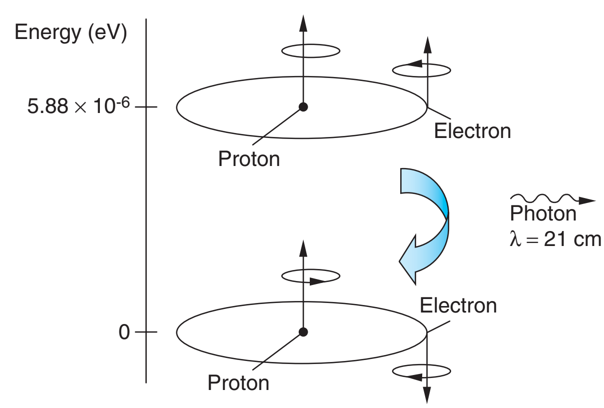

Figure 13-23 The hyperfine spitting of the hydrogen atom ground state is the origin of the 21-cm radiation used to map gas clouds in the ISM.

enabling the atom to release the excess energy as heat or it can spontaneously flip the spin back antiparallel to that of the proton, emitting a photon with wavelength 21 cm in the process. The likelihood of either of these occurring is very small. For a given atom, collisions only occur every few hundred years and spontaneous return to the lower state may take millions of years. Even so, the number of atoms in the huge clouds is so large that there is a faint continuous emission of the 21-cm photons that enables mapping of the clouds by radiotelescopes.

Together, the interstellar dust and the clouds of gas account for an estimated 2 to 3 percent of the total mass (ordinary and dark matter) of our Galaxy. It is nearly certain that there is not enough unseen gas and dust to account for the Galaxy`s dark matter.

Gaseous Nebulae

Though most gas clouds, or nebulae, in interstellar space are irregular in shape, a few are circular, leading to speculation that they are self-gravitating and represent the very early stages of new star formation. Some large hydrogen clouds have spherical inner regions of ionized hydrogen, with a quite sharp demarcation between the H and H^+ regions. Astrophysicists believe that the ionized region is maintained by ultraviolet photons with frequencies above the Lyman limit emitted by a hot, newly formed star at the center of the region. The view that new stars form in the nebulae in an ongoing process is strongly supported by the observation that, although the Galaxy is of the order of 10^{10} years old, our Galaxy contains main sequence stars that are no more than 2 to 3×10^6 years old. Furthermore, high-resolution radioastronomy has in recent years located numerous newly forming stars embedded in clouds of dust and gas that are completely opaque to optical wavelengths.

Classification of Galaxies

Although fuzzy, extended objects, at one time called "nebulae" (not to be confused with planetary nebulae defined in Section 13-3), that were obviously not stars had been observed in the night sky since the 1700s, what and where they were was a matter of active scientific debate until well into the twentieth century. The answer had to await the development of telescopes with sufficient resolution and light gathering power and a theoretical means of computing distances from observations made with them. These came together in the mid-1920s when Edwin Hubble[16] used the 2.5 m telescope on Mount Wilson, the largest in existence at the time, to measure the intensities of rare stars, called Cepheid variables[17] that he discovered in three "nebulae." One of those nebulae, the great spiral Andromeda, he measured to be 2×10^6 light-years away. In one stroke, he was able to demonstrate that the "nebulae" were in fact galaxies much like our own, as had first been suggested by the philosopher Emmanuel Kant 150 years earlier, and that they were far outside the Milky Way. Exploring Hubble's discovery will take us into the realm of cosmology, the study of the large-scale structure of the universe.

Following his discovery that these "nebulae" were in reality distant galaxies, Hubble conducted a systematic study of the enormous number that were visible. He found that all but a very few fit into four general categories. Most had regular geometrical shapes and occur in two varieties: *ellipticals* which are roundish, rather like a football, and *disks*. The disks in turn had two subgroups, *ordinary spirals* and *barred spirals* (i.e., spirals with a "bar" of stars across the center). The small percentage that did not have regular shapes he called *irregular galaxies*. Figure 13-24 shows an example of each type of galaxy. The Milky Way is a large barred spiral.

Figure 13-24 In Hubble's galaxy classification scheme, (*a*) is an example of an elliptical galaxy, (*b*) illustrates an ordinary spiral, (*c*) is a barred spiral, and (*d*) is an irregular galaxy. The Milky Way is thought to be a spiral with a faint bar. [*(a) NASA, ESA, and The Hubble Heritage Team (STScI/AURA). (b) NASA and ESA. (c) NASA, ESA, and The Hubble Heritage Team (STScI/AURA). (d) NASA, ESA, and The Hubble Heritage Team (STScI/AURA).*]

In addition to their geometrical differences, the four types of galaxies have other dissimilarities. A large fraction of the motion of the stars in spirals is rotational about the galactic center, whereas the motion of stars in ellipticals is generally random with only a relatively small rotational component. Ellipticals also seem to have very little interstellar gas and dust, while spirals and many irregulars have a substantial amount. The fact that most ellipticals have no young stars is probably a consequence of that absence. With a few exceptions, ellipticals are much smaller than spirals, typically having only about 20 percent of the diameter of an average spiral and only a thousandth of the mass.

Quiet and Active Galaxies

Most of the approximately 10^{10} galaxies in the observable universe appear to be *quiet galaxies*—i.e., there is very little activity other than what might be expected for such dynamic systems. The vast majority of these galaxies are so distant that our instruments cannot resolve internal details. Therefore, only the composite spectra and radiant flux F for the entire galaxy can be observed. The range of velocities Δv that exists in the stars of the regular galaxies, measured by the Doppler broadening of the spectral lines, turns out to be related to the total luminosity L by

$$L \propto (\Delta v)^4 \qquad \textbf{13-26}$$

Since L is related to F and r, the distance to the galaxy, by Equation 13-8, the distance r can be found from measurements of the redshift and the apparent brightness of the galaxy, assuming that L is known.

In a very small percentage of galaxies something extremely violent, even by comparison with stellar supernovae, is occurring. Such systems are called *active galaxies*. There are several distinct types, some of which may not even be galaxies at all. The first discovered were *Seyfert galaxies*, named after Carl Seyfert, who first identified many of them. They are spirals with extremely bright, central starlike cores, or nuclei. In many of them, light coming from the core exceeds that from all of the stars in the galaxy and may vary in intensity by a factor of two or more in less than a year. Such a rapid variation in the total intensity means that the source must be less than one light-year in extent while producing as much energy as 10^{11} stars. Even more incredible, if possible, is the fact that the light emitted by a Seyfert galaxy consists of broad emission lines originating in both allowed and forbidden transitions in highly ionized atomic systems superimposed on a continuum, but without the absorption lines typical of stars. That suggests that its enormous energy is not coming from thermonuclear reactions. The source is not yet understood.

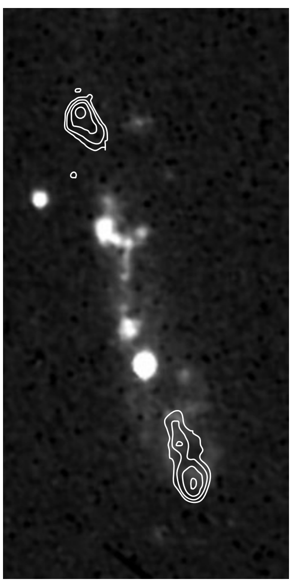

Radio galaxy 3C368. The contours show the centers of strong radio emission. The bright knots may be regions of star formation in this elliptical galaxy. [*NASA, NRAO, VLA, HST, WFPC 2, M. Longair (U. Cambridge).*]

A similar sort of extreme activity occurs in a few ellipticals called *N galaxies* and *BL Lac objects*. N galaxies are elliptical counterparts of Seyfert galaxies, that is, they have very bright centers. BL Lac objects seem to be like N galaxies, but exhibit substantial short-term intensity variations. In these, an intensity variation of a factor of two can occur within a week and a complete reversal of the polarization of the emitted light within one day, suggesting that the energy source is only one light-day in diameter. BL Lac objects are now thought to be giant ellipticals about 10^9 $c \cdot$y from Earth.

Some of the giant ellipticals are also strong emitters in the radio region of the spectrum. Study of these *radio galaxies* has been intense, and the results have been astonishing. For example, the radio source Centaurus A is double-lobed with a small radio-emitting nucleus midway between the lobes. It is one of the brightest radio-emitting objects in the universe. Analyses of its spectra indicate that the initial energy release represented by the radiation that we now see amounted to 10^{56} J, which is about the equivalent of all the stars in the Milky Way undergoing supernova explosions simultaneously! The nature of such a colossal event is not currently understood.

In a universe of strange phenomena, *quasars*, short for quasi-stellar radio sources, are among the strangest. Discovered as radio sources, their optical images look like stars; that is, they have no resolved structure. Their spectra resemble that of a Seyfert galaxy. Resolved radio images of some quasars show that a few of them are double-lobed, like the radio galaxies, which makes their identification ambiguous. The Sloan Digital Sky Survey (SDSS) has catalogued 46,420 quasars; of those, 520 have redshifts ≥ 4, the most distant at a redshift of $z = 5.41$. There is also a group of objects about 10 times more numerous than quasars, radio sources that were earlier called

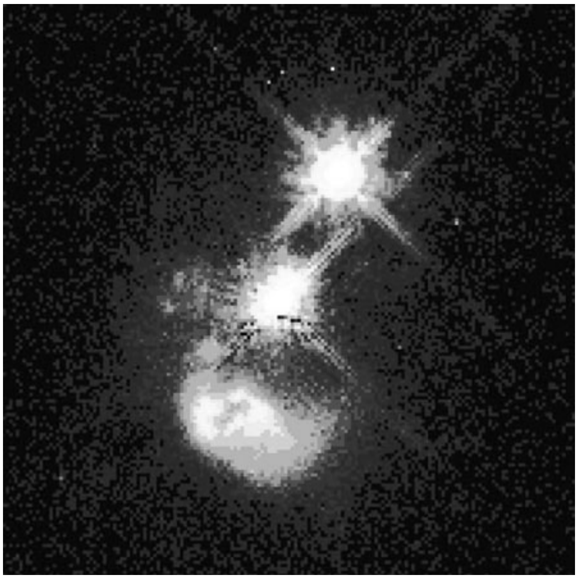

Debris from the catastrophic collision of two galaxies may be fueling quasar IRAS04505-2958. The quasar is about 3×10^9 $c \cdot$ y from Earth. Astronomers believe the collision ripped out the core of a spiral galaxy (bottom of the picture). The ring lies in front of the quasar (the bright object in the middle) at a distance of 15,000 $c \cdot$ y (one-seventh of the diameter of the Milky Way). The bright object just above the quasar is a foreground star. [*John Bahsall (Institute for Advanced Study, Princeton), Mike Disney (University of Wales), and NASA.*]

quasi-stellar objects. These are like quasars in every major way, except that they are not radio-emitters. Current terminology refers to both types as quasars, the radio sources as *radio-loud quasars* (QSRs) and the others as *radio-quiet quasars* (QSOs).

Perhaps the strangest thing about the quasars is the magnitude of the redshift of their spectra, which is very large. It implies that some quasars are receding directly away from us at greater than 0.95 c. This would make them the most distant massive objects, of the order of 10^{10} $c \cdot$ y from Earth. Their radiant flux F together with the great distance imply power outputs of 10^{40} W, greater than that of 10^{12} Suns. Not only that, but the intensities of some quasars vary over only a few hours, suggesting dimensions of only a few light-hours.

Hubble's law

E. P. Hubble was the first astronomer to recognize that there is a relation between the redshifts of the spectra of galaxies and their *distances* from us. This relation is illustrated in Figure 13-25 for a group of spiral galaxies used by astronomers for calibrating distances. The recession velocity v of a galaxy is related to its distance r from us by *Hubble's law:*

$$v = H_0 r \qquad \textbf{13-27}$$

where H_0 is the *Hubble constant*.

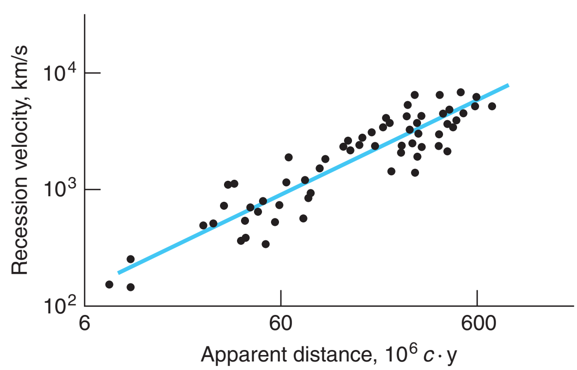

Figure 13-25 A plot of the recession velocities of individual galaxies versus apparent distance illustrates Hubble's law. The slope of the line is H_0.

In principle, the value of H_0 is easy to obtain, since it relies on the direct calculation of v from redshift measurements. However, recall that astronomical distances are very difficult to obtain and that they have been measured for only a miniscule fraction of the 10^{10} or so galaxies in the observable universe. Thus, the value of H_0 changes as the interpretation of distance calibration data is refined. The currently accepted value of the Hubble constant is

$$H_0 = 71 \pm 4 \text{ km/s per Mpc} = 22 \pm 2 \text{ km/s per } 10^6\ c \cdot \text{y} \qquad \textbf{13-28}$$

Notice that the basic unit of H_0 is reciprocal time. The quantity $1/H_0$ is called the *Hubble time* and equals about 1.3×10^{10} years. This would correspond to the age of the universe if gravitational pull on the receding galaxies were ignored.

The redshift z, defined in Section 1-5, is given by

$$z = \frac{f_0 - f}{f} = \frac{\lambda - \lambda_0}{\lambda_0} \qquad \textbf{13-29}$$

where f_0 and λ_0 are measured in the rest system of the star or galaxy (the emitter) and f and λ are measured at Earth (the observer). Figure 13-26 shows the redshifted spectra of five galaxies whose distances from us range from 2.6 to 287.5 Mpc.

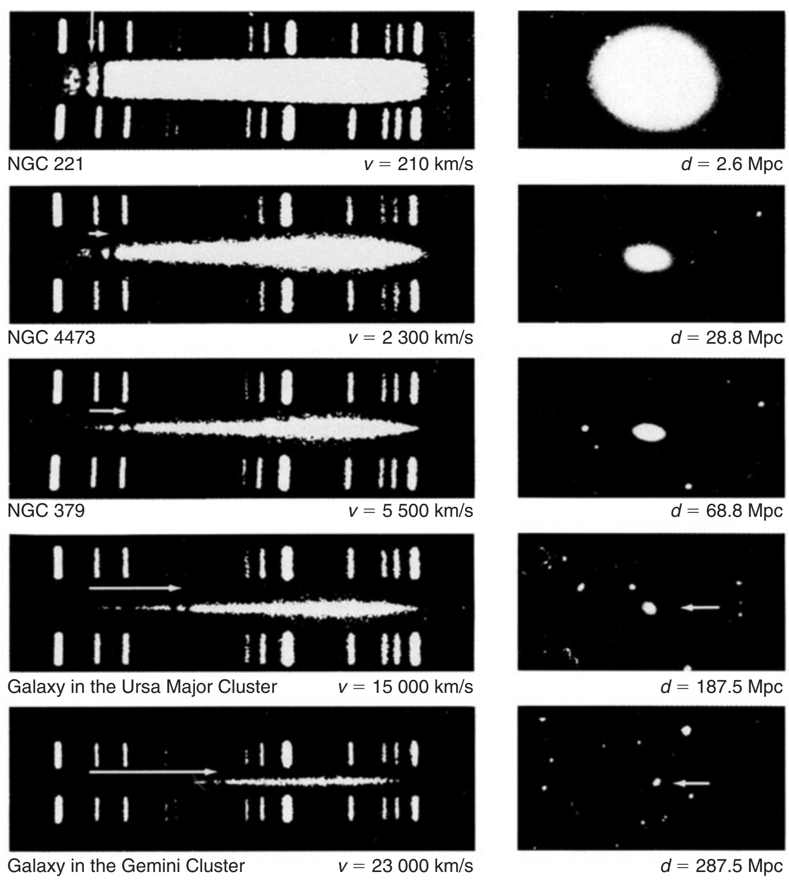

Figure 13-26 The redshifts of the Ca, H, and K absorption spectral lines are shown for five galaxies at different distances from us. The line spectra above and below the absorption spectrum are standards used for determining the amount of shift accurately. [*California Institute of Technology.*]

EXAMPLE 13-5 Distance to a Galaxy in Virgo Redshift measurements on a galaxy in the constellation Virgo yields a recession velocity of 1200 km/s. How far is it to Virgo?

SOLUTION

Using Hubble's law, we obtain

$$r = \frac{v}{H_0} = \frac{1200 \text{ km/s}}{21 \text{ km/s per } 10^6\, c \cdot \text{y}} = \frac{(1200 \text{ km/s})(10^6\, c \cdot \text{y})}{21 \text{ km/s}} = 57 \times 10^6\, c \cdot \text{y}$$

$$= 17.5 \text{ Mpc}$$

Remarks: *Compare this result with distance measurements to Virgo made by some of the standard astronomical distance-measuring methods given in Table 13-4.*

Hubble's law tells us that the galaxies are all receding from us, with those the farthest away moving the fastest. However, there is no reason why our location in the universe should be special. An observer in any galaxy would make the same observations and compute the same Hubble constant. (See Problem 13-25.) Thus, Hubble's law states that all of the galaxies are receding from each other at an average speed of 71 km/s per Mpc of separation. In other words, *the universe—space itself—is expanding*. This is a profound discovery with enormous theoretical implications.

All galaxies participate in the general expansion of the universe. As a result, the wavelengths of light emitted toward Earth by galaxies (and stars and anything else out there) is lengthened or stretched along with the space through which it is moving, producing the *cosmological redshift*. It is the cosmological redshift that is described by Hubble's law. This redshift is not related to the galaxy's recessional velocity by the relativistic Doppler effect equation that we developed in Chapter 1 (Equation 1-38), even though astronomers often use that equation to express a measured redshift z as the radial velocity of a galaxy as if it were moving through space, rather than the actual velocity with which it receding from us due to the expansion of space. That this practice provides a reasonable estimate of relatively nearby distances can be seen as follows: Substituting Equation 13-27 into Equation 13-29 and solving for r yields

$$r = \frac{c}{H_0} \frac{(z + 1)^2 - 1}{(z + 1)^2 + 1} \qquad \textbf{13-30}$$

For $z \leq 2$, Equation 13-30 yields values of r within about 5 percent of the values measured by the methods listed in Table 13-4. If $z \ll 1$, then the nonrelativistic equation $r = cz/H_0$ can be used and, e.g., for $z < 0.1$ the error is about the same as above. However, always remember that the cosmological redshift has nothing to do with the Doppler effect.

Table 13-4 Distance measurements to Virgo

Method	Cepheids	Novae	Brightness fluctuations	Type Ia supernovae
Distance to Virgo (Mpc)	15 – 25	21.1 ± 3.9	15.9 ± 0.9	19.4 ± 5.0
Maximum useful distance (Mpc)	<29	<20	<50	> 1000

The fractional change in the wavelength for the cosmological redshift is equal to the fractional change in the "size" or scale R of the universe since the time when the light was emitted. This allows us to also write the redshift as

$$z = \frac{\lambda - \lambda_0}{\lambda_0} = \frac{R - R_0}{R_0} = \frac{R_{\text{observed}} - R_{\text{emitted}}}{R_{\text{emitted}}} \Rightarrow \frac{R_{\text{observed}}}{R_{\text{emitted}}} = 1 + z \qquad \textbf{13-31}$$

Equation 13-31 says, for example, that a galaxy with $z = 2$ is now three times farther from Earth than it was when the observed light was emitted. Looking at regions in space that are cosmologically nearby or close to us provides a "snapshot" of what the universe looks like everywhere *now*. At Earth at the present time (t_0), $z = 0$. That is, galaxies close by the Milky Way have no (measurable) cosmological redshift. Looking at objects with higher z values corresponds to looking back in time. Thus, at redshift z we are seeing the universe as it appeared when it was $1/(1 + z)$ of its size now.

The discovery and analysis of the redshifts and luminosities of the quasars has significantly furthered our understanding of the expansion and evolution of the universe. Observations show that bright quasars are more numerous at large z than at small z, that is, the space or volume density of bright quasars was larger at earlier times than it is now. This could be because there where more of them in earlier times or their luminosities could have been higher or both. Or it could be that the observations are simply the result of the general expansion of space and the volume density and luminosities of the quasars have not changed over time. To remove the complicating effect of the expansion, astrophysicists and cosmologists define *comoving coordinates* and, correspondingly, for our purposes here *comoving space density*. The former we will return to in Section 13-8. The latter removes the effect of the expanding universe by dividing the number density of objects per cubic Mpc at redshift z by $(1 + z)^3$. This converts the number density of objects to the value it would have at $z = 0$ (today). Thus, if the number density and/or brightness have been constant over time, their comoving space density and brightness will be constant. Changes signal a change in the number density or an evolution of the quasars or both.

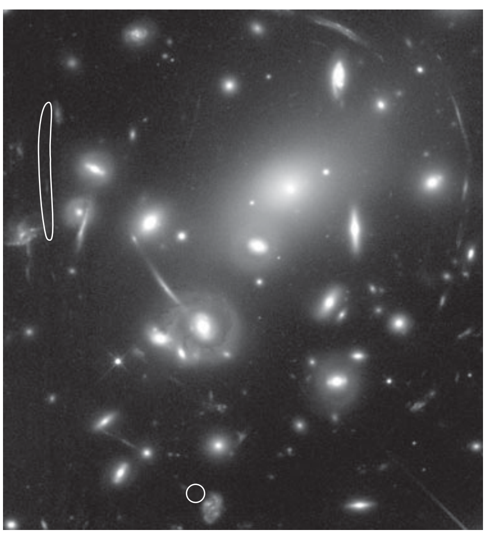

The oval encircles the most distant galaxy yet discovered (as of 2007). The faint streaks are the galaxy's image as gravitationally lensed by galaxy cluster Abell 2218. Its redshift of 6.6 puts it about $13 \times 10^9\ c \cdot y$ from Earth moving away from us at about 0.97 c. The light that formed this image left the galaxy when the universe was only 700 million years old. [*NASA, Andrew Fruchter and the ERO Team [Sylvia Baggett (STScI), Richard Hook (ST-ECF), Zoltan Levay (STScI)] (STScI).*]

Observations of the comoving space density of bright quasars show that they are more than 1000 times more numerous at $z = 2$ than they are today (at $z = 0$), *but* the total number of quasars has not changed back to about $z = 2$. Therefore, observations indicate that the luminosity of quasars evolves over time, but not their comoving space density. That is, at least back to $z = 2$, there appears to be a constant number of quasars growing dimmer as the universe expands. Further back than $z = 2$, measurements have reached about $z = 6$. In this range the picture is more complicated, the comoving space density declining after about $z \approx 3$, diminishing by approximately a factor of 10 by $z = 4$. The meaning of the decrease is a focus of continuing research.

An obvious question is whether there are other observational results that support Hubble's conclusion. For example, is the observed expansion general, or could it be a statistical accident—a consequence of our having measured distances to only a fraction of the 250,000 (out of the 10^{10} galaxies in the observable universe) whose redshifts have been measured to date? Thus, redshift surveys of the universe are an important first step in studying Hubble's expansion.

Redshift surveys establish the existence of large scale structure in the universe and, together with independent distance measurements for individual galaxies, determine the Hubble constant. Such surveys have been underway for several years and about 10^{-5} of the volume of the visible universe has now been mapped. These surveys have yielded several unexpected discoveries, but have not yet answered the question above conclusively. There are huge voids in space—regions where the density of galaxies is only 20 percent or so of the average for the universe. In addition, the galaxies themselves tend to be grouped into clusters and the clusters into superclusters. The Milky Way is a part of the Local Cluster that contains about a dozen galaxies. The galaxies also tend to lie on thin, sheetlike structures. How such structures might have evolved in the general expansion described by Hubble's law presents a challenge to cosmological models. The most successful cosmological model thus far has been the Λ Cold Dark Matter (ΛCDM) model, where Λ is Einstein's cosmological constant. One of the largest of the galaxy mapping projects has been the 2dF Galaxy Redshift Survey (2dF GRS; Figure 13-27). The project, completed in 2002, obtained high-quality spectra and redshifts for 245,591objects, mainly galaxies. Still underway is the largest survey, the Sloan Digital Sky Survey (SDSS). The SDSS first phase was completed in 2005 after measuring the spectra of 675,000 galaxies, 90,000 quasars, and 185,000 individual stars. The SDSS second phase of measurements is currently underway at the project's dedicated 2.5-m telescope in New Mexico.

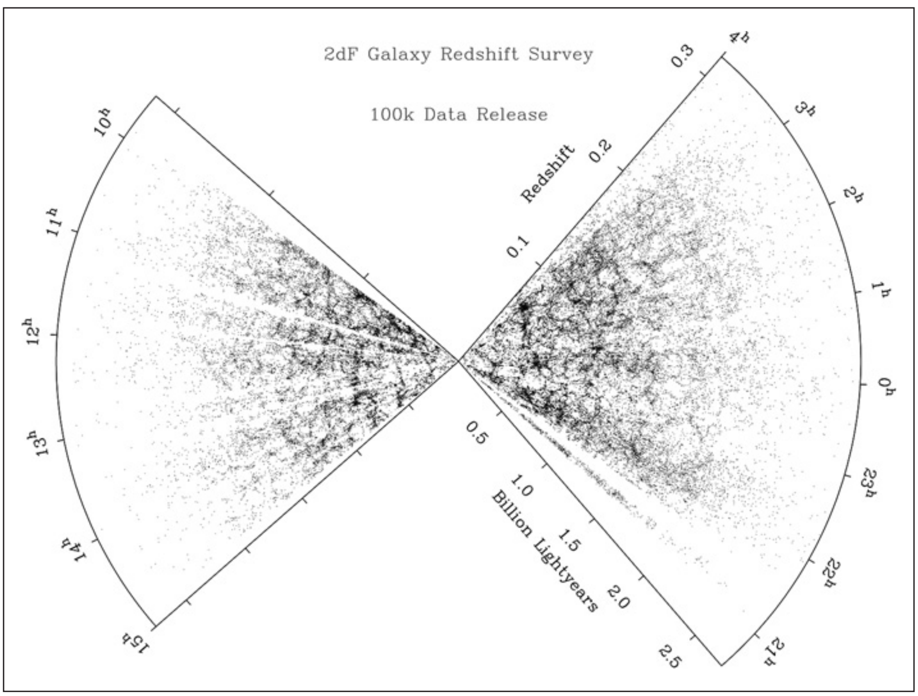

Figure 13-27 The 2dF Galaxy Redshift Survey (2dF GRS) is a major spectroscopic survey utilizing unique facilities built by the Anglo-Australian Observatory. By the survey's completion in 2002 it had recorded precise spectra for 245,591 objects enabling a wide range of new analyses including, for example, the first direct comparison with the microwave background anisotropy on the same spatial scale and studies of galaxy clustering to test inflationary cosmological models of the early universe. The survey is integrated with the 2dF Quasi Stellar Objects survey. [*Matthew Colless and the 2dF Galaxy Redshift Survey Team.*]

13-7 Cosmology and Gravitation

We have seen that applying Hubble's law to the observations of galaxies leads inescapably to the conclusion that the universe is expanding and provides us with a measure, $1/H_0$, of how long ago that expansion began. In this section, we will examine the basic theoretical framework that suggests possible tests of that conclusion. The basis for this discussion is the philosophical view that at large scale the universe is homogeneous and isotropic at any instant in time. That is, at any given instant the universe has the same physical properties everywhere and looks the same in all directions from every location. This is called the *cosmological principle*. Note that Hubble's law is consistent with the cosmological principle.

We have already seen that the cosmological principle clearly does *not* hold on a local scale. Galaxies are clustered into local groups. Even on a scale of $10^8\ c \cdot y$, the dimension typical of galactic superclusters, the universe is neither homogeneous nor isotropic. However, when maps of very distant space are examined (Figure 13-28), the distribution does appear to be statistically homogeneous and isotropic. Redshift survey maps like Figure 13-27, which extend to about $4 \times 10^9\ c \cdot y$, do indeed show homogeneity and isotropy in a statistical sense.

The Critical Energy Density of the Universe

Noting that the Hubble age $1/H_0 = 1.3 \times 10^{10}$ years ignores the effect of gravity and ignoring for the moment the recently discovered acceleration of the expansion, the expectation is that gravity tends to slow the expansion over time. Is the gravity in the universe strong enough to eventually reverse the expansion and cause the universe to collapse? Or will the expansion continue forever? The answer depends upon the mass density ρ_0 of the universe. We can understand this by considering the motion of a single galaxy of mass m at a very large distance R from Earth. Let M be the total mass of all the galaxies within the spherical volume of radius R. The gravitational potential energy of our single galaxy is $-GMm/R$. The total energy of the galaxy is

$$E = K + U = \frac{1}{2}mv^2 - \frac{GMm}{R} \qquad \textbf{13-32}$$

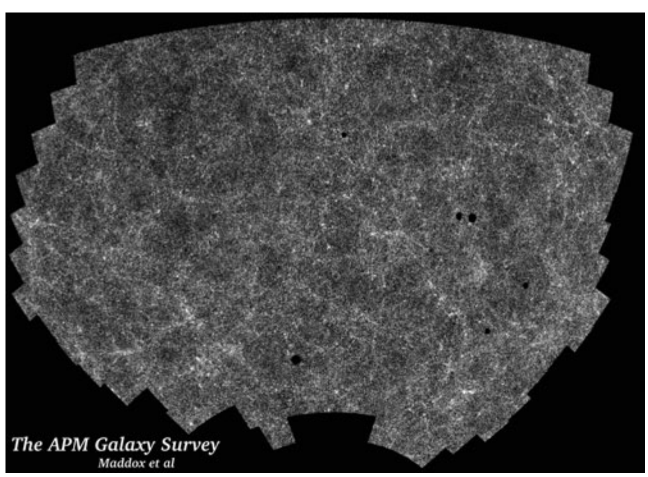

Figure 13-28 A map showing approximately 2 million galaxies ranging up to $2 \times 10^9\ c \cdot y$ away. The distribution of the galaxies looks essentially homogeneous and isotropic. This is a composite of 185 contiguous photos taken by the Schmidt telescope at the European Southern Observatory. The south Galactic pole is at the bottom center. [*S. Maddox (Nottingham U.) et al., APM Survey, Astrophys. Dept. Oxford U.*]

If we project an object with some speed v from Earth, the object will escape if its total energy is greater than or equal to zero, but if the total energy is negative, the particle will eventually stop and fall back to Earth. Similarly, if the total energy of the galaxy is greater than or equal to zero, it will continue to move away from Earth forever, but if the total energy is negative, the galaxy will eventually stop moving away from Earth and start moving back toward Earth. We can see from Equation 13-32 that the total energy of the galaxy depends on the mass density $\rho = M/(4/3\pi R^3)$. We can find the critical mass density of the universe ρ_c by setting the total energy in Equation 13-32 equal to zero:

$$\frac{1}{2}mv^2 = \frac{GMm}{R}$$

Substituting $v = H_0R$ from Hubble's law (Equation 13-27), we obtain

$$\frac{1}{2}m(H_0R)^2 = \frac{GMm}{R}$$

$$\frac{1}{2}H_0^2 = \frac{GM}{R^3}$$

Then

$$\rho_c = \frac{M}{\left(\frac{4}{3}\right)\pi R^3} = \frac{3H_0^2}{8\pi G} \qquad \textbf{13-33}$$

Substituting the values for H_0 and G, we obtain for the critical mass density of the universe:

$$\rho_c \approx 10^{-26}\ \text{kg/m}^3$$

This corresponds to about five hydrogen atoms per cubic meter of space.

Determining the present mass density ρ_0 of the universe is thus an important goal. If it is larger than ρ_c, the expansion will reverse and the universe will collapse. If it is smaller, then the expansion will continue forever. If it should happen that $\rho_0 = \rho_c$, the expansion will coast to a stop, but will not begin to contract. It should also be clear that if ρ_0 is greater than ρ_c now, it will always be so because it is actually the conservation of energy that determines whether contraction or continued expansion will occur. Since ρ_0 must decline over time as expansion progresses, the Hubble constant must also decline over time to ensure that ρ_0 remains larger than ρ_c. In other words, the Hubble constant must be a function of time $H(t)$, that is, $H_0 \equiv H(t_0)$. The value of ρ_0 based on the *visible* (baryonic matter) universe is only about 4 percent of ρ_c, suggesting that the universe will expand forever. However, the dark matter of the universe discussed earlier affects the value of ρ_0. Together, the visible matter and dark matter account for about 26 percent of the mass necessary to make $\rho_0 = \rho_c$. Examination of the recession rates of the Type Ia "standard candle" supernovae suggests that dark energy provides the additional 74 percent needed. Recalling that they have very similar brightness and light curves, the discovery that for a given brightness the redshifts of distant Type Ia supernovae are less than expected implies that the universe was expanding at less than the expected rate in the past. Therefore, the universe is expanding at an accelerated rate today. The implication is that dark energy corresponds to a repulsive force that is speeding up the expansion.

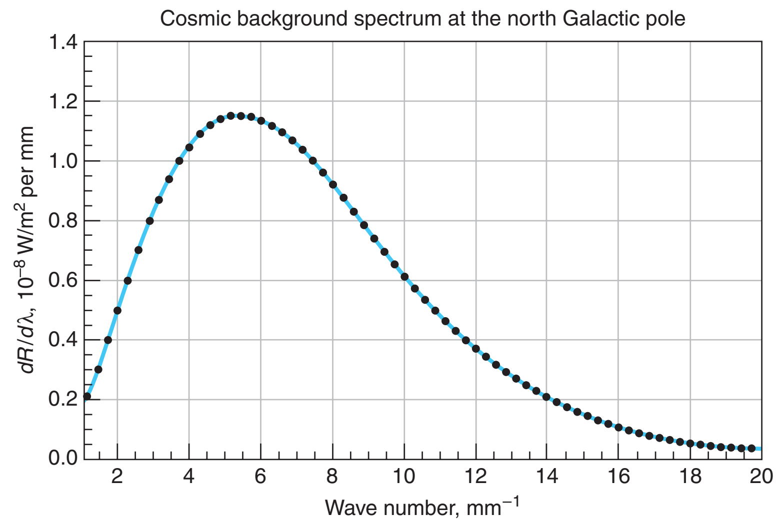

(*a*)

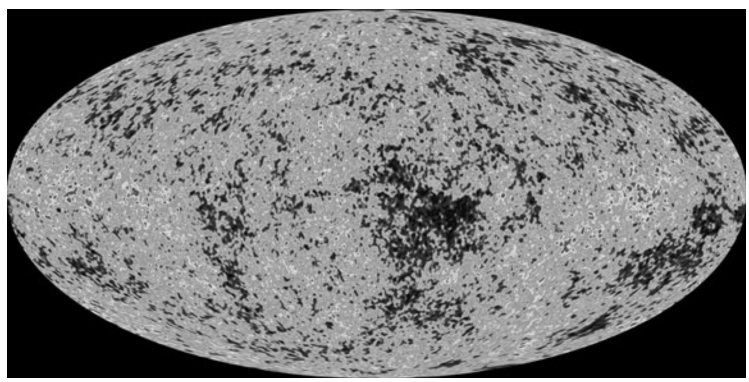

(*b*)

Figure 13-29 (*a*) The spectrum of the cosmic background radiation measured by NASA's *Cosmic Background Explorer* (COBE) spacecraft. The dots are the data points. The solid curve is the Planck radiation curve for a blackbody at 2.725 K. [*CERN Courier, June 1991, p. 2, courtesy of NASA*.] (*b*) This detailed all-sky picture of the infant universe includes three years of WMAP data. It shows 13.7×10^9-years-old temperature fluctuations that were the seeds that eventually became the galaxies and provides new clues regarding events that occurred in the first trillionth of a second following the Big Bang. The range of the temperature fluctuations is ± 200 μK. [*NASA/WMAP Science Team.*]

This view is independently supported by very recent research that compares the temperature fluctuations in the cosmic microwave background shown in Figure 13-29*b* with their origin in the "lumpiness" of matter in the 2dF GRS (see Figure 13-27).

13-8 Cosmology and the Evolution of the Universe

Following his completion of general relativity in 1915, Einstein turned to cosmology. He based his early work on the assumption that the universe was not only homogeneous and isotropic, but also constant in time. This is sometimes called the *perfect cosmological principle*. He quickly discovered that, like a universe described by Newton's gravitational theory, only an empty (no mass) universe can be static. He found that a static universe could be metastable if it contained mass and a *cosmological constant*, thereby committing what he later described as the biggest blunder of his life. On learning of Hubble's discovery of the expansion of the universe, he abandoned the cosmological constant. However, dark energy is essentially a revision of the cosmological constant for an expanding universe. Since the constant, in effect, generated the mass of the universe, adjusting its value could shift some of the predicted mass into energy, thereby accounting for the unseen mass.

One difficulty with the steady-state model is a problem known as *Olber's paradox*, first posed by Edmund Halley in 1720, but named after the nineteenth-century physician-astronomer Wilhelm Olbers who publicized it widely. If there is a uniform distribution of stars throughout an infinite space, then no matter in which direction you look, you will eventually see a star. Since stars are bright, the night sky should look as bright as the surface of the average star. (This is analogous to standing in an infinitely large forest in which all the trees are painted white. Along any line of sight, you will eventually see a white tree, so you should see white in all directions.) Why then is the night sky dark? The solution offered by Olber himself was that interstellar dust absorbs the light from distant stars. But this is no help since the dust would eventually be heated to glowing, so the night sky should still be bright.

The solution to this problem came in part with Hubble's discovery of the expansion of the universe. The point is not that light is redshifted out of the visible region,[18] but that the energy of every photon is diminished, since $E = hc/\lambda$. However, redshift can account for only a very small part of the solution. The key is that, since the velocity of light is finite, looking into space means looking back in time. Looking deeper into space we eventually would be looking at a time before the stars began to form, that is, at a time greater than the Hubble age. (In terms of our forest analogy, the distant trees have not yet been painted white; therefore, if the separation of the trees is great enough, many lines of sight will end on dark trees.)

A Simple Cosmology Model[19]

To a considerable extent, descriptions of the origin and evolution of the universe depend on the cosmology model that is used to interpret observations. The appearance of galaxies at cosmological distances is directly affected by the curvature of spacetime through which the light travels on its trip to Earth. One would reasonably expect that the distortion of spacetime would be more complex at higher redshifts when the visible universe was smaller and the mass density larger than now, which is understandably a region of high interest to cosmologists. A proper interpretation of observations at high redshifts necessarily requires the use of the general theory of relativity. Such an application is beyond the scope of our discussions; however, we can develop a useful, albeit approximate view of the expansion of the universe with the aid of cosmological a model based on Newtonian mechanics and the cosmological principle, then follow up with a very brief look at the current state of the theory based on general relativity and measurements from the Wilkinson Microwave Anisotropy Project (WMAP).

Consider a thin spherical shell of radius r in our homogeneous, isotropic universe (Figure 13-30a). The shell contains and uniformly distributed total mass m.

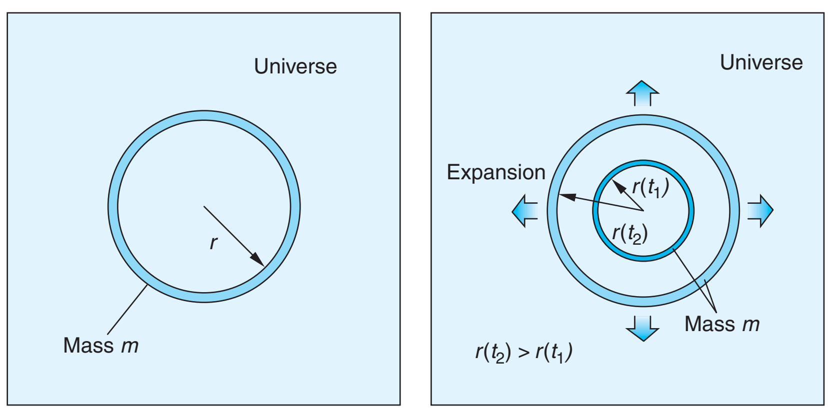

(*a*) (*b*)

Figure 13-30 (*a*) Cross section of a thin spherical shell containing mass m in an isotropic, homogeneous universe. (*b*) The same shell as it has expanded from its size at time t_1 to time t_2. The thickness of the shell also expands; however, the mass in the shell is constant. The shell's comoving coordinate $r(t_0)$ remains unchanged.

Our shell, like all such shells, expands along with the general expansion of the universe, becoming both large and thicker; however, m remains constant. Assuming gravity to be the only interaction present, the total energy of the mass m within the shell is the kinetic energy plus the gravitational potential energy:

$$E = K + U = \frac{1}{2}mv^2(t) - \frac{GM_r m}{r(t)} \qquad \textbf{13-34}$$

where $v(t)$ is the recessional velocity of the shell and M_r is the mass within the sphere that is enclosed by the shell. Like m, M_r also remains constant because $M_r = (4/3)\pi r^3 \rho$ and, although r and ρ are both functions of time, $\rho \propto r^{-3}$. The mass of our universe outside the shell exerts no net gravitational force on m. (Why not?) As the shell expands the gravitational force due to M_r causes the kinetic energy of m to decrease and the gravitational potential energy to increase, i.e., to become less negative. Conservation of energy requires that the total energy E be unchanged, so we will, with remarkable foresight, write the total energy as

$$E = -\frac{1}{2}kmc^2 r^2(t_0) \qquad \textbf{13-35}$$

where $r(t_0)$ is the radius of the shell at $t_0 = now$ and k is a constant with units $(\text{length})^{-2}$. As we will see, the constant k determines the geometry of the universe. Combining Equations 13-34 and 13-35, substituting for M_r, and cancelling m yield

$$v^2(t) - \frac{8}{3}\pi G\rho(t)\, r^2(t) = -kc^2 r^2(t_0) \qquad \textbf{13-36}$$

Referring to Equation 13-36, note that:

- If $k > 0$, then the total energy of the mass m is negative. In that event there is a radius $r(t)$ beyond which the shell cannot expand because v is (instantaneously) zero and we say that the universe is *closed* or *bounded*. The shell will then begin to contract due to the mass M_r interior to the shell and undergo a time-reversed copy of the expansion back to what is sometimes called the "Big Crunch."
- If $k = 0$, then the total energy of the mass m is zero. In that case as $t \rightarrow \infty$, $r(t) \rightarrow \infty$ the recession velocity $v(t) \rightarrow 0$ and the shell (and universe) coast forever toward a halt. We refer to such a universe as *flat*.
- If $k < 0$, then the total energy of the mass m is positive. In that event, as $r(t)$ increases, the gravitational potential energy becomes steadily more negative. But $v^2(t)$ must continually increase in order to keep the total energy positive. We then say that the universe is *open* and will continue to expand forever.

Since the cosmological principle requires that all shells, including ours in Figure 13-30*a*, must expand in the same way, that is, the time required for the radii of all shells to, say, triple, must be the same, we can express the radius $r(t)$ of our shell (or any shell) as

$$r(t) = R(t)r(t_0) \qquad \textbf{13-37}$$

where $r(t)$ is the distance from the coordinate origin to the shell (see Figure 13-30*a*) and $R(t)$ is the *scale factor* first introduced in Equation 13-31 which describes the expansion or contraction of the universe. Since there is nothing special about our shell, $R(t)$ is the same for *all* shells. The constant $r(t_0)$ that in effect labels the shell is called the *comoving coordinate* (see Figure 13-30*b*). Assuming that the present is t_0, $R(t_0) = 1$ and, as we have noted, the present radius of our shell is $r(t_0)$. In Equation 13-31 R refers to the rest frame of the observer and R_0 to that of the emitting star or galaxy. Since $R(t_0) = 1$, the scale factor $R(t)$ and the redshift z are related by

$$1 + z = \frac{1}{R(t)} \qquad \textbf{13-38}$$

For example, looking back in time to redshift $z = 2$, the scale factor $R = 1/3$, that is, the visible universe was one-third of its present size. Hubble's law can now be written as

$$v\,(t) = H(t)r(t) = H(t)R(t)r(t_0) \qquad \textbf{13-39}$$

Differentiating Equation 13-37 with respect to time, substituting into Equation 13-36, and cancelling $r^2(t_0)$ yield

$$\left(H^2(t) - \frac{8}{3}\pi G\,\rho(t)\right)R^2(t) = -kc^2 \qquad \textbf{13-40}$$

Cosmologists define the *density parameter* $\Omega = \rho(t)/\rho_c(t)$ whose present value is

$$\Omega_0 = \frac{\rho_0}{\rho_{c0}} = \frac{8\pi G\rho_0}{3H_0^3} \qquad \textbf{13-41}$$

and since, as you will show in Problem 13-26, $\rho(z) = \rho(1 + z)^3$,

$$\frac{\Omega}{\Omega_0} = (1 + z)^3\frac{H_0^2}{H^2} \qquad \textbf{13-42}$$

In relativistic cosmology models, universes are described in terms of three components: matter (including dark matter) Ω_m, relativistic particles (e.g., neutrinos) Ω_{rel}, and dark energy (the cosmological constant) Ω_Λ. Current data suggests that relativistic particles do not contribute significantly to the energy density at the present time. Cosmologists, like all scientists, use graphical representations whenever possible, in this situation employing a two-dimensional graph of $\Omega_{\Lambda 0}$ versus Ω_{m0} to assess the current state of the universe. It is reproduced as Figure 13-31. The coordinates $(\Omega_{\Lambda 0}, \Omega_{m0})$ for the best values of the density parameters based on current WMAP observations are $(0.73 \pm 0.04, 0.27 \pm 0.04)$. Delving further into this and related issues is on the leading edge of cosmological research, but regretfully beyond the scope of this book.

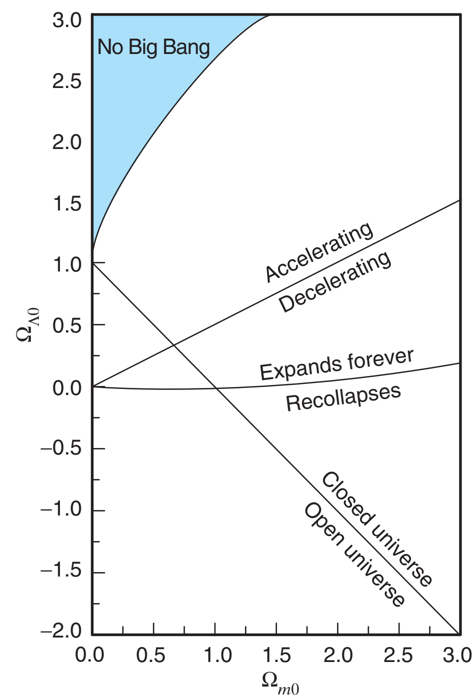

Figure 13-31 Every point in the $\Omega_{\Lambda 0} - \Omega_{m0}$ plane represents a possible universe. The lines drawn are based on various parameters from general relativity analyses. The line with negative slope starting in the lower right corner corresponds to the geometry parameter $k = 0$ (see Equation 13-36).

The Big Bang

Over the past century cosmologists have developed a well-defined *standard model of the universe* that fits a comprehensive set of very precise, constraining measurements and observations. The foundation of the standard model is the Big Bang theory. It is the observational foundation of the theory that $(13.7 \pm 0.2) \times 10^9$ years ago[20] the universe was in a hot, dense state and at that particular time a single event, the Big Bang,[21] initiated an expansion and cooling that has continued to the present time. Two major astrophysical discoveries made in the 1960s were the first of several that have convinced most scientists that the model is correct. The first of the two discoveries that supported the evolving universe model was Martin Ryle's[22] observations revealing that there is a higher comoving space density of distant radio galaxies than nearby ones. Since distant observations correspond to earlier times, this meant that the universe had looked different at earlier times than it does now; that is, it has evolved over time.

The second discovery was monumental, as important as Hubble's discovery of the expansion of the universe itself. In investigating ways of accounting for the cosmic abundance of elements heavier than hydrogen, cosmologists recognized that nucleosynthesis in stars could explain the abundance of those heavier than helium but not that of helium itself. (See Figure 13-32.) Helium must therefore have been formed during the Big Bang. Synthesizing the amount of helium that would account for its present abundance requires that the Big Bang occurred at an extremely high initial temperature to provide the necessary reaction rate before the fusion was shut down by the decreasing density due to the very rapid initial expansion. The high temperature implies a corresponding thermal (blackbody) radiation field that would cool as the expansion progressed. Theoretical analysis predicted that from the Big Bang to the present, the remnants of the radiation field should have cooled to a temperature of

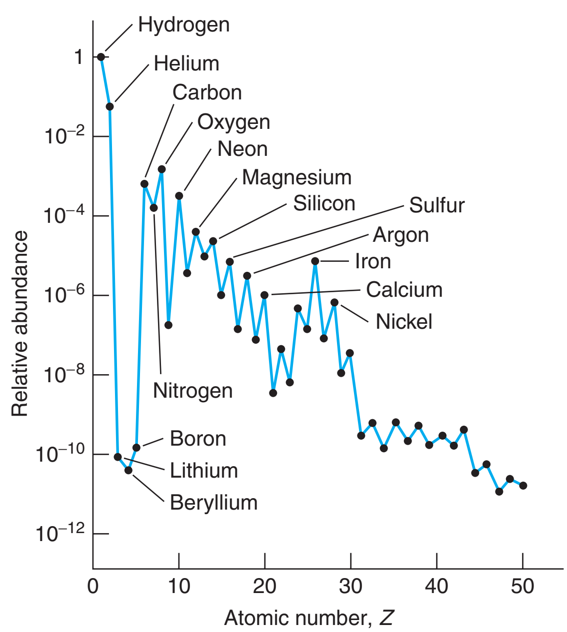

Figure 13-32 The abundances, relative to hydrogen, of elements in the Milky Way up to $Z = 50$ (tin). Note the peak at $Z = 26$ (iron), the sharp decline in abundances after iron, and the extremely low relative abundances of lithium, beryllium, and boron.

about 3 K, corresponding to a blackbody spectrum with peak wavelength λ_{max} in the microwave region. In 1965, the predicted Cosmic Microwave Background (CMB) radiation was discovered by Arno Penzias and Robert Wilson[23] at Bell Labs. Since this landmark discovery, analysis of data from the Cosmic Background Explorer (COBE) satellite by John Mather and George Smoot[24] and by the Wilkinson Microwave Anisotropy Project (WMAP) collaborators have established the temperature of the background field at 2.725 ± 0.001 K with deviations from that value of no more than a few thousandths of a percent. These results show that the CMB has the isotropic distribution in space that is absolutely essential for a universe that satisfies the cosmological principle. Indeed, the Cosmic Microwave Background is the most precise blackbody known in nature (see Figure 13-29*a*). In addition, the WMAP detection of temperature fluctuations in the range of 30 μK (see Figure 13-29*b*) provided the first evidence for density inhomogeneities that cosmologists believe seeded all of the galactic structure of the universe.

The Very Early History of the Universe

What was the Big Bang like? The singular event that initiated the expansion of the universe must have been a huge explosion of space that occurred throughout the entire hot, dense state. Most cosmologists favor the standard model as the theoretical description of the evolution of the universe following the Big Bang. It relies heavily on recent experimental discoveries and theoretical advances in particle physics and reflects the increasing overlap of frontier research in those areas of physics over the past several years. The standard model's account of how the universe evolved from $t = 0$ to now, when $t \approx 10^{10}$ years, is outlined in the following discussion and illustrated in Figure 13-33.

In the beginning the universe was dominated by energy at negative pressure which led to an early exponentially accelerated expansion referred to as *inflation*. The theoretical basis for inflation comes from general relativity and the cosmological principle which together give the acceleration equation (not intended to be obvious) below.

$$\frac{1}{R(t)}\frac{d^2R}{dt^2} = -\frac{4\pi G}{3c^2}(\rho c^2 + 3P) \qquad \textbf{13-43}$$

where $R(t)$ is the dimensionless scale factor discussed earlier, ρc^2 is the energy density of the universe, and P is the pressure. Notice that in situations where negative pressure dominates, the expansion has positive acceleration. This very early period of inflation for which, bear in mind, we have no direct evidence, is nonetheless successful in resolving several cosmological questions, including (1) Why is the CMB temperature so uniform in every direction? (2) Why is the geometry of the universe so close to being flat? (3) Why do we not see magnetic monopoles? (4) What is the origin of the anisotropies measured by WMAP? Following that brief, but extremely rapid inflation, the universe was dominated by radiation, then subsequently by matter. Recently, cosmologically speaking, it has again become dominated by a negative energy pressure which is driving a new, but slower acceleration of the general expansion. Today, as we have alluded to earlier, matter accounts for only about 26 percent of the energy density of the universe, only 4 percent being ordinary matter. (See Figure13-34). The other 22 percent is the cold dark matter (CDM) discussed earlier that neither emits nor reflects light or is affected by radiation pressure, but does participate in the gravitational interaction. Figure 13-34*c* shows what may be the first indirect observation of dark matter. Dark energy, the remaining 74 percent of the energy density of the universe, is apparently driving the new acceleration.

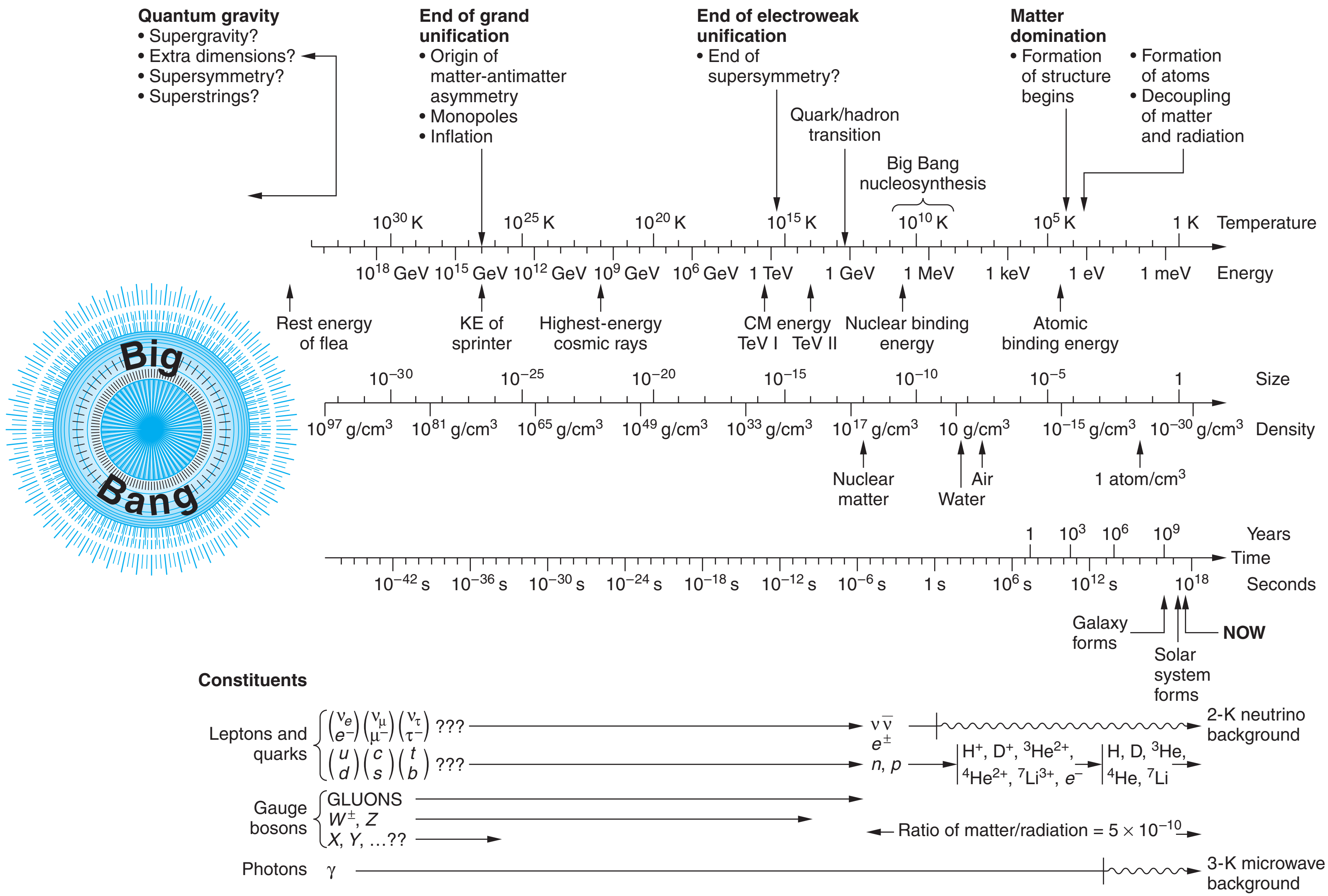

Figure 13-33 The evolution of the universe from time $t = 0$ to the present, according to the standard model.

(a) (c)

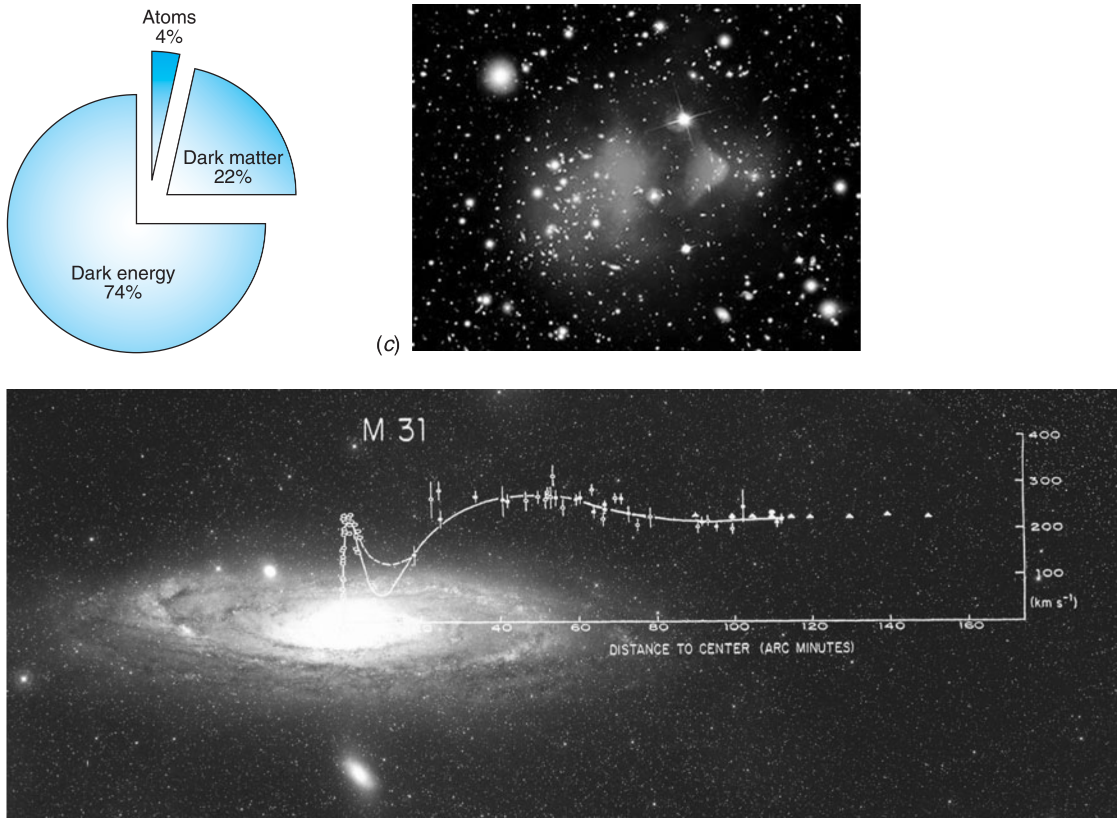

(b)

Figure 13-34 (*a*) The mass-energy content of the universe. Recent observations indicate that the dark energy is driving a renewed acceleration of the general expansion of the universe. (*b*) Stellar velocities in M31. Newton's law of gravitation requires that constant velocity implies $M \propto r$. Thus, in M31 much of the mass lies well beyond the visible extent of the galaxy, a very early indicator of dark matter. (*c*) Galaxy cluster 1E0657-558 resulted from a small cluster passing through a larger one some time in the past. Using this cluster as a gravitational lens for more distant galaxies made possible the mapping of the gravitational potential of 1E0657-588 (the large fuzzy "cloud"). X-ray emission recorded by the Chandra X-Ray Observatory of the two central, darker portions of the "cloud" reveal the hot gases (ordinary matter) of the two original colliding clusters. The lighter portions to the outside of the "cloud" are inferred to be dark matter. [The authors thank Vera Rubin for permission to use image (*b*). *(b) Vera Rubin and Janice Dunlap. (c) X-ray courtesy NASA/CXC/CfA/M Markevitch et al.; optical courtesy NASA/STScl; Magellan/U Arizona/D Clowe et al.; lensing map courtesy NASA/STScl; ESO WFI; Magellan/U Arizona/D Clowe et al.)*]

Initially, the four forces of nature (strong, electromagnetic, weak, and gravity) were unified into a single force. Physicists have been successful in developing theoretical descriptions that unify the first three, but a theory of quantum gravity, needed for the extreme densities of the single-force period, does not yet exist. Consequently, until the cooling universe "froze" or "condensed out" the gravitational force about 10^{-43} seconds after the Big Bang when the temperature was still 10^{32} K, we have no means of describing what was occurring. At this point the average energy of the particles would have been about 10^{19} GeV. As the universe continued to cool below 10^{32} K the three forces other than gravity remained unified and are described by grand unification theories (GUTs). Quarks and leptons were indistinguishable and particle quantum numbers were not conserved. It was during this period that a slight excess of quarks over antiquarks occurred, roughly 1 in 10^9, that ultimately resulted in the matter that we now observe in the universe.

At 10^{-35} seconds, the universe had expanded sufficiently to cool to about 10^{27} K at which point another phase transition occurred as the strong force condensed out of the grand unified group, leaving only the electromagnetic and weak forces still unified as the *electroweak force*. During this period the previously free quarks in the dense mixture of roughly equal numbers of quarks, leptons, their antiparticles, and photons began to combine into hadrons and their antiparticles, including the nucleons. By the time the universe had cooled to about 10^{13} K, at about $t = 10^{-6}$ s, the hadrons had mostly disappeared through annihilation. This is because 10^{13} K corresponds to $kT \sim 1$ GeV, which is the minimum energy needed to create nucleons and antinucleons from the photons present via the reactions

$$\gamma \longrightarrow p^+ + p^- \qquad \textbf{13-44}\boldsymbol{a}$$

and

$$\gamma \longrightarrow n + \bar{n} \qquad \textbf{13-44}\boldsymbol{b}$$

The particle-antiparticle pairs annihilated and there was no new production to replace them. Only the slight earlier excess of quarks led to a slight excess of protons and neutrons over their antiparticles. The annihilations resulted in photons and leptons and after about $t = 10^{-4}$ seconds, those particles in roughly equal numbers dominated the universe. This was the *lepton era*. At about $t = 10$ seconds the temperature had fallen to 10^{10} K (kT $\sim$ 1 MeV). Further expansion and cooling dropped the average photon energy below that needed to form an electron-positron pair. Annihilation then removed all of the positrons as it had the antiprotons and antineutrons earlier, leaving only the small excess of electrons arising from charge conservation, and the *radiation era* began. The particles present were primarily photons and neutrinos.

Within a few more minutes, the temperature dropped sufficiently to enable fusing protons and neutrons to form nuclei that were not immediately photodisintegrated. Deuterium, helium, and a bit of lithium were produced in this *nucleosynthesis period*, but the rapid expansion soon dropped the temperature too low for the fusion to continue and the formation of heavier elements had to await the birth of stars.

A long time later, when the temperature dropped to about 3000 K as the universe grew to about 1/1000 of its present size, kT dropped below typical atomic ionization energies and atoms were formed. By then the expansion had cooled the radiation field so that the total radiation energy was now about equal to the energy represented by the remaining mass. This occurred when the scale factor $R(t)$ reached about 2.8×10^{-4}. As expansion and cooling continued, the energy of the steadily redshifting radiation declined until matter came to dominate the universe, its energy density exceeding that of today's 2.725 K radiation remaining from the Big Bang by about a factor of 1000. Now, once again, energy at negative pressure appears to dominate.

Unanswered Questions and the Limits of Knowledge

The standard model of the evolution of the universe and the current theories of stellar and galactic genesis and evolution have been amazingly successful. Still, some fundamental questions that have arisen during our discussions remain unanswered. Will the universe expand forever or rebound to its initial state and repeat the Big Bang? The answer depends on whether the present average matter density is greater or less than the critical density of about 10^{-26} kg/m^3. The uncertainty in the current measurements would allow either possibility, but the value is tantalizingly close to the critical value. If it does equal the critical value, an intriguing additional question is, Why? We have noted the serious problem of the dark matter and how it might be explained. Answering some of these questions requires that we probe at the current limits of physical knowledge.

For example, near a mass m, general relativity prevents our seeing events occurring at dimensions less than the Schwarzschild radius, the *event horizon*,

$$R_S = \frac{2Gm}{c^2} \qquad \textbf{13-45}$$

On the other hand the uncertainty principle in quantum theory places this limit at the Compton wavelength λ_c:

$$\lambda_c = \frac{h}{mc} \qquad \textbf{13-46}$$

Equating these, $m = \sqrt{hc/2G}$, an expression for m that depends only on universal constants, where $m \approx 10^{-8}$ kg. That relation for m together with Equation 13-46 allows the corresponding definition of a length unit dependent only on universal constants. That length $L = \lambda_c \approx 10^{-35}$ m and the time for light to travel across that length can be similarly expressed as

$$t = \left(\frac{Gh}{c^5}\right)^{1/2} = 1.35 \times 10^{-43}\ \text{s} \qquad \textbf{13-47}$$

In terms of these units the mass density of the universe is such that a mass m is contained within a volume of dimensions $L^3 \sim (10^{-35})^3$ m^3. The definition of the units of mass, length, and time in terms of fundamental constants was originally pointed out by Planck[25] and are the basis for Planck units, the topic of the Exploring section that follows.

Some cosmologists have suggested that, if the universe had evolved even slightly differently than it has, perhaps due to a slightly different value for h or e or some other fundamental constant, life on Earth and maybe Earth itself would be impossible. This can be attributed to the *anthropic principle*, that the universe looks as it does because we are here to see it.

EXPLORING
"Natural" Planck Units

Not long after Max Planck had introduced the constant h in fitting physical theory to the emission spectrum of a blackbody, he pointed out that a system of "natural" units for the fundamental quantities of mass, length, time, and temperature could be constructed from the three fundamental constants $\hbar$, c, and G, where $\hbar$ = Planck's constant$/2\pi$, c = speed of light, and G = Newton's gravitation constant.

Planck mass:

$$M_P = (\hbar c/G)^{1/2} = 2.2 \times 10^{-8}\ \text{kg}$$

Planck length:

$$l_P = (\hbar G/c^3)^{1/2} = 1.6 \times 10^{-35}\ \text{m}$$

Planck time:

$$t_P = (\hbar G/c^5)^{1/2} = 5.4 \times 10^{-44}\ \text{s}$$

Planck energy:

$$E_P = M_P c^2 = 2.0 \times 10^9\ \text{J} = 1.2 \times 10^{22}\ \text{MeV}$$

Planck temperature:

$$T_P = \frac{E_P}{k_B} = \frac{\hbar^{1/2} c^{5/2}}{G^{1/2} k_B} = 1.4 \times 10^{32}\ \text{K}$$

> If length, mass, temperature, and time are measured in Planck units, the result is the "natural" units often used by particle physicists, astrophysicists, and cosmologists: $c = k_B = \hbar = G = 1$.

When first proposed, Planck's suggested units had little basis in fundamental physics, but over time that has changed. As Frank Wilczek[26] has pointed out, Planck's proposal has now become compelling: the constant $\hbar$ is now the fundamental unit of action and c the fundamental unit of velocity. These are the primary units of measurement in the two great theories of modern physics, quantum mechanics and special relativity. The corresponding unit in general relativity is G (actually $1/Gc^4$).

As Wilczek speculates, with the natural units of measure it may soon be possible to understand why, compared to the other forces in nature, the gravitational force is so weak and how we can account for the value of the proton's mass. In addition, he suggests that we have the beginnings of a quantum theory of gravity that agrees accurately with all existing experimental data. Thus, Einstein's goal of the unification of the four natural forces may be just over the horizon.

Summary

TOPIC	RELEVANT EQUATIONS AND REMARKS	
1. The Sun	The solar energy received at the top of Earth's atmosphere, called the solar constant, is	
	$f = 1.365 \times 10^3\ \mathrm{W/m^2}$	**13-1**
	The rate at which the Sun emits energy is the luminosity $L_\odot$:	
	$L_\odot = 3.85 \times 10^{26}\ \mathrm{W}$	**13-2**
Surface temperature	Assuming that the Sun radiates as a blackbody, its effective surface temperature T_e can be computed from the Stefan-Boltzmann law:	
	$T_e = 5780\ \mathrm{K}$	
Source of Sun's energy	The source of the Sun's energy in nuclear fusion, mainly via the proton-proton cycle which starts with the reaction	
	${}^1\mathrm{H} + {}^1\mathrm{H} \longrightarrow {}^2\mathrm{H} + e^+ + \nu_e + 0.42\ \mathrm{MeV}$	**13-5**
2. The stars	Stars are classed as either population I or population II, based on their composition. The former have 2 to 3 percent of their mass composed of elements heavier than helium; the latter are nearly devoid of those elements.	
The Milky Way	Our galaxy, the Milky Way, consists of about 10^{10} stars. The Sun is about 28,000 $c \cdot$y from the center of the Galaxy, which is in the direction of the constellation Sagittarius from us. Only about 4 percent of the mass of the Galaxy is accounted for by the visible stars and the gas and dust of the ISM.	
3. Evolution of the stars	The Hertzsprung-Russell diagram displays the evolution of stars, relating their luminosities to their effective temperatures. Both quantities are related to the stellar mass.	
	$L \propto M^4$	**13-14**
	$T_e = \left(\dfrac{L}{4\pi R^2 \sigma}\right)^{1/4} \propto M^{1/2}$	**13-17**
	Stars "burning" hydrogen to helium fall on the main sequence of the H-R diagram.	

TOPIC	RELEVANT EQUATIONS AND REMARKS
Final states of stars	Following exhaustion of their hydrogen fuel, stars evolve to one of three possible final states, dependent on their mass: white dwarf, neutron star, or black hole. It is in cataclysmic events accompanying evolution to these states that elements heavier than Fe are formed.
4. Galaxies	Edwin Hubble grouped galaxies into four general categories: ellipticals, spirals, barred spirals, and irregulars.
Hubble's law	Hubble showed that the universe was expanding and, using spectral redshifts to determine the velocities of galaxies, that the recession velocities v were proportional to the distance r from us according to
	$v = H_0 r$ **13-27**
	where the Hubble constant H_0 is
	$H_0 = 71 \pm 4$ km/s per Mpc $= 22 \pm 2$ km/s per $10^6\ c \cdot y$ **13-28**
	The quantity $1/H_0 = 1.3 \times 10^{10}$ y is the Hubble age. It would correspond to the age of the universe under a constant velocity expansion if gravitational pull on receding galaxies were ignored.
5. Gravitation and cosmology	The cosmological principle states that the universe has the same physical properties everywhere and looks the same in every direction from every location. The current theory of cosmology, called the standard model, describes the universe as having begun with the Big Bang 13.7×10^{10} years ago. It has substantial theoretical and observational support.
Inflation	The standard model holds that the very early universe underwent a period of exponentially accelerated growth which explains many features of the current universe. After a long period of slowing, the expansion of the universe is again accelerating.

General References

The following general references are written at a level appropriate for the readers of this book.

Akerlof, C. W., and M. A. Srednicki, *Relativistic Astrophysics and Particle Cosmology*, New York Academy of Sciences, New York, 1993.

Bahcall, J. N., *Neutrino Astrophysics*, Cambridge University Press, New York, 1989.

Bennett, J., M. Donahue, N. Schneider, and M. Voit, *Stars, Galaxies, and Cosmology*, 2d ed., Addison Wesley, San Francisco, 2002.

Carroll, B. W., and D. A. Ostlie, *An Introduction to Modern Astrophysics*, 2d ed., Pearson Addison Wesley, San Francisco, 2007.

Comins, N. F., and W. J. Kaufmann III, *Discovering the Universe*, 6th ed., W. H. Freeman, New York, 2003.

Frauenfelder, H., and E. M. Henley, *Subatomic Physics*, 2d ed., Prentice Hall, Englewood Cliffs, N.J., 1991.

Pasachoff, J. M., *Contemporary Astronomy*, Saunders, Philadelphia, 1977.

Rees, M., *Before the Beginning*, Addison Wesley, San Francisco, 1997.

Ryden, B., *Introduction to Cosmology*, Addison Wesley, San Francisco, 2003.

Shu, F. H., *The Physical Universe*, University Science Books, Mill Valley, Calif., 1982.

Weinberg, S., *The First Three Minutes*, updated ed., Basic Books, New York, 1993.

Notes

1. Hans Albrecht Bethe (1906–2005). He made the proposal concerning stellar energy sources in 1938. One of those who worked on the Manhattan Project during World War II, he received the Nobel Prize for his work on the Sun's energy source in 1967.

2. John Bahcall (1934–2005), American physicist. His definitive theoretical analysis of the solar neutrino spectrum provided the benchmark for experimentalists whose measurements ultimately confirmed neutrino oscillations.

3. The reaction by which Davis's detector detected neutrinos is $^{37}_{17}\text{Cl} + \nu_e \rightarrow ^{37}_{18}\text{Ar} + e^-$. Seventy-seven percent of the neutrinos producing this reaction were from the ^{8}B decay, step 6 of the *p-p* cycle shown in Table 13-1.

4. The term *galaxy* is derived from the Greek word for milk.

5. Apart from the Sun, Sirius is the brightest star in the sky.

6. Annie Jump Cannon (1863–1941). An astronomer at the Harvard Observatory, her work on stellar classification systems forms the basis of the *Henry Draper Catalogue* which contains the spectral classifications of 225,300 stars.

7. Hipparchus (circa 190 B.C.–circa 120 B.C.). The greatest of the Greek astronomers, he created the stellar magnitude system of classifying stars by brightness. He measured the size and distance to the Sun and Moon and made the first accurate star map showing the positions of about 1000 of the brightest stars.

8. Astronomers customarily capitalize the word *Galaxy* when it refers to the Milky Way.

9. Harlow Shapley (1885–1972). A long-time director of the Harvard Observatory, he was an early and vocal supporter of civil liberties and peace movements in the United States.

10. The term "right ascension" for the celestial longitude apparently comes from the appearance of the stars as rising vertically, i.e., at a right angle to the line of sight to the horizon each night.

11. *Equinox* means day and night are equal; *solstice* means "standing Sun."

12. Edouard A. Roche (1820–1883). A French astronomer, he also showed that a small body orbiting a large body would be broken up by tidal forces if it comes within 2.5 times the radius of the larger body. The distance is referred to as Roche's limit. It corresponds approximately to the outer limit of planetary ring systems in the solar system.

13. Subrahmanyan Chandrasekhar (1910–1995). He received his Ph.D. under P. A. M. Dirac and spent most of his career at the University of Chicago. He shared the 1983 Nobel Prize in Physics for his work on the evolution of stars. The Chandra X-Ray Observatory is named for him.

14. The possibility of black holes was first suggested by Rev. John Mitchell, an English amateur astronomer, in 1783. He observed that a star with the same density, but 500 times the radius of the Sun would have an escape velocity greater than the speed of light. He speculated that light could not leave such a star. The name black hole was coined by physicist John Wheeler.

15. Gamma-ray bursts are named according to the first date of observation: GRB yymmdd

16. Edwin P. Hubble (1889–1953). Trained as a lawyer, he was influenced to take up astronomy partly by R. A. Millikan. In recognition of his many contributions, he was accorded the honor of being the first user of the 5-m Hale telescope on Mount Palomar.

17. Cepheid variables are rare stars for which a relation exists connecting the period of intensity variation to the brightness and, hence, to the distance from the Sun. They were one of the earliest means of measuring astronomical distances. Polaris, the current Pole Star, is a Cepheid variable.

18. Light beyond the blue of the visible region would be shifted into the visible. Indeed, the visible region might even get brighter!

19. This discussion is based on the development in the early part of Chapter 29 of Carroll and Ostlie (see General References).

20. This age of the universe results from measurements made by the Wilkinson Microwave Anisotropy Project.

21. The term *Big Bang* was coined by the eminent astronomer Fred Hoyle, a steadfast proponent of the steady-state universe, intending the term as derision of the expanding universe cosmology.

22. Sir Martin Ryle (1918–1984). His invention of long-baseline radiointerferometry resulted in his sharing the Nobel Prize in 1974.

23. Arno Allan Penzias (b. 1933), German-American physicist, and Robert Woodrow Wilson (b. 1936), American radioastronomer. Their discovery of the cosmic microwave background radiation, first predicted by George Gamow 20 years earlier, earned each of them a share of the 1978 Nobel Prize in Physics.

24. Frank C. Mather (b. 1946) and George F. Smoot (b. 1945), American physicists, shared the 2006 Nobel Prize in Physics for this work which provides very strong support for the Big Bang theory.

25. M. Planck, Sitzungsber. "Dtsh. Akad. Wiss," Berlin, *Math-Phys. Tech. Kl.*, 440 (1899).

26. Frank Wilczek, American physicist, in the series "Scaling Mount Planck" in *Physics Today*, June 2001, November 2001, and August 2002. He shared the Nobel Prize in Physics in 2004 for his contributions to quark theory.

Problems

Level I

Section 13-1 The Sun

13-1. Measurement of the Doppler shift of spectral lines in light from the east and west limbs of the Sun at the solar equator reveal that the tangential velocities of the limbs differ by 4 km/s. Use this result to compute the approximate period of the Sun's rotation. ($R_\odot = 6.96 \times 10^5$ km)

13-2. The gravitational potential energy U of a self-gravitating spherical body of mass M and radius R is a function of the details of the mass distribution. For the Sun $U_\odot = -2GM_\odot^2/R_\odot$. What would be the approximate lifetime of the Sun, radiating at its present rate, if the source of its emitted energy were entirely derived from gravitational contraction? ($M_\odot = 1.99 \times 10^{30}$ kg)

Section 13-2 The Stars

13-3. Lithium, beryllium, and boron ($Z = 3, 4$, and 5, respectively) have very low abundances in the cosmos compared to many heavier elements. (See Figure 13-32.) Considering the fusion of He to C, explain these low abundances.

13-4. The Sun is moving with speed 2.5×10^5 m/s in a circular orbit about the center of the Galaxy. How long (in Earth years) does it take to complete one orbit? How many orbits has it completed since it was formed?

13-5. The reason that massive neutrinos were considered as a candidate for solving the missing mass problem is that, at the conclusion of the lepton era, the universe contained about equal numbers of photons and neutrinos. They are still here, for the most part. The former can be observed and their density is measured to be about 500 photons/cm^3; thus, there must be about that number density of neutrinos in the universe, too. If neutrinos have a nonzero mass and if the cosmological expansion has reduced their average speed so that their energy is now primarily mass, what would be the individual neutrino mass (in eV/c^2) necessary to account for the missing mass of the universe? Recall that the observed mass of the stars and galaxies (including the dust and gas) accounts for only about 4 percent of that needed to close the universe.

13-6. Using data from Table 13-3, construct a graph that demonstrates the validity of Equation 13-17.

13-7. Recalling that the light-year $c \cdot y$ is the distance light travels in one year, compute in meters the distance equivalent to 1 light-second, 1 light-minute, 1 light-hour, and 1 light-day.

Section 13-3 The Evolution of Stars

13-8. A unit of length often used by astronomers to measure distances in "nearby" space is the parsec (pc), defined as the distance at which a star subtends a parallax angle of one arc second due to Earth's orbit around the Sun. (See Equation 13-11 and Example 13-4.) The practical limit of such measurements is 0.01 arc second. (*a*) How many light-years is 1 pc? (*b*) If the density of stars in the Sun's region of the Milky Way is 0.08 stars/pc^3 , how many stars could, in principle, have their distances from us measured by the trigonometric parallax method?

13-9. Astronomers often use the *apparent magnitude m* as a means of comparing the visual brightness of stars and relating the comparison to the luminosity and distance to "standard" stars, such as the Sun. (See Equation 13-9.) The difference in the apparent magnitudes of two stars m_1 and m_2 is defined as $m_2 - m_1 = 2.5 \log (f_1/f_2)$, a relation based on the logarithmic response of the human eye to the brightness of objects. Pollux, one of the "twins" in the constellation Gemini, has apparent magnitude 1.16 and is 12 pc away. Betelgeuse, the star at Orion's right shoulder, has apparent magnitude 0.41. How far away is Betelgeuse, if they have the same luminosity?

13-10. Using the H-R diagram (Figure 13-17), determine the effective temperature and the luminosity of a star whose mass is (*a*) $0.3M_\odot$ and (*b*) $3M_\odot$. (*c*) Compute the radius of each star. (d) Determine their expected lifetimes, relative to that of the Sun.

13-11. Two stars in a binary system are located 100 $c \cdot y$ from Earth and separated from each other by 10^8 km. What is the angular separation of the stars in arc seconds? In degrees?

Section 13-4 Cataclysmic Events

13-12. Compute the energy required (in MeV) to produce each of the photodisintegration reactions in Equations 13-19 and 13-20.

13-13. The gas shell of a planetary nebula shown at the right in Figure 13-18 is expanding at 24 km/s. Its diameter is 1.5 $c \cdot y$. (*a*) How old is the gas shell? (*b*) If the central star of the planetary nebula is 12 times as luminous as the Sun and 15 times hotter, what is the radius of the central star in units of $R_\odot$?

Section 13-5 Final States of Stars

13-14. Calculate the Schwarzschild radius of a star whose mass is equal to that of (*a*) the Sun, (*b*) Jupiter, (*c*) Earth. (The mass of Jupiter is approximately 318 times that of Earth.)

13-15. Consider a neutron star whose mass equals $2M_\odot$. (*a*) Compute the star's radius. (*b*) If the neutron star is rotating at 0.5 rev/s and assuming its density to be uniform, what is its rotational kinetic energy? (*c*) If its rotation slows by 1 part in 10^8 per day and the lost kinetic energy is all radiated, what is the star's luminosity?

13-16. If the 90 percent of the Milky Way's mass which is "missing" resides entirely in a large black hole at the center of the Galaxy, what would be the black hole's (*a*) mass and (*b*) radius?

Section 13-6 Galaxies

13-17. Redshift measurements for a particular galaxy indicate that it has a recession velocity of 72,000 km/s. (*a*) Compute the distance to the galaxy. (*b*) The value of Hubble's constant depends critically on calibration distance measurements which are difficult to make. If the calibration distance measurements are in error by 10 percent, by how much is the age calculated from Equation 13-28 in error?

13-18. The bright core of a certain Seyfert galaxy had a luminosity of $10^{10}L_\odot$. The luminosity increased by 100 percent in a period of 18 months. Show that this means that the energy source of the core is less than 9.45×10^4 AU in diameter. How does this compare to the diameter of the Milky Way?

Section 13-7 Cosmology and Gravitation

13-19. Evaluate Equation 13-33 for the critical density of the universe.

Section 13-8 Cosmology and the Evolution of the Universe

13-20. Cosmological theory suggests that the average separation of galaxies, i.e., the scale of the universe, is inversely proportional to the absolute temperature. If that is true, relative to the present size, how large was the universe compared to the scale today (*a*) 2000 years ago, (*b*) 10^6 years ago, (*c*) $t = 10$ s after the Big Bang, (*d*) when $t = 1$ s and, (*e*) when $t = 10^{-6}$ s?

13-21. Determine the value of the mass density of the universe for $t =$ Planck time. How does this compare to the density of the proton? Of osmium?

13-22. At what wavelength is the blackbody radiation distribution of the cosmic microwave background at a maximum?

13-23. How long after the Big Bang did it take the universe to cool to the threshold temperature for the formation of muons? What would be the mass of a particle-antiparticle pair that could be formed by the average energy of the current 2.725 K background radiation?

13-24. Show that the present mass density of the universe $\rho_0 = R(t)\rho(t)$.

Level II

13-25. If Hubble's Law is true for an observer in the Milky Way (i.e., us), prove that it must also be true for observers in other galaxies. (Hint: Use the vector property of the velocity.)

13-26. Show that the mass density of the universe at redshift z is given by $\rho(z) = \rho(1 + z)^3$.

13-27. When the Sun was formed about 75 percent of its mass was hydrogen, of which only about 13 percent ever becomes available for fusion. (The rest is in regions of the Sun where the temperature is too low for fusion reactions to occur.) $M_\odot = 2 \times 10^{30}$ kg and the Sun fuses about 6×10^{11} kg/s. (*a*) Compute the total mass of hydrogen available for fusion during the Sun's lifetime. (*b*) How long (in years) will the Sun's initial supply of hydrogen last? (*c*) Since the solar system is currently about 4.6×10^9 years old, when should we begin to worry about the Sun running out of hydrogen for fusion?

13-28. Supernova SN1987A was first visible at Earth in 1987. (*a*) How many years B.P. (before present) did the explosion occur? (*b*) If protons with 100 GeV of kinetic energy were produced in the event, when should they arrive at Earth?

13-29. Assume that the Sun when it first formed was composed of 70 percent hydrogen. How many hydrogen nuclei were there in the Sun at that time? How much energy would ultimately be released if all of the hydrogen nuclei fused into helium? Astrophysicists have predicted that the Sun can radiate energy at its current rate until about 23 percent of the hydrogen has been "burned." What total lifetime for the Sun does that prediction imply? Compare these results with the corresponding ones from Problem 13-27.

13-30. Kepler's third law states that the square of a planet's orbital speed is proportional to the cube of its average orbital radius. Use Kepler's third law to answer each of the following questions. (*a*) The Moon's orbital radius is 3.84×10^5 km and it orbits Earth once every 27.3 d. Neglecting the Moon's mass, compute the mass of Earth. (*b*) Io (one of Jupiter's moons) orbits Jupiter once every 42.5 h in a near-circular orbit of average radius 4.22×10^5 km. Neglecting

Io's mass, compute the mass of Jupiter. (*c*) Compute the orbital period of the International Space Station as it orbits 300 km above Earth's surface. (*d*) Charon, a moon of Pluto, orbits that planet once every 6.4 d at an average distance of 1.97×10^4 km. Compute the total mass of Pluto and Charon. What fraction of Earth's mass is this? (*e*) Using the data for the star S2, compute the volume (upper limit) that confines the black hole at the center of the Milky Way. Compare the result with the volume of the Sun.

13-31. Consider an eclipsing binary whose orbital plane is parallel to our line of sight. Doppler measurements of the radial velocity of each component of the binary are shown in Figure 13-35. Assume that the mass $m_1 > m_2$ and that the orbits of each component about the center of mass are circular. (*a*) What is the period T and the angular frequency ω of the binary? (*b*) Show that in this case $(m_1 + m_2) = (\omega^2 r^3)/G$, where r = separation of the binary. (*c*) Compute the values of m_1, m_2, and r from the data in the v versus t graph.

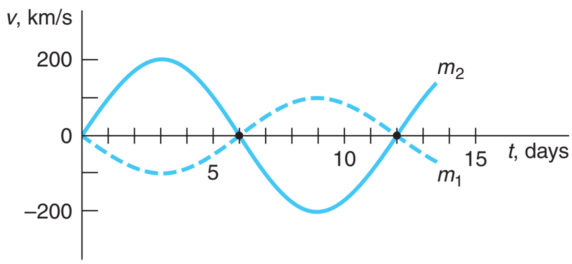

Figure 13-35

13-32. Prove that the total energy of Earth's orbital motion $E = (mv^2/2) + (-GM_\odot m/r)$ is equal to one-half of its gravitational potential energy $(-GM_\odot m/r)$, where r is Earth's orbit radius.

13-33. Given the currently accepted value of the Hubble constant and the fact that the average matter density of the universe is one H atom/m^3, what creation rate of new H atoms would be necessary in a steady-state model to maintain the present mass density, even though the universe is expanding? (Give your answer in H atoms/m^3 per 10^6 years.) Would you expect such a spontaneous creation rate to be readily observable?

Level III

13-34. The ability of a planet to retain particular gases in an atmosphere depends on the temperature that its atmosphere has (or would have) and the escape velocity for the planet. In general, if the average speed of a particular gas molecule exceeds 1/6 of the escape velocity, that gas will disappear from the atmosphere in about 10^8 years. (*a*) Graph the average speed of H_2O, CO_2, O_2, CH_4, H_2, and He from 50 K to 1000 K. On the same graph show the points representing 1/6 of the escape velocity versus average temperature of the atmosphere for the planets in Table 13-5 below. (*b*) Show that the escape speed v from a planet is given by

$$\frac{v}{v_{\text{Earth}}} = \sqrt{\frac{(M/M_{\text{Earth}})}{(R/R_{\text{Earth}})}}$$

Table 13-5 Atmospheric temperatures

Average T_{atmo}(K)	Planet	M/M_{Earth}	R/R_{Earth}
300	Earth	1.00	1.00
390	Venus	0.81	0.95
600	Mercury	0.06	0.38
150	Jupiter	318.00	11.00
60	Neptune	17.00	3.90
290	Mars	0.11	0.53

(*c*) Which of the six gases plotted probably would and would not currently be found in the atmospheres of the solar system bodies in the table? Explain *each* answer briefly.

13-35. Using the parallax technique, compute the distance to (*a*) Alpha Centauri (parallax angle 0.742 arc seconds) and (*b*) Procyon (parallax angle 0.0286 arc second. Express each answer in both light-years and parsecs.

13-36. As the Sun evolves into a red giant star, suppose that its luminosity increases by a factor of 10^2. Show that Earth's oceans will evaporate, but that the water vapor will not escape from the atmosphere.

13-37. The approximate mass of dust in the Galaxy can be computed from the observed extinction of starlight. Assuming the mean radius of dust grains to be R with a uniform number density n grains/cm^3, (*a*) show that the mean free path d_0 of a photon in interstellar dust is given by $d_0 = 1/(n\pi R^2)$. (*b*) Starlight traveling toward an Earth observer a distance d from the star has intensity

$$I = I_0 e^{-d/d_0}$$

In the vicinity of the Sun, a measurement of I yields $d_0 = 3000\ c \cdot \mathrm{y}$. If $R = 10^{-5}$ cm, calculate n. (*c*) The average mass density of solid material in the Galaxy is 2 g/cm^3 and in the disk the density of stars is about $1M_\odot/300\ (c \cdot y)^3$. Compute the ratio of the mass density of dust to the mass density of stars, assuming $1\ M_\odot$ in $300\ (c \cdot \mathrm{y})^3$.

13-38. The supernova SN1987A certainly produced some heavy elements. Compared to the energy released in fusing 56 ^{1}H atoms into one ^{56}Fe atom starting from the proton-proton cycle, how much energy would be required to fuse two ^{56}Fe atoms into one ^{112}Cd atom?

13-39. Current theory suggests that black holes evaporate by the emission of Hawking radiation in a time t that depends on the mass M of the black hole according to the following relation:

$$t = (1.024 \times 10^4 \pi^2\ \mathrm{m^3/s^2}) G^2 M^2 / hc^4$$

(*a*) Explain without calculating anything why the formula implies that high-mass black holes have longer lifetimes than low-mass ones and why the rate of evaporation accelerates as the black hole loses mass. (*b*) Compute the lifetime of a black hole whose mass equals $1M_\odot$. Compare this time with the current age of the universe. (*c*) According to some theories, the largest black hole that could conceivably form would have a mass $10^{12}\ M_\odot$, of the order of the mass of an entire galaxy. What would be the lifetime of a black hole that large?

APPENDIX A

Table of Atomic Masses

Z	Element	Symbol	Chemical atomic weight	Mass number (* indicates radioactive)	Atomic mass	Percent abundance	Half-life and decay mode (if unstable)	
0	(Neutron)	n		1*	1.008665		10.4 m	β^-
1	Hydrogen	H	1.00798	1	1.007825	99.985		
	Deuterium	D		2	2.014102	0.015		
	Tritium	T		3*	3.016049		12.33 y	β^-
2	Helium	He	4.00260	3	3.016029	0.00014		
				4	4.002602	99.99986		
				6*	6.018886		0.81 s	β^-
				8*	8.033922		0.12 s	β^-
3	Lithium	Li	6.941	6	6.015121	7.5		
				7	7.016003	92.5		
				8*	8.022486		0.84 s	β^-
				9*	9.026789		0.18 s	β^-
				11*	11.043897		8.7 ms	β^-
4	Beryllium	Be	9.0122	7*	7.016928		53.3 d	ec
				9	9.012174	100		
				10*	10.013534		1.5×10^6 y	β^-
				11*	11.021657		13.8 s	β^-
				12*	12.026921		23.6 ms	β^-
				14*	14.042866		4.3 ms	β^-
5	Boron	B	10.811	8*	8.024605		0.77 s	β^+
				10	10.012936	19.9		
				11	11.009305	80.1		
				12*	12.014352		0.0202 s	β^-
				13*	13.017780		17.4 ms	β^-
				14*	14.025404		13.8 ms	β^-
				15*	15.031100		10.3 ms	β^-
6	Carbon	C	12.011	9*	9.031030		0.13 s	β^+
				10*	10.016854		19.3 s	β^+
				11*	11.011433		20.4 m	β^+
				12	12.000000	98.90		
				13	13.003355	1.10		
				14*	14.003242		5730 y	β^-
				15*	15.010599		2.45 s	β^-
				16*	16.014701		0.75 s	β^-
				17*	17.022582		0.20 s	β^-

(*Continued*)

Z	Element	Symbol	Chemical atomic weight	Mass number (* indicates radioactive)	Atomic mass	Percent abundance	Half-life and decay mode (if unstable)
7	Nitrogen	N	14.0067	12*	12.018613		0.0110 s β^+
				13*	13.005738		9.96 m β^+
				14	14.003074	99.63	
				15	15.000108	0.37	
				16*	16.006100		7.13 s β^-
				17*	17.008450		4.17 s β^-
				18*	18.014082		0.62 s β^-
				19*	19.017038		0.24 s β^-
8	Oxygen	O	15.9994	13*	13.024813		8.6 ms β^+
				14*	14.008595		70.6 s β^+
				15*	15.003065		122 s β^+
				16	15.994915	99.71	
				17	16.999132	0.039	
				18	17.999160	0.20	
				19*	19.003577		26.9 s β^-
				20*	20.004076		13.6 s β^-
				21*	21.008595		3.4 s β^-
9	Fluorine	F	18.99840	17*	17.002094		64.5 s β^+
				18*	18.000937		109.8 m β^+
				19	18.998404	100	
				20*	19.999982		11.0 s β^-
				21*	20.999950		4.2 s β^-
				22*	22.003036		4.2 s β^-
				23*	23.003564		2.2 s β^-
10	Neon	Ne	20.180	18*	18.005710		1.67 s β^+
				19*	19.001880		17.2 s β^+
				20	19.992435	90.48	
				21	20.993841	0.27	
				22	21.991383	9.25	
				23*	22.994465		37.2 s β^-
				24*	23.993999		3.38 m β^-
				25*	24.997789		0.60 s β^-
11	Sodium	Na	22.98977	21*	20.997650		22.5 s β^+
				22*	21.994434		2.61 y β^+
				23	22.989767	100	
				24*	23.990961		14.96 h β^-
				25*	24.989951		59.1 s β^-
				26*	25.992588		1.07 s β^-
12	Magnesium	Mg	24.3051	23*	22.994124		11.3 s β^+
				24	23.985042	78.99	
				25	24.985838	10.00	
				26	25.982594	11.01	
				27*	26.984341		9.46 m β^-
				28*	27.983876		20.9 h β^-
				29*	28.375346		1.30 s β^-

Z	Element	Symbol	Chemical atomic weight	Mass number (* indicates radioactive)	Atomic mass	Percent abundance	Half-life and decay mode (if unstable)	
13	Aluminum	Al	26.98154	25*	24.990429		7.18 s	β^+
				26*	25.986892		7.4×10^5 y	β^+
				27	26.981538	100		
				28*	27.981910		2.24 m	β^-
				29*	28.980445		6.56 m	β^-
				30*	29.982965		3.60 s	β^-
14	Silicon	Si	28.086	27*	26.986704		4.16 s	β^+
				28	27.976927	92.23		
				29	28.976495	4.67		
				30	28.973770	3.10		
				31*	30.975362		2.62 h	β^-
				32*	31.974148		172 y	β^-
				33*	32.977928		6.13 s	β^-
15	Phosphorus	P	30.97376	30*	29.978307		2.50 m	β^+
				31	30.973762	100		
				32*	31.973762		14.26 d	β^-
				33*	32.971725		25.3 d	β^-
				34*	33.973636		12.43 s	β^-
16	Sulfur	S	32.066	31*	30.979554		2.57 s	β^+
				32	31.972071	95.02		
				33	32.971459	0.75		
				34	33.967867	4.21		
				35*	34.969033		87.5 d	β^-
				36	35.967081	0.02		
17	Chlorine	Cl	35.453	34*	33.973763		32.2 m	β^+
				35	34.968853	75.77		
				36*	35.968307		3.0×10^5 y	β^-
				37	36.965903	24.23		
				38*	37.968010		37.3 m	β^-
18	Argon	Ar	39.948	36	35.967547	0.337		
				37*	36.966776		35.04 d	ec
				38	37.962732	0.063		
				39*	38.964314		269 y	β^-
				40	39.962384	99.600		
				42*	41.963049		33 y	β^-
19	Potassium	K	39.0983	39	38.963708	93.2581		
				40*	39.964000	0.0117	1.28×10^9 y	β^+, ec, β^-
				41	40.961827	6.7302		
				42*	41.962404		12.4 h	β^-
				43*	42.960716		22.3 h	β^-

(Continued)

Z	Element	Symbol	Chemical atomic weight	Mass number (* indicates radioactive)	Atomic mass	Percent abundance	Half-life and decay mode (if unstable)
20	Calcium	Ca	40.078	40	39.962591	96.941	
				41*	40.962279		1.0×10^5 y ec
				42	41.958618	0.647	
				43	42.958767	0.135	
				44	43.955481	2.086	
				46	45.953687	0.004	
				48	47.952534	0.187	
21	Scandium	Sc	44.9559	41*	40.969250		0.596 s β^+
				43*	42.961151		3.89 h β^+
				45	44.955911	100	
				46*	45.955170		83.8 d β^-
22	Titanium	Ti	47.88	44*	43.959691		49 y ec
				46	45.952630	8.0	
				47	46.951765	7.3	
				48	47.947947	73.8	
				49	48.947871	5.5	
				50	49.944792	5.4	
23	Vanadium	V	50.9415	48*	47.952255		15.97 d β^+
				50*	49.947161	0.25	1.5×10^{17} y β^+
				51	50.943962	99.75	
24	Chromium	Cr	51.996	48*	47.954033		21.6 h ec
				50	49.946047	4.345	
				52	51.940511	83.79	
				53	52.940652	9.50	
				54	53.938883	2.365	
25	Manganese	Mn	54.93805	53*	52.941292		3.74×10^6 y ec
				54*	53.940361		312.1 d ec
				55	54.938048	100	
				56*	55.938908		2.58 h β^-
26	Iron	Fe	55.847	54	53.939613	5.9	
				55*	54.938297		2.7 y ec
				56	55.934940	91.72	
				57	56.935396	2.1	
				58	57.933278	0.28	
				60*	59.934078		1.5×10^6 y β^-
27	Cobalt	Co	58.93320	57*	56.936294		271.8 d ec
				58*	57.935755		70.9 h ec, β^+
				59	58.933198	100	
				60*	59.933820		5.27 y β^-
				61*	60.932478		1.65 h β^-

Z	Element	Symbol	Chemical atomic weight	Mass number (* indicates radioactive)	Atomic mass	Percent abundance	Half-life and decay mode (if unstable)	
28	Nickel	Ni	58.693	58	57.935346	68.077		
				59*	58.934350		7.5×10^4 y	ec, β^+
				60	59.930789	26.223		
				61	60.931058	1.140		
				62	61.928346	3.634		
				63*	62.929670		100 y	β^-
				64	63.927967	0.926		
29	Copper	Cu	63.546	63	62.929599	69.17		
				64*	63.929765		12.7 h	ec
				65	64.927791	30.83		
				66*	65.928871		5.1 m	β^-
30	Zinc	Zn	65.39	64	63.929144	48.6		
				66	65.926035	27.9		
				67	66.927129	4.1		
				68	67.924845	18.8		
				70	69.925323	0.6		
31	Gallium	Ga	69.723	69	68.925580	60.108		
				70*	69.926027		21.1 m	β^-
				71	70.924703	39.892		
				72*	71.926367		14.1 h	β^-
32	Germanium	Ge	72.61	69*	68.927969		39.1 h	ec, β^+
				70	69.924250	21.23		
				72	71.922079	27.66		
				73	72.923462	7.73		
				74	73.921177	35.94		
				76	75.921402	7.44		
				77*	76.923547		11.3 h	β^-
33	Arsenic	As	74.9216	73*	72.923827		80.3 d	ec
				74*	73.923928		17.8 d	ec, β^+
				75	74.921594	100		
				76*	75.922393		1.1 d	β^-
				77*	76.920645		38.8 h	β^-
34	Selenium	Se	78.96	74	73.922474	0.89		
				76	75.919212	9.36		
				77	76.919913	7.63		
				78	77.917307	23.78		
				79*	78.918497		$\leq 6.5 \times 10^4$ y	β^-
				80	79.916519	49.61		
				82*	81.916697	8.73	1.4×10^{20} y	$2\beta^-$

(*Continued*)

Z	Element	Symbol	Chemical atomic weight	Mass number (* indicates radioactive)	Atomic mass	Percent abundance	Half-life and decay mode (if unstable)	
35	Bromine	Br	79.904	79	78.918336	50.69		
				80*	79.918528		17.7 m	β^+
				81	80.916287	49.31		
				82*	81.916802		35.3 h	β^-
36	Krypton	Kr	83.80	78	77.920400	0.35		
				80	79.916377	2.25		
				81*	80.916589		2.11×10^5 y	ec
				82	81.913481	11.6		
				83	82.914136	11.5		
				84	83.911508	57.0		
				85*	84.912531		10.76 y	β^-
				86	85.910615	17.3		
37	Rubidium	Rb	85.468	85	84.911793	72.17		
				86*	85.911171		18.6 d	β^-
				87*	86.909186	27.83	4.75×10^{10} y	β^-
				88*	87.911325		17.8 m	β^-
38	Strontium	Sr	87.62	84	83.913428	0.56		
				86	85.909266	9.86		
				87	86.908883	7.00		
				88	87.905618	82.58		
				90*	89.907737		29.1 y	β^-
39	Yttrium	Y	88.9058	88*	87.909507		106.6 d	ec, β^+
				89	88.905847	100		
				90*	89.914811		2.67 d	β^-
40	Zirconium	Zr	91.224	90	89.904702	51.45		
				91	90.905643	11.22		
				92	91.905038	17.15		
				93*	92.906473		1.5×10^6 y	β^-
				94	93.906314	17.38		
				96	95.908274	2.80		
41	Niobium	Nb	92.9064	91*	90.906988		6.8×10^2 y	ec
				92*	91.907191		3.5×10^7 y	ec
				93	92.906376	100		
				94*	93.907280		2×10^4 y	β^-
42	Molybdenum	Mo	95.94	92	91.906807	14.84		
				93*	92.906811		3.5×10^3 y	ec
				94	93.905085	9.25		
				95	94.905841	15.92		
				96	95.904678	16.68		
				97	96.906020	9.55		
				98	97.905407	24.13		
				100	99.907476	9.63		

Z	Element	Symbol	Chemical atomic weight	Mass number (* indicates radioactive)	Atomic mass	Percent abundance	Half-life and decay mode (if unstable)	
43	Technetium	Tc		97*	96.906363		2.6×10^6 y	ec
				98*	97.907215		4.2×10^6 y	β^-
				99*	98.906254		2.1×10^5 y	β^-
44	Ruthenium	Ru	101.07	96	95.907597	5.54		
				98	97.905287	1.86		
				99	98.905939	12.7		
				100	99.904219	12.6		
				101	100.905558	17.1		
				102	101.904348	31.6		
				104	103.905428	18.6		
45	Rhodium	Rh	102.9055	102*	101.906794		207 d	ec
				103	102.905502	100		
				104*	103.906654		42 s	β^-
46	Palladium	Pd	106.42	102	101.905616	1.02		
				104	103.904033	11.14		
				105	104.905082	22.33		
				106	105.903481	27.33		
				107*	106.905126		6.5×10^6 y	β^-
				108	107.903893	26.46		
				110	109.905158	11.72		
47	Silver	Ag	107.868	107	106.905091	51.84		
				108*	107.905953		2.39 m	ec, β^+, β^-
				109	108.904754	48.16		
				110*	109.906110		24.6 s	β^-
48	Cadmium	Cd	112.41	106	105.906457	1.25		
				108	107.904183	0.89		
				109*	108.904984		462 d	ec
				110	109.903004	12.49		
				111	110.904182	12.80		
				112	111.902760	24.13		
				113*	112.904401	12.22	9.3×10^{15} y	β^-
				114	113.903359	28.73		
				116	115.904755	7.49		
49	Indium	In	114.82	113	112.904060	4.3		
				114*	113.904916		1.2 m	β^-
				115*	114.903876	95.7	4.4×10^{14} y	β^-
				116*	115.905258		54.4 m	β^-

(*Continued*)

Z	Element	Symbol	Chemical atomic weight	Mass number (* indicates radioactive)	Atomic mass	Percent abundance	Half-life and decay mode (if unstable)
50	Tin	Sn	118.71	112	111.904822	0.97	
				114	113.902780	0.65	
				115	114.903345	0.36	
				116	115.901743	14.53	
				117	116.902953	7.68	
				118	117.901605	24.22	
				119	118.903308	8.58	
				120	119.902197	32.59	
				121*	120.904237		55 y β^-
				122	121.903439	4.63	
				124	123.905274	5.79	
51	Antimony	Sb	121.76	121	120.903820	57.36	
				123	122.904215	42.64	
				125*	124.905251		2.7 y β^-
52	Tellurium	Te	127.60	120	119.904040	0.095	
				122	121.903052	2.59	
				123*	122.904271	0.905	1.3×10^{13} y ec
				124	123.902817	4.79	
				125	124.904429	7.12	
				126	125.903309	18.93	
				128*	127.904463	31.70	$>8 \times 10^{24}$ y $2\beta^-$
				130*	129.906228	33.87	1.2×10^{21} y $2\beta^-$
53	Iodine	I	126.9045	126*	125.905619		13 d ec, β^+, β^-
				127	126.904474	100	
				128*	127.905812		25 m β^-, ec, β^+
				129*	128.904984		1.6×10^{7} y β^-
54	Xenon	Xe	131.29	124	123.905894	0.10	
				126	125.904268	0.09	
				128	127.903531	1.91	
				129	128.904779	26.4	
				130	129.903509	4.1	
				131	130.905069	21.2	
				132	131.904141	26.9	
				134	133.905394	10.4	
				136	135.907215	8.9	
55	Cesium	Cs	132.9054	133	132.905436	100	
				134*	133.906703		2.1 y β^-
				135*	134.905891		2×10^{6} y β^-
				137*	136.907078		30 y β^-

Z	Element	Symbol	Chemical atomic weight	Mass number (* indicates radioactive)	Atomic mass	Percent abundance	Half-life and decay mode (if unstable)	
56	Barium	Ba	137.33	130	129.906289	0.106		
				132	131.905048	0.101		
				133*	132.905990		10.5 y	ec
				134	133.904492	2.42		
				135	134.905671	6.593		
				136	135.904559	7.85		
				137	136.905816	11.23		
				138	137.905236	71.70		
57	Lanthanum	La	138.905	137*	136.906462		6×10^4 y	ec
				138*	137.907105	0.0902	1.05×10^{11} y	ec, β^+
				139	138.906346	99.9098		
58	Cerium	Ce	140.12	136	135.907139	0.19		
				138	137.905986	0.25		
				140	139.905434	88.43		
				142	141.909241	11.13		
59	Praseodymium	Pr	140.9076	140*	139.909071		3.39 m	ec, β^+
				141	140.907647	100		
				142*	141.910040		25.0 m	β^-
60	Neodymium	Nd	144.24	142	141.907718	27.13		
				143	142.909809	12.18		
				144*	143.910082	23.80	2.3×10^{15} y	α
				145	144.912568	8.30		
				146	145.913113	17.19		
				148	147.916888	5.76		
				150	149.920887	5.64		
61	Promethium	Pm		143*	142.910928		265 d	ec
				145*	144.912745		17.7 y	ec
				146*	145.914698		5.5 y	ec
				147*	146.915134		2.623 y	β^-
62	Samarium	Sm	150.36	144	143.911996	3.1		
				146*	145.913043		1.0×10^8 y	α
				147*	146.914894	15.0	1.06×10^{11} y	α
				148*	147.914819	11.3	7×10^{15} y	α
				149	148.917180	13.8		
				150	149.917273	7.4		
				151*	150.919928		90 y	β^-
				152	151.919728	26.7		
				154	153.922206	22.7		

(*Continued*)

Z	Element	Symbol	Chemical atomic weight	Mass number (* indicates radioactive)	Atomic mass	Percent abundance	Half-life and decay mode (if unstable)	
63	Europium	Eu	151.96	151	150.919846	47.8		
				152*	151.921740		13.5 y	ec, β^+
				153	152.921226	52.2		
				154*	153.922975		8.59 y	β^-
				155*	154.922888		4.7 y	β^-
64	Gadolinium	Gd	157.25	148*	147.918112		75 y	α
				150*	149.918657		1.8×10^6 y	α
				152*	151.919787	0.20	1.1×10^{14} y	α
				154	153.920862	2.18		
				155	154.922618	14.80		
				156	155.922119	20.47		
				157	156.923957	15.65		
				158	157.924099	24.84		
				160	159.927050	21.86		
65	Terbium	Tb	158.9253	158*	157.925411		180 y	ec, β^+, β^-
				159	158.925345	100		
				160*	159.927551		72.3 d	β^-
66	Dysprosium	Dy	162.50	156	155.924277	0.06		
				158	157.924403	0.10		
				160	159.925193	2.34		
				161	160.926930	18.9		
				162	161.926796	25.5		
				163	162.928729	24.9		
				164	163.929172	28.2		
67	Holmium	Ho	164.9303	165	164.930316	100		
				166*	165.932282		1.2×10^3 y	β^-
68	Erbium	Er	167.26	162	161.928775	0.14		
				164	163.929198	1.61		
				166	165.930292	33.6		
				167	166.932047	22.95		
				168	167.932369	27.8		
				170	169.935462	14.9		
69	Thulium	Tm	168.9342	169	168.934213	100		
				171*	170.936428		1.92 y	β^-
70	Ytterbium	Yb	173.04	168	167.933897	0.13		
				170	169.934761	3.05		
				171	170.936324	14.3		
				172	171.936380	21.9		
				173	172.938209	16.12		
				174	173.938861	31.8		
				176	175.942564	12.7		

Z	Element	Symbol	Chemical atomic weight	Mass number (* indicates radioactive)	Atomic mass	Percent abundance	Half-life and decay mode (if unstable)	
71	Lutetium	Lu	174.967	173*	172.938930		1.37 y	ec
				175	174.940772	97.41		
				176*	175.942679	2.59	3.8×10^{10} y	β^-
72	Hafnium	Hf	178.49	174*	173.940042	0.162	2.0×10^{15} y	α
				176	175.941404	5.206		
				177	176.943218	18.606		
				178	177.943697	27.297		
				179	178.945813	13.629		
				180	179.946547	35.100		
73	Tantalum	Ta	180.9479	180	179.947542	0.012		
				181	180.947993	99.988		
74	Tungsten (Wolfram)	W	183.85	180	179.946702	0.12		
				182	181.948202	26.3		
				183	182.950221	14.28		
				184	183.950929	30.7		
				186	185.954358	28.6		
75	Rhenium	Re	186.207	185	184.952951	37.40		
				187*	186.955746	62.60	4.4×10^{10} y	β^-
76	Osmium	Os	190.2	184	183.952486	0.02		
				186*	185.953834	1.58	2.0×10^{15} y	α
				187	186.955744	1.6		
				188	187.955744	13.3		
				189	188.958139	16.1		
				190	189.958439	26.4		
				192	191.961468	41.0		
				194*	193.965172		6.0 y	β^-
77	Iridium	Ir	192.2	191	190.960585	37.3		
				193	192.962916	62.7		
78	Platinum	Pt	195.08	190*	189.959926	0.01	6.5×10^{11} y	α
				192	191.961027	0.79		
				194	193.962655	32.9		
				195	194.964765	33.8		
				196	195.964926	25.3		
				198	197.967867	7.2		
79	Gold	Au	196.9665	197	196.966543	100		
				198*	197.968217		2.70 d	β^-
				199*	198.968740		3.14 d	β^-

(Continued)

Z	Element	Symbol	Chemical atomic weight	Mass number (* indicates radioactive)	Atomic mass	Percent abundance	Half-life and decay mode (if unstable)
80	Mercury	Hg	200.59	196	195.965806	0.15	
				198	197.966743	9.97	
				199	198.968253	16.87	
				200	199.968299	23.10	
				201	200.970276	13.10	
				202	201.970617	29.86	
				204	203.973466	6.87	
81	Thallium	Tl	204.383	203	202.972320	29.524	
				204*	203.973839		3.78 y β^-
				205	204.974400	70.476	
		(Ra E″)		206*	205.976084		4.2 m β^-
		(Ac C″)		207*	206.977403		4.77 m β^-
		(Th C″)		208*	207.981992		3.053 m β^-
		(Ra C″)		210*	209.990057		1.30 m β^-
82	Lead	Pb	207.2	202*	201.972134		5×10^4 y ec
				204	203.973020	1.4	
				205*	204.974457		1.5×10^7 y ec
				206	205.974440	24.1	
				207	206.975871	22.1	
				208	207.976627	52.4	
		(Ra D)		210*	209.984163		22.3 y β^-
		(Ac B)		211*	210.988734		36.1 m β^-
		(Th B)		212*	211.991872		10.64 h β^-
		(Ra B)		214*	213.999798		26.8 m β^-
83	Bismuth	Bi	208.9803	207*	206.978444		32.2 y ec, β^+
				208*	207.979717		3.7×10^5 y ec
				209	208.980374	100	
		(Ra E)		210*	209.984096		5.01 d α, β^-
		(Th C)		211*	210.987254		2.14 m α
				212*	211.991259		60.6 m α, β^-
		(Ra C)		214*	213.998692		19.9 m β^-
				215*	215.001836		7.4 m β^-
84	Polonium	Po		209*	208.982405		102 y α
		(Ra F)		210*	209.982848		138.38 d α
		(Ac C′)		211*	210.986627		0.52 s α
		(Th C′)		212*	211.988842		0.30 μs α
		(Ra C′)		214*	213.995177		164 μs α
		(Ac A)		215*	214.999418		0.0018 s α
		(Th A)		216*	216.001889		0.145 s α
		(Ra A)		218*	218.008965		3.10 m α
85	Astatine	At		215*	214.998638		≈ 100 μs α
				218*	218.008685		1.6 s α
				219*	219.011297		0.9 m α

Z	Element	Symbol	Chemical atomic weight	Mass number (* indicates radioactive)	Atomic mass	Percent abundance	Half-life and decay mode (if unstable)	
86	Radon	Rn						
		(An)		219*	219.009477		3.96 s	α
		(Tn)		220*	220.011369		55.6 s	α
		(Rn)		222*	222.017571		3.823 d	α
87	Francium			221*	221.01425		4.18 m	α
		Fr		222*	222.017585		14.2 m	β^-
		(Ac K)		223*	223.019733		22 m	β^-
88	Radium	Ra		221*	221.01391		29 s	α
		(Ac X)		223*	223.018499		11.43 d	α
		(Th X)		224*	224.020187		3.66 d	α
				225*			14.9 d	β^-
		(Ra)		226*	226.025402		1600 y	α
		($MsTh_1$)		228*	228.031064		5.75 y	β^-
89	Actinium	Ac		225*			10 d	α
		(Ms Th_2)		227*	227.027749		21.77 y	β^-
				228*	228.031015		6.15 h	β^-
				229*			1.04 h	β^-
90	Thorium	Th	232.0381					
		(Rd Ac)		227*	227.027701		18.72 d	α
		(Rd Th)		228*	228.028716		1.913 y	α
				229*	229.031757		7300 y	α
		(Io)		230*	230.033127		75,000 y	α, sf
		(UY)		231*	231.036299		25.52 h	β^-
		(Th)		232*	232.038051	100	1.40×10^{10} y	α
		(UX_1)		234*	234.043593		24.1 d	β^-
91	Protactinium	Pa		231*	231.035880		32,760 y	α
		(UZ)		234*	234.043300		6.7 h	β^-
92	Uranium	U	238.0289	231*	231.036264		4.2 d	β^+
				232*	232.037131		69 y	α
				233*	233.039630		1.59×10^5 y	α
		(UII)		234*	234.040946	0.0055	2.45×10^5 y	α
		(Ac U)		235*	235.043924	0.720	7.04×10^8 y	α
		(UI)		236*	236.045562		2.34×10^7 y	α
				238*	238.050784	99.2745	4.47×10^9 y	α
				239*	239.054290		23.5 m	β^-
93	Neptunium	Np		235*	235.044057		396 d	α
				236*	236.046559		1.54×10^5 y	ec
				237*	237.048168		2.14×10^6 y	α

(Continued)

Z	Element	Symbol	Chemical atomic weight	Mass number (* indicates radioactive)	Atomic mass	Percent abundance	Half-life and decay mode (if unstable)	
94	Plutonium	Pu		236*	236.046033		2.87 y	α, sf
				238*	238.049555		87.7 y	α, sf
				239*	239.052157		24,120 y	α, sf
				240*	240.053808		6560 y	α, sf
				241*	241.056846		14.4 y	β^-
				242*	242.058737		3.7×10^5 y	α, sf
				244*	244.064200		8.1×10^7 y	α, sf
95	Americium	Am		240*	240.055285		2.12 d	ec
				241*	241.056824		432 y	α, sf
96	Curium	Cm		247*	247.070347		1.56×10^7 y	α
				248*	248.072344		3.4×10^5 y	α, sf
97	Berkelium	Bk		247*	247.070300		1380 y	α
				249*	249.074979		327 d	β^-
98	Californium	Cm		250*	250.076400		13.1 y	α, sf
				251*	251.079580		898 y	α
99	Einsteinium	Es		252*	252.082974		1.29 y	α
				253*	253.084817		2.02 d	α, sf
100	Fermium	Fm		253*	253.085173		3.00 d	ec
				254*	254.086849		3.24 h	α, sf
101	Mendelevium	Md		256*	256.093988		75.6 m	ec, β^+
				258*	258.098594		55 d	α
102	Nobelium	No		257*	257.096855		25 s	α
				259*	259.100932		58 m	α, sf
103	Lawrencium	Lr		259*	259.102888		6.14 s	α, sf
				260*	260.105346		3.0 m	α, sf
104	Rutherfordium	Rf		260*	260.160302		24 ms	sf
				261*	261.108588		65 s	α, sf
105	Dubnium	Db		261*	261.111830		1.8 s	α
				262*	262.113763		35 s	α
106	Seaborgium	Sg		263*	263.118310		0.78 s	α, sf
107	Bohrium	Bh		262*	262.123081		0.10 s	α, sf
108	Hassium	Hs		265*	265.129984		1.8 ms	α
				267*	267.131770		60 ms	α
109	Meitnerium	Mt		266*	266.137789		3.4 ms	α, sf
				268*	268.138820		70 ms	α

Z	Element	Symbol	Chemical atomic weight	Mass number (* indicates radioactive)	Atomic mass	Percent abundance	Half-life and decay mode (if unstable)
110	Darmstadtium	Ds		269*	269.145140		0.17 ms α
				271*	271.146080		1.1 ms α
				273*	272.153480		8.6 ms α
111	Roentgenium	Rg		272*	272.153480		1.5 ms α
112	Ununbium	Unb		277*	?		0.2 ms α
113	Ununtrium	Unt		284*	?		? α
114	Ununquadium	Unq		289*	?		? α
115	Ununpentium	Unp		288*	?		? α
116	Ununhexium	Unh		292*	?		? α
117							
118	Ununoctium	Uno		294*	?		? α

APPENDIX B1

Probability Integrals

When calculating various average values using the Maxwell-Boltzmann distribution, integrals of the following type occur:

$$I_n = \int_0^\infty x^n e^{-\lambda x^2} dx$$

where n is an integer. These can be obtained from I_0 and I_1 by differentiation. Consider I_n to be a function of λ and take the derivative with respect to λ:

$$\frac{dI_n}{d\lambda} = \int_0^\infty -x^2 x^n e^{-\lambda x^2}\, dx = -I_{n+2} \qquad \textbf{B1-1}$$

Thus, if I_0 is known, all the I_n for even n can be obtained, and if I_1 is known, all the I_n for odd n can be obtained from Equation B1-1. I_1 can easily be evaluated. Using the substitution $u = \lambda x^2$, then $du = 2\lambda x\, dx$ and

$$I_1 = \int_0^\infty x e^{-\lambda x^2}\, dx = \frac{1}{2}\lambda^{-1}\int_0^\infty e^{-u}\, du = \frac{1}{2}\lambda^{-1}$$

Then I_3 and I_5 are

$$I_3 = -\frac{d\left(\frac{1}{2}\lambda^{-1}\right)}{d\lambda} = \frac{1}{2}\lambda^{-2} \qquad \text{and} \qquad I_5 = -\frac{dI_3}{d\lambda} = \lambda^{-3}$$

The evaluation of I_0 is more difficult, but it can be done using a trick. We evaluate I_0^2:

$$I_0^2 = \int_0^\infty e^{-\lambda x^2}\, dx \int_0^\infty e^{-\lambda y^2}\, dy = \int_0^\infty \int_0^\infty e^{-\lambda(x^2+y^2)}\, dx\, dy \qquad \textbf{B1-2}$$

where we have used y as the dummy variable of integration in the second integral. If we now consider this to be an integration over the xy plane, we can change to polar coordinates $r^2 = x^2 + y^2$ and $\tan\varphi = y/x$. The element of area $dx\,dy$ becomes $r\,dr\,d\varphi$ and the integration over positive x and y becomes an integration from $r = 0$ to $r = \infty$ and from $\varphi = 0$ to $\varphi = \pi/2$. Then we have

$$I_0^2 = \int_0^\infty \int_0^{\pi/2} e^{-\lambda r^2} r\, dr\, d\varphi = \frac{\pi}{2} I_1 = \frac{\pi}{4}\lambda^{-1}$$

and

$$I_0 = \frac{1}{2}\sqrt{\pi}\,\lambda^{-1/2}$$

We then obtain $I_2, I_4, \ldots$ by differentiation. For example,

$$I_2 = -\frac{dI_0}{d\lambda} = \frac{1}{4}\sqrt{\pi}\,\lambda^{-3/2}$$

Table B1-1 lists the values of the integral I_n calculated as above for values of n from 0 to 5.

Table B1-1 Values of the integral $I_n = \int_0^{\infty} x^n e^{-\lambda x^2}\,dx$ for $n = 0$ to $n = 5$

n	I_n
0	$\frac{1}{2}\pi^{1/2}\lambda^{-1/2}$
1	$\frac{1}{2}\lambda^{-1}$
2	$\frac{1}{4}\pi^{1/2}\lambda^{-3/2}$
3	$\frac{1}{2}\lambda^{-2}$
4	$\frac{3}{8}\pi^{1/2}\lambda^{-5/2}$
5	λ^{-3}
If n is even	$\int_{-\infty}^{+\infty} x^n e^{-\lambda x^2}\,dx = 2I_n$
If n is odd	$\int_{-\infty}^{+\infty} x^n e^{-\lambda x^2}\,dx = 0$

APPENDIX B2

Binomial and Exponential Series

Binomial Series

$$(1 + x)^m = 1 + mx + \frac{m(m-1)}{2!}x^2 + \frac{m(m-1)(m-2)}{3!}x^3 + \cdots$$

$$+ \frac{m(m-1)(m-2)\cdots(m-n+2)}{(n-1)!}x^{n-1} + R_n$$

where

$$R_n = \frac{m(m-1)(m-2)\cdots(m-n+1)}{n!}x^n(1+ax)^{m-n}$$

for all cases where $0 < a < 1$.

$$R_n < \left|\frac{m(m-1)(m-2)\cdots(m-n+1)}{n!}x^n\right| \quad \text{if } x > 0$$

$$R_n < \left|\frac{m(m-1)(m-2)\cdots(m-n+1)}{n!}\,\frac{x^n}{(1+x)^{n-m}}\right| \quad \text{for } x < 0, \quad n > m$$

$$R_n < |x^n|(1+x)^m \quad \text{if} \quad -1 < m < 0$$

If m is a negative integer or a positive or negative fraction, the binomial expansion is valid only when $|x| < 1$. Except when m is a positive integer, a binomial such as $(a + b)^m$ must be written in one of the following forms before expanding it:

$$a^m\left(1 + \frac{b}{a}\right)^m \quad \text{if} \quad a > b \qquad b^m\left(1 + \frac{a}{b}\right)^m \quad \text{if} \quad b > a$$

Exponential Series

$$e^x = 1 + x + \frac{x^2}{2!} + \frac{x^3}{3!} + \cdots + \frac{x^{n-1}}{(n-1)!} + \frac{x^n}{n!} + \cdots$$

$$a^x = 1 + x\log a + \frac{(x\log a)^2}{2!} + \cdots + \frac{(x\log a)^{n-1}}{(n-1)!} + \frac{(x\log a)^n}{n!} + \cdots$$

APPENDIX B3

Diagrams of Crystal Unit Cells

Crystalline solids are classified according to their symmetries into 7 crystal systems and 14 lattices. A **lattice** is defined as an infinite array of points each of which has surroundings identical to those of all other points. In three dimensions this definition is expressed by three **translation vectors a**, **b**, and **c**, such that the array of atoms in the crystal when viewed from point **r** looks the same when viewed from any other point **r**′, where **r**′ is reached by translations of integer multiples of the $\mathbf{a}_i$, that is,

$$\mathbf{r}' = \mathbf{r} + m_1\mathbf{a} + m_2\mathbf{b} + m_3\mathbf{c}$$

where m_i are integers. The translation vectors are usually (but not always) used to specify the three axes of the crystal's **unit cell**. The volume of the unit cell is $\mathbf{a} \cdot (\mathbf{b} \times \mathbf{c})$, and no cell of smaller volume can serve as the unit to assemble the crystal.

Figure B3-1 illustrates the orientations of the translation vectors and the standard designations of the angles between them. Figure B3-2 illustrates diagrams of the 14 lattices.

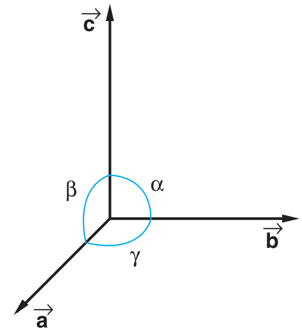

Figure B3-1 The directions of the translation vectors are often used to define the directions of the crystal axes, the angles between each axis pair defining the shape of the cell.

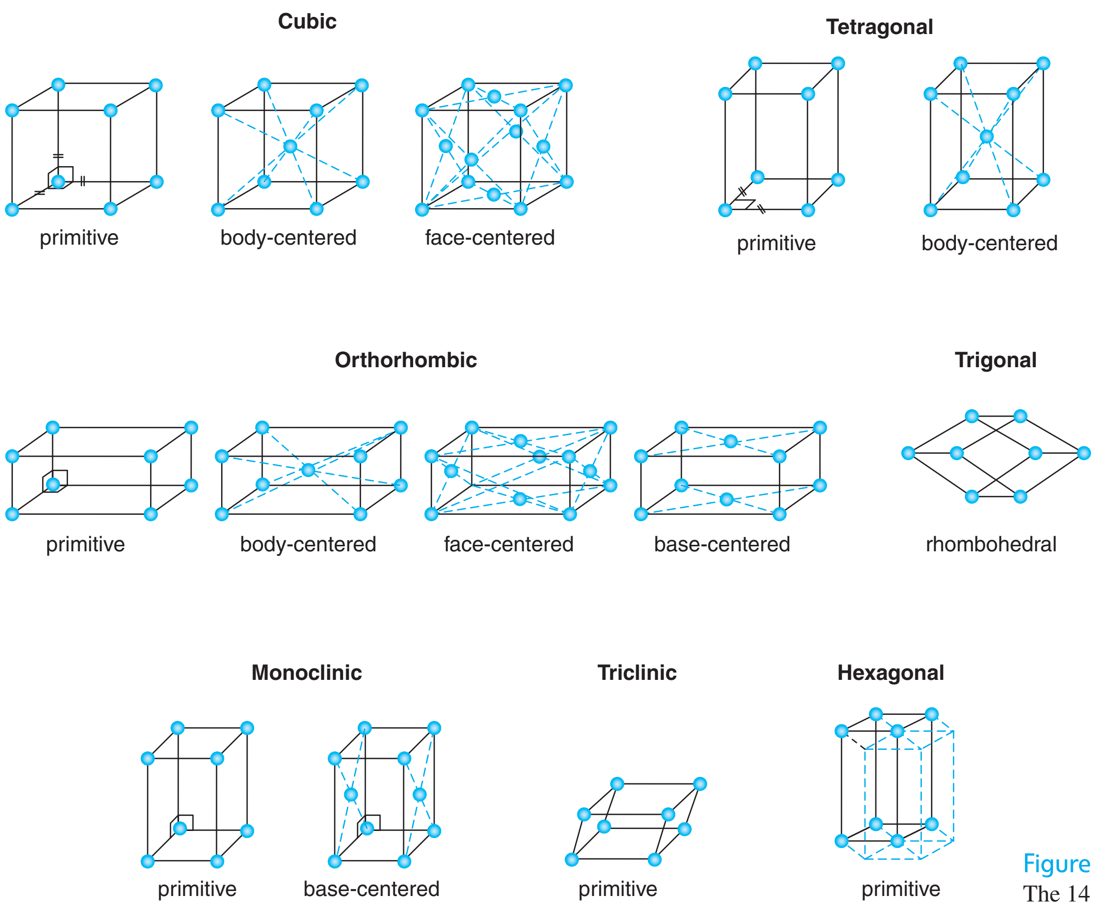

Figure B3-2 The 14 crystal lattices.

APPENDIX C

Electron Configurations

Electron configurations of the atoms in their ground states. For a few of the rare earth elements ($Z = 57$ to 71) and the heavy elements ($Z > 89$), the configurations are not firmly established.

Z	Element	Ionization energy (eV)	K $n:1$ $l:s$	L 2 $s\ p$	M 3 $s\ p\ d$	N 4 $s\ p\ d\ f$	O 5 $s\ p\ d\ f$	P 6 $s\ p\ d$	Q 7 $s\ p$
1	H (hydrogen)	13.6	1						
2	He (helium)	24.5	2						
3	Li (lithium)	5.4	2	1					
4	Be (beryllium)	9.3	2	2					
5	B (boron)	8.3	2	2 1					
6	C (carbon)	11.3	2	2 2					
7	N (nitrogen)	14.5	2	2 3					
8	O (oxygen)	13.6	2	2 4					
9	F (flourine)	17.4	2	2 5					
10	Ne (neon)	21.6	2	2 6					
11	Na (sodium)	5.1	2	2 6	1				
12	Mg (magnesium)	7.6	2	2 6	2				
13	Al (aluminum)	6.0	2	2 6	2 1				
14	Si (silicon)	8.1	2	2 6	2 2				
15	P (phosphorus)	10.5	2	2 6	2 3				
16	S (sulfur)	10.4	2	2 6	2 4				
17	Cl (chlorine)	13.0	2	2 6	2 5				
18	Ar (argon)	15.8	2	2 6	2 6				

Z	Element	Ionization energy (eV)	K	L	M	N	O	P	Q
			n : 1	2	3	4	5	6	7
			l : s	s p	s p d	s p d f	s p d f	s p d	s p
19	K (potassium)	4.3	2	2 6	2 6 .	1			
20	Ca (calcium)	6.1	2	2 6	2 6 .	2			
21	Sc (scandium)	6.5	2	2 6	2 6 1	2			
22	Ti (titanium)	6.8	2	2 6	2 6 2	2			
23	V (vanadium)	6.7	2	2 6	2 6 3	2			
24	Cr (chromium)	6.8	2	2 6	2 6 5	1			
25	Mn (manganese)	7.4	2	2 6	2 6 5	2			
26	Fe (iron)	7.9	2	2 6	2 6 6	2			
27	Co (cobalt)	7.9	2	2 6	2 6 7	2			
28	Ni (nickel)	7.6	2	2 6	2 6 8	2			
29	Cu (copper)	7.7	2	2 6	2 6 10	1			
30	Zn (zinc)	9.4	2	2 6	2 6 10	2			
31	Ga (gallium)	6.0	2	2 6	2 6 10	2 1			
32	Ge (germanium)	7.9	2	2 6	2 6 10	2 2			
33	As (arsenic)	9.8	2	2 6	2 6 10	2 3			
34	Se (selenium)	9.8	2	2 6	2 6 10	2 4			
35	Br (bromine)	11.8	2	2 6	2 6 10	2 5			
36	Kr (krypton)	14.0	2	2 6	2 6 10	2 6			
37	Rb (rubidium)	4.2	2	2 6	2 6 10	2 6 . .	1		
38	Sr (strontium)	5.7	2	2 6	2 6 10	2 6 . .	2		
39	Y (yttrium)	6.4	2	2 6	2 6 10	2 6 1 .	2		
40	Zr (zirconium)	6.8	2	2 6	2 6 10	2 6 2 .	2		
41	Nb (niobium)	6.9	2	2 6	2 6 10	2 6 4 .	1		
42	Mo (molybdenum)	7.1	2	2 6	2 6 10	2 6 5 .	1		
43	Tc (technetium)	7.3	2	2 6	2 6 10	2 6 6 .	1		

(Continued)

Z	Element	Ionization energy (eV)	*K* *n*: 1 *l*: *s*	*L* 2 *s p*	*M* 3 *s p d*	*N* 4 *s p d f*	*O* 5 *s p d f*	*P* 6 *s p d*	*Q* 7 *s p*
44	Ru (ruthenium)	7.4	2	2 6	2 6 10	2 6 7 .	1		
45	Rh (rhodium)	7.5	2	2 6	2 6 10	2 6 8 .	1		
46	Pd (palladium)	8.3	2	2 6	2 6 10	2 6 10 .			
47	Ag (silver)	7.6	2	2 6	2 6 10	2 6 10 .	1		
48	Cd (cadmium)	9.0	2	2 6	2 6 10	2 6 10 .	2		
49	In (indium)	5.8	2	2 6	2 6 10	2 6 10 .	2 1		
50	Sn (tin)	7.3	2	2 6	2 6 10	2 6 10 .	2 2		
51	Sb (antimony)	8.6	2	2 6	2 6 10	2 6 10 .	2 3		
52	Te (tellurium)	9.0	2	2 6	2 6 10	2 6 10 .	2 4		
53	I (iodine)	10.5	2	2 6	2 6 10	2 6 10 .	2 5		
54	Xe (xenon)	12.1	2	2 6	2 6 10	2 6 10 .	2 6		
55	Cs (cesium)	3.9	2	2 6	2 6 10	2 6 10 .	2 6 . .	1	
56	Ba (barium)	5.2	2	2 6	2 6 10	2 6 10 .	2 6 . .	2	
57	La (lanthanum)	5.6	2	2 6	2 6 10	2 6 10 .	2 6 1 .	2	
58	Ce (cerium)	5.6	2	2 6	2 6 10	2 6 10 1	2 6 1 .	2	
59	Pr (praseodymium)	5.5	2	2 6	2 6 10	2 6 10 3	2 6 . .	2	
60	Nd (neodymium)	5.5	2	2 6	2 6 10	2 6 10 4	2 6 . .	2	
61	Pm (promethium)	5.5	2	2 6	2 6 10	2 6 10 5	2 6 . .	2	
62	Sm (samarium)	5.6	2	2 6	2 6 10	2 6 10 6	2 6 . .	2	
63	Eu (europium)	5.7	2	2 6	2 6 10	2 6 10 7	2 6 . .	2	
64	Gd (gadolinium)	6.2	2	2 6	2 6 10	2 6 10 7	2 6 1 .	2	
65	Tb (terbium)	6.0	2	2 6	2 6 10	2 6 10 9	2 6 . .	2	
66	Dy (dysprosium)	6.8	2	2 6	2 6 10	2 6 10 10	2 6 . .	2	
67	Ho (holmium)	6.0	2	2 6	2 6 10	2 6 10 11	2 6 . .	2	

Z	Element	Ionization energy (eV)	*K* *n* : 1 *l* : *s*	*L* 2 *s p*	*M* 3 *s p d*	*N* 4 *s p d f*	*O* 5 *s p d f*	*P* 6 *s p d*	*Q* 7 *s p*
68	Er (erbium)	6.1	2	2 6	2 6 10	2 6 10 12	2 6 . .	2	
69	Tm (thulium)	5.8	2	2 6	2 6 10	2 6 10 13	2 6 . .	2	
70	Yb (ytterbium)	6.2	2	2 6	2 6 10	2 6 10 14	2 6 . .	2	
71	Lu (lutetium)	5.1	2	2 6	2 6 10	2 6 10 14	2 6 1 .	2	
72	Hf (hafnium)	7.0	2	2 6	2 6 10	2 6 10 14	2 6 2 .	2	
73	Ta (tantalum)	7.9	2	2 6	2 6 10	2 6 10 14	2 6 3 .	2	
74	W (tungsten)	8.0	2	2 6	2 6 10	2 6 10 14	2 6 4 .	2	
75	Re (rhenium)	7.9	2	2 6	2 6 10	2 6 10 14	2 6 5 .	2	
76	Os (osmium)	8.5	2	2 6	2 6 10	2 6 10 14	2 6 6 .	2	
77	Ir (iridium)	9.0	2	2 6	2 6 10	2 6 10 14	2 6 7 .	2	
78	Pt (platinum)	9.0	2	2 6	2 6 10	2 6 10 14	2 6 9 .	1	
79	Au (gold)	9.2	2	2 6	2 6 10	2 6 10 14	2 6 10 .	1	
80	Hg (mercury)	10.4	2	2 6	2 6 10	2 6 10 14	2 6 10 .	2	
81	Tl (thallium)	6.1	2	2 6	2 6 10	2 6 10 14	2 6 10 .	2 1	
82	Pb (lead)	7.4	2	2 6	2 6 10	2 6 10 14	2 6 10 .	2 2	
83	Bi (bismuth)	7.3	2	2 6	2 6 10	2 6 10 14	2 6 10 .	2 3	
84	Po (polonium)	8.4	2	2 6	2 6 10	2 6 10 14	2 6 10 .	2 4	
85	At (astatine)	9.5	2	2 6	2 6 10	2 6 10 14	2 6 10 .	2 5	
86	Rn (radon)	10.7	2	2 6	2 6 10	2 6 10 14	2 6 10 .	2 6	
87	Fr (francium)	4.0	2	2 6	2 6 10	2 6 10 14	2 6 10 .	2 6 .	1
88	Ra (radium)	5.3	2	2 6	2 6 10	2 6 10 14	2 6 10 .	2 6 .	2
89	Ac (actinium)	6.9	2	2 6	2 6 10	2 6 10 14	2 6 10 .	2 6 1	2
90	Th (thorium)	7.0	2	2 6	2 6 10	2 6 10 14	2 6 10 .	2 6 2	2
91	Pa (protactinium)		2	2 6	2 6 10	2 6 10 14	2 6 10 1	2 6 2	2

(Continued)

Z	Element	Ionization energy (eV)	*K* *n* : 1 *l* : *s*	*L* 2 *s p*	*M* 3 *s p d*	*N* 4 *s p d f*	*O* 5 *s p d f*	*P* 6 *s p d*	*Q* 7 *s p*
92	U (uranium)	6.1	2	2 6	2 6 10	2 6 10 14	2 6 10 3	2 6 1	2
93	Np (neptunium)		2	2 6	2 6 10	2 6 10 14	2 6 10 4	2 6 1	2
94	Pu (plutonium)	5.8	2	2 6	2 6 10	2 6 10 14	2 6 10 6	2 6 .	2
95	Am (americium)	6.0	2	2 6	2 6 10	2 6 10 14	2 6 10 7	2 6 .	2
96	Cm (curium)		2	2 6	2 6 10	2 6 10 14	2 6 10 7	2 6 1	2
97	Bk (berkelium)		2	2 6	2 6 10	2 6 10 14	2 6 10 8	2 6 1	2
98	Cf (californium)		2	2 6	2 6 10	2 6 10 14	2 6 10 10	2 6 .	2
99	Es (einsteinium)		2	2 6	2 6 10	2 6 10 14	2 6 10 11	2 6 .	2
100	Fm (fermium)		2	2 6	2 6 10	2 6 10 14	2 6 10 12	2 6 .	2
101	Md (mendelevium)		2	2 6	2 6 10	2 6 10 14	2 6 10 13	2 6 .	2
102	No (nobelium)		2	2 6	2 6 10	2 6 10 14	2 6 10 14	2 6 .	2
103	Lw (lawrencium)		2	2 6	2 6 10	2 6 10 14	2 6 10 14	2 6 1	2
104	Rf (rutherfordium)		2	2 6	2 6 10	2 6 10 14	2 6 10 14	2 6 2	2
105	Du (dubnium)		2	2 6	2 6 10	2 6 10 14	2 6 10 14	2 6 3	2
106	Sg (seaborgium)		2	2 6	2 6 10	2 6 10 14	2 6 10 14	2 6 4	2
107	Bh (bohrium)		2	2 6	2 6 10	2 6 10 14	2 6 10 14	2 6 5	2
108	Hs (hassium)		2	2 6	2 6 10	2 6 10 14	2 6 10 14	2 6 6	2
109	Mt (meitnerium)		2	2 6	2 6 10	2 6 10 14	2 6 10 14	2 6 7	2
110	Ds (darmstadtium)		2	2 6	2 6 10	2 6 10 14	2 6 10 14	2 6 9	1
111	Rg (roentgenium)		2	2 6	2 6 10	2 6 10 14	2 6 10 14	2 6 10	1
112	Unb (ununbium)		2	2 6	2 6 10	2 6 10 14	2 6 10 14	2 6 10	2
113	Unt (ununtrium)		2	2 6	2 6 10	2 6 10 14	2 6 10 14	2 6 10	2 1
114	Unq (ununquadium)		2	2 6	2 6 10	2 6 10 14	2 6 10 14	2 6 10	2 2
115	Unp (ununpentium)		2	2 6	2 6 10	2 6 10 14	2 6 10 14	2 6 10	2 3

Z	Element	Ionization energy (eV)	*K* *n*: 1 *l*: *s*	*L* 2 *s p*	*M* 3 *s p d*	*N* 4 *s p d f*	*O* 5 *s p d f*	*P* 6 *s p d*	*Q* 7 *s p*
116	Unh (ununhexium)		2	2 6	2 6 10	2 6 10 14	2 6 10 14	2 6 10	2 4
117									
118	Uno (ununoctium)		2	2 6	2 6 10	2 6 10 14	2 6 10 14	2 6 10	2 6

APPENDIX D

Fundamental Physical Constants

This set of fundamental physical constants consists of selected values recommended by CODATA, the Committee on Data for Science and Technology of the International Council of Scientific Unions, resulting from the most recent (2002) compilation and computations. The digits in parentheses are the one-standard-deviation uncertainties in the last digits. (Reference: P. J. Mohr and B. N. Taylor, http://www.physicstoday.org/guide/fundconst.pdf.)

Quantity	Symbol	Value	Units
Universal constants			
Speed of light in vacuum (exact)	c	299,792,458	$\mathrm{m \cdot s^{-1}}$
Permeability of vacuum (magnetic constant) (exact)	μ_0	$4\pi \times 10^{-7} = 12.566370614 \times 10^{-7}$	$\mathrm{N \cdot A^{-2}}$
Permittivity of vacuum (electric constant) (exact)	ϵ_0	$1/\mu_0 c^2 = 8.854187817$	$10^{-12}\ \mathrm{F \cdot m^{-1}}$
Newtonian constant of gravitation	G	6.6742 (10)	$10^{-11}\ \mathrm{m^3 \cdot kg^{-1} \cdot s^{-2}}$
Planck constant	h	6.6260693 (11)	$10^{-34}\ \mathrm{J \cdot s}$
in electron volts, $h/\{e\}$		4.13566743 (35)	$10^{-15}\ \mathrm{eV \cdot s}$
$h/2\pi$	$\hbar$	1.05457168 (18)	$10^{-34}\ \mathrm{J \cdot s}$
in electron volts, $\hbar/\{e\}$		6.58211915 (56)	$10^{-16}\ \mathrm{eV \cdot s}$
Planck mass, $(\hbar c/G)^{1/2}$	m_p	2.17654 (16)	10^{-8} kg
Planck temperature, $(\hbar c^5/G)^{1/2}/k$	T_p	1.41679 (11)	10^{32} K
Planck length, $\hbar/m_p c = (\hbar G/c^3)^{1/2}$	l_p	1.61624 (12)	10^{-35} m
Planck time, $(l_p/c) = (\hbar G/c^5)^{1/2}$	t_p	5.39121 (40)	10^{-44} s
Electromagnetic constants			
Elementary charge	e	1.60217653 (14)	10^{-19} C
	e/h	2.41798940 (21)	$10^{14}\ \mathrm{A \cdot J^{-1}}$
Magnetic flux quantum, $h/2e$	Φ_0	2.06783372 (18)	10^{-15} Wb
Josephson constant $2e/h$	K_J	483597.879 (41)	$10^{9}\ \mathrm{Hz \cdot V^{-1}}$
von Klitzing constant, $h/e^2 = \mu_0 c/2\alpha$	R_K	25812.807449 (86)	Ω
Bohr magneton, $e\hbar/2m_e$	μ_B	927.400949 (80)	$10^{-24}\ \mathrm{J \cdot T^{-1}}$
in eV/T		5.788381804 (39)	$10^{-5}\ \mathrm{eV \cdot T^{-1}}$
Nuclear magneton, $e\hbar/2m_p$	μ_N	5.05078343 (43)	$10^{-27}\ \mathrm{J \cdot T^{-1}}$
in eV/T		3.152451259 (24)	$10^{-8}\ \mathrm{eV \cdot T^{-1}}$
Atomic constants			
Fine-structure constant, $e^2/4\pi\epsilon_0\hbar c$	α	7.297352568 (24)	10^{-3}
inverse fine-structure constant	α^{-1}	137.03599911 (46)	
Rydberg constant, $m_e c\alpha^2/2h$	R_∞	10,973,731.568525 (73)	$\mathrm{m^{-1}}$
in hertz, $R_\infty c$		3.289841960360 (22)	10^{15} Hz
in joules, $R_\infty hc$		2.17987209 (37)	10^{-18} J
in eV, $R_\infty hc/\{e\}$		13.6056923 (12)	eV
Bohr radius	a_0	0.5291772108 (18)	10^{-10} m
Electron			
Mass	m_e	9.1093826 (16)	10^{-31} kg
		5.4857990945 (24)	10^{-4} u
in electron volts, $m_e c^2/\{e\}$		0.510998918 (44)	MeV

Quantity	Symbol	Value	Units
Electron-muon mass ratio	m_e/m_μ	4.83633167 (13)	10^{-3}
Electron-tau mass ratio	m_e/m_τ	2.87564 (47)	10^{-4}
Electron-proton mass ratio	m_e/m_p	5.4461702173 (25)	10^{-4}
Electron-deuteron mass ratio	m_e/m_d	2.7244371095 (13)	10^{-4}
Electron-α-particle mass ratio	m_e/m_α	1.37093355575 (61)	10^{-4}
Specific charge	$-e/m_e$	−1.75882012 (15)	10^{11} C · kg^{-1}
Molar mass	$M(e)$	5.4857990945 (24)	10^{-7} kg · mol^{-1}
Compton wavelength, h/m_ec	λ_C	2.426310238 (16)	10^{-12} m
$\lambda_C/2\pi = \alpha a_0 = \alpha^2/4\pi R_\infty$	$\lambdabar_C$	386.1592678 (26)	10^{-15} m
Classical radius, $\alpha^2 a_0$	r_e	2.817940325 (28)	10^{-15} m
Thomson cross section, $(8\pi/3)r_e^2$	σ_e	0.665245873 (13)	10^{-28} m^2
Magnetic moment	μ_e	−928.476412 (80)	10^{-26} J · T^{-1}
in Bohr magnetons	μ_e/μ_B	−1.0011596521859 (38)	
in nuclear magnetons	μ_e/μ_N	−1838.28197107 (85)	
Magnetic moment anomaly, $\lvert\mu_e\rvert/\mu_B - 1$	a_e	1.1596521859 (38)	10^{-3}
g factor, $-2(1 + a_e)$	g_e	−2.0023193043718 (75)	
Electron-muon magnetic moment ratio	μ_e/μ_μ	206.7669894 (54)	
Electron-proton magnetic moment ratio	μ_e/μ_p	−658.2106862 (66)	
Muon			
Mass	m_μ	1.88353140 (33)	10^{-28} kg
		0.1134289264 (30)	u
in electron volts, $m_\mu c^2/\{e\}$		105.6583692 (94)	MeV
Muon-electron mass ratio	m_μ/m_e	206.7682838 (54)	
Muon-tau mass ratio	$m_\mu/m\tau$	5.94592 (97)	
Molar mass	$M(\mu)$	1.134289264 (34)	10^{-4} kg · mol^{-1}
Magnetic moment	μ_μ	−4.49044799 (40)	10^{-26} J T^{-1}
in Bohr magnetons	μ_μ/μ_B	4.84197085 (15)	10^{-3}
in nuclear magnetons	μ_μ/μ_N	8.89059770 (27)	
Magnetic moment anomaly, $\lvert\mu_\mu\rvert/(e\hbar/2\,m_\mu) - 1$	a_μ	1.16591981 (62)	10^{-3}
g factor, $-2(1 + a_\mu)$	g_μ	−2.0023318396 (12)	
Muon-proton magnetic moment ratio	μ_μ/μ_p	−3.183345118 (89)	
Tau			
Mass	m_τ	3.16777 (52)	10^{-27} kg
		1.90768 (31)	u
in electron volts		1776.99 (29)	MeV
Proton			
Mass	m_p	1.67262171 (29)	10^{-27} kg
		1.00727646688 (13)	u
in electron volts		938.272029 (80)	MeV
Proton-electron mass ratio	m_p/m_e	1836.15267261 (85)	
Proton-muon mass ratio	m_p/m_μ	8.88024333 (23)	
Specific charge	e/m_p	9.57883376 (82)	10^7 C · kg^{-1}
Molar mass	$M(p)$	1.00727646688 (13)	10^{-3} kg · mol^{-1}
Compton wavelength, h/m_pc	$\lambda_{C,p}$	1.3214098555 (88)	10^{-15} m
$\lambda_{C,p}/2\pi$	$\lambdabar_C$	2.103089104 (14)	10^{-16} m

(Continued)

Quantity	Symbol	Value	Units
Magnetic moment	μ_p	1.41060671 (12)	10^{-26} J · T^{-1}
in Bohr magnetons	μ_p/μ_B	1.521032206 (15)	10^{-3}
in nuclear magnetons	μ_p/μ_N	2.792847351 (28)	
Diamagnetic shielding correction for protons			
(H_2O spherical sample, 25°C), $1 - \mu'_p/\mu_p$	σ_{H_2O}	25.687 (15)	10^{-6}
Shielded proton moment			
(H_2O spherical sample, 25°C)	μ'_p	1.41057047 (12)	10^{-26} J · T^{-1}
in Bohr magnetons	μ'_p/μ_B	1.520993132 (16)	10^{-3}
in nuclear magnetons	μ'_p/μ_N	2.792775604 (30)	
Gyromagnetic ratio	γ_p	26,752.2205 (23)	10^4 sec^{-1} · T^{-1}
	$\gamma_p/2\pi$	42.5774813 (37)	MHz · T^{-1}
uncorrected (H_2O, spherical sample, 25°C)	γ'_p	26,751.5333 (23)	10^4 sec^{-1} · T^{-1}
	$\gamma'_p/2\pi$	42.5763875 (37)	MHz · T^{-1}
Neutron			
Mass	m_n	1.67492728 (29)	10^{-27} kg
		1.00866491560 (55)	u
in electron volts, $m_n c^2/\{e\}$		939.565360 (81)	MeV
Neutron-electron mass ratio	m_n/m_e	1838.6836598 (13)	
Neutron-proton mass ratio	m_n/m_p	1.00137841870 (58)	
Molar mass	$M(n)$	1.00866491560 (55)	10^{-3} kg · mol^{-1}
Compton wavelength, $h/m_n c$	$\lambda_{C,n}$	1.3195909067 (88)	10^{-15} m
$\lambda_{C,n}/2\pi$	$\bar{\lambda}_{C,n}$	2.100194157 (14)	10^{-16} m
Magnetic moment	μ_n	−0.96623645 (24)	10^{-26} J · T^{-1}
in Bohr magnetons	μ_n/μ_B	−1.04187563 (25)	10^{-3}
in nuclear magnetons	μ_n/μ_N	−1.91304273 (45)	
Neutron-electron magnetic moment ratio	μ_n/μ_e	1.04066882 (25)	10^{-3}
Neutron-proton magnetic moment ratio	μ_n/μ_p	−0.68497934 (16)	
Deuteron			
Mass	m_d	3.34358335 (57)	10^{-27} kg
		2.01355321270 (35)	u
in electron volts, $m_d c^2/\{e\}$		1875.61282 (16)	MeV
Deuteron-electron mass ratio	m_d/m_e	3670.4829652 (18)	
Deuteron-proton mass ratio	m_d/m_p	1.99900750082 (41)	
Molar mass	$M(d)$	2.01355321270 (35)	10^{-3} kg · mol^{-1}
Magnetic moment	μ_d	0.433073482 (38)	10^{-26} J · T^{-1}
in Bohr magnetons	μ_d/μ_B	0.4669754567 (50)	10^{-3}
in nuclear magnetons	μ_d/μ_N	0.8574382329 (92)	
Deuteron-electron magnetic moment ratio	μ_d/μ_e	−0.4664345548 (50)	10^{-3}
Deuteron-proton magnetic moment ratio	μ_d/μ_p	0.3070122084 (45)	
Alpha particle			
Mass	m_α	6.6446565 (11)	10^{-27} kg
in electron volts		3727.37917 (32)	MeV
Physiochemical constants			
Avogadro constant	N_A, L	6.0221415 (10)	10^{23} mol^{-1}
Atomic mass constant, $m(C^{12})/12$	m_u	1.66053886 (28)	10^{-27} kg
in electron volts, $m_u c^2/\{e\}$		931.494043 (80)	MeV

Quantity	Symbol	Value	Units
Faraday constant	F	96,485.3383 (83)	$C \cdot mol^{-1}$
Molar Planck constant	$N_A h$	3.990312716 (27)	$10^{-10}\ J \cdot s \cdot mol^{-1}$
	$N_A hc$	0.11962656572 (80)	$J \cdot m \cdot mol^{-1}$
Molar gas constant	R	8.314472 (15)	$J \cdot mol^{-1} \cdot K^{-1}$
Boltzmann constant, R/N_A	k	1.3806505 (24)	$10^{-23}\ J \cdot K^{-1}$
in electron volts, $k/\{e\}$		8.617343 (15)	$10^{-5}\ eV \cdot K^{-1}$
in hertz, k/h		2.0836644 (36)	$10^{10}\ Hz \cdot K^{-1}$
in wavenumbers, k/hc		69.50356 (12)	$m^{-1}\ K^{-1}$
Molar volume (ideal gas), RT/p (at 273.15 K, 101 325 Pa)	V_m	22.413996 (39)	$10^{-3}\ m^{-3} \cdot mol^{-1}$
Loschmidt constant, N_A/V_m	n_0	2.6867773 (47)	$10^{25}\ m^{-3}$
Stefan-Boltzmann constant, $(\pi^2/60)k^4/h^3c^2$	σ	5.670400 (40)	$10^{-8}\ W \cdot m^{-2} \cdot K^{-4}$
First radiation constant, $2\pi hc^2$	c_1	3.74177138 (64)	$10^{-16}\ W \cdot m^2$
Second radiation constant, hc/k	c_2	1.4387752 (25)	$10^{-2}\ m \cdot K$
Wien displacement law constant, $\lambda_{max} T = c_2/4.96511423\ldots$	b	2.8977686 (51)	$10^{-3}\ m \cdot K$
Conversion factors and units			
Electron volt, $(e/C)J = \{e\}J$	eV	1.60217653 (14)	$10^{-19}\ J$
Atomic mass unit (unified), $m_u = m(C^{12})/12$	u	1.66053886 (28)	$10^{-27}\ kg$
Standard atmosphere	atm	101,325	Pa
Standard acceleration of gravity	g_n	9.80665	$m \cdot s^{-2}$

APPENDIX E

Conversion Factors

Conversion factors are written as equations for simplicity; relations marked with an asterisk are exact.

Length

- 1 km = 0.6215 mi
- 1 mi = 1.609 km
- 1 m = 1.0936 yd = 3.281 ft = 39.37 in
- *1 in = 254 cm
- *1 ft = 12 in = 30.48 cm
- *1 yd = 3 ft = 91.44 cm
- 1 light-year = 1 $c \cdot$ y = 9.467×10^{15} m
- *1 Å = 0.1 nm

Area

- *1 $m^2 = 10^4\ cm^2$
- 1 $km^2 = 0.3861\ mi^2$ = 247.1 acres
- 1 hectare = $10^4\ m^2$ = 2.471 acres
- *1 $in^2 = 6.4516\ cm^2$
- 1 $ft^2 = 9.29 \times 10^{-2}\ m^2$
- 1 $m^2 = 10.76\ ft^2$
- *1 acre = 43,560 ft^2
- 1 mi^2 = 640 acres = 2.590 km^2

Volume

- *1 $m^3 = 10^6\ cm^3$
- *1 L = 1000 $cm^3 = 10^{-3}\ m^3$
- 1 gal = 3.786 L
- 1 gal = 4 qt = 8 pt = 128 oz = 231 in^3
- 1 $in^3 = 16.39\ cm^3$
- 1 $ft^3 = 1728\ in^3$ = 28.32 L = $2.832 \times 10^4\ cm^3$

Time

- *1 h = 60 min = 3.6 ks
- *1 d = 24 h = 1440 min = 86.4 ks
- 1 y = 365.24 d = 31.56 Ms

Speed

- 1 km/h = 0.2778 m/s = 0.6215 m/h
- 1 mi/h = 0.4470 m/s = 1.609 km/h
- 1 mi/h = 1.467 ft/s

Angle and angular speed

- *π rad = 180°
- 1 rad = 57.30°
- 1° = 1.745×10^{-2} rad
- 1 rev/min = 0.1047 rad/s
- 1 rad/s = 9.549 rev/min

Mass

- *1 kg = 1000 g
- *1 metric ton = 1000 kg = 1 Mg
- 1 u = 1.6606×10^{-27} kg
- 1 kg = 6.022×10^{26} u
- 1 slug = 14.59 kg
- 1 kg = 6.852×10^{-2} slug
- 1 u = 931.50 MeV/c^2

Density

- *1 g/cm^3 = 1000 kg/m^3 = 1 kg/L
- (1 g/cm^3)g = 62.4 lb/ft^3

Force

- 1 N = 0.2248 lb = 10^5 dyn
- 1 lb = 4.4482 N
- (1 kg)g = 2.2046 lb

Pressure

- *1 Pa = 1 N/m^2
- *1 atm = 101.325 kPa = 1.01325 bars
- 1 atm = 14.7 lb/in^2 = 760 mmHg
  = 29.9 inHg = 33.8 ftH_2O
- 1 lb/in^2 = 6.895 kPa
- 1 torr = 1 mmHg = 133.32 Pa
- 1 bar = 100 kPa

Energy

- *1 kW $\cdot$ h = 3.6 MJ
- *1 cal = 4.1840 J
- 1 ft $\cdot$ lb = 1.356 J = 1.286×10^{-3} Btu
- *1 L $\cdot$ atm = 101.325 J
- 1 L $\cdot$ atm = 24.217 cal
- 1 Btu = 778 ft $\cdot$ lb = 252 cal = 1054.35 J
- 1 eV = 1.602×10^{-19} J
- 1 u $\cdot\, c^2$ = 931.50 MeV
- *1 erg = 10^{-7} J

Power

- 1 horsepower = 550 ft $\cdot$ lb/s = 745.7 W
- 1 Btu/min = 17.58 W
- 1 W = 1.341×10^{-3} horsepower
  = 0.7376 ft $\cdot$ lb/s
- 1 W = 1 J/s

Magnetic field

- *1 G = 10^{-4} T
- *1 T = 10^4 G

Thermal conductivity

- 1 W/m $\cdot$ K = 6.938 Btu $\cdot$ in/h $\cdot$ ft^2 $\cdot$ F°
- 1 Btu $\cdot$ in/h $\cdot$ ft^2 $\cdot$ F° = 0.1441 W/m $\cdot$ K

APPENDIX F

Nobel Laureates in Physics

Listed are the names and a brief quotation from the award citation for all Nobel laureates in physics. Included, too, are a few Nobel laureates in chemistry whose work was very closely related to physics, this latter group with a (C) following their names. (The Royal Swedish Academy of Sciences, which awards the prizes, has generally considered the discovery of new elements to be chemistry rather than physics.)

Year	Nobel laureate		Citation for
1901	Wilhelm Konrad Roentgen	1845–1923	discovery of X rays
1902	Hendrik Antoon Lorentz Pieter Zeeman	1853–1928 1865–1943	their researches into the influence of magnetism upon radiation phenomena
1903	Antoine Henri Bequerel Pierre Curie Marie Sklowdowska-Curie	1852–1908 1859–1906 1867–1934	his discovery of spontaneous radioactivity their joint researches on the radiation phenomena discovered by Henri Bequerel
1904	Lord Rayleigh (John William Strutt) Sir William Ramsay (C)	1842–1919 1851–1939	investigations of the densities of the most important gases and his discovery of argon his discovery of the inert gaseous elements in air and his determination of their place in the periodic system
1905	Philipp Eduard Anton von Lenard	1862–1947	his work on cathode rays
1906	Joseph John Thomson	1856–1940	his theoretical and experimental investigations on the conduction of electricity by gases
1907	Albert Abraham Michelson	1852–1931	his optical precision instruments and the spectroscopic and metrological investigations carried out with their aid
1908	Gabriel Lippman Ernest Rutherford (C)	1845–1921 1871–1937	his method of reproducing colors photographically based on the phenomena of interference his investigations into the disintegration of the elements and the chemistry of radioactive substances
1909	Guglielmo Marconi Carl Ferdinand Braun	1874–1937 1850–1918	their contributions to the development of wireless telegraphy
1910	Johannes Diderik van der Waals	1837–1923	his work on the state of equations of gases and liquids
1911	Wilhelm Wien Marie Curie (C)	1864–1928 1867–1934	his discoveries regarding the laws governing the radiation of heat her services to the advancement of chemistry by the discovery of the elements radium and polonium and by the isolation of radium and the study of its nature and compounds
1912	Nils Gustaf Dalén	1869–1937	his invention of automatic regulators for use in conjunction with gas accumulators for illuminating lighthouses and buoys

(*Continued*)

Year	Nobel laureate		Citation for
1913	Heike Kamerlingh Onnes	1853–1926	his investigations of the properties of matter at low temperatures, which led, *inter alia,* to the production of liquid helium
1914	Max von Laue	1879–1960	his discovery of the diffraction of X rays by crystals
1917	Charles Glover Barkla	1877–1944	his discovery of the characteristic X rays of the elements
1918	Max Planck	1858–1947	his discovery of energy quanta
1919	Johannes Stark	1874–1957	his discovery of the Doppler effect in canal rays and of the splitting of spectral lines in electric fields
1920	Charles-Édouard Guillaume	1861–1938	the service he has rendered to precise measurement in physics by his discovery of anomalies in nickel steel alloys
1921	Albert Einstein	1879–1955	his services to theoretical physics, and especially for his discovery of the law of the photoelectric effect
	Frederick Soddy (C)	1877–1956	his contributions to our knowledge of the chemistry of radioactive substances, and his investigations into the origin and nature of isotopes
1922	Neils Bohr	1885–1962	his investigation of the structure of atoms and the radiation emanating from them
	Francis W. Aston (C)	1877–1945	his discovery, by means of his mass spectrograph, of isotopes in a large number of nonradioactive elements, and for his enunciation of the whole-number rule
1923	Robert Andrews Millikan	1868–1953	his work on the elementary charge of electricity and on the photoelectric effect
1924	Karl Manne Georg Siegbahn	1886–1978	his discoveries and researches in the field of X-ray spectroscopy
1925	James Franck Gustav Hertz	1882–1964 1887–1975	their discovery of the laws governing the impact of an electron upon an atom
1926	Jean-Baptiste Perrin	1870–1942	his work on the discontinuous structure of matter, and especially for his discovery of sedimentation equilibrium
1927	Arthur Holly Compton	1892–1962	his discovery of the effect named after him
	Charles Thomson Rees Wilson	1869–1959	his method of making the paths of electrically charged particles visible by condensation of vapor
1928	Owen Willans Richardson	1879–1959	his work on the thermionic phenomenon, and especially for the discovery of the law named after him
1929	Prince Louis-Victor de Broglie	1892–1987	his discovery of the wave nature of electrons
1931	Werner Heisenberg	1901–1976	the creation of quantum mechanics, the application of which has, *inter alia*, led to the discovery of the allotropic forms of hydrogen
1933	Erwin Schrödinger Paul Adrien Maurice Dirac	1887–1961 1902–1984	their discovery of new productive forms of atomic theory

Year	Nobel laureate		Citation for
1934	Harold C. Urey (C)	1893–1991	his discovery of heavy hydrogen
1936	Victor Franz Hess Carl David Anderson Peter Debye (C)	1883–1964 1905–1991 1884–1966	his discovery of cosmic radiation his discovery of the positron his contributions to our knowledge of molecular structure through his investigations on dipole moments and on the diffraction of X rays and electrons in gases
1937	Clinton Joseph Davisson George Paget Thomson	1881–1958 1892–1975	their experimental discovery of the diffraction of electrons by crystals
1938	Enrico Fermi	1901–1954	his demonstrations of the existence of new radioactive elements produced by neutron irradiation, and for his related discovery of nuclear reactions brought about by slow neutrons
1939	Ernest Orlando Lawrence	1901–1958	the invention and development of the cyclotron and for results obtained with it, especially with regard to artificial radioactive elements
1943	Otto Stern	1888–1969	his contributions to the development of the molecular ray method and his discovery of the magnetic moment of the proton
1944	Isidor Issac Rabi Otto Hahn (C)	1898–1988 1879–1968	his resonance method for recording the magnetic properties of atomic nuclei his discovery of the fission of heavy nuclei
1945	Wolfgang Pauli	1900–1958	his discovery of the exclusion principle, also called the Pauli principle
1946	Percy Williams Bridgman	1882–1961	the invention of an apparatus to produce extremely high pressures and for the discoveries he made in the field of high pressure physics
1947	Sir Edward Victor Appleton	1892–1965	his investigations of the physics of the upper atmosphere, especially for the discovery of the Appleton layer
1948	Patrick Maynard Stuart Blackett	1897–1974	his development of the Wilson cloud chamber method and his discoveries therewith in nuclear physics and cosmic radiation
1949	Hideki Yukawa	1907–1981	his prediction of the existence of mesons on the basis of theoretical work on nuclear forces
1950	Cecil Frank Powell	1903–1969	his development of the photographic method of studying nuclear processes and his discoveries regarding mesons made with this method
1951	Sir John Douglas Cockcroft Ernest Thomas Sinton Walton Edwin M. McMillan (C) Glenn T. Seaborg (C)	1897–1967 1903–1995 1907–1991 1912–1999	their pioneer work on the transmutation of atomic nuclei by artificially accelerated atomic particles their discoveries in the chemistry of the transuranium elements
1952	Felix Bloch Edward Mills Purcell	1905–1983 1912–1997	the development of new methods for nuclear magnetic precision measurements and discoveries in connection therewith

(Continued)

Year	Nobel laureate		Citation for
1953	Frits Zernike	1888–1966	his demonstration of the phase contrast method, especially for his invention of the phase contrast microscope
1954	Max Born	1882–1970	his fundamental research in quantum mechanics, especially his statistical interpretation of the wave function
	Walter Bothe	1891–1957	the coincidence method and his discoveries made therewith
1955	Willis Eugene Lamb Jr.	b. 1913	his discoveries concerning the fine structure of the hydrogen spectrum
	Polykarp Kusch	1911–1993	his precision determination of the magnetic moment of the electron
1956	William Shockley	1910–1989	their investigations on semiconductors and their discovery of the transistor effect
	John Bardeen	1908–1991	
	Walter Houser Brattain	1902–1987	
1957	Chen Ning Yang	b. 1922	their penetrating investigation of the parity laws, which led to important discoveries regarding elementary particles
	Tsung Dao Lee	b. 1926	
1958	Pavel Alekseyevich Cherenkov	1904–1990	their discovery and interpretation of the Cherenkov effect
	Ilya Mikhaylovich Frank	1908–1990	
	Igor Yevgenyevich Tamm	1895–1971	
1959	Emilio Gino Segrè	1905–1989	their discovery of the antiproton
	Owen Chamberlain	1920–2006	
1960	Donald Arthur Glaser	b. 1926	the invention of the bubble chamber
	Willard F. Libby (C)	1908–1980	his method to use ^{14}C for age determination in several branches of science
1961	Robert Hofstadter	1915–1990	his pioneering studies of electron scattering in atomic nuclei and for his discoveries concerning the structure of the nucleon achieved thereby
	Rudolf Ludwig Mössbauer	b. 1929	his researches concerning the resonance absorption of γ rays his discovery in this connection of the effect that bears his name
1962	Lev Davidovich Landau	1908–1968	his pioneering theories of condensed matter, especially liquid helium
1963	Eugene Paul Wigner	1902–1995	his contributions to the theory of the atomic nucleus and the elementary particles, particularly through the discovery and application of fundamental symmetry principles
	Maria Goeppert Mayer	1906–1972	their discoveries concerning nuclear shell structure
	J. Hans D. Jensen	1907–1973	
1964	Charles H. Townes	b. 1915	fundamental work in the field of quantum electronics, which has led to the construction of oscillators and amplifiers based on the maser-laser principle
	Nikolai G. Basov	1922–2001	
	Alexander M. Prokhorov	1916–2002	
1965	Shin'ichiro Tomonaga	1906–1979	their fundamental work in quantum electrodynamics, with profound consequences for the physics of elementary particles
	Julian Schwinger	1918–1994	
	Richard P. Feynman	1918–1988	

Year	Nobel laureate		Citation for
1966	Alfred Kastler	1902–1984	the discovery and development of optical methods for studying Hertzian resonance in atoms
1967	Hans Albrecht Bethe	1906–2005	his contributions to the theory of nuclear reactions, especially his discoveries concerning the energy production in stars
1968	Luis W. Alvarez	1911–1988	his decisive contributions to elementary particle physics, in particular the discovery of a large number of resonance states made possible through his development of the techniques of using the hydrogen bubble chamber and data analysis
1969	Murray Gell-Mann	b. 1929	his contributions and discoveries concerning the classification of elementary particles and their interactions
1970	Hannes Alfvén	1908–1995	fundamental work and discoveries in magnetohydrodynamics with fruitful applications in different parts of plasma physics
	Louis-Eugène-Félix Néel	1904–2000	fundamental work and discoveries concerning antiferromagnetism and ferrimagnetism, which have led to important applications in solid-state physics
1971	Dennis Gabor	1900–1979	his invention and development of the holographic method
1972	John Bardeen Leon N. Cooper J. Robert Schrieffer	1908–1991 b. 1930 b. 1931	their theory of superconductivity, usually called the BCS theory
1973	Leo Esaki Ivar Giaever	b. 1925 b. 1929	their experimental discoveries of tunneling phenomena in semiconductors and superconductors, respectively
	Brian D. Josephson	b. 1940	his theoretical predictions of the properties of a supercurrent through a tunnel barrier, in particular those phenomena which are generally known as Josephson effects
1974	Antony Hewish	b. 1924	the discovery of pulsars
	Sir Martin Ryle	1918–1984	his observations and inventions in radio astronomy
1975	Aage Bohr Ben R. Mottleson L. James Rainwater	b. 1922 b. 1926 1917–1986	the discovery of the connection between collective motion and particle motion in atomic nuclei and for the theory of the structure of the atomic nucleus based on this connection
1976	Burton Richter Samuel Chao Chung Ting	b. 1931 b. 1936	their pioneering work in the discovery of a heavy elementary particle of a new kind
1977	Philip Warren Anderson Nevill Francis Mott John Hasbrouck Van Vleck	b. 1923 1905–1996 1899–1980	their fundamental theoretical investigations of the electronic structure of magnetic and disordered systems
1978	Pyotr L. Kapitza	1894–1984	his basic inventions and discoveries in the area of low-temperature physics
	Arno A. Penzias Robert Woodrow Wilson	b. 1933 b. 1936	their discovery of cosmic microwave background radiation

(*Continued*)

Year	Nobel laureate		Citation for
1979	Sheldon Lee Glashow Abdus Salam Steven Weinberg	b. 1932 1926–1996 b. 1933	their contributions to the theory of the unified weak and electromagnetic interaction between elementary particles, including, *inter alia*, the prediction of the weak neutral current
1980	James W. Cronin Val L. Fitch	b. 1931 b. 1923	the discovery of violations of fundamental symmetry principles in the decay of neutral K-mesons
1981	Nicolaas Bloembergen Arthur L. Schawlow	b. 1920 1921–1999	their contributions to the development of laser spectroscopy
	Kai M. Siegbahn	b. 1918	his contribution to the development of high-resolution electron spectroscopy
1982	Kenneth G. Wilson	b. 1936	his theory for critical phenomena in connection with phase transitions
1983	Subrahmanyan Chandrasekhar	1910–1995	his theoretical studies of the physical processes of importance to the structure and evolution of the stars
	William A. Fowler	1911–1995	his theoretical and experimental studies of the nuclear reactions of importance in the formation of the chemical elements in the universe
1984	Carlo Rubbia Simon van der Meer	b. 1934 b. 1925	their decisive contributions to the large project, which led to the discovery of the field particles W and Z, communicators of the weak interaction
1985	Klaus von Klitzing	b. 1943	the discovery of the quantized Hall effect
1986	Ernst Ruska	1906–1988	his fundamental work in electron optics and for the design of the first electron microscope
	Gerd Binnig Heinrich Rohrer	b. 1947 b. 1933	their design of the scanning tunneling microscope
1987	J. Georg Bednorz Karl Alex Müller	b. 1950 b. 1927	their important breakthrough in the discovery of superconductivity in ceramic materials
1988	Leon M. Lederman Melvin Schwartz Jack Steinberger	b. 1922 1932–2006 b. 1921	the neutrino beam method and the demonstration of the doublet structure of the leptons through the discovery of the muon neutrino
1989	Hans G. Dehmelt Wolfgang Paul	b. 1922 1913–1993	their development of the ion trap technique
	Norman F. Ramsey	b. 1915	the invention of the separated oscillatory fields method and its use in the hydrogen maser and other atomic clocks
1990	Jerome I. Friedman Henry W. Kendall Richard E. Taylor	b. 1930 1926–1999 b. 1929	their pioneering investigations concerning deep inelastic scattering of electrons on protons and bound neutrons which have been of essential importance for the development of the quark model in particle physics

Year	Nobel laureate		Citation for
1991	Pierre-Gilles de Gennes	1932–2007	his discovering that methods developed for studying ordered phenomena in simple systems can be generalized to more complex forms of matter, in particular, to liquid crystals and polymers
1992	Georges Charpak	b. 1924	his invention and development of particle detectors, particularly multi-wire proportional counters
1993	Joseph H. Taylor, Jr. Russell A. Hulse	b. 1941 b. 1950	their discovery of rare binary pulsars
1994	Bertram N. Brockhouse Clifford G. Shull	1918–2003 1915–2001	their pioneering contributions to the development of neutron scattering techniques for studies of condensed matter
1995	Martin Perl Frederick Reines	b. 1927 1918–1998	for his discovery of the tau lepton for his discovery of the neutrino
1996	David Lee Douglas Osheroff Robert Richardson	b. 1931 b. 1945 b. 1937	for their discovery of the superfluid phase of ^{3}He
1997	Steven Chu Claude Cohen-Tannoudji William Phillips	b. 1948 b. 1933 b. 1948	for their development of techniques to chill atoms to millionths of a kelvin above absolute zero and to trap them with laser light
1998	Robert B. Laughlin Horst L. Störmer Daniel C. Tsui	b. 1950 b. 1949 b. 1939	for their discovery of a new form of quantum fluid with fractiionally charged excitations
1999	Gerardus ‘t Hooft Martinus J. G. Veltman	b. 1946 b. 1931	for elucidating the quantum structure of electroweak interactions in physics
2000	Zhores I. Alferov Herbert Kroemer Jack S. Kilby	b. 1930 b. 1928 1923–2005	for basic work on information technology for his part in the invention of the integrated circuit
2001	Eric A. Cornell Wolfgang Ketterle Carl E. Weiman	b. 1961 b. 1957 b. 1951	for the achievement of Bose-Einstein condensation in dilute gases of alkali atoms and early fundamental studies of the properties of the condensates
2002	Raymond Davis, Jr. Masatoshi Koshiba Riccardo Giacconi	1914–2006 b. 1926 b. 1931	their pioneering contributions to astrophysics, in particular the detection of cosmic neutrinos his pioneering contributions to astrophysics, which have led to the discovery of cosmic x-ray sources
2003	Alexei A. Abrikosov Vitaly L. Ginzburg Anthony J. Leggett	b. 1928 b. 1916 b. 1938	for pioneering contributions to the theory of superconductors and superfluids

(*Continued*)

Year	Nobel laureate		Citation for
2004	David J. Gross H. David Politzer Frank Wilczek	b. 1941 b. 1949 b. 1951	for the discovery of asymptotic freedom in the theory of the strong interaction
2005	Roy J. Glauber John L. Hall Theodor W. Hänsch	b. 1925 b. 1934 b. 1941	for his contribution to the quantum theory of optical coherence for their contributions to the development of laser-based precision spectroscopy, including the optical frequency combo technique
2006	John C. Mather George F. Smoot	b. 1946 b. 1945	for their discovery of the blackbody form and anisotropy of the cosmic microwave background radiation

Answers

These results are usually rounded to three significant figures. Differences in the third significant figure may result from rounding and are not important. When the solution is a diagram, graph, derivation, or proof, reference is made to the *Students Solution Manual* (*SSM*) where the solution appears.

Chapter 1

1-1. (a) 4.4×10^8 m/s (b) No, since the droid is moving faster than light speed relative to Hoth.

1-5. (a) At $t = 2$ s, a bright circle reflected from great circle perpendicular to the motion. (b) At $t = 2$ s, the entire interior lights up.

1-9. $\Delta t \approx 4.63 \times 10^{-13}$ s

1-13. (a) 3.76×10^{-5} s (b) 2.0×10^{-5} s

1-17. (a) See *Students Solution Manual (SSM)* (b) When 10 s have passed on the rocket's clock, only 6 s have passed on the lab clock.

1-21. $0.14c$

1-25. $0.527c$

1-29. (a) In S': $V' = 16$ m^3; in S: $V = 12.2$ m^3 (b) See *SSM*

1-33. 657.0 nm, 662.9 nm, 725.6 nm

1-37. 3.0 m

1-41. 9.6 ms

1-45. (a) See *SSM* (b) $v = 1.44 \times 10^8$ m/s (c) 4.39 μs (d) 4.39 μs

1-49. (a) $v = 0.5c$ in the $-x$ direction (b) 0.58 y (c) 0.866 $c \cdot$ y (d) spacelike (e) 0.866 $c \cdot$ y

1-53. $\theta' = 0.494\, v_y/c$

1-57. (a) 120 min (b) 240 min (c) identical

1-61. (a) $A \rightarrow B$: $T/2 + 2vL/(c^2 - v^2)$; $B \rightarrow A$: $T/2 + 2vL/(c^2 - v^2)$ (b) $4vL/(c^2 - v^2)$

Chapter 2

2-1. See *SSM*

2-5. 1.1×10^{-16} kg, mass increases

2-9. (a) $0.99998898c$ (b) 3.94×10^4 GeV/c (c) 3.31×10^9 GeV; -3.31×10^9 GeV/c

2-13. (a) 3.5×10^{-7} (b) 0.0079

2-17. 6.26 MeV

2-21. 280 MeV

2-25. See *SSM*

2-29. $m = 1673$ MeV/c^2, $u = 0.286c$

2-33. (c) is correct.

2-37. 8.62 ms

2-41. (a) 1.73×10^5 m/s (b) 1.5×10^5 m/s (c) 155 kg

2-45. See *SSM*

2-49. (a) $v = E/Mc$ (b) $\Delta x = EL/Mc^2$ (c) $m \approx E/c^2$

2-53. (a) See *SSM* (b) See *SSM*

Chapter 3

3-1. proton 6.5×10^{-2} m; electron 3.6×10^{-5} m; deuteron 0.13 m; H_2 0.13 m; helium 0.26 m

3-5. (a) 2.2 mm (b) 9.1×10^9 Hz, 1.1×10^{-10} s

3-9. See *SSM*

3-13. 5.67×10^{-8} W/m^2 K^4

3-17. 16 R_1

3-21. 278.3 K (5.3 °C)

3-25. (a) 255 nm (b) 1.4×10^{-4}

3-29. (a) 1.03×10^{15} Hz (b) ultraviolet

3-33. 4.14×10^{-3} nm; 5.8%

3-37. 0.243 nm

3-41. (a) electron 0.00243 nm; proton 1.32 fm (b) electron 0.510 MeV; proton 939 MeV

3-45. (a) 2.08 eV (b) 4.95×10^{14} Hz (c) 4.19×10^{-15} eV/Hz

3-49. See *SSM*

3-53. See *SSM*

3-57. (a) 0.0309 nm, 0.1259 nm (b) 9.90 keV

Chapter 4

4-1. Lyman 91.16 nm; Balmer 364.6 nm; Paschen 820.4 nm

4-5. 4103 nm

4-9. 45.5 fm; 29.5 fm; 19.0 fm

4-13. (a) 1.91 nm (b) 0.95 nm

4-17. 8.22×10^{14} Hz, 8.22×10^6 revolutions

4-21. See *SSM*

4-25. (a) 19.0 μm (b) 3.65×10^3 m/s

4-29. 680 fm

4-33. 1.90×10^{-8} Hz$^{-1/2}$

4-37. 10.2 V

4-41. (a) 1.054×10^{-3} A (b) 9.27×10^{-24} A · m^2

4-45. (a) Lyman α: $n = 6 \rightarrow n = 3$ Lyman β: $n = 9 \rightarrow n = 3$ (b) $\Delta\lambda = 0.056$ nm

4-49. (a) $b = R\cos(\theta/2)$ (b) $I_0 R^2 \cos^2(\theta/2)$ (c) πR^2 (d) See *SSM*

4-53. For $n = 1$: $v = 0.0075cZ^{1/2}$; $E = -14.4Z$ eV

4-57. 10; 1,042

Chapter 5

5-1. (a) 2.1×10^{-23} m (b) 2.1×10^{-21} m/y
5-5. 0.0276 nm
5-9. (a) 0.445 fm (b) 6.18×10^{-3} fm
5-13. $\lambda = 0.523$ nm; $E_k = 3.0 \times 10^{-3}$ eV
5-17. (a) See *SSM* (b) 50 m/s (c) 50 m/s (d) $\Delta x = 5\pi$ m; $\Delta k = 0.4$ m^{-1}
5-21. 3.2×10^{-5} s
5-25. (a) $A^2\,dx$ (b) $0.61A^2\,dx$ (c) $0.14A^2\,dx$ (d) $x = 0$
5-29. 1.99×10^{-21} eV
5-33. (a) 5.3×10^{-10} (b) 1.32×10^{-7} eV
5-37. See *SSM*
5-41. (a) See *SSM* (b) See *SSM*
5-45. (a) 1840 MeV (b) 2.02 fm (c) 1.22 fm (d) 0.76 fm
5-49. (a) 0.243 nm (b) 0.511 MeV (c) 0.511 MeV/c (d) 2.43×10^{-3} nm
5-53. 1.2×10^{-6} eV, 1.2 eV

Chapter 6

6-1. See *SSM*
6-5. See *SSM*
6-9. (a) 0.021 eV (b) 205 MeV
6-13. (a) $\Delta x = 10^{-6}$ m; $\Delta p = 10^{-16}$ kg·m/s (b) 9×10^{11}
6-17. See *SSM*
6-21. 1.21×10^{-7} N
6-25. 0.87 nm
6-29. (a) $L/2$ (b) $0.320L^2$
6-33. $\langle x \rangle = 0$; $\langle x^2 \rangle = \hbar/(2m\omega)$
6-37. (a) See *SSM* (b) $\langle x \rangle = 0$ (c) $\langle x^2 \rangle = 3\hbar/(2m\omega)$ (d) $\langle V(x) \rangle = 3\hbar\omega/4$
6-41. (a) 2.33×10^{-34} J (b) 2.1×10^{28} (c) 0.70 Hz
6-45. (a) 4.3×10^{-6} is the transmitted fraction (b) See *SSM*
6-49. (a) $R = 0.111$; $T = 0.889$ (b) $R = 0.111$; $T = 0.889$
6-53. $\langle E_k \rangle = \hbar^2/(2mL^2)$
6-57. (a) 4.95×10^{-13} (b) 0.197
6-61. (a) $0.39c$ (b) See *SSM* (c) 8.03×10^5 eV (d) 3.76×10^5 eV

Chapter 7

7-1. $11E_0$, $12E_0$, $14E_0$, The 1st, 2nd, 3rd, and 5th excited states are degenerate.
7-5. (a) See *SSM* (b) 1, 1, 4 and 1, 2, 2
7-9. (a) 0, 1, 2 (b) For $\ell = 0$, $m = 0$; for $\ell = 1$, $m = \pm 1, 0$; for $\ell = 2$, $m = \pm 2, \pm 1, 0$
(c) 18
7-13. (a) $2\hbar^2$ (b) $6\hbar^2$ (c) $5\hbar^2$ (d) $n = 3$
7-17. (a) $n = 6$, $\ell = 3$ (b) -0.38 eV (c) 3.65×10^{-34} J·s
(d) $\pm 3\hbar$, $\pm 2\hbar$, $\pm\hbar$, 0
7-21. See *SSM*

7-25. (a) $0.606(1/a_0)^{3/2}/\sqrt{32\pi}$ (b) $0.368(1/a_0)^3/(32\pi)$ (c) $0.368/(8a_0)$

7-29. See *SSM*

7-33. (a) 4 (b) 3

7-37. See *SSM*

7-41. See *SSM*

7-45. Sn: $1s^2 2s^2 2p^6 3s^2 3p^6 3d^{10} 4s^2 4p^6 4d^{10} 5s^2 5p^2$
Nd: $1s^2 2s^2 2p^6 3s^2 3p^6 3d^{10} 4s^2 4p^6 4d^{10} 5s^2 5p^6 4f^4 6s^2$
Yb: $1s^2 2s^2 2p^6 3s^2 3p^6 3d^{10} 4s^2 4p^6 4d^{10} 4f^{14} 5s^2 5p^6 6s^2$

7-49. (a) silicon, Si (b) calcium, Ca

7-53. Similar to H: Li, Rb, Ag, and Fr
Similar to He: Ca, Ti, Cd, Ba, Hg, and Ra

7-57. $D_{5/2} \rightarrow P_{1/2}$ is j-forbidden

7-61. (a) 2.90×10^{-6} eV (b) 7.83×10^{-4} nm (c) 0.638 T

7-65. (a) 1.67×10^6 m/s^2 (b) 1.95 cm

7-69. (a) See *SSM* (b) See *SSM*

7-73. (a) through (e) See *SSM*

Chapter 8

8-1. (a) 1930 m/s (b) 1.01×10^4 K

8-5. (a) 3400 J (b) One mole of any gas has the same translational energy at the same temperature.

8-9. See *SSM*

8-13. $C_v = R$, $C_p = 2R$, and $\gamma = 2$

8-17. (a) n_2/n_1 and n_3/n_1 are both ≈ 0 (b) 19,760 K (c) 0.7%

8-21. See *SSM*

8-25. See *SSM*

8-29. See *SSM*

8-33. See *SSM*

8-37. (a) $f_{FD}(E) = [e^{10(E-E_F)/E_F} + 1]^{-1}$ (b) See *SSM*

8-41. $\langle E_{K(\text{escape})} \rangle = 2kT$

8-45. See *SSM*

Chapter 9

9-1. (a) 23.06 kcal/mol (b) 98.5 kcal/mol (c) 1.08 eV/molecule

9-5. (a) -5.39 eV (b) 4.83 eV (c) 0.46 eV

9-9. For KBr: 0.19 eV For RbCl: 0.23 eV

9-13. 2.63×10^{-29} C · m

9-17. (a) 0.67 nm (b) 55 nm (c) See *SSM*

9-21. 1.78×10^{-4} eV

9-25. (a) 18.6 u (b) 0.280 nm

9-29. 0.04×10^{-5} eV

9-33. about 5.5×10^{31}

9-37. 1.28×10^{16}/s

9-41. (a) 8.47×10^{-5} radians (b) 5.08×10^{-3} W/cm^2

9-45. (a) $E_3 = 1.44 \times 10^{-3}$ eV, $E_2 = 9.61 \times 10^{-4}$ eV, $E_1 = 4.79 \times 10^{-4}$ eV, vibrational states (note equal spacing); See *SSM* (b) 0.215 nm

9-49. 480 N/m

9-53. (a) 0.31 eV (b) 8.9×10^{-14} eV · nm^{20}

9-57. (a) 4.58×10^{-48} kg · m^2 (b) 1.32×10^{14} Hz

Chapter 10

10-1. 4.64

10-5. 4.09 eV/atom

10-9. 4.18

10-13. (a) 5.86×10^{22}/cm^3 (b) 5.90×10^{22}/cm^3

10-17. 1.87 eV

10-21. (a) 34.2 nm (b) 41.4 nm (c) 43.1 nm

10-25. 6.7×10^{-3}

10-29. (a) 0.37 eV (b) 4300 K

10-33. See *SSM*

10-37. (a) 27.8 mV (b) −12.0 mV

10-41. For ^{206}Pb: 7.217 K; for ^{207}Pb: 7.200 K; for ^{208}Pb: 7.183 K

10-45. (a) 0.95 (b) 0.71 (c) 0.32

10-49. (a) See *SSM* (b) *See SSM* (c) 0.0055

10-53. silicon: 3.17 nm; germanium: 8.46 nm

10-57. (a) 1.28×10^{13} Hz (b) 23.4 μm

Chapter 11

11-1. See *SSM*

11-5. See *SSM*

11-9. (a) 6.46 MeV/nucleon (b) 7.47 MeV/nucleon (c) 8.77 MeV/nucleon

11-13. (a) 2.70 fm; 3.53 fm (b) 4.26 fm; 5.57 fm (c) 6.34 fm; 8.30 fm

11-17. (a) 5.21 h (b) 3.11×10^6 atoms

11-21. 33.2 min

11-25. $A = 191$; $B = -72.2$

11-29. 1.00 MeV

11-33. 93 keV

11-37. 789 MeV/c^2

11-41. ^{36}S, ^{53}Mn, ^{82}Ge, ^{88}Sr, ^{94}Ru, ^{131}In, ^{145}Eu

11-45. $^{30}_{14}$Si, $j = 0$; $^{37}_{17}$Cl, $j = 3/2$; $^{55}_{27}$Co, $j = 7/2$; $^{90}_{40}$Zr, $j = 0$; $^{107}_{49}$In, $j = 9/2$

11-49. (a) −4.97 MeV (b) 1.92 MeV

11-53. 224 MeV

11-57. 1.78×10^{14} atoms/s

11-61. (a) 8.78×10^{12} J (b) 145 y

11-65. 1.90×10^9 y

11-69. (a) 10^{13} (b) 0.149 mg (c) 2.15×10^4 y

11-73. See *SSM*

11-77. (a) 5.06×10^{-6} eV (b) 4.71×10^{-2} eV (c) 1.17 cm/s

11-81. (a) ^{141}Ba : 6.24×10^{-15} m; ^{92}Kr : 5.42×10^{-15} m (b) 249 MeV

11-85. 7.03×10^{8} y

11-89. (a) See *SSM* (b) 51.7 MeV (c) 1.43 MeV (c) 96.5 MeV

11-93. (a) See *SSM* (b) See *SSM* (c) See *SSM* (d) See *SSM* (e) See *SSM*

11-97. (a) See *SSM* (b) 8.66×10^{4}

11-101. (a) 137% (b) 0.00498

Chapter 12

12-1. (a) See *SSM* (b) 139.6 MeV (c) 8.88 fm

12-5. (a) 1.711 MeV (b) 78.5 eV (c) 2.16 MeV/c

12-9. (a) weak (b) electromagnetic (c) strong (d) weak

12-13. $m \approx 22$ eV/c^2

12-17. (a) Conservation of energy and lepton number are violated. (b) Conservation of energy is violated. (c) Conservation of linear momentum is violated. (d) No conservation laws are violated. (e) Conservation of lepton number is violated. (f) Conservation of baryon number is violated.

12-21. (a) Conservation of lepton number is violated. (b) Allowed. (c) Allowed. (d) Conservation of baryon number and angular momentum are violated. (e) Allowed.

12-25. See *SSM*

12-29. *uuu*

12-33. −138.3 MeV Energy is not conserved.

12-37. (a) $c\bar{d}$ (b) $\bar{c}d$

12-41. (a) Energy is not conserved. (b) Angular momentum is not conserved. (c) Angular momentum is not conserved.

12-45. (a) The final products are all stable. (b) See *SSM* (c) See *SSM* (d) No. Energy is not conserved.

12-49. (a) No conservation laws are violated. (b) Conservation of energy and baryon number are violated. (c) No conservation laws are violated.

12-53. (a) 1193 MeV (b) 77 MeV/c (c) 2.66 MeV (d) 74.3 MeV/c

Chapter 13

13-1. 25.3 d

13-5. 10.4 eV/c^2

13-9. 17.0 pc

13-13. (a) 9400 y (b) $R_{star} = 1.96R_{\odot}$ using the T_e relation

13-17. (a) 3.27×10^{9} $c \cdot$ y (b) 10%

13-21. 5.5×10^{97} kg/m^3; 1.67×10^{18} kg/m^3; 2.45×10^{4} kg/m^3

13-25. See *SSM*

13-29. (a) 8.33×10^{56} (b) 8.89×10^{44} J (c) 1.7×10^{10} y

13-33. $\approx$ 0.001 "new" H atoms/m$^3 \cdot 10^6$ y; No.

13-37. (a) See *SSM* (b) 1.1×10^{-12} cm^3 (c) $\approx 0.1\%$ $M_{\odot}$

INDEX

boldface indicates a definition
italics indicates a figure
t indicates a table
* indicates a MORE section on the home page: www.whfreeman.com/tiplermodernphysics5e
# indicates a Classical Concept Review section on the home page: www.whfreeman.com/tiplermodernphysics5e

FËUE

The Greek Alphabet

Alpha	A	α	Iota	I	ι	Rho	P	ρ
Beta	B	β	Kappa	K	κ	Sigma	Σ	σ
Gamma	Γ	γ	Lambda	Λ	λ	Tau	T	τ
Delta	Δ	δ	Mu	M	μ	Upsilon	Υ	υ
Epsilon	E	ϵ	Nu	N	ν	Phi	Φ	ϕ
Zeta	Z	ζ	Xi	Ξ	ξ	Chi	X	χ
Eta	H	η	Omicron	O	o	Psi	Ψ	ψ
Theta	Θ	θ	Pi	Π	π	Omega	Ω	ω

Prefixes for Powers of 10

Multiple	**Prefix**	**Abbreviation**
10^{18}	exa	E
10^{15}	peta	P
10^{12}	tera	T
10^{9}	giga	G
10^{6}	mega	M
10^{3}	kilo	k
10^{2}	hecto	h
10^{1}	deka	da
10^{-1}	deci	d
10^{-2}	centi	c
10^{-3}	milli	m
10^{-6}	micro	μ
10^{-9}	nano	n
10^{-12}	pico	p
10^{-15}	femto	f
10^{-18}	atto	a

Mathematical Symbols

$=$	is equal to	Δx	change in x
$\neq$	is not equal to	$\lvert x \rvert$	absolute value of x
$\approx$	is approximately equal to	$n!$	$n(n-1)(n-2)\cdots 1$
$\sim$	is of the order of	Σ	sum
$\propto$	is proportional to	lim	limit
$>$	is greater than	$\Delta t \to 0$	Δt approaches zero
$\geq$	is greater than or equal to	$\frac{dx}{dt}$	derivative of x with respect to t
$\gg$	is much greater than		
$<$	is less than	$\frac{\partial x}{\partial t}$	partial derivative of x with respect to t
$\leq$	is less than or equal to		
$\ll$	is much less than	$\int$	integral

Abbreviations for Units

A	ampere	keV	kilo-electron volts
Å	angstrom (10^{-10} m)	L	liter
atm	atmosphere	m	meter
Btu	British thermal unit	MeV	mega-electron volts
Bq	becquerel	min	minute
C	coulomb	mm	millimeter
°C	degree Celsius	ms	millisecond
cal	calorie	N	newton
Ci	curie	nm	nanometer (10^{-9} m)
cm	centimeter	rev	revolution
eV	electron volt	R	roentgen
°F	degree Fahrenheit	Sv	seivert
fm	femtometer, fermi (10^{-15} m)	s	second
G	gauss	T	tesla
Gy	gray	u	unified mass unit
g	gram	V	volt
H	henry	W	watt
h	hour	Wb	weber
Hz	hertz	y	year
J	joule	μm	micrometer (10^{-6} m)
K	kelvin	μs	microsecond
kg	kilogram	μC	microcoulomb
km	kilometer	Ω	ohm

Some Useful Combinations

$$hc = 1.9864 \times 10^{-25}\ \mathrm{J\cdot m} = 1239.8\ \mathrm{eV\cdot nm}$$

$$\hbar c = 3.1615 \times 10^{-26}\ \mathrm{J\cdot m} = 197.33\ \mathrm{eV\cdot nm}$$

$$\text{Bohr radius } a_0 = \frac{4\pi\boldsymbol{\varepsilon}_0\hbar^2}{m_e e^2} = 5.2918 \times 10^{-11}\ \mathrm{m}$$

$$ke^2 = 1.440\ \mathrm{eV\cdot nm}$$

$$\text{Fine structure constant } \alpha = \frac{e^2}{4\pi\boldsymbol{\varepsilon}_0\hbar c} = 0.0072974 \approx \frac{1}{137}$$

$$kT = 2.5249 \times 10^{-2}\ \mathrm{eV} \approx \tfrac{1}{40}\ \mathrm{eV\ at\ } T = 293\ \mathrm{K}$$

Some Physical Constants

(See Appendix D for a complete list of fundamental constants.)

Avogadro's number	N_A	6.022142×10^{23} particles/mol
Boltzmann's constant	k	1.380650×10^{-23} J/K
Bohr magneton	$m_B = e\hbar$	$9.2740095 \times 10^{-24}$ J/T
Coulomb constant	$k = 1/4\pi\epsilon_0$	$8.987551788 \times 10^{9}\ \mathrm{N \cdot m^2/C^2}$
Compton wavelength	$\lambda_c = h/m_e c$	$2.42631024 \times 10^{-12}$ m
Fundamental charge	e	1.602176×10^{-19} C
Gas constant	$R = N_A k$	8.31447 J/mol·K = 1.987 22 cal/mol·K
		$= 8.20578 \times 10^{-2}$ L·atm/mol·K
Gravitational constant	G	$6.6742 \times 10^{-11}\ \mathrm{N \cdot m^2/kg^2}$
Mass, of electron	m_e	9.109382×10^{-31} kg
		$= 510.9989\ \mathrm{keV}/c^2$
of proton	m_p	1.672622×10^{-27} kg
		$= 938.2722\ \mathrm{MeV}/c^2$
of neutron	m_n	1.674927×10^{-27} kg
		$= 939.5653\ \mathrm{MeV}/c^2$
Permeability of free space	μ_0	$4\pi \times 10^{-7}\ \mathrm{N/A^2}$
Planck's constant	h	6.626069×10^{-34} J·s
		$= 4.135667 \times 10^{-15}$ eV·s
	$\hbar$	1.054572×10^{-34} J·s
		$= 6.582119 \times 10^{-16}$ eV·s
Speed of light	c	2.99792458×10^{8} m/s
Unified mass unit	u	1.660539×10^{-27} kg
		$= 931.49401\ \mathrm{MeV}/c^2$

Some Conversion Factors

1 yr = 3.156×10^{7} s	1 T = 10^{4} G
1 light-year = 9.461×10^{15} m	1 Ci = 3.7×10^{10} Bq
1 cal = 4.186 J	1 barn = $10^{-28}\ \mathrm{m^2}$
1 MeV/c = 5.344×10^{-22} kg·m/s	1 u = 1.66054×10^{-27} kg
1 eV = 1.6022×10^{-19} J	1 parsec = 3.26 light-years
1 kW·h = 3.6 MJ	1 rad = 57.30°

Some Particle Masses and Rest Energies

	kg	**MeV/c^2**	**u**
Electron	9.1094×10^{-31}	0.51100	5.4858×10^{-4}
Muon	1.8835×10^{-28}	105.66	0.11343
Proton	1.6726×10^{-27}	938.27	1.00728
Neutron	1.6749×10^{-27}	939.57	1.00866
Deuteron	3.3436×10^{-27}	1875.61	2.01355
α particle	6.6447×10^{-27}	3727.38	4.00151
W	1.43×10^{-25}	80×10^{3}	85.9
Z°	1.63×10^{-25}	91.2×10^{3}	97.9

Periodic Table

1	2	3	4	5	6	7	8	9	10	11	12	13	14	15	16	17	18
1 **H** Hydrogen 1.007 94(7)																	2 **He** Helium 4.002 602(2)
3 **Li** Lithium 6.941(2)	4 **Be** Beryllium 9.012 182(3)											5 **B** Boron 10.811(7)	6 **C** Carbon 12.0107(8)	7 **N** Nitrogen 14.0067(2)	8 **O** Oxygen 15.9994(3)	9 **F** Fluorine 18.998 4032(5)	10 **Ne** Neon 20.1797(6)
11 **Na** Sodium 22.989 769 28(2)	12 **Mg** Magnesium 24.3050(6)											13 **Al** Aluminum 26.981 538 6(8)	14 **Si** Silicon 28.0855(3)	15 **P** Phosphorus 30.973 762(2)	16 **S** Sulfur 32.065(5)	17 **Cl** Chlorine 35.453(2)	18 **Ar** Argon 39.948(1)
19 **K** Potassium 39.0983(1)	20 **Ca** Calcium 40.078(4)	21 **Sc** Scandium 44.955 912 (6)	22 **Ti** Titanium 47.867(1)	23 **V** Vanadium 50.9415(1)	24 **Cr** Chromium 51.9961(6)	25 **Mn** Manganese 54.938 045(5)	26 **Fe** Iron 55.845(2)	27 **Co** Cobalt 58.933 195(5)	28 **Ni** Nickel 58.6934(2)	29 **Cu** Copper 63.546(3)	30 **Zn** Zinc 65.409(4)	31 **Ga** Gallium 69.723(1)	32 **Ge** Germanium 72.64(1)	33 **As** Arsenic 74.921 60(2)	34 **Se** Selenium 78.96(3)	35 **Br** Bromine 79.904(1)	36 **Kr** Krypton 83.798(2)
37 **Rb** Rubidium 85.4678(3)	38 **Sr** Strontium 87.62(1)	39 **Y** Yttrium 88.905 85(2)	40 **Zr** Zirconium 91.224(2)	41 **Nb** Niobium 92.906 38 (2)	42 **Mo** Molybdenum 95.94(2)	43 **Tc** Technetium [97.9072]	44 **Ru** Ruthenium 101.07(2)	45 **Rh** Rhodium 102.905 50(2)	46 **Pd** Palladium 106.42(1)	47 **Ag** Silver 107.8682(2)	48 **Cd** Cadmium 112.411(8)	49 **In** Indium 114.818(3)	50 **Sn** Tin 118.710(7)	51 **Sb** Antimony 121.760(1)	52 **Te** Tellurium 127.60(3)	53 **I** Iodine 126.904 47(3)	54 **Xe** Xenon 131.293(6)
55 **Cs** Cesium 132.905 451 9 (2)	56 **Ba** Barium 137.327(7)	57-71 Lanthanoids	72 **Hf** Hafnium 178.49(2)	73 **Ta** Tantalum 180.947 88(2)	74 **W** Tungsten 183.84(1)	75 **Re** Rhenium 186.207(1)	76 **Os** Osmium 190.23(3)	77 **Ir** Iridium 192.217(3)	78 **Pt** Platinum 195.084(9)	79 **Au** Gold 196.966 569(4)	80 **Hg** Mercury 200.59(2)	81 **Tl** Thallium 204.3833(2)	82 **Pb** Lead 207.2(1)	83 **Bi** Bismuth 208.980 40(1)	84 **Po** Polonium [208.9824]	85 **At** Astatine [209.9871]	86 **Rn** Radon [222.0176]
87 **Fr** Francium [223]	88 **Ra** Radium [226]	89-103 Actinoids	104 **Rf** Rutherfordium [261]	105 **Db** Dubnium [262]	106 **Sg** Seaborgium [266]	107 **Bh** Bohrium [264]	108 **Hs** Hassium [277]	109 **Mt** Meitnerium [268]	110 **Ds** Darmstadtium [271]	111 **Rg** Roentgenium [272]	112 **UUb** [277]	113 **Uut** [284]	114 **Uuq** [289]	115 **Uup** [288]	116 **Uuh** [292]		118 **Uuo** [294]

57 **La** Lanthanum 138.905 47(7)	58 **Ce** Cerium 140.116(1)	59 **Pr** Praseodymium 140.907 65(2)	60 **Nd** Neodymium 144.242(3)	61 **Pm** Promethium [145]	62 **Sm** Samarium 150.36(2)	63 **Eu** Europium 151.964(1)	64 **Gd** Gadolinium 157.25(3)	65 **Tb** Terbium 158.925 35(2)	66 **Dy** Dysprosium 162.500(1)	67 **Ho** Holmium 164.930 32(2)	68 **Er** Erbium 167.259(3)	69 **Tm** Thulium 168.934 21(2)	70 **Yb** Ytterbium 173.04(3)	71 **Lu** Lutetium 174.967(1)
89 **Ac** Actinium [227]	90 **Th** Thorium 232.038 06(2)	91 **Pa** Protactinium 231.035 88(2)	92 **U** Uranium 238.028 91(3)	93 **Np** Neptunium [237]	94 **Pu** Plutonium [244]	95 **Am** Americium [243]	96 **Cm** Curium [247]	97 **Bk** Berkelium [247]	98 **Cf** Californium [251]	99 **Es** Einsteinium [252]	100 **Fm** Fermium [257]	101 **Md** Mendelevium [258]	102 **No** Nobelium [259]	103 **Lr** Lawrencium [262]

Notes

- Symbols for elements 112 through 118 are temporary placeholders. The corresponding Latin names are, using 115 as an example, Ununpentium, meaning element one, one, five.

4197

Chemistry

SEVENTH EDITION

ZUMDAHL | ZUMDAHL

Chemistry

Seventh Edition

Steven S. Zumdahl
University of Illinois

Susan A. Zumdahl
University of Illinois

Houghton Mifflin Company Boston New York

Executive Editor: Richard Stratton
Developmental Editor: Rebecca Berardy Schwartz
Senior Project Editor: Cathy Labresh Brooks
Editorial Assistant: Susan Miscio
Senior Art & Design Coordinator: Jill Haber
Composition Buyer: Chuck Dutton
Manufacturing Coordinator: Renee Ostrowski
Senior Marketing Manager: Katherine Greig
Marketing Assistant: Naveen Hariprasad

Cover image: Masaaki Kazama/Photonica

Photo credits: Page A39.

Printed in the U.S.A.

Library of Congress Catalog Card Number: 2005929890

Student edition:
ISBN 13: 978-0-618-52844-8
ISBN 10: 0-618-52844-X
Instructor's Annotated Edition:
ISBN 13: 978-0-618-52845-5
ISBN 10: 0-618-52845-8
Advanced Placement edition:
ISBN 13: 978-0-618-71370-7
ISBN 10: 0-618-71370-0

123456789-WEB-09 08 07 06 05

Contents

5 Gases 178

6 Thermochemistry 228

7 Atomic Structure and Periodicity 274

8 Bonding: General Concepts 328


STATFJORD C
BLOKK 33/9

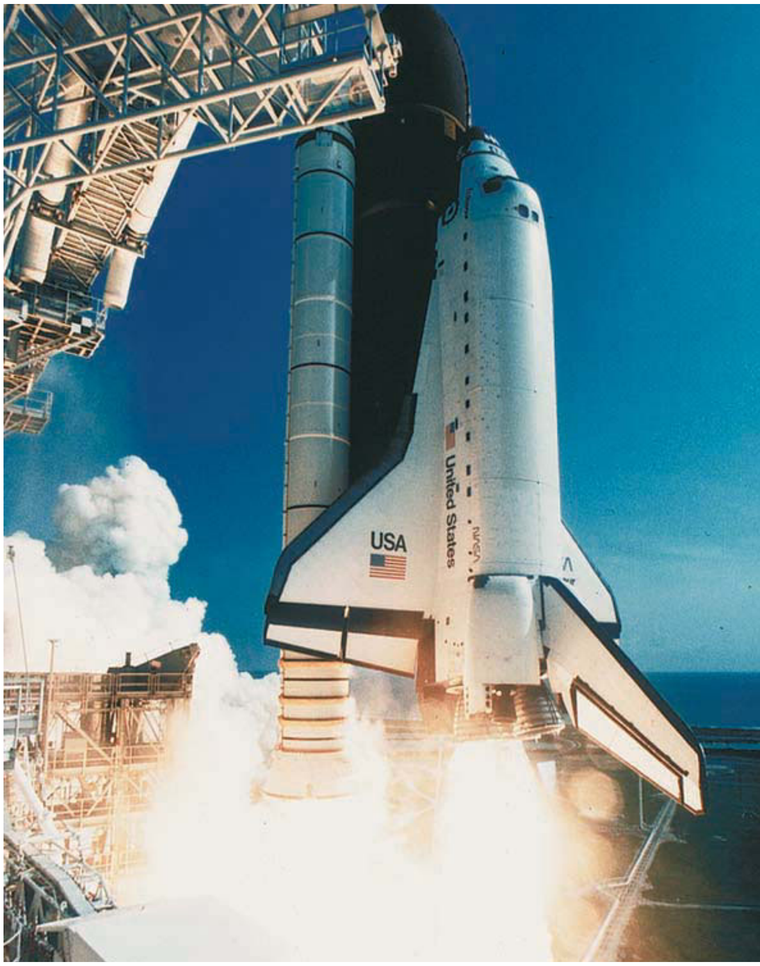
USA
United States

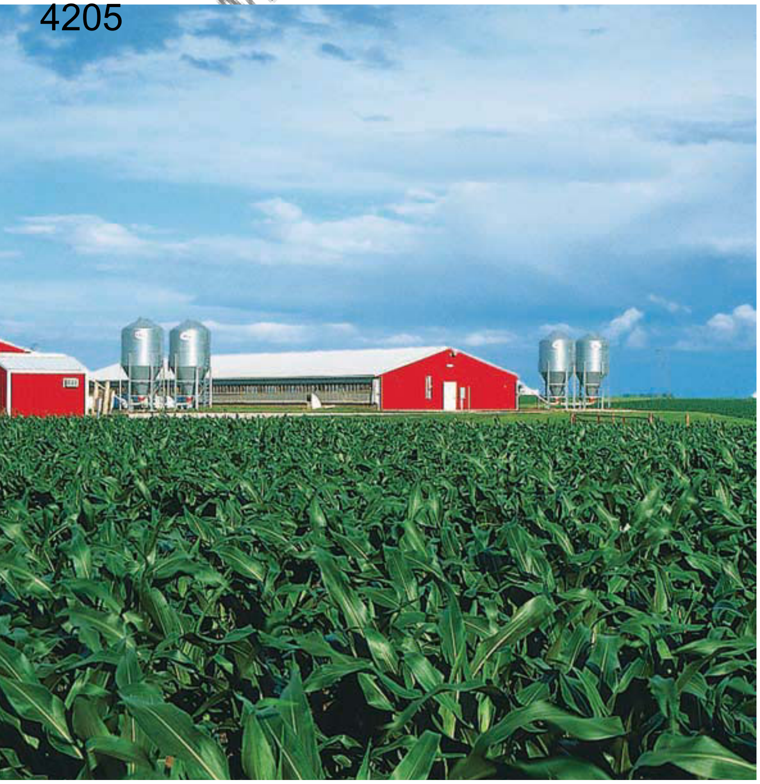

To the Professor

With this edition of *Chemistry,* students and instructors alike will experience a truly integrated learning program. The textbook's strong emphasis on conceptual learning and problem solving is extended through the numerous online media assignments and activities. It was our mission to create a media program that embodies the spirit of the textbook so that, when instructors and students look online for either study aids or online homework, that each resource supports the goals of the textbook—a strong emphasis on models, real-world applications, and visual learning.

We have gone over every page in the sixth edition thoroughly, fine-tuning in some cases and rewriting in others. In doing so, we have incorporated numerous constructive suggestions from instructors who used the previous edition. Based on this feedback new content has been added, such as the treatment of real gases in Chapter 5, which has been expanded to include a discussion of specific gases, and also coverage of photoelectric effect has been added to Chapter 7. In addition, the *Sample Exercises* in Chapter 2 have been revised to cover the naming of compounds given the formula and the opposite process of writing the formula from the name. To help students review key concepts, the For Review section of each chapter has been reorganized to provide an easy-to-read bulleted summary; this section includes new review questions. The art program has been enhanced to include electrostatic potential maps to show a more accurate distribution of charge in molecules.

In the media program instructors will find a variety of resources to assign additional practice, study, and quiz material. *ChemWork* interactive assignments, end-of-chapter online homework, *HM Testing,* and classroom response system applications allow you to assess students in multiple ways. The Online Study Center promotes self-study with animations, video demonstrations, and practice exercises.

Important Features of *Chemistry*

- *Chemistry* contains numerous discussions, illustrations, and exercises aimed at *overcoming common misconceptions.* It has become increasingly clear from our own teaching experience that students often struggle with chemistry because they misunderstand many of the fundamental concepts. In this text, we have gone to great lengths to provide illustrations and explanations aimed at giving students more accurate pictures of the fundamental ideas of chemistry. In particular, we have attempted to represent the microscopic world of chemistry so that students have a picture in their minds of "what the atoms and molecules are doing." The art program along with animations emphasize this goal. Also, we have placed a larger emphasis on the qualitative understanding of concepts before quantitative problems are considered. Because using an algorithm to correctly solve a problem often masks misunderstanding—students assume they understand the material because they got the right "answer"—it is important to probe their understanding in other ways. In this vein the text includes a number of Active Learning Questions (previously called In-Class Discussion Questions) at the end of each chapter that are intended for group discussion. It is our experience that students often learn the most when they teach each other. Students are forced to recognize their own lack of conceptual understanding when they try and fail to explain a concept to a colleague.
- With a strong *problem-solving orientation,* this text talks to the student about how to approach and solve chemical problems. We have made a strong pitch to students for using a thoughtful and logical approach rather than simply memorizing procedures. In particular, an innovative method is given for dealing with acid–base equilibria, the material the typical student finds most difficult and frustrating. The key to this approach involves first deciding what species are present in solution, then thinking about the chemical properties of these species. This method provides a general framework for approaching all types of solution equilibria.
- The text contains *almost 300 sample exercises,* with many more examples given in the discussions leading to sample exercises or used to illustrate general strategies. When a specific strategy is presented, it is summarized, and the sample exercise that follows it reinforces the step-by-step attack on the problem. In general, in approaching problem solving we emphasize understanding rather than an algorithm-based approach.
- We have presented a thorough *treatment of reactions* that occur in solution, including acid–base reactions. This material appears in Chapter 4, directly after the chapter on chemical stoichiometry, to emphasize the connection between solution reactions and chemical reactions in general. The early presentation of this material provides an opportunity to cover some interesting descriptive chemistry and also supports the lab, which typically involves a great deal of aqueous chemistry. Chapter 4 also includes oxidation–reduction reactions, because a large number of interesting and important chemical reactions involve redox processes. However, coverage of oxidation–reduction is optional at this point and depends on the needs of a specific course.

- *Descriptive chemistry* and chemical principles are thoroughly integrated in this text. Chemical models may appear sterile and confusing without the observations that stimulated their invention. On the other hand, facts without organizing principles may seem overwhelming. A combination of observations and models can make chemistry both interesting and understandable. In addition, in those chapters that deal with the chemistry of the elements systematically, we have made a continuous effort to show how properties and models correlate. Descriptive chemistry is presented in a variety of ways—as applications of the principles in separate sections, in Sample Exercises and exercise sets, in photographs, and in Chemical Impact features.
- Throughout the book a strong *emphasis on models* prevails. Coverage includes how they are constructed, how they are tested, and what we learn when they inevitably fail. Models are developed naturally, with pertinent observations always presented first to show why a particular model was invented.
- Everyday-life *applications* of chemistry that should be of interest to students taking general chemistry appear throughout the text. For example, the Chemical Impact "Pearly Whites" illustrates the procedures for keeping teeth white, and "Thin is In" discusses the new technology being used to produce plasma flat-panel displays. Many industrial applications have also been incorporated into the text.
- A double-helix icon in the *Instructor's Annotated Edition* highlights organic and biological examples of applications that are integrated throughout the text, in end-of-chapter problems, in exercises, or in-text discussions or examples. This feature allows instructors to quickly locate material that will be of particular interest to students in pre-medicine, biology, or other health-related fields.
- Judging from the favorable comments of instructors and students who have used the sixth edition, the text seemed to work very well in a variety of courses. We were especially pleased that *readability* was cited as a key strength when students were asked to assess the text. Thus, although the text has been fine-tuned in many areas, we have endeavored to build on the basic descriptions, strategies, analogies, and explanations that were successful in the previous editions.

New to the Seventh Edition

The seventh edition of *Chemistry* incorporates many significant improvements and is accompanied by new and enhanced media products and support services.

- Electrostatic potential maps have been added to Chapter 8 to show a more accurate distribution of charge in molecules. These maps are based on *ab initio* molecular modeling calculations and provide a convenient method for better student understanding of bond and molecular polarity.
- Additional topics have been added to the text, which include a treatment of real gases in Chapter 5 and coverage of photoelectric effect to Chapter 7. In addition, the Sample Exercises in Chapter 2 have been revised to cover the naming of compounds given the formula and the opposite process of writing the formula from the name.
- The end-of-chapter exercises and problems have been revised, providing approximately 20% new problems, including some that feature molecular art. End-of-chapter problems include: *Active Learning Questions* to test students' conceptual grasp of the material; *Questions* to help review important facts; *Exercises* that are paired and organized by topic; *Additional Exercises,* which are not keyed by topic; *Challenge Problems,* which require students to combine skills and problems; and *Marathon Problems,* which are the most comprehensive and challenging type of problem. New to the seventh edition are *Integrative Problems* that require students to understand multiple concepts across chapters.
- The *For Review* section, at the beginning of the end-of-chapter exercises, has been reorganized to help students more easily identify key concepts and test themselves on these concepts with review questions.
- A large number of new Chemical Impacts have been included in the seventh edition to continue the emphasis on up-to-date application of chemistry in the real world. These essays feature intriguing topics such as "Faux Snow," and "Closest Packing of M&M's®."
- To support the use of active learning in chemical education, we have created new PowerPoint presentations—*Active Learning PowerPoints with Lecture Outlines.* These PowerPoint presentations feature in-class discussion questions called *Reacts,* chemical demonstrations, animations, and figures from the text. This material is designed to help instructors present chemistry using an interactive teaching style, which we believe is most effective in promoting student learning. An *Active Learning Guide* includes the discussion questions and supporting information in a workbook format. The questions are repeated in the workbook (with space to record answers) so that students can focus on participation in class sessions. This guide can then be used effectively for independent student review outside of class.
- The Online Study Center has been enhanced to include a variety of tools to support visual learning and to give students extra practice. A *For Review* section summarizes the key topics of each chapter and helps students visualize the concepts with animations and video demonstrations. *Visualization* quiz questions allow students to test their knowledge of the concepts presented through the animations and video demonstrations. *ACE* practice tests allow students to practice problems on their own, and get immediate feedback. Additional resources include a molecule library, interactive periodic table, and flashcards to help students study key terms.

- A very important feature accompanying the seventh edition is the online homework in the Eduspace® online learning tool. In addition to new algorithmic end-of-chapter questions, Eduspace also includes *ChemWork*™ interactive online homework. *ChemWork* is structured to help students learn chemistry in a conceptual way and is a series of text-based assignments. The system is modeled on a one-to-one teacher- student problem session. When a student cannot answer a given question, instead of giving him/her the correct answer, a system of interactive hints is available to help them think through each problem. Often the hints are in the form of a question on which the student receives feedback. Links to text material are also available for reference to key concepts at points of learning. The philosophy behind the homework is to help students understand the material so that they can arrive at the correct answer by their own efforts, supported by the kind of help an instructor would provide in a one-to-one tutoring session.

  Another important feature of this homework system is that each student, even in a very large course, receives a unique set of tasks for each homework assignment, which is accomplished using random number–generation and similar versions of algorithmic problems. Each student's work is assessed by the system, and the score for each task in the assignment is recorded in the electronic gradebook for immediate access by both student and instructor. The system also encourages increased student responsibility by setting firm deadlines for assignments. From the instructor's perspective, Eduspace encourages student study without the burden of tracking student efforts through grading. Our experience with a similar system at the University of Illinois convinces us that this interactive homework represents an important breakthrough in helping students learn chemistry.

Flexibility of Topic Order

The order of topics in the text was chosen because it is preferred by the majority of instructors. However, we consciously constructed the book so that many other orders are possible. During our tenure at the University of Illinois, for a two-chapter sequence, we used the chapters in this order: 1–6, 13–15, 7–9, 18, 21, 12, 10, 11, 16, 17, and parts of 22. Sections of Chapters 19, 20, and parts of 22 are used throughout the two semesters as appropriate. This order, chosen because of the way the laboratory is organized, is not necessarily recommended, but it illustrates the flexibility of order built into the text.

Some specific points about topic order:

- About half of chemistry courses present kinetics before equilibria; the other half present equilibria first. This text is written to accommodate either order.
- The introductory aspects of thermodynamics are presented relatively early (in Chapter 6) because of the importance of energy in various chemical processes and models, but the more subtle thermodynamic concepts are left until later (Chapter 16). These two chapters may be used together if desired.
- To make the book more flexible, the derivation of the ideal gas law from the kinetic molecular theory and quantitative analysis using spectroscopy are presented in the appendixes. Although mainstream general chemistry courses typically do not cover this material, some courses may find it appropriate. By using the optional material in the appendixes and by assigning the more difficult end-of-chapter exercises (from the additional exercises section), an instructor will find the level of the text appropriate for many majors courses or for other courses requiring a more extensive coverage of these topics.
- Because some courses cover bonding using only a Lewis structure approach, orbitals are not presented in the introductory chapter on bonding (Chapter 8). In Chapter 9 both hybridization and the molecular orbital model are covered, but either or both of these topics may be omitted if desired.
- Chapter 4 can be tailored to fit the specific course involved. Used in its entirety where it stands in the book, it provides interesting examples of descriptive chemistry and supports the laboratory program. Material in this chapter can also be skipped entirely or covered at some later point, whenever appropriate. For example, the sections on oxidation and reduction can be taught with electrochemistry. Although many instructors prefer early introduction of this concept, these sections can be omitted without complication since the next few chapters do not depend on this material.

Supplements

An extensive teaching and learning package has been designed to make this book more useful to both instructors and students.

Technology: For Instructors

Chemistry is accompanied by a complete suite of teaching and learning tools, including the customizable media resources below. Whether online or via CD, these integrated resources are designed to save you time and help make class preparation, presentation, assessment, and course management more efficient and effective.

- **Media Integration Guide for Instructors** is your portal to the digital assets for this text. It includes the CDs described below as well as a user name and password to the Online Teaching Center, giving you instant access to text-related materials.

  HM ClassPrep™ CD includes everything an instructor needs to develop lectures: *Active Learning PowerPoints with Lecture Outlines;* virtually all text figures, tables, and photos in PowerPoint slides and as JPEGs; the *Instructor's Resource Guide* in Word; Word files of the printed *Test Bank;* and Word files of the *Complete Solutions Manual*.

HM Testing™ (powered by *Diploma*®) is Houghton Mifflin's new version of *HM Testing.* It significantly improves on functionality and ease of use by offering instructors all the tools they will need to create, author, deliver, and customize multiple types of tests—including authoring and editing algorithmic questions. New content includes 150 new *Conceptual Questions,* skill-level coding, and preprogrammed, algorithmic questions. HM Testing combines a flexible test-editing program with a comprehensive gradebook function for easy administration and tracking. It enables instructors to administer tests via print, network server, or the web. The HM Testing database contains a wealth of questions and can produce multiple-choice, true/false, fill-in-the-blank, and essay tests. Questions can be customized based on the chapter being covered, the question format, level of difficulty, and specific topics. Available on the HM ClassPrep CD.

HM ClassPresent™ 2006: General Chemistry features new animations and video demonstrations. HM ClassPresent provides a library of high-quality, scaleable lab demonstrations and animations covering core chemistry concepts arranged by chapter and topic. The resources within it can be browsed by thumbnail and description or searched by chapter, title, or keyword. Instructors can export the animations and videos into a variety of presentation formats or use for presentation directly from the CD. Full transcripts accompany all audio commentary to reinforce visual presentations and to cater to different learning styles.

Online Teaching Center includes classroom presentation and preparation materials. Animations; videos; virtually all figures, tables, and photos from the text are available in JPEG and PowerPoint format; the *Transition Guide* from the sixth to seventh edition; *Active Learning PowerPoints with Lecture Outlines;* and classroom response system content are all available online.

Eduspace (powered by Blackboard™), Houghton Mifflin's complete course-management solution, features algorithmic, end-of-chapter questions along with **ChemWork** interactive online homework. Both types of homework problems include links to relevant pages from the text. These integrated resources allow students to reference core concepts at the point of learning. *ChemWork* assignments help students learn the process of thinking like a chemist: as students work through unique, text-based assignments, a system of interactive hints is available to help them think through each problem. Eduspace includes all of Blackboard's powerful features for teaching and learning, and comes preloaded with course materials including videos and animations, and a link to SMARTHINKING™ live online tutoring. Customized functions allow instructors to tailor these materials to their specific needs, select, create and post homework assignments and tests, communicate with students in a variety of different ways, track student progress, and manage their portfolio of course work in the gradebook. To help instructors best utilize the media that accompanies the textbook, lesson plans have been created based on the sections of the book. Each section correlates the relevant *ChemWork* assignments, Visualization (animations and videos), and online end-of-chapter questions. **Please note: instructors who want their students to use Eduspace must request a *Getting Started Guide for Students* which will be bundled free with new copies of the text. Instructors who adopt Eduspace will receive a separate *Getting Started Guide for Instructors* for the program with a passkey to set up their course.**

- **Classroom Response System (CRS)** compatible content on the Online Teaching Center, HM ClassPrep CD, and in Eduspace allows professors to perform "on-the-spot" assessments, deliver quick quizzes, gauge students' understanding of a particular question or concept, and take their class roster easily. Students get immediate feedback on how well they know the content and where they need to improve. Two sets of questions are available in PowerPoint slides: one based on *Test Bank* content and the other with unique, conceptual questions. Both question types are correlated to sections in the textbook. The conceptual questions are also correlated to relevant media and art from the book.
- **TeamUP Integration Services**
  http://teamup.college.hmco.com
  Houghton Mifflin aims to provide customers with quality textbooks, technology, and superior training and implementation services. TeamUP, our integration program, offers flexible, personalized training and consultative services by phone, online, or on campus. Experienced faculty advisors and media specialists will assist you and your department in using our products most effectively.
- **Course-Management Software** is available through *WebCT* and *Blackboard.* These two distributed learning systems allow instructors to create a virtual classroom without any knowledge of HTML. Features include: assessment tools, a gradebook, online file exchange between instructors and students, online syllabi, and course descriptions. The customized *Chemistry* cartridges feature *Test Bank* questions, lecture materials, and study aids related to the text.

Print Supplements: For Instructors

- *Complete Solutions Guide,* by Thomas J. Hummel, Susan Arena Zumdahl, and Steven S. Zumdahl, presents detailed solutions for all of the end-of-chapter exercises in the text for the convenience of faculty and staff involved in instruction and for instructors who wish their students to have solutions for all exercises. Departmental approval is required for the sale of the *Complete Solutions Guide* to students.
- *Instructor's Resource Guide,* by Donald J. DeCoste, includes suggestions for alternative orders of topics, suggested responses to the *Active Learning Questions,* amplification

of strategies used in various chapters, lesson plans of media resources correlated to section, answers to *Reacts,* and a section on notes for teaching assistants.

- *Lecture Demonstration Guide,* by Fred Jurgens of the University of Wisconsin—Madison, lists the sources for over 750 classroom demonstrations that can be used in general chemistry courses. Icons in the margins of the *Instructor's Annotated Edition* of the text key the demonstrations to their corresponding text discussions.
- *Instructor's Resource Guide for Experimental Chemistry,* Seventh Edition, by James F. Hall, contains tips including hints on running experiments, approximate times for each experiment, and answers to all prelab and postlab questions posed in the laboratory guide.
- *Bibliobase (www.bibliobase.com)* allows instructors to create a completely customized lab manual by mixing and matching from 88 general chemistry labs—including all the labs from *Experimental Chemistry*—and 56 labs for the course in general, organic, and biochemistry. At the Online Teaching Center, instructors search through the database of labs, make their selections, organize the sequence of the manual, and submit their order via the Internet. Customized, printed, and bound lab manuals are delivered to the bookstore within weeks.
- *Test Item File,* by Steven S. Zumdahl, Susan Arena Zumdahl, and Gretchen Adams (available to adopters), offers a printed version of more than 2000 exam questions, 10 percent of which are new to this edition, referenced to the appropriate text section. Questions are in multiple-choice, open-ended, and true-false formats.
- *Transparencies,* in a full-color set of 255, are available to adopters of the seventh edition of the text.

Technology: For Students

Chemistry is supported by an array of learning tools designed to help students succeed in their chemistry course. It includes the following media resources:

A passkey to the Online Study Center is bound into the front of the textbook. From the Online Study Center, students have access to practice, visualization, and self-study aids. *Visualization* animations and video demonstrations help students see key concepts, and each *Visualization* is accompanied by quiz questions for students' review. A *For Review* section helps students review key topics at a glance and includes video demonstrations and animations for additional reinforcement. *Flashcards* and *ACE* practice tests help students study key concepts and problem-solve. A molecule library, glossary, and interactive periodic table are also available for support. A *Student CD,* with many of these Online Study Center resources, is available upon request for students who do not have Internet access.

Eduspace (powered by *Blackboard*), Houghton Mifflin's complete course-management solution, features algorithmic end-of-chapter questions along with *ChemWork* interactive online homework. Through Eduspace, students can also access the Online Study Center and SMARTHINKING live, online tutoring. Instructors who adopt Eduspace will receive a separate user guide for the program with a passkey to set up their course. Students using Eduspace will also receive a separate user guide and passkey.

SMARTHINKING live, online tutoring is also available free with new books upon instructor request. Students may also purchase stand-alone access to it. SMARTHINKING provides personalized, text-specific tutoring and is available during peak study hours when students need it most. Limits apply; terms and hours of SMARTHINKING service are subject to change.

Print Supplements: For Students

- *Study Guide,* by Paul B. Kelter of the University of Illinois—Urbana. Written to be a self-study aid for students, this guide includes alternate strategies for solving problems, supplemental explanations for the most difficult material, and self-tests. There are approximately 500 worked examples and 1200 practice problems (with answers), designed to give students mastery and confidence.
- *Student Solutions Manual,* by Thomas J. Hummel, Susan Arena Zumdahl, and Steven S. Zumdahl, all of the University of Illinois, Urbana, provides detailed solutions for half of the end-of-chapter exercises (designated by the blue question numbers) using the strategies emphasized in the text. To ensure the accuracy of the solutions, this supplement and the *Complete Solutions Guide* were checked independently by several instructors.
- *Active Learning Guide,* by Donald J. DeCoste. This printed workbook can be used in lecture or recitation in conjunction with the instructor PowerPoint slides. It provides a complete set of *React* questions with space for student answers. Students can use the workbook as a self-study aid outside of class.
- *Solving Equilibrium Problems with Applications to Qualitative Analysis,* by Steven S. Zumdahl. Successfully used by thousands of students, this book offers thorough, step-by-step procedures for solving problems related to equilibria taking place both in the gas phase and in solution. Containing hundreds of sample exercises, test exercises with complete solutions, and end-of-chapter exercises with answers, the text utilizes the same problem-solving methods found in *Chemistry* and is an excellent source of additional drill-type problems. The last chapter presents an exploratory qualitative analysis experiment with explanations based on the principles of aqueous equilibria.
- *Experimental Chemistry,* Seventh Edition, by James F. Hall of the University of Massachusetts—Lowell, provides an extensively revised laboratory program compatible with the text. The 48 experiments present a wide variety of chemistry, and many experiments offer choices of procedures. Safety is strongly emphasized throughout the program.

Acknowledgments: This book represents the efforts of many talented and dedicated people. We particularly want to thank Richard Stratton, Executive Editor, for his vision and oversight of this project. Richard's knowledge, judgment, and enthusiasm have contributed immeasurably to the success of this text. He is not only an outstanding editor but also one of the nicest people in the business.

We also want to thank Cathy Brooks, Senior Project Editor, who did a miraculous job of coordinating the production of an incredibly complex project with grace and good humor. We also especially appreciate the excellent work of Rebecca Berardy Schwartz, Developmental Editor, who managed the revision process in a very supportive and organized manner.

We are especially grateful to Tom Hummel, who managed the revision of the end-of-chapter problems and the solutions manuals. Tom's extensive experience teaching general chemistry and his high standards of accuracy and clarity have resulted in great improvements in the quality of the problems and the solutions in this edition. In addition, we very much appreciate the contributions of Don DeCoste, who has helped us comprehend more clearly the difficulties students have with conceptual understanding and who contributed the Challenge Problems.

We also extend our thanks to Jason Overby, who rendered the electrostatic potential maps and who contributed the Integrative Problems. Our thanks and love also go to Leslie, Steve, Whitney, Scott, Tyler, Sunshine, and Tony for their continuing support.

Thanks to the others at Houghton Mifflin who supplied valuable assistance on this revision: Jill Haber, Senior Art/Design Coordinator; Sharon Donahue, Photo Researcher; Katherine Greig, Senior Marketing Manager; Naveen Hariprasad, Marketing Assistant; and Susan Miscio, Editorial Assistant.

Special thanks go to the following people who helped shape this edition by offering suggestions for its improvement:

Dawood Afzal, Truman State (media reviewer); Carol Anderson, University of Connecticut—Avery Point (media reviewer); Jeffrey R. Appling, Clemson University (media reviewer); Dave Blackburn, University of Minnesota; Robert S. Boikess, Rutgers University; Ken Carter, Truman State (media reviewer); Bette Davidowitz, University of Cape Town; Natalie Foster, Lehigh University; Tracy A. Halmi, Penn State Erie, The Behrend College; Carl A. Hoeger, UC—San Diego; Ahmad Kabbani, Lebanese American University; Arthur Mar, University of Alberta; Jim McCormick, Truman State (media reviewer); Richard Orwell, Blue Ridge Community College (media reviewer); Jason S. Overby, College of Charleston; Robert D. Pike, The College of William and Mary; Daniel Raftery, Purdue University; Jimmy Rogers, University of Texas—Arlington (media reviewer); Raymond Scott, Mary Washington College; Alan Stolzenberg, West Virginia University; Rashmi Venkateswaran, University of Ottawa. *AP reviewers*: Annis Hapkiewicz, Okemos High School; Tina Ohn-Sabatello, Maine Township HS East. *Interactive Course Guide Reviewers:* Lynne C. Cary, Ph.D., Bethel College; Craig C. Martens, University of California—Irvine; Jeffrey P. Osborne, Manchester College; Donald W. Shive, Muhlenberg College; Craig Sockwell, Northwest Shoals Community College; Richard Pennington, College of St. Mary. *Accuracy reviewers:* Linda Bush (textbook reviewer), Jon Booze (media reviewer)

Reviewers of the sixth edition:

Ramesh D. Arasasingham, University of California—Irvine; Stanley A. Bajue, Medgar Evans College, CUNY; V.G. Berner, New Mexico Junior College; Dave Blackburn, University of Minnesota; Steven R. Boone, Central Missouri State University; Gary S. Buckley, Cameron University; Lara L. Chappell, SUNY College at Oswego; David Cramb, University of Calgary; Philip W. Crawford, Southeast Missouri State University; Philip Davis, University of Tennessee; Michael P. Garoutte, Missouri Southern State College; Daniel Graham, Loyola University; David R. Hawkes, Lambuth University; Dale Hawley, Kansas State University; Thomas B. Higgins, Harold Washington College; John C. Hogan, Louisiana State University; Donald P. Land, University of California—Davis; Michael P. Masingale, LeMoyne College; Julie T. Millard, Colby College; Robert H. Paine, Rochester Institute of Technology; Brenda Ross, Cottey College; Jay S. Shore, South Dakota State University; Richard T. Toomey, Northwest Missouri State University; Robert Zoellner, Humboldt State University.

To the Student

The major purpose of this book, of course, is to help you learn chemistry. However, this main thrust is closely linked to two other goals: to show how important and how interesting the subject is, and to show how to think like a chemist. To solve complicated problems the chemist uses logic, trial and error, intuition, and, above all, patience. A chemist is used to being wrong. The important thing is to learn from a mistake, recheck assumptions, and try again. A chemist thrives on puzzles that seem to defy solutions.

Many of you using this text do not plan to be practicing chemists. However, the nonchemist can benefit from the chemist's attitude. Problem solving is important in all professions and in all walks of life. The techniques you will learn from this book will serve you well in any career you choose. Thus, we believe that the study of chemistry has much to offer the nonmajor, including an understanding of many fascinating and important phenomena and a chance to hone problem-solving skills.

This book attempts to present chemistry in a manner that is sensible to the novice. Chemistry is not the result of an inspired vision. It is the product of countless observations and many attempts, using logic and trial and error, to account for these observations. In this book the concepts are developed in a natural way: The observations come first and then models are constructed to explain the observed behavior.

Models are a major focus in this book. The uses and limitations of models are emphasized, and science is treated as a human activity, subject to all the normal human foibles. Mistakes are discussed as well as successes.

A central theme of this book is a thoughtful, systematic approach to problem solving. Learning encompasses much more than simply memorizing facts. Truly educated people use their factual knowledge as a starting point—a base for creative approaches to solving problems.

Read through the material in the text carefully. For most concepts, illustrations or photos will help you visualize what is going on. To further help you visualize concepts by using animations and videos, we have included *Visualization* exercises on the Online Study Center or on an optional free CD. Icons in the text margin signal that there is companion material available on the CD.

Often a given type of problem is "walked through" in the text before the corresponding Sample Exercises appear. Strategies for solving problems are given throughout the text.

Thoroughly examine the Sample Exercises and the problem-solving strategies. The strategies summarize the approach taken in the text; the Sample Exercises follow the strategies step-by-step. Schematics in Chapter 15 also illustrate the logical pathways to solving aqueous equilibrium problems.

Throughout the text, we have used margin notes to highlight key points, to comment on an application of the text material, or to reference material in other parts of the book. Chemical Impact, the boxed feature that appears frequently throughout the text, discusses especially interesting applications of chemistry to the everyday world.

Each chapter has a summary and key terms list for review, and the glossary gives a quick reference for definitions.

Learning chemistry requires working the end-of-chapter exercises assigned by your professor. Answers to exercises denoted by blue question numbers are in the back of the book, and complete solutions to those exercises are in the *Partial Solutions Guide.* To help you assess your level of proficiency, the Online Study Center (college.hmco.com/PIC/zumdahl7e) offers quizzes and electronic homework assignments that feature instant feedback.

The *Study Guide* contains extra practice problems and many worked examples. The supplement, *Solving Equilibrium Problems with Applications to Qualitative Analysis,* reinforces in great detail the text's step-by-step approach to solving equilibrium problems and contains many worked examples and self-quiz questions.

It is very important to use the exercises and electronic homework assignments to your best advantage. Your main goal should not be to simply get the correct answer but to *understand the process* for getting the answer. Memorizing the solutions for specific problems is not a very good way to prepare for an exam. There are too many pigeonholes required to cover every possible problem type. Look within the problem for the solution. Use the concepts you have learned along with a systematic, logical approach to find the solution. Learn to trust yourself to think it out. You will make mistakes, but the important thing is to learn from these errors. The only way to gain confidence is to do lots of practice problems and use these to diagnose your weaknesses.

Be patient and thoughtful and work hard to understand rather than simply memorize. We wish you an interesting and satisfying year.

Features of **Chemistry** Seventh Edition

Conceptual Understanding and Problem Solving

8.13 Molecular Structure: The VSEPR Model

The structures of molecules play a very important role in determining their chemical properties. As we will see later, this is particularly important for biological molecules; a slight change in the structure of a large biomolecule can completely destroy its usefulness to a cell or may even change the cell from a normal one to a cancerous one.

Many accurate methods now exist for determining **molecular structure,** the three-dimensional arrangement of the atoms in a molecule. These methods must be used if precise information about structure is required. However, it is often useful to be able to predict the approximate molecular structure of a molecule. In this section we consider a simple model that allows us to do this. This model, called the **valence shell electron-pair repulsion (VSEPR) model,** is useful in predicting the geometries of molecules formed from nonmetals. The main postulate of this model is that *the structure around a given atom is determined principally by minimizing electron-pair repulsions.* The idea here is that the bonding and nonbonding pairs around a given atom will be positioned as far apart as possible. To see how this model works, we will first consider the molecule $BeCl_2$, which has the Lewis structure

$$:\ddot{\underset{..}{Cl}}—Be—\ddot{\underset{..}{Cl}}:$$

The authors' emphasis on **modeling** (or chemical theories) throughout the text addresses the problem of rote memorization by helping students better understand and appreciate the process of scientific thinking.

By stressing the limitations and uses of **scientific models**, the authors show students how chemists think and work.

ight Bonding: General Concepts

Fundamental Properties of Models

- Models are human inventions, always based on an incomplete understanding of how nature works. *A model does not equal reality.*
- Models are often wrong. This property derives from the first property. Models are based on speculation and are always oversimplifications.
- Models tend to become more complicated as they age. As flaws are discovered in our models, we "patch" them and thus add more detail.
- It is very important to understand the assumptions inherent in a particular model before you use it to interpret observations or to make predictions. Simple models usually involve very restrictive assumptions and can be expected to yield only qualitative information. Asking for a sophisticated explanation from a simple model is like expecting to get an accurate mass for a diamond using a bathroom scale.

  For a model to be used effectively, we must understand its strengths and weaknesses and ask only appropriate questions. An illustration of this point is the simple aufbau principle used to account for the electron configurations of the elements. Although this model correctly predicts the configuration for most atoms, chromium and copper, for example, do not agree with the predictions. Detailed studies show that the configurations of chromium and copper result from complex electron interactions that are not taken into account in the simple model. However, this does not mean that we should discard the simple model that is so useful for most atoms. Instead, we must apply it with caution and not expect it to be correct in every case.
- When a model is wrong, we often learn much more than when it is right. If a model makes a wrong prediction, it usually means we do not understand some fundamental characteristics of nature. We often learn by making mistakes. (Try to remember this when you get back your next chemistry test.)

8.8 Covalent Bond Energies and Chemical Reactions

In this section we will consider the energies associated with various types of bonds and see how the bonding concept is useful in dealing with the energies of chemical reactions. One important consideration is to establish the sensitivity of a particular type of bond its molecular environment. For example, consider the stepwise decomposition of thane:

Process	Energy Required (kJ/mol)
$CH_4(g) \rightarrow CH_3(g) + H(g)$	435
$CH_3(g) \rightarrow CH_2(g) + H(g)$	453
$CH_2(g) \rightarrow CH(g) + H(g)$	425
$CH(g) \rightarrow C(g) + H(g)$	339
	Total = 1652

$$\text{Average} = \frac{1652}{4} = 413$$

Sample Exercise 5.5 Avogadro's Law

Avogadro's law also can be written as

$$\frac{V_1}{n_1} = \frac{V_2}{n_2}$$

Suppose we have a 12.2-L sample containing 0.50 mol oxygen gas (O_2) at a pressure of 1 atm and a temperature of 25°C. If all this O_2 were converted to ozone (O_3) at the same temperature and pressure, what would be the volume of the ozone?

Solution

The balanced equation for the reaction is

$$3O_2(g) \longrightarrow 2O_3(g)$$

To calculate the moles of O_3 produced, we must use the appropriate mole ratio:

$$0.50\ \cancel{\text{mol } O_2} \times \frac{2 \text{ mol } O_3}{3\ \cancel{\text{mol } O_2}} = 0.33 \text{ mol } O_3$$

Avogadro's law states that $V = an$, which can be rearranged to give

$$\frac{V}{n} = a$$

Since a is a constant, an alternative representation is

$$\frac{V_1}{n_1} = a = \frac{V_2}{n_2}$$

where V_1 is the volume of n_1 moles of O_2 gas and V_2 is the volume of n_2 moles of O_3 ga In this case we have

$$n_1 = 0.50 \text{ mol} \qquad n_2 = 0.33 \text{ mol}$$
$$V_1 = 12.2 \text{ L} \qquad V_2 = ?$$

Solving for V_2 gives

$$V_2 = \left(\frac{n_2}{n_1}\right)V_1 = \left(\frac{0.33\ \cancel{\text{mol}}}{0.50\ \cancel{\text{mol}}}\right)12.2 \text{ L} = 8.1 \text{ L}$$

Reality Check: Note that the volume decreases, as it should, since fewer moles of ga molecules will be present after O_2 is converted to O_3.

See Exercises 5.35 and 5.3

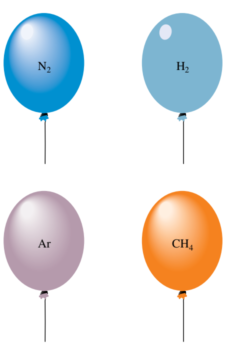

FIGURE 5.10
These balloons each hold 1.0 L of gas at 25°C and 1 atm. Each balloon contains 0.041 mol of gas, or 2.5×10^{22} molecules.

Sample Exercises model a step-by-step approach to solving problems. Cross-references to similar end-of-chapter exercises are provided at the end of each Sample Exercise. **Reality Checks** appear after the solutions in selected exercises, helping students evaluate their answers to ensure that they are reasonable.

Connections

Each chapter begins with an engaging introduction that demonstrates how chemistry is related to everyday life.

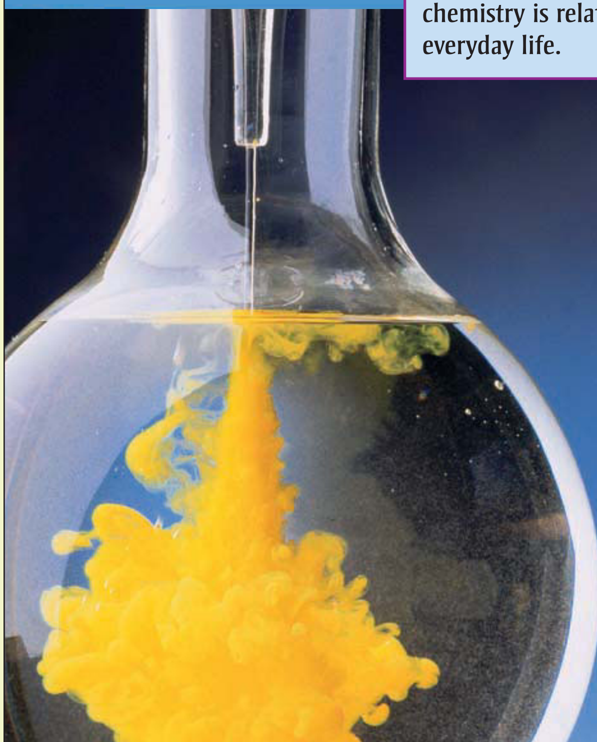

Much of the chemistry that affects each of us occurs among substances dissolved in water. For example, virtually all the chemistry that makes life possible occurs in an aqueous environment. Also, various medical tests involve aqueous reactions, depending heavily on analyses of blood and other body fluids. In addition to the common tests for sugar, cholesterol, and iron, analyses for specific chemical markers allow detection of many diseases before obvious symptoms occur.

Aqueous chemistry is also important in our environment. In recent years, contamination of the groundwater by substances such as chloroform and nitrates has been widely publicized. Water is essential for life, and the maintenance of an ample supply of clean water is crucial to all civilization.

To understand the chemistry that occurs in such diverse places as the human body, the atmosphere, the groundwater, the oceans, the local water treatment plant, your hair as you shampoo it, and so on, we must understand how substances dissolved in water react with each other.

However, before we can understand solution reactions, we need to discuss the nature of solutions in which water is the dissolving medium, or *solvent*. These solutions are called **aqueous solutions.** In this chapter we will study the nature of materials after they are dissolved in water and various types of reactions that occur among these substances. You will see that the procedures developed in Chapter 3 to deal with chemical reactions work very well for reactions that take place in aqueous solutions. To understand the types of reactions that occur in aqueous solutions, we must first explore the types of species present. This requires an understanding of the nature of water.

4.1 Water, the Common Solvent

Water is one of the most important substances on earth. It is essential for sustaining the reactions that keep us alive, but it also affects our lives in many indirect ways. Water helps moderate the earth's temperature; it cools automobile engines, nuclear power plants, and many industrial processes; it provides a means of transportation on the earth's surface and a medium for the growth of a myriad of creatures we use as food; and much more.

One of the most valuable properties of water is its ability to dissolve many different substances. For example, salt "disappears" when you sprinkle it into the water used to cook vegetables, as does sugar when you add it to your iced tea. In each case the "disappearing" substance is obviously still present—you can taste it. What happens when a solid dissolves? To understand this process, we need to consider the nature of water. Liquid water consists of a collection of H_2O molecules. An individual H_2O molecule is "bent" or V-shaped, with an H—O—H angle of approximately 105 degrees:

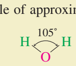

The O—H bonds in the water molecule are covalent bonds formed by electron sharing between the oxygen and hydrogen atoms. However, the electrons of the bond are not shared equally between these atoms. For reasons we will discuss in later chapters, oxygen has a greater attraction for electrons than does hydrogen. If the electrons were shared equally between the two atoms, both would be electrically neutral because, on average, the number of electrons around each would equal the number of protons in that nucleus.

127

CHEMICAL IMPACT

The Chemistry of Air Bags

Most experts agree that air bags represent a very important advance in automobile safety. These bags, which are stored in the auto's steering wheel or dash, are designed to inflate rapidly (within about 40 ms) in the event of a crash, cushioning the front-seat occupants against impact. The bags then deflate immediately to allow vision and movement after the crash. Air bags are activated when a severe deceleration (an impact) causes a steel ball to compress a spring and electrically ignite a detonator cap, which, in turn, causes sodium azide (NaN_3) to decompose explosively, forming sodium and nitrogen gas:

$$2NaN_3(s) \longrightarrow 2Na(s) + 3N_2(g)$$

This system works very well and requires a relatively small amount of sodium azide (100 g yields 56 L $N_2(g)$ at 25°C and 1.0 atm).

When a vehicle containing air bags reaches the end of its useful life, the sodium azide present in the activators must be given proper disposal. Sodium azide, besides being explosive, has a toxicity roughly equal to that of sodium cyanide. It also forms hydrazoic acid (HN_3), a tox explosive liquid, when treated with acid.

The air bag represents an application of chemis has already saved thousands of lives.

Inflated air bags.

Chemical Impact boxes describe current applications of chemistry. These special-interest boxes cover such topics as preserving works of art, molecules as a means of communication, and the heat of chili peppers.

4215

Visualization

Electrostatic potential maps help students visualize the distribution of charge in molecules.

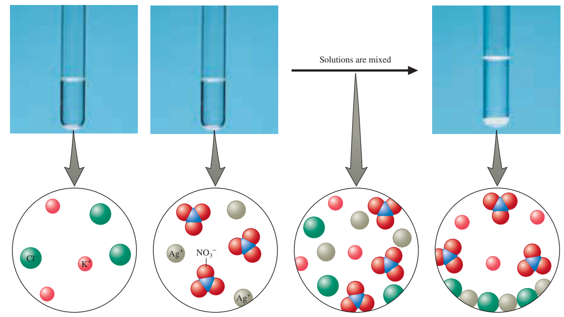

FIGURE 4.17
Photos and accompanying molecular-level representations illustrating the reaction of KCl(*aq*) with $AgNO_3$(*aq*) to form AgCl(*s*). Note that it is not possible to have a photo of the mixed solution before the reaction occurs, because it is an imaginary step that we use to help visualize the reaction. Actually, the reaction occurs immediately when the two solutions are mixed.

The art program emphasizes molecular-level interactions that help students visualize the **"micro-macro"** connection.

Since the equation for lattice energy contains the product Q_1Q_2, the lattice energy for a solid with 2+ and 2− ions should be four times that for a solid with 1+ and 1− ions. That is,

$$\frac{(+2)(-2)}{(+1)(-1)} = 4$$

For MgO and NaF, the observed ratio of lattice energies (see Fig. 8.11) is

$$\frac{-3916 \text{ kJ}}{-923 \text{ kJ}} = 4.24$$

more negative than that for combining gaseous Na^+ and F^- ions to form NaF(*s*). Thus the energy released in forming a solid containing Mg^{2+} and O^{2-} ions rather than Mg^+ and O^- ions more than compensates for the energies required for the processes that produce the Mg^{2+} and O^{2-} ions.

If there is so much lattice energy to be gained in going from singly charged to doubly charged ions in the case of magnesium oxide, why then does solid sodium fluoride contain Na^+ and F^- ions rather than Na^{2+} and F^{2-} ions? We can answer this question by recognizing that both Na^+ and F^- ions have the neon electron configuration. Removal of an electron from Na^+ requires an extremely large quantity of energy (4560 kJ/mol) because a 2*p* electron must be removed. Conversely, the addition of an electron to F^- would require use of the relatively high-energy 3*s* orbital, which is also an unfavorable process. Thus we can say that for sodium fluoride the extra energy required to form the doubly charged ions is greater than the gain in lattice energy that would result.

This discussion of the energies involved in the formation of solid ionic compounds illustrates that a variety of factors operate to determine the composition and structure of these compounds. The most important of these factors involve the balancing of the energies required to form highly charged ions and the energy released when highly charged ions combine to form the solid.

8.6 Partial Ionic Character of Covalent Bonds

Recall that when atoms with different electronegativities react to form molecules, the electrons are not shared equally. The possible result is a polar covalent bond or, in the case of a large electronegativity difference, a complete transfer of one or more electrons to form ions. The cases are summarized in Fig. 8.12.

How well can we tell the difference between an ionic bond and a polar covalent bond? The only honest answer to this question is that there are probably no totally ionic bonds between *discrete pairs of atoms.* The evidence for this statement comes from calculations of the percent ionic character for the bonds of various binary compounds in the gas phase. These calculations are based on comparisons of the measured dipole moments for molecules of the type X—Y with the calculated dipole moments for the completely ionic case, X^+Y^-. The percent ionic character of a bond can be defined as

$$\text{Percent ionic character of a bond} = \left(\frac{\text{measured dipole moment of X—Y}}{\text{calculated dipole moment of } X^+Y^-}\right) \times 100\%$$

Application of this definition to various compounds (in the gas phase) gives the results shown in Fig. 8.13, where percent ionic character is plotted versus the difference in the electronegativity values of X and Y. Note from this plot that ionic character increases with electronegativity difference, as expected. However, none of the bonds reaches 100% ionic character, even though compounds with the maximum possible electronegativity differences are considered. Thus, according to this definition, no individual bonds are completely ionic. This conclusion is in contrast to the usual classification of many of these compounds (as ionic solids). All the compounds shown in Fig. 8.13 with more than 50% ionic character are normally considered to be ionic solids. Recall, however, the results in Fig. 8.13 are for the gas p
not necessarily be assume
vored by the multiple ion

Another complication
contain polyatomic ions. F
contains Na^+ and SO_4^{2-}
by covalent bonds. Thus,
ambiguous.

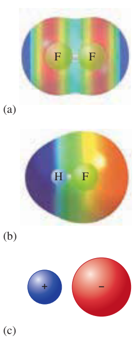

FIGURE 8.12
The three possible types of bonds: (a) a covalent bond formed between identical F atoms; (b) the polar covalent bond of HF, with both ionic and covalent components; and (c) an ionic bond with no electron sharing.

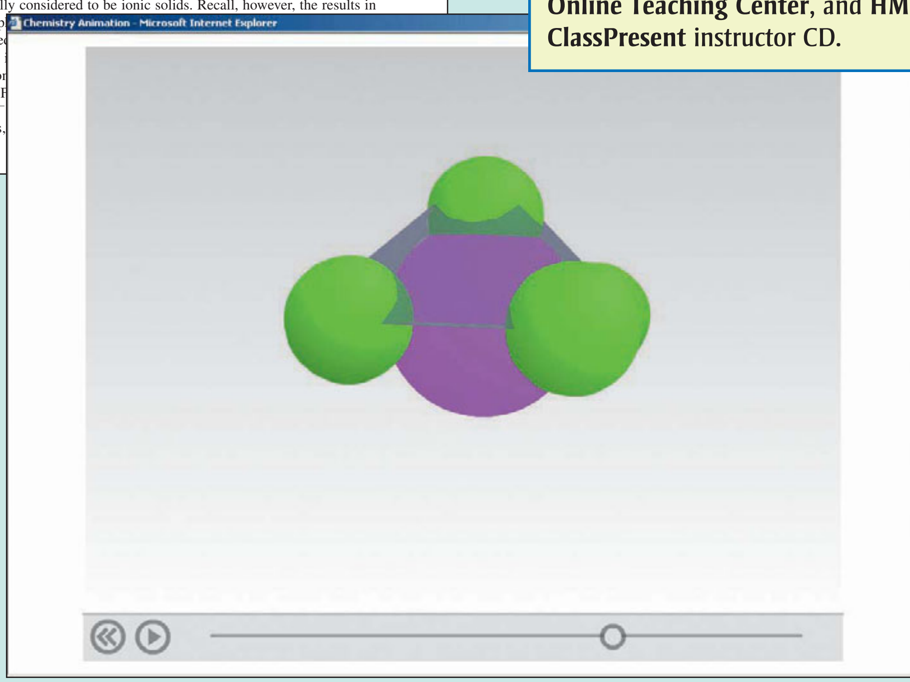

Visualization animations and video demonstrations help students further understand and visualize chemical concepts. Animations and videos (Visualizations) are found via the **Online Study Center and Online Teaching Center**, and **HM ClassPresent** instructor CD.

4216

Practice

Active Learning Questions are designed to promote discussion among groups of students in class.

Active Learning Questions

These questions are designed to be used by groups of students in class. The questions allow students to explore their understanding of concepts through discussion and peer teaching. The real value of these questions is the learning that occurs while students talk to each other about chemical concepts.

1. Consider the following apparatus: a test tube covered with a nonpermeable elastic membrane inside a container that is closed with a cork. A syringe goes through the cork.

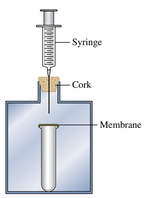

   a. As you push down on the syringe, how does the membrane covering the test tube change?
   b. You stop pushing the syringe but continue to hold it down. In a few seconds, what happens to the membrane?
2. Figure 5.2 shows a picture of a barometer. Which of the following statements is the best explanation of how this barometer works?
   a. Air pressure outside the tube causes the mercury to move in the tube until the air pressure inside and outside the tube is equal.
   b. Air pressure inside the tube causes the mercury to move in the tube until the air pressure inside and outside the tube is equal.
   c. Air pressure outside the tube counterbalances the weight of the mercury in the tube.
   d. Capillary action of the mercury causes the mercury to go up the tube.
   e. The vacuum that is formed at the top of the tube holds up the mercury.

   Justify your choice, and for the choices you did not pick, explain what is wrong with them. Pictures help!
3. The barometer below shows the level of mercury at a given atmospheric pressure. Fill all the other barometers with mercury for that same atmospheric pressure. Explain your answer.

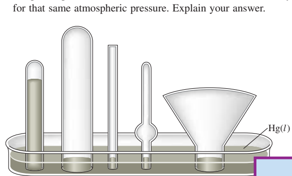

4. As you increase the temperature c… tainer, what happens to the density… be the same if you did the same e… a piston at constant pressure? (Se…
5. A diagram in a chemistry book … flask of air as follows:

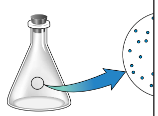

   What do you suppose is between t… molecules)?
   a. air
   b. dust
   c. pollutants
   d. oxygen
   e. nothing
6. If you put a drinking straw in wa… opening, and lift the straw out of t… the straw. Explain.
7. A chemistry student relates the f… tires were a bit low and went to th… the tires, I thought about the kinet… noticed the tires because the volum… I was increasing both the pressu… "Hmmm," I thought, "that goes ag… istry, where I was told pressure a… portional." What is the fault in the… in this situation? Explain *why* we… be inversely related (draw pictures and use the KMT).
8. Chemicals X and Y (both gases) react to form the gas XY, but it takes a bit of time for the reaction to occur. Both X and Y a… placed in a container with a piston (free to move), and you no… the volume. As the reaction occurs, what happens to the volu… of the container? (See Fig. 5.18.)
9. Which statement best explains why a hot-air balloon rises wh… the air in the balloon is heated?
   a. According to Charles's law, the temperature of a gas … directly related to its volume. Thus the volume of the ballo… increases, making the density smaller. This lifts the balloo…
   b. Hot air rises inside the balloon, and this lifts the balloon.
   c. The temperature of a gas is directly related to its pressu… The pressure therefore increases, and this lifts the balloo…
   d. Some of the gas escapes from the bottom of the balloon, th… decreasing the mass of gas in the balloon. This decreases t… density of the gas in the balloon, which lifts the balloon.
   e. Temperature is related to the root mean square velocity of t… gas molecules. Thus the molecules are moving faster, hitti… the balloon more, and thus lifting the balloon.

Key Terms

Section 5.1
barometer
manometer
mm Hg
torr
standard atmosphere
pascal

Section 5.2
Boyle's law
ideal gas
Charles's law
absolute zero
Avogadro's law

Section 5.3
universal gas constant
ideal gas law

Section 5.4
molar volume
standard temperature and pressure (STP)

Section 5.5
Dalton's law of partial pressures
partial pressure
mole fraction

Section 5.6
kinetic molecular theory (KMT)
root mean square velocity
joule

Section 5.7
diffusion
effusion
Graham's law of effusion

Section 5.8
real gas
van der Waals equation

Section 5.10
atmosphere
air pollution
photochemical smog
acid rain

For Review

State of a gas
- The state of a gas can be described completely by specifying its pressure (P), volume (V), temperature (T) and the amount (moles) of gas present (n)
- Pressure
  - Common units

    1 torr = 1 mm Hg

    1 atm = 760 torr
  - SI unit: pascal

    1 atm = 101,325 Pa

Gas laws
- Discovered by observing the properties of gases
- Boyle's law: $PV = k$
- Charles's law: $V = bT$
- Avogadro's law: $V = an$
- Ideal gas law: $PV = nRT$
- Dalton's law of partial pressures: $P_{total} = P_1 + P_2$ … the partial pressure of component n in a mixture o…

Kinetic molecular theory (KMT)
- Model that accounts for ideal gas behavior
- Postulates of the KMT:
  - Volume of gas particles is zero
  - No particle interactions
  - Particles are in constant motion, colliding with … pressure
  - The average kinetic energy of the gas particles … temperature of the gas in kelvins

Gas properties
- The particles in any gas sample have a range of ve…
- The root mean square (rms) velocity for a gas repr… of the particle velocities

$$u_{rms} = \sqrt{\frac{3RT}{M}}$$

- Diffusion: the mixing of two or more gases
- Effusion: the process in which a gas passes through a small hole into an empty chamber

Real gas behavior
- Real gases behave ideally only at high temperatures and low pressures
- Understanding how the ideal gas equation must be modified to account for real gas behavior helps us understand how gases behave on a molecular level
- Van der Waals found that to describe real gas behavior we must consider particle interactions and particle volumes

REVIEW QUESTIONS

1. Explain how a barometer and a manometer work to measure the pressure of the atmosphere or the pressure of a gas in a container.

Each chapter has a **For Review** section to reinforce key concepts, and includes review questions. **Key Terms** are printed in bold type and are defined where they first appear. They are also grouped at the end of the chapter and in the **Glossary** at the back of the text.

25°C. The air has a mole fraction of nitrogen of 0.790, the rest being oxygen.
   a. Explain why the balloon would float when heated. Make sure to discuss which factors change and which remain constant, and why this matters. Be complete.
   b. Above what temperature would you heat the balloon so that it would float?

123. You have a helium balloon at 1.00 atm and 25°C. You want to make a hot-air balloon with the same volume and same lift as the helium balloon. Assume air is 79.0% nitrogen, 21.0% oxygen by volume. The "lift" of a balloon is given by the difference between the mass of air displaced by the balloon and the mass of gas inside the balloon.
   a. Will the temperature in the hot-air balloon have to be higher or lower than 25°C? Explain.
   b. Calculate the temperature of the air required for the hot-air balloon to provide the same lift as the helium balloon at 1.00 atm and 25°C. Assume atmospheric conditions are 1.00 atm and 25°C.

…4. We state that the ideal gas law tends to hold best at low pressures and high temperatures. Show how the van der Waals equation simplifies to the ideal gas law under these conditions.

…5. Atmospheric scientists often use mixing ratios to express the concentrations of trace compounds in air. Mixing ratios are often expressed as ppmv (parts per million volume):

$$\text{ppmv of } X = \frac{\text{vol. of } X \text{ at STP}}{\text{total vol. of air at STP}} \times 10^6$$

On a recent autumn day, the concentration of carbon monoxide in the air in downtown Denver, Colorado, reached 3.0×10^2 ppmv. The atmospheric pressure at that time was 628 torr, and the temperature was 0°C.
   a. What was the partial pressure of CO?
   b. What was the concentration of CO in molecules per cubic centimeter?

…6. Nitrogen gas (N_2) reacts with hydrogen gas (H_2) to form ammonia gas (NH_3). You have nitrogen and hydrogen gases in a 15.0-L container fitted with a movable piston (the piston allows the container volume to change so as to keep the pressure constant inside the container). Initially the partial pressure of each reactant gas is 1.00 atm. Assume the temperature is constant and that the reaction goes to completion.
   a. Calculate the partial pressure of ammonia in the container after the reaction has reached completion.
   b. Calculate the volume of the container after the reaction has reached completion.

…tegrative Problems

…ese problems require the integration of multiple concepts to find the …lutions.

…7. In the presence of nitric acid, UO^{2+} undergoes a redox process. It is converted to UO_2^{2+} and nitric oxide (NO) gas is produced according to the following unbalanced equation:

$$NO_3^-(aq) + UO^{2+}(aq) \longrightarrow NO(g) + UO_2^{2+}(aq)$$

If 2.55×10^2 mL of NO(g) is isolated at 29°C and 1.5 atm, what amount (moles) of UO^{2+} was used in the reaction?

128. Silane, SiH_4, is the silicon analogue of methane, CH_4. It is prepared industrially according to the following equations:

$$Si(s) + 3HCl(g) \longrightarrow HSiCl_3(l) + H_2(g)$$
$$4HSiCl_3(l) \longrightarrow SiH_4(g) + 3SiCl_4(l)$$

   a. If 156 mL of $HSiCl_3$ (d = 1.34 g/mL) is isolated when 15.0 L of HCl at 10.0 atm and 35°C is used, what is the percent yield of $HSiCl_3$?
   b. When 156 mL of $HSiCl_3$ is heated, what volume of SiH_4 at 10.0 atm and 35°C will be obtained if the percent yield of the reaction is 93.1%?

129. Solid thorium(IV) fluoride has a boiling point of 1680°C. What is the density of a sample of gaseous thorium(IV) fluoride at its boiling point under a pressure of 2.5 atm in a 1.7-L container? Which gas will effuse faster at 1680°C, thorium(IV) fluoride or uranium(III) fluoride? How much faster?

130. Natural gas is a mixture of hydrocarbons, primarily methane (CH_4) and ethane (C_2H_6). A typical mixture might have $\chi_{methane} = 0.915$ and $\chi_{ethane} = 0.085$. What are the partial pressures of the two gases in a 15.00-L container of natural gas at 20.°C and 1.44 atm? Assuming complete combustion of both gases in the natural gas sample, what is the total mass of water formed?

Marathon Problem*

This problem is designed to incorporate several concepts and techniques into one situation. Marathon Problems can be used in class by groups of students to help facilitate problem-solving skills.

131. Use the following information to identify element A and compound B, then answer questions a and b.

An empty glass container has a mass of 658.572 g. It has a mass of 659.452 g after it has been filled with nitrogen gas at a pressure of 790. torr and a temperature of 15°C. When the container is evacuated and refilled with a certain element (A) at a pressure of 745 torr and a temperature of 26°C, it has a mass of 660.59 g.

Compound B, a gaseous organic compound that consists of 85.6% carbon and 14.4% hydrogen by mass, is placed in a stainless steel vessel (10.68 L) with excess oxygen gas. The vessel is placed in a constant-temperature bath at 22°C. The pressure in the vessel is 11.98 atm. In the bottom of the vessel is a container that is packed with Ascarite and a desiccant. Ascarite is asbestos impregnated with sodium hydroxide; it quantitatively absorbs carbon dioxide:

$$2NaOH(s) + CO_2(g) \longrightarrow Na_2CO_3(s) + H_2O(l)$$

*Used with permission from the *Journal of Chemical Education,* Vol. 68, No. 11, 1991, pp. 919–922; copyright © 1991, Division of Chemical Education, Inc.

Questions give students an opportunity to review key concepts; **Exercises** (paired and organized by topic) reinforce students' understanding of each section; **Additional Exercises** require students to identify and apply the appropriate concepts themselves; **Challenge Problems** take students one step further and challenge students more rigorously than Additional Exercises; **Integrative Problems** combine concepts from multiple chapters; **Marathon Problems** also combine concepts from multiple chapters, and they are the most challenging problems in the end-of-chapter material.

Online Problem Solving and Practice

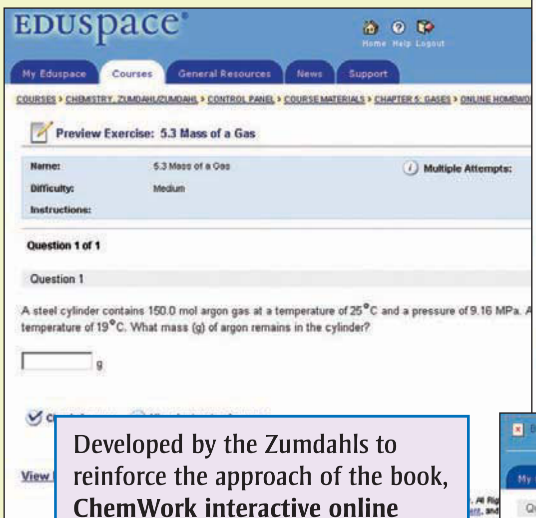

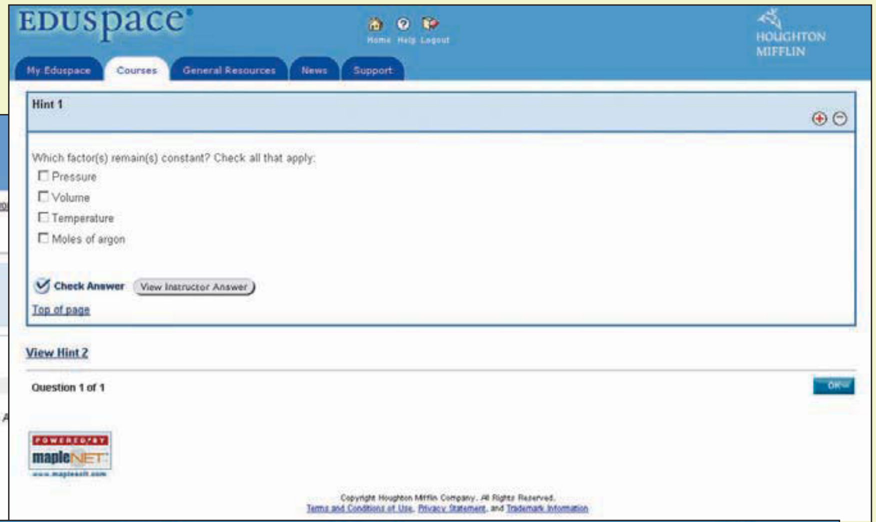

Developed by the Zumdahls to reinforce the approach of the book, **ChemWork interactive online homework** offers problems accompanied by hints to help students as they think through each problem. *ChemWork* assignments are offered in **Eduspace**—Houghton Mifflin's course-management system.

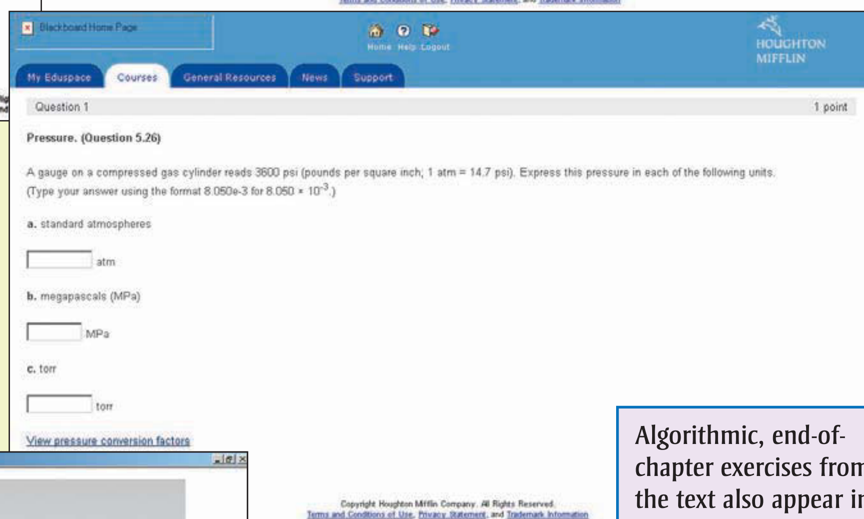

Algorithmic, end-of-chapter exercises from the text also appear in **Eduspace.** Exercises also include helpful links to art, tables, and equations from the textbook.

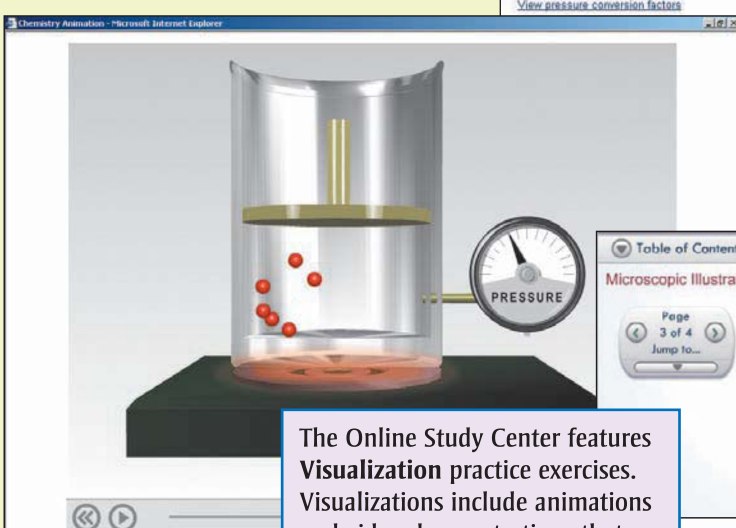

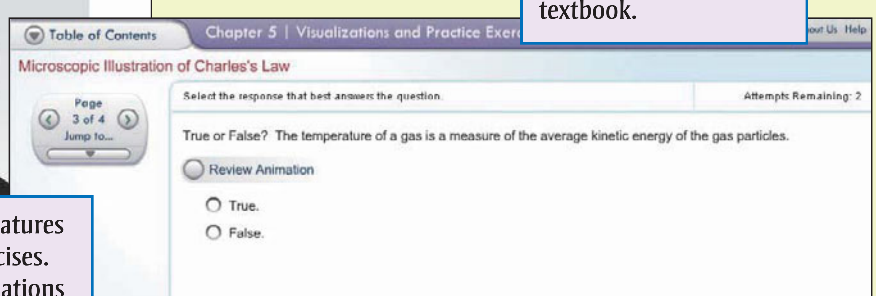

The Online Study Center features **Visualization** practice exercises. Visualizations include animations and video demonstrations that help students to further understand chemical concepts. Each Visualization is accompanied by quiz questions.

Media Resources for Instructors

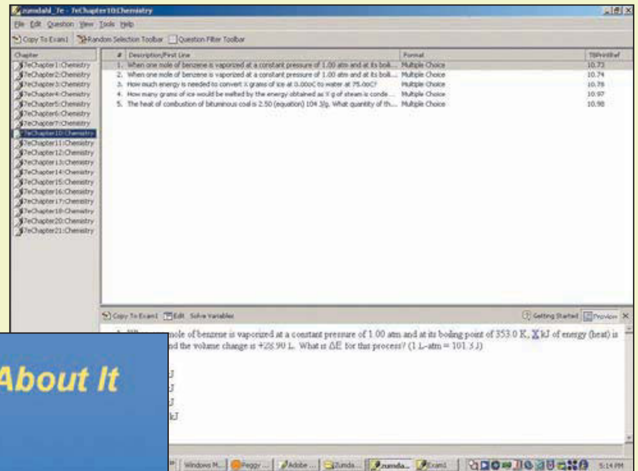

HM ClassPrep with **HM Testing (powered by Diploma) CD** is a cross-platform CD that contains extensive text-specific resources for instructors to incorporate into their lecture presentations. These customizable assets include PowerPoint slides, Word files of the printed *Test Bank* and *Solutions Manual,* figures from the text, the *Instructor's Resource Guide* and more. HM Testing (powered by Diploma) is Houghton Mifflin's new flexible test-editing program, which features algorithmically generated questions, conceptual questions, and factual questions coded by level of difficulty to allow you to more easily choose appropriate test items. Select from 2400 test items designed to measure the concepts and principles covered in the seventh edition.

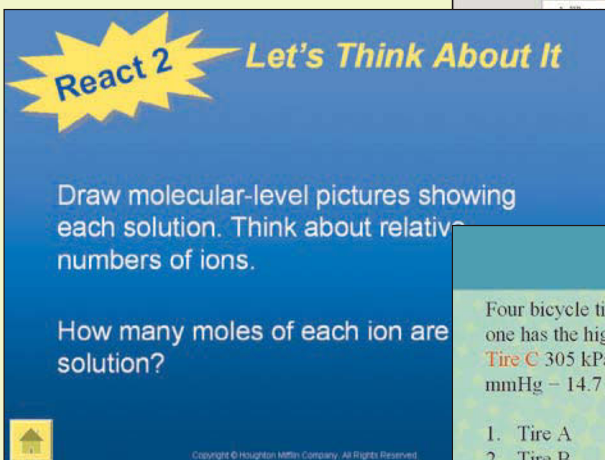

HM ClassPresent includes animations and video demonstrations that can be used to illustrate concepts and ideas that will help students further understand and visualize chemical concepts. Animations and videos can be projected directly from the CD, exported to your computer, and also come embedded in PowerPoint files.

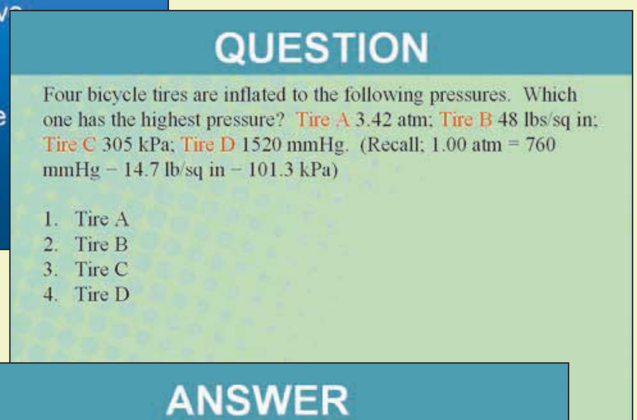

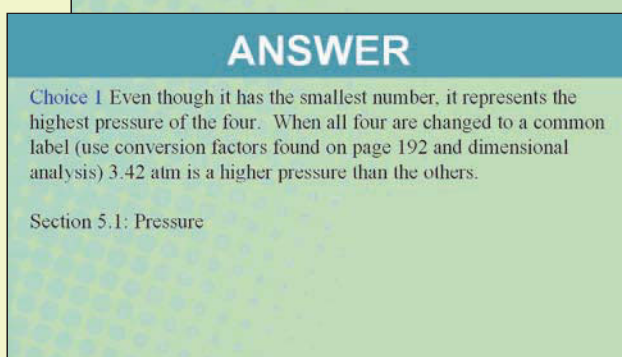

Online Teaching Center for *Chemistry* offers access to lecture preparation materials; PowerPoint presentation resources; JPEGs of virtually all text illustrations, tables, and photos; video demonstrations and animations; molecule library with CHIME; as well as service and support. Also included on the Online Teaching Center, you will find classroom response-system slides. These slides allow you to get on-the-spot feedback on how well your students are grasping key concepts.

Eduspace, featuring online homework, is Houghton Mifflin's course-management system. Eduspace allows for online delivery of course materials, chat and discussion tools, and includes two types of algorithmic online homework: *ChemWork* and end-of-chapter exercises. *ChemWork* helps students learn the process of problem solving with interactive hints that help students think through each problem.